

PhD Thesis

School of Chemistry

Cardiff University



The application of Cs-exchanged tungstophosphoric acid as an additive in the direct synthesis of hydrogen peroxide and the use of Au-Pd / TS-1 in a one-pot approach to cyclohexanone oxime production.

Thesis submitted in accordance with the requirements of the University of Cardiff for the degree of doctor in philosophy by:

Richard Lewis

2016

Summary.

The work presented within this thesis can be separated into two distinct parts. The first investigates the direct synthesis of hydrogen peroxide from molecular hydrogen and oxygen using gold-palladium supported catalysts and caesium exchanged tungstophosphoric acid as an acidic additive. The direct synthesis of H₂O₂ presents an environmentally friendly alternative to the current industrial, anthraquinone process. However for the direct route to be viable a variety of issues must be addressed. Primarily catalytic selectivity towards H₂O₂ is a major concern for the majority of catalysts active for H₂O₂ synthesis, with the degradation of H₂O₂ through hydrogenation or decomposition reported for a number of catalysts within the literature.

The use of acid either during catalyst preparation or as part of the reaction solution has previously been shown to improve selectivity towards H₂O₂. Furthermore acidic supports, including heteropolyacid, have been observed to produce catalysts with greater selectivity than those with a higher isoelectric point and in turn provide higher yields of H₂O₂. This work investigates the ability of caesium exchanged heteropolyacids to improve catalytic activity towards H₂O₂ when used in addition to Au-Pd supported catalysts, in particular 2.5 wt. % Au – 2.5 wt. Pd / TiO₂.

The second part of this work is concerned with the ammoximation of cyclohexanone to cyclohexanone oxime via the *in-situ* formation of H₂O₂, in a one-pot style process. The conditions associated with ammoximation of cyclohexanone that is the presence of elevated temperatures and basic conditions, are considered extremely harsh for H₂O₂ stability. The *in-situ* generation of H₂O₂ during the ammoximation of cyclohexanone to cyclohexanone oxime would yield significant reductions in overall costs of the ammoximation reaction. Primarily these costs are associated with the purchasing, transport, storage and dilution of H₂O₂. This work determines the feasibility of a one-pot ammoximation process via *in-situ* H₂O₂ formation. Firstly, reaction conditions are established for this process and following this the role of catalyst design in improving selectivity towards cyclohexanone oxime as well as cyclohexanone conversion for this reaction is studied.

Acknowledgements

I would like to express my gratitude to my research supervisor Professor Graham Hutchings, who provided me with the opportunity to conduct this research as a member of the renowned Cardiff Catalysis Institute. His encouragement, guidance and insights throughout this work was invaluable.

Secondly I would like to thank Dr. Jennifer Edwards, Dr. Simon Freakley and Dr. Gregory Shaw, their willingness to give advice during my three years of laboratory work as well as during the writing of this thesis is very much appreciated, as has been their support during the difficult times that inevitably occur during three and a half years of research. My gratitude is extended to Professor Pelham Hawker, Dr. Brian Harrison and Professor Jacob Moulijn for their advice and constructive recommendations on their numerous visits to Cardiff. I gratefully acknowledge the staff in the chemistry department at Cardiff University, in particular Alun Davies and Steve Morris who always managed to save the day, when technical issues arose.

I wish to acknowledge UBE Industries for their support and contribution to this project. In particular my special thanks to Dr. Yukimasa Fukuta and Mr. Kenji Ueura who's expertise was invaluable.

I would like to thank all the numerous PhD students and post docs who I have had the pleasure to work alongside during my PhD. In particular the '*hydrogen peroxide team*' Dr. Adeeba Akram, Dr. Ouardia Adkim, David Crole, Ricci Underhill and Jonathan HARRY but also Dr. Benjamin Yeo, Dr. Rob Armstrong, Gavin King, Christopher Evans and Christopher Williams all of whom have played a role in maintaining my sanity while conducting this work and were always available to share ideas or provide coffee, as many a PhD student knows this is something that is relied upon more and more throughout a PhD.

Most importantly I would like to thank my family who have been a constant support and an inspiration to me, not just during my PhD, but in everything I do. They more than anyone have been there for me when I needed them and for this I will always be grateful.

1 Contents

1	Contents.....	3
1.	Introduction.....	7
1.1	Overview.....	7
1.2.	Catalysis, basic concepts and definitions.....	10
1.3.	Introduction to hydrogen peroxide.....	14
1.4.	Historical note and current synthesis method.....	15
1.5.	The proposed mechanism in the direct synthesis of H ₂ O ₂ from H ₂ and O ₂	19
1.7.	Gold based catalysts in the synthesis of hydrogen peroxide.....	25
1.8.	Bimetallic catalysts for the direct synthesis of hydrogen peroxide.....	28
1.9.	The effect of the calcination process on the effectiveness of bimetallic catalysts in the direct formation of hydrogen peroxide.....	32
1.10.	Particle morphology in bimetallic Au-Pd supported catalysts.....	35
1.11.	The role of the support in the direct synthesis of H ₂ O ₂	38
1.12.	The role of additives in the direct synthesis of hydrogen peroxide.....	43
1.11.	Heteropolyacid based catalysts in the direct synthesis of hydrogen peroxide.....	47
1.12.	The ammoximation of cyclohexanone to cyclohexanone oxime, utilising TS-1.....	50
1.13.	The structure of TS-1.....	51
1.14.	The ammoximation of cyclohexanone to cyclohexanone oxime.....	52
1.15.	Thesis Aims.....	56
1.17.	References.....	57
2.	Experimental.....	62
2.1.	Materials used.....	62
2.2.	Catalyst Preparation.....	63
2.2.1.	Gold, Palladium and Gold-Palladium Catalysts prepared by wet impregnation.....	63
2.2.2.	Gold, Palladium, Platinum and Gold - Palladium - Platinum Catalysts prepared by wet impregnation.....	63
2.2.3.	Cs-exchanged tungstophosphoric acid.....	63
2.3.	Catalyst Testing.....	64
2.3.1.	The Direct Synthesis of H ₂ O ₂	64
2.3.2.	Degradation of H ₂ O ₂	66
2.3.3.	Direct synthesis of H ₂ O ₂ under ammoximation conditions.....	66
2.3.4.	Degradation of H ₂ O ₂ under ammoximation conditions.....	67
2.3.5.	The ammoximation of cyclohexanone to cyclohexanone oxime via H ₂ O ₂ addition.....	67

2.3.6. Catalyst re-use for the ammoximation of cyclohexanone to cyclohexanone oxime via H ₂ O ₂ addition.	67
2.3.7. The ammoximation of cyclohexanone to cyclohexanone oxime via <i>in-situ</i> synthesis of H ₂ O ₂	68
2.3.8. Hot filtration for the ammoximation of cyclohexanone to cyclohexanone oxime via in-situ synthesis of H ₂ O ₂	68
2.4. Gas Chromatography.	69
2.4.1. GC setup for analysis of gas from H ₂ O ₂ direct synthesis reaction.	69
2.4.2. GC set up for analysis of reaction mixture from ammoximation of cyclohexanone.	69
2.4.3. Quantitative Analysis by Gas Chromatography.	71
2.5. X-Ray Diffraction (XRD).	72
2.6. BET Surface Area Analysis.	74
2.7. Microwave Plasma Atomic Emission Spectroscopy (MP-AES).	76
2.8. Electron Microscopy (EM).	77
2.8.1. Transmission electron microscopy (TEM).	77
2.8.2. Scanning Transmission Electron Microscopy (STEM).	78
2.8.3. Energy Dispersive X-ray Spectroscopy (EDX).	79
2.9. X-ray photoelectron spectroscopy (XPS).	79
2.10. Temperature Programmed Desorption (TPD).	81
2.11. Infra-red Spectroscopy (IR).	82
2.12. CO Chemisorption.	83
2.13. References	84
Appendix. 2. 1	85
3. The Direct Synthesis of H ₂ O ₂ using supported Gold Palladium Catalysts and Heteropolyacid based additives.	87
3.1. Introduction.	87
3.2. Results and discussion.	89
3.2.1. The direct synthesis of H ₂ O ₂ using 2.5 wt. % Au – 2.5 wt. % Pd / TiO ₂ catalyst and Cs-exchanged heteropolyacids.	89
3.2.2. The effect of Cs-exchanged of tungstophosphoric acid on the promotion of 2.5 wt. % Au – 2.5 wt. % Pd / TiO ₂ towards the direct synthesis of H ₂ O ₂	90
3.2.3. The effect of adding Cs _{0.1} H _{2.9} PW ₁₂ O ₄₀ to supported bimetallic catalysts.	102
3.2.4. The Effect of Reaction Conditions on the direct synthesis of H ₂ O ₂ using Cs _{0.1} H _{2.9} PW ₁₂ O ₄₀ as a solid acid additive for 2.5 wt. % Au – 2.5 wt. % Pd / TiO ₂	103
3.2.4.1. Effect of gas feed composition.	104
3.2.4.2. Effect of reaction temperature.	107
3.2.4.3. The effect of reaction time.	109

3.2.4.4. The effect of stirring speed.	111
3.2.4.5. The effect of catalyst mass.	113
3.2.4.6. Effect of Cs _{0.1} H _{2.9} PW ₁₂ O ₄₀ mass.	114
3.2.4.7. Effect of solvent mass.	117
3.2.4.8. Effect of H ₂ O / CH ₃ OH ratio.	118
3.2.5.1. Variation in pH of the water-methanol working solution using common supports as an additive to 2.5 Wt. % Au – 2.5 Wt. % Pd / TiO ₂	119
3.2.5.2. Variation in pH of the water-methanol working solution using nitric and tungstic acid as an additive to 2.5 wt. % Au – 2.5 wt. % Pd / TiO ₂	121
3.2.7. Reusability of the Cs-exchanged HPAs in the direct synthesis of H ₂ O ₂	124
3.3. Conclusion.	126
3.4. References	128
4. Ammoximation of cyclohexanone via in-situ H ₂ O ₂ synthesis.	130
4.1. Introduction.	130
4.2. Results.	131
4.2.1. H ₂ O ₂ synthesis activity of monometallic and bimetallic Au-Pd catalysts supported on TS-1.	132
4.2.2. The direct synthesis of H ₂ O ₂ , using 5 wt. % Pd/ TS-1 as a model catalyst, moving towards ammoximation conditions.	134
4.2.3. The degradation of H ₂ O ₂ using 5 wt. % Pd / TS-1 as a model catalyst, moving towards ammoximation conditions.	136
4.2.4. The ammoximation of cyclohexanone to cyclohexanone oxime via H ₂ O ₂ addition.	137
4.3. Optimisation of Reaction Conditions for the Ammoximation of Cyclohexanone to Cyclohexanone Oxime.	139
4.3.1. Reaction temperature optimisation.	140
4.3.2. Catalyst mass optimisation.	142
4.3.3. Solvent composition optimisation	143
4.3.4. Cyclohexanone concentration optimization.	145
4.3.5. Ammonia concentration optimization.	146
4.3.6. Reaction time optimisation.	147
4.3.7. Reactant gas composition optimization.	148
4.3.8. Total reactant gas pressure, while maintaining H ₂ : O ₂	150
4.3.9. Stirring speed optimization.	151
4.4. Determining the activity of leached metal towards the ammoximation of cyclohexanone <i>via in-situ</i> synthesis of H ₂ O ₂	153
4.5. Conclusion.	156
4.6. References.	160

5. Catalyst Design in the ammoximation of cyclohexanone via the <i>in-situ</i> synthesis of H ₂ O ₂ .	161
5.1. Introduction.	161
5.2. Results and discussion	162
5.2.1. Effect of Pd loading on the ammoximation of cyclohexanone to cyclohexanone oxime via direct synthesis of H ₂ O ₂ from H ₂ and O ₂ .	162
5.2.3. The effect of Au-Pd metal ratio on the ammoximation of cyclohexanone to cyclohexanone oxime via direct synthesis of H ₂ O ₂ from H ₂ and O ₂ .	171
5.2.4. Investigating the role of Au in improving catalytic selectivity towards cyclohexanone oxime.	175
5.2.5. The effect of calcination temperature on 2.5 wt. % Au – 2.5 wt. % Pd / TS-1 activity towards the ammoximation of cyclohexanone.	178
5.2.6. Investigation of the effect of total metal loading for Au-Pd catalysts for the ammoximation of cyclohexanone.	184
5.2.7. Mono – bi – and tri-metallic Pd / Pt / Au / catalysts supported on TS-1 for the ammoximation of cyclohexanone.	186
5.2.8. The effect of calcination temperature on 2 wt. % Au – 2 wt. % Pd – 1 wt. % Pt / TS-1 activity towards the ammoximation of cyclohexanone.	193
5.2.9. The effect of calcination temperature of 5 wt. % Au-Pd-Pt / TS-1 catalysts for the ammoximation of cyclohexanone via direct synthesis of H ₂ O ₂ .	198
5.3. Conclusion.	202
5.4. References.	205
Appendix 5.1	206
Appendix 5.2.	209
Appendix 5.3.	210
6. Conclusion and Future Work.	212
6.1 .Conclusion.	212
6.2. Future Work.	220
6.2.1 Improved use of metal.	220
6.2.2. Catalyst Stability.	220
6.2.3. Catalyst synthesis technique.	221
6.2.4. The use of cheaper metals.	222
6.2.5. Particle composition.	222
6.2.6. Determine the activity of TS-1 supported catalysts towards the ammoximation of other substrates.	223
6.2.7. Determine the role of phosphate present in Cs _x H _{3-x} PW ₁₂ O ₄₀ salts in improving the stability H ₂ O ₂ .	223
6.3. References.	224

1. Introduction.

1.1 Overview.

The vast majority of hydrogen peroxide (H_2O_2) produced globally is done so *via* the indirect or anthraquinone auto-oxidation (AO) process, which involves the hydrogenation of an alkyl anthraquinone which is subsequently oxidised. This process has been continually improved since it was first developed in 1939 by Riedel and Pfeleiderer¹ and so is highly energy efficient. Although problems of scale and the environmentally unfriendly nature of solvent systems used present a considerable downside to the indirect process.

The direct synthesis of H_2O_2 has been a challenge for the scientific community for over 100 years, with the first patent, for a Pd catalyst, filed in 1914² and until recently investigation into the catalysis of the direct route have been based upon Pd catalysts.³⁻⁷ Figure 1.1 shows the synthesis route for H_2O_2 as well as the sequential hydrogenation / decomposition steps. It is known that catalysts active towards the synthesis of H_2O_2 are almost always active towards its subsequent break down and it is these side reactions that result in a loss of catalytic selectivity and therefore reduce the net formation of H_2O_2 . Although it has been reported recently that catalyst design can be modified in order to limit or even inhibit these subsequent reactions.⁸⁻¹⁰

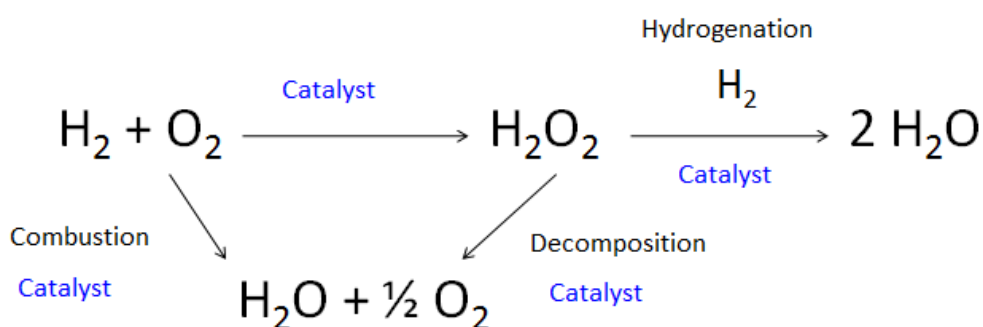


Figure 1.1 The direct synthesis of H_2O_2 and its subsequent degradation pathways.

The issue of catalyst selectivity can be understood as the formation of water from H_2 and O_2 is thermodynamically favorable, in comparison to the formation of H_2O_2 as summarized by Equations 1-2.

1. $\text{H}_2(\text{g}) + \text{O}_2(\text{g}) \rightarrow \text{H}_2\text{O}_2(\text{l}) \quad \Delta G_{298} = -120.5 \text{ kJ/mol}$
2. $\text{H}_2(\text{g}) + \frac{1}{2} \text{O}_2(\text{g}) \rightarrow \text{H}_2\text{O}_2(\text{l}) \quad \Delta G_{298} = -237.2 \text{ kJ/mol}$

Furthermore the undesired subsequent H_2O_2 decomposition and hydrogenation reactions are also thermodynamically favorable:

3. $\text{H}_2\text{O}_2(\text{l}) \rightarrow \text{H}_2\text{O}(\text{l}) + \frac{1}{2} \text{O}_2(\text{g}) \quad \Delta G_{298} = -116.7 \text{ kJ/mol}$
4. $\text{H}_2\text{O}_2(\text{l}) + \text{H}_2(\text{g}) \rightarrow 2 \text{H}_2\text{O}(\text{l}) \quad \Delta G_{298} = -354.0 \text{ kJ/mol}$

The direct synthesis of H_2O_2 , therefore demonstrates the need for catalyst design to balance selectivity and activity carefully, as well as the selection of reaction conditions that inhibit the degradation of H_2O_2 . It is known that H_2O_2 is highly unstable at high temperatures or in the presence of basic conditions¹¹. It can be demonstrated that through the use of low reaction temperatures it is possible to limit the thermodynamic favorability of the subsequent H_2O_2 degradation reactions. By decreasing temperature it is possible to decrease the entropic contribution to the Gibbs free energy (ΔG), which clearly favors the degradation of H_2O_2 to H_2O .

As discussed above the use of Pd as a catalyst for the direct synthesis of H_2O_2 has been highly reported. Hutchings' seminal study¹² showed that catalysts containing Au also had some activity towards H_2O_2 synthesis, however the crucial finding was that bimetallic Au-Pd supported catalysts were significantly more effective than either monometallic Au or Pd catalyst for the direct synthesis of H_2O_2 .¹³ Subsequent work by Hutchings and co-workers has shown this to be true on a variety of supports, including Al_2O_3 ¹², Fe_2O_3 ¹³, SiO_2 ¹⁴ and TiO_2 ¹⁵ and where the addition of Au to Pd improves catalytic selectivity and enhances the rate of H_2O_2 synthesis.

Various studies have shown that supports with lower isoelectric points, effectively more acidic supports^{16, 17}, such as carbon as well as the addition of acid additives including HCl ¹⁸, H_3PO_4 ¹⁹ and H_2SO_4 ¹⁹ can aid in the suppression of H_2O_2 decomposition thus improving catalytic selectivity. Indeed it has recently been shown by Hutchings and co-workers⁸ that it is possible to 'switch off' the hydrogenation and decomposition activity of a carbon supported bimetallic catalyst *via* an acid pre-treatment of the support. This has been shown to increase gold dispersion by producing smaller Au-Pd nanoparticles which are believed to be able to block the catalytic sites responsible for H_2O_2 hydrogenation / decomposition. Further work by Hutchings and co-workers has shown that this acidic pre-treatment can also inhibit the degradation of H_2O_2 by Au-Pd catalysts supported on TiO_2 ²⁰ and SiO_2 ⁹, however

the pre-treatment is unable to completely inhibit H₂O₂ degradation as seen when utilising a carbon support.

It is this work which has led to the investigation of highly acidic supports as a means by which catalyst selectivity towards H₂O₂ may be improved. Sun and co-workers²¹ have shown that Pd based heteropolyacid (HPA) catalysts offer both greater rates of H₂O₂ synthesis, as well as improved selectivity towards H₂O₂ synthesis in comparison to Pd catalysts utilizing more conventional supports. This work has led Hutchings and co-workers to investigate bi-metallic Au-Pd exchanged heteropolyacids in the direct synthesis of H₂O₂^{22,23}.

The first part of the work reported herein attempts to build further on these earlier studies. However, instead of utilising Cs-exchanged HPAs as a support for metals known to be active towards H₂O₂ synthesis, as studied previously within the Hutchings' group, their ability to promote catalyst activity towards H₂O₂ synthesis is investigated when they are utilised as an additive in addition to a well-established H₂O₂ synthesis catalyst.

The second part of this work is concerned with the formation of H₂O₂ under the relatively challenging conditions associated with the ammoximation of cyclohexanone, that is the presence of elevated temperatures and basic conditions. The *in-situ* generation of H₂O₂ during the ammoximation of cyclohexanone to cyclohexanone oxime would yield significant reductions in overall costs of the ammoximation reaction. Primarily these costs are associated with the purchasing, transport, storage and dilution of H₂O₂.

A suggested reaction scheme for the ammoximation of cyclohexanone is shown below, in Figure 1.2. It is observed that there are a number of competing, unwanted, side reactions that may contribute towards a decrease in the overall yield of cyclohexanone oxime. The role of catalyst design and reaction process optimization has been investigated in an attempt to improve the yield of cyclohexanone oxime.

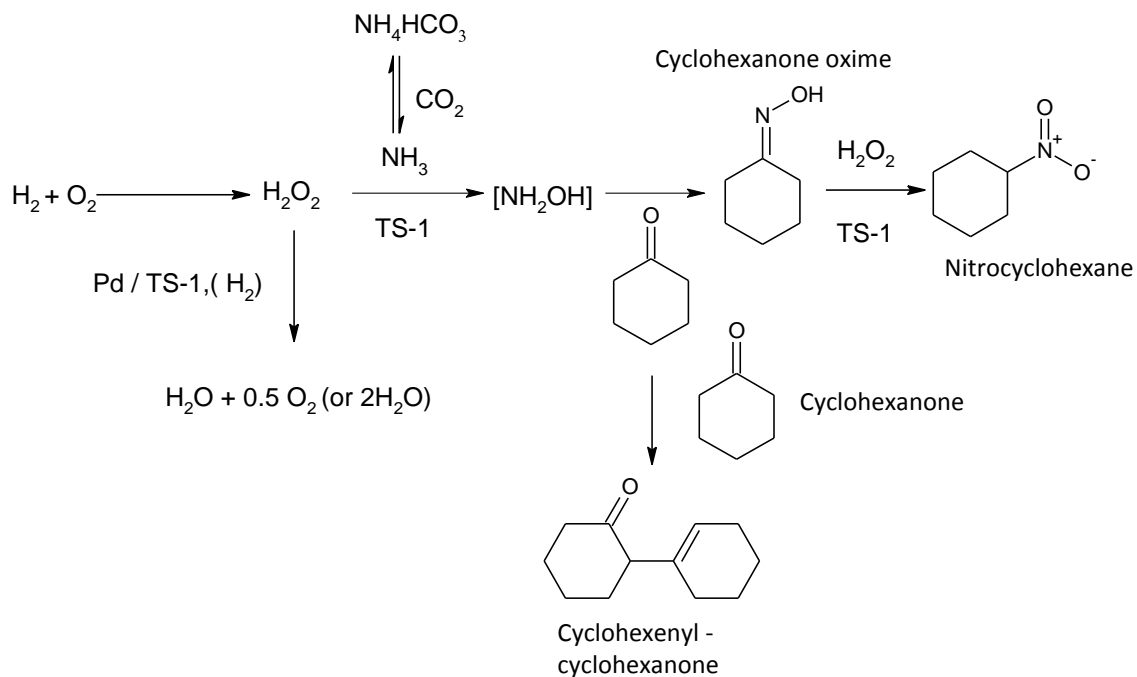


Figure 1.2. Proposed reaction scheme for the ammoxidation of cyclohexanone via the in-situ synthesis of H_2O_2 .

1.2. Catalysis, basic concepts and definitions.

Perhaps one of the most important industrial chemical reactions is the Haber-Bosch process, which leads to the production of artificial fertilisers and allows for the mass production of food. Without this process it is difficult to imagine how different the modern world would be. However the Haber-Bosch process is only one of a vast list of chemical processes that relies on the use of catalysis.

A large proportion of these catalysed reactions utilise a heterogeneous catalyst, where the catalyst itself is in a different phase to the reactants, often a solid catalyst with reactants in the liquid or gaseous phase. In comparison a homogenous catalyst exists in the same phase as the reactants, typically both catalyst and reactant will be gaseous or in the liquid phase.

It is possible to define a catalyst as a material that increases the rate of a chemical reaction by reducing the activation energy of a reaction (E_A), but which is left unaltered at the end of the reaction. The lowering of the activation energy is achieved by the catalyst providing an alternative reaction pathway for the reaction to proceed, possibly through several intermediates or transition states, as seen in Figure 1.3. It can be seen that the activation barrier of the catalysed pathway is significantly lower than that on the un-catalysed route.

However, the Gibbs free energy of the system (G) is the same regardless of whether the reaction occurs in the presence of a catalyst or not. The Gibbs free energy may be defined in terms of enthalpy (H) and entropy (S) as the thermodynamic function of a system that is equal to the enthalpy minus the product of the absolute temperature (T) and entropy and an exact definition of G is therefore given by:

$$5. \quad G = H - TS$$

The Gibbs free energy is a measure of the tendency for a reaction to take place (a criterion of spontaneous change) as well as a measure of the useful work of a process. That is it combines two state functions and so it must be a state function itself. This means that the value of Gibbs free energy is dependent only on the initial and final state of the system. As such the presence of a catalyst will not alter the value of Gibbs free energy as a catalyst only provides a different pathway, of lower activation energy, for the reaction to proceed and does not alter the initial or final states of the system.

When a chemical reaction occurs the system is attempting to satisfy two opposing tendencies:

- 1) Towards maximum energy (maximum stability) and
- 2) Towards maximum entropy (maximum freedom).

Therefore the change in Gibbs free energy (ΔG) is a measure of the tendency of a reaction to proceed and can be defined as:

$$6. \quad \Delta G = \Delta H - T\Delta S$$

The magnitude and sign of ΔG provides information to how a reaction will proceed, with a large, negative value meaning that the reaction proceeds from reactants to products spontaneously. That is if a reaction results in a lowering of free energy it will be spontaneous. However, this means that it is possible that the reaction can occur not that it is certain to occur. Often a reaction may be highly favorable thermodynamically but occurs very slowly. It is kinetically unfavorable, as it has a high activation energy. The utilization of a catalyst will therefore affect the kinetics of the reaction.

At low reaction temperatures, the $T\Delta S$ term will be relatively small in comparison to ΔH so that ΔG is insensitive towards the sign of the entropy change. The sign of ΔG is therefore determined by the sign of ΔH . At low temperatures the entropic contribution can be negative or positive but the Gibbs free energy change will be negative. Therefore, for a spontaneous

reaction ΔH must be negative. However at high temperatures the $(-T \Delta S)$ term will be dominant so that a positive ΔS is needed for Gibbs free energy to be negative²⁴.

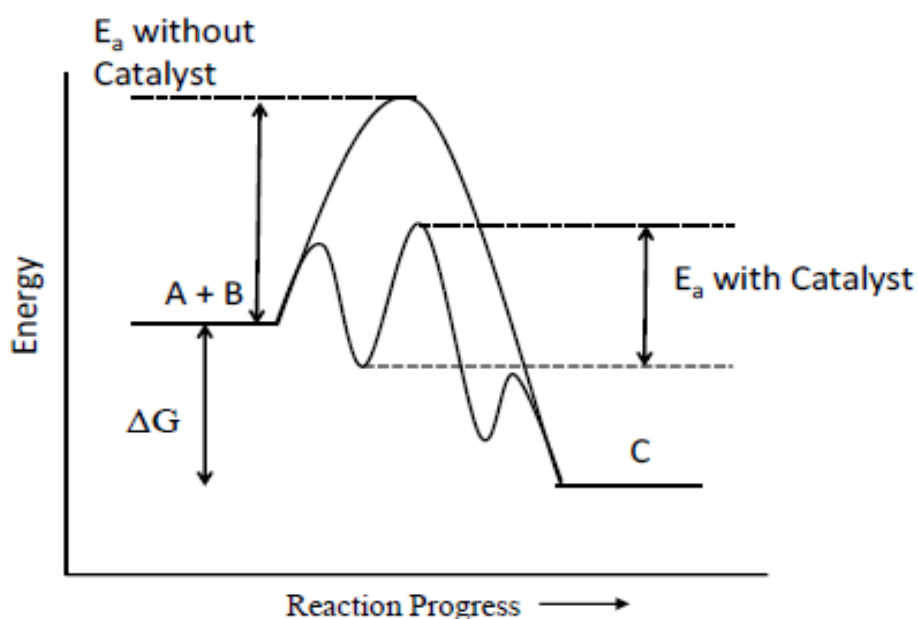
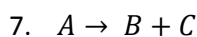


Figure 1.3. Energy level diagram to compare the difference in the activation energy of a catalysed and non-catalysed reaction.²⁴

Heterogeneous catalysts have a distinct advantage over homogeneous catalysts, mainly the ease in which they can be recovered and re-used. They provide a means for reactants to be brought together, on the active site of the catalyst, in such a way that reaction to the desired products are possible. It is therefore possible to correlate catalytic activity and the total number of active sites, in turn a high active surface area is often key in producing a highly active catalyst. The activity of a catalyst may be defined as the rate of reactant consumption (units: moles / dm³/s), although the activity to a particular product may also be quantified.

For a general reaction:



Catalytic activity towards A, B and C may be defined as:

$$8. \quad \text{Activity towards A} = (-d[A])/dt$$

$$9. \quad \text{Activity towards B} = (d[B])/dt$$

$$10. \quad \text{Activity towards C} = (d[C])/dt$$

A further term, known as specific activity can also be defined as:

$$11. A_{Sv} = \frac{-1}{Sv} * \frac{d[A]}{dt}$$

Where:

S_v = total number of active sites per unit volume.

The specific activity is often very important for industrial application of catalysts, where the reactors used have a fixed volume for a catalyst to fill. Specific activity may also be expressed per unit weight of catalyst. Instead of expression in terms of unit volume it is possible to express specific activity per unit surface area, as shown in Equation 12.

$$12. A_{SV} = \frac{1}{b * S_A} * \frac{d[B]}{dt}$$

Where:

b = the stoichiometric number of the conversion of one mole of reactant A to product B.

S_A = the number of active sites per unit area of catalyst surface.

Finally an alternative expression, the turnover frequency (TOF), gives the rate in terms of molecules of A reacted per site per unit of time (usually seconds).

$$13. TOF = A_{SV} * N_A$$

Where N_A is Avagadro's number

To quantify the number of active sites (S_A) it is first important to determine the total surface area of the catalytic metals on the surface of the support. This may be done through a process known as selective gas chemisorption, which is discussed in Chapter 2.

Often catalytic activity is improved through the dispersion of metal nanoparticles, often on an inert support. Typically metal oxides are utilised as they provide important physical features, such as high melting and decomposition temperatures, the ability to maintain a specific surface area when exposed to high temperatures, particularly when metal nanoparticles are affixed to them via thermal treatment. Furthermore other features such as pore volume and pore distribution can be established and provide significant benefit to the catalyst. With many reactions that utilise catalysts both the properties of the active phase and the support bring about the functionality of the catalyst.

A general description of a catalytic process can be broken down into a number of basic steps; reactant adsorption onto the active site of the catalyst, breaking of the reactant bonds, reaction to form the products and the subsequent desorption of the newly formed products. These various steps are shown in Figure 1.4.

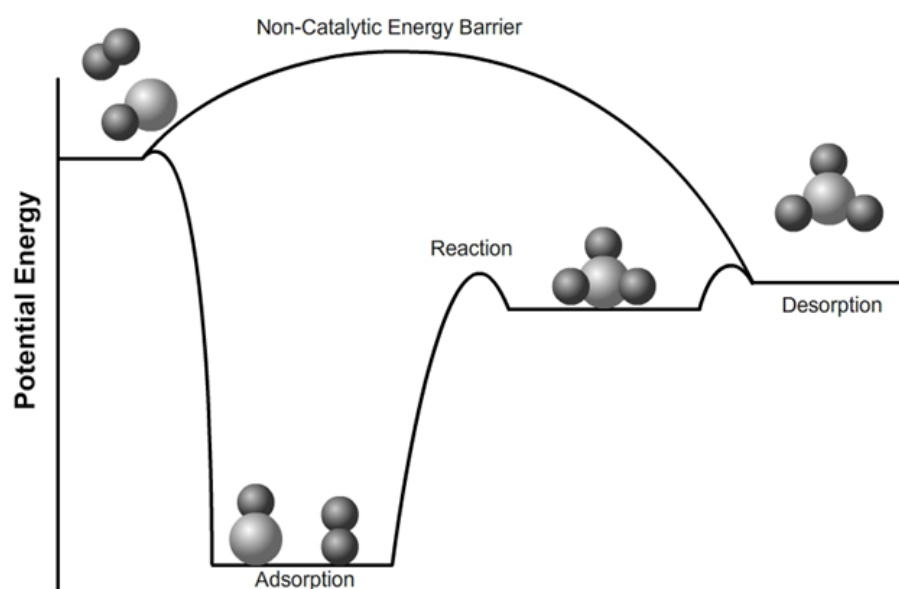


Figure 1.4. A basic energy diagram to show the potential steps that occur in a catalysed reaction²⁵.

1.3. Introduction to hydrogen peroxide.

Hydrogen peroxide is a powerful, environmentally friendly, oxidant that is able to oxidise both inorganic and organic substrates, under mild conditions, and has a number of applications, summarized in Figure 1.5.²⁶

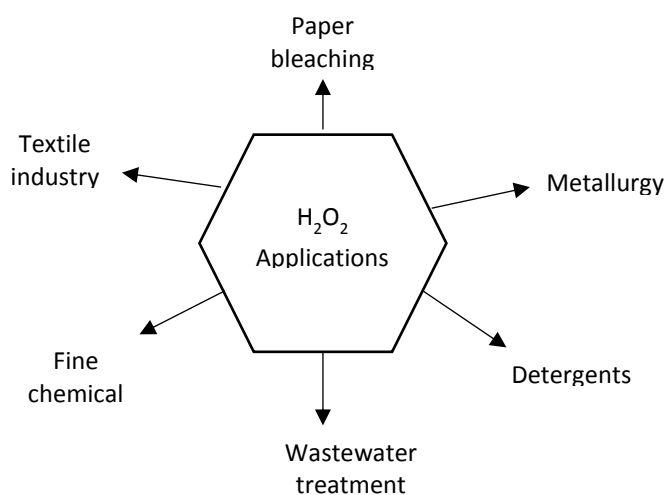


Figure 1.5. Applications of H₂O₂²⁶.

The global production of H₂O₂ is estimated to exceed 2.2 million tons per annum and demand is believed to be growing at a rate of approximately 4 % per annum²⁷. The principal industries that utilise H₂O₂ are the pulp / paper bleaching and textile industries as well as water treatment where it is increasingly superseding chlorine containing oxidants¹¹. In particular it is known that H₂O₂ is able to destroy toxic chemicals present in industrial waste water such as thiocyanate, nitrate and hypochlorite. Furthermore H₂O₂ finds use in mining, in particular in the extraction of gold and uranium¹¹.

H₂O₂ has also been used in many application in the chemical sector, where it is used either directly or indirectly in the production of both organic and inorganic chemicals, such as hydrazine, ferric sulphate, iodic acid and perborates²⁶, while typical uses of H₂O₂ in organic synthesis include epoxidation²⁸, hydroxylation²⁹ and oxidation²⁹.

Furthermore H₂O₂ is considered a reasonably safe chemical when handled in the correct manner and has the additional benefit of being soluble in water as well as a range of organic solvents. Hydrogen peroxides green credentials are well founded since the only by product of its oxidations is water and this, coupled with its nature as a highly effective oxidant, due to its high active oxygen content, has been a contributing factor in the growth in demand for H₂O₂. Indeed H₂O₂ has been reported to be the best single-oxygen donor, next to molecular oxygen²⁶. Owing to its low molecular weight H₂O₂ is a more efficient oxidizing agent than other oxidants, such as sodium hypochlorite. Table 1.1 shows the efficiency of common industrially utilized oxidizing agents.

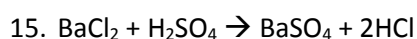
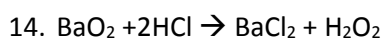
Table 1.1. The oxidizing efficiency of common industrial oxidants.

Oxidant	Active oxygen (% w/w)	By-product
H ₂ O ₂	47.1	H ₂ O
^t BuOOH	17.8	^t BuOH
HNO ₃	25.0	NO _x , N ₂ O, N ₂
NaClO	21.6	NaCl
NaBrO	13.4	NaBr

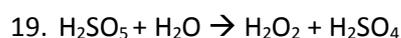
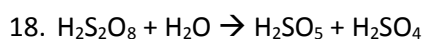
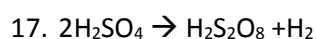
1.4. Historical note and current synthesis method.

The manufacture of hydrogen peroxide can be traced back to its isolation by L .J. Thenard³⁰ in 1818, who reacted barium peroxide with nitric acid to give rise to a low concentration of aqueous hydrogen peroxide. It was discovered that this process can be improved greatly through the use of hydrochloric acid. The hydrogen peroxide is formed in combination with

barium chloride, which is removed by precipitation with sulphuric acid, shown in Equation 14. Thernard's process however had some major drawbacks; firstly only three per cent aqueous hydrogen peroxide solutions were produced using the barium peroxide based process and this led to high production costs and thus limited the market availability. Also the high level of impurities caused the stability of H₂O₂ to be very poor. Thernard's route to H₂O₂ is shown in Equations 14-16.



These difficulties were mostly alleviated when Meidinger discovered in 1853 that hydrogen peroxide could be formed electrolytically from sulphuric acid³¹. The electrochemical production process of aqueous H₂O₂ is seen in Equations 17 - 19.



In 1901 Machot observed that autoxidizable compounds, such as hydroquinones react under alkaline conditions to form peroxides³². Subsequent to the work of Walton and Filson, who proposed the formation of H₂O₂ via alternating oxidation and reduction of hydrazobenzene, Pfleiderer developed a process for the alkaline autoxidation of hydrazobenzenes to produce sodium peroxide. In the Pfleiderer approach sodium amalgam was utilised to reduce the azobenzene³².

Based on the work of Pfleiderer ¹ BASF developed the indirect anthraquinone process (AO process) in between 1939 and 1945, seen in Figure 1.6. This follows a route which involves the hydrogenation of a substituted anthraquinone, dissolved in a suitable solvent mixture at temperatures between 40-50 °C and under a partial pressure of hydrogen of no more than 4 bar. Carrier solutions are used, such as 2-tert-amylanthraquinone and 2-ethylanthraquinone, to yield a 'working' solution. The features of the AO process can be described as follows. A 2-alkylanthraquinone is dissolved in a suitable solvent and is catalytically hydrogenated to the corresponding 2-alkylanthrahydroquinone. The working

solution, containing 2-alkylanthrahydroquinone is then separated from the hydrogenation catalyst, usually palladium or nickel³¹. This is followed by aeration to reform the alkylanthraquinone and also produce hydrogen peroxide; demineralised water is then used to obtain H₂O₂ in a counter current column. The hydrogen peroxide produced is approximately 30 % by weight and distillation techniques are employed to concentrate this to 70 % by weight and also remove impurities³¹.

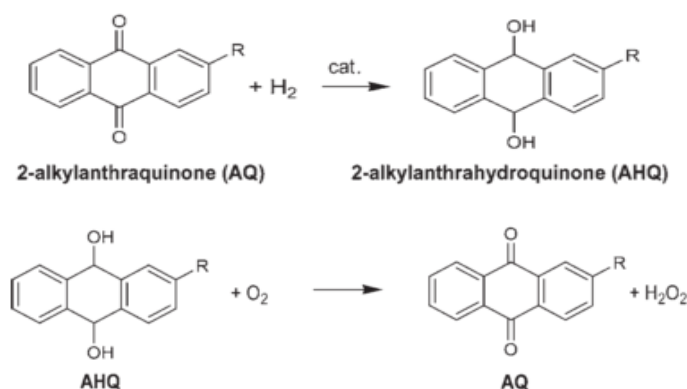


Figure 1.6. The basic reaction scheme of the anthraquinone oxidation process.

The hydrogenation step in the original reduction of alkylanthraquinone employed a Raney nickel based catalysts. However, there were a number of drawbacks associated with this including limited selectivity, rapid deactivation and the pyrophoric nature of Raney nickel. A new generation of amorphous Ni / B³³ and Ni /Cr /B catalysts have been developed, which have proved to show selective carbonyl hydrogenation; hydrogenation of the aromatic rings of alkylanthraquinone is blocked. This is believed to be due to the ability of amorphous alloys to bond tightly with hydrogen.¹⁵ It has been shown that Cr(III) promotes the hydrogenation of carbonyl groups by accepting the lone pair of the oxygen³⁴. This activation favours attack of the carbon of the carbonyl group by dissociated hydrogen, adsorbed on to the nickel catalyst and causes greater selectivity of alkylanthraquinone in comparison to the alkylanthrahydroquinone. The most common catalysts employed in the hydrogenation of alkylanthraquinone are based on palladium, usually supported on Al₂O₃, SiO₂ and Al₂SO₃ / SiO₂²⁶.

The indirect synthesis of hydrogen peroxide has been established on an industrial scale for many decades and as a result has become relatively efficient. However, a number of problems still exist. Firstly there is the inherent risk of using an oxygen-hydrogen gaseous mixture, under high pressure. The flammability limits of hydrogen in oxygen are between 4

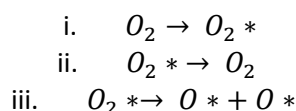
and 94 %¹¹ and therefore it is prudent to use concentrations of hydrogen below 4%, however this can result in decreased hydrogen peroxide yields. The fact that the anthraquinone process is only economically viable for large scale production means that the production of hydrogen peroxide occurs at a particular site, often some distance from where it will be utilised, followed by its transportation. The transport of highly concentrated hydrogen peroxide has associated safety concerns since H₂O₂ can be explosive if allowed to decompose. Furthermore the catalytic reduction of the 2-alkylhydroanthraquinone dictates the need for continual replacement of the 2-alkylanthraquinone, this coupled with the need for continual regeneration of the catalyst represents two significant drawbacks to the AO process.

Even though the anthraquinone process has been made highly efficient its limitations have meant that other routes to the production of hydrogen peroxide are being investigated. This includes the use of photocatalysis³⁵, electrolysis and the direct synthesis route, which strives to produce hydrogen peroxide from hydrogen and oxygen in a 'greener', one hundred per cent atom efficient route, which utilises a less expensive and less toxic solvent system.

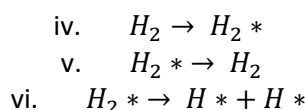
1.5. The proposed mechanism in the direct synthesis of H₂O₂ from H₂ and O₂

It has generally been assumed that the formation of H₂O₂ takes place via a two-step hydrogenation mechanism³⁶⁻³⁹, where a number of side reactions are involved. Possible elementary steps in the formation of H₂O₂ and the competing side reactions are listed below.

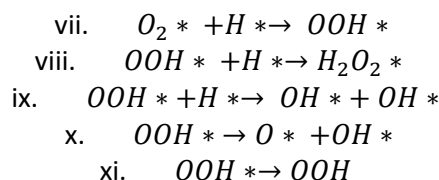
For the reactant O₂:



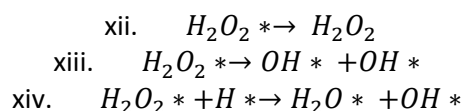
For the reactant H₂



For the intermediate OOH:



For the product H₂O₂:



Where the asterisks (*) represents the surface species on the metal catalyst, the hydrogenation steps vii and viii constitute the main reaction steps for the direct synthesis of H₂O₂. Steps ii, v and xi are the desorption of O₂, H₂ and OOH respectively; and steps iii, vi, xi and xii are the dissociation of O₂, H₂, OOH or H₂O₂. The hydrogenation of OOH in step ix as well as the cleavage of the O-O bond present in the OOH species in step x hydrogenation of OOH leads to the cleavage of the O-O bond and as a result the formation of OH (hydroxyl species), subsequent hydrogenation of the OH species will then result in the formation of

water. Step xiv is the hydrogenation of H_2O_2 to water and an OH group. All these side reactions involve the cleavage of the O-O bond and result in the formation of H_2O .

The comprehensive review by Yoshizawa and Li⁴⁰ reported the improved selectivity observed for a Au-Pd catalyst in comparison to the a mono-metallic Pd only catalyst. Several extremely interesting findings are reported. Firstly, it is suggested that H_2 adsorption and dissociation occurs at the Pd sites, as H_2 dissociation is very facile and almost without an activation barrier. Secondly, on a Au-Pd bimetallic surface O_2 will be located on a top-bridge-top position over one Au and one Pd atom. The formation of H_2O_2 and undesired side reactions can be considered to be a competition between the formation of the O-O bond and the O-M bond (where M is Pd or Au). The O-Pd bond is calculated to be stronger than the O-O bond in the OOH and H_2O_2 species, while the O-Au bond is much weaker, as a result the Au-Pd bimetallic surface shows improved selectivity towards H_2O_2 than a pure Pd surface. However, it should be noted that this is based on the assumption that the more active Pd sites are occupied by dissociated H atoms. The need to maintain the O-O bond is considered key in the formation of H_2O_2 . Lunsford has reported through isotopic labelling that the O-O bond is indeed maintained in the formation of H_2O_2 , while O-O bond cleavage results in the formation of H_2O .

1.6. The palladium based catalyst in the synthesis of hydrogen peroxide.

The direct synthesis of H_2O_2 has long since been a research objective, with the very first patent being filed in 1914 by Henkel and Weber² and until quite recently the investigation of catalysts that may be appropriate for the direct synthesis of hydrogen peroxide have been solely based on palladium. However these earlier investigations utilised H_2 / O_2 mixtures within the explosive range, which has obvious associated dangers, which would be magnified greatly for any commercial operation.

The work of Lunsford^{4,6,41} has shown that palladium supported catalysts show high activity towards the direct formation of hydrogen peroxide, however as with previous studies involving palladium only catalysts the presence of halides is required in order for the catalyst to show high selectivity. Further work by Lunsford^{5,42} has indicated that the high activity of palladium catalysts can be attributed to the formation of colloidal palladium, particularly

when PdCl₂ and Pd / SiO₂ were used as the catalyst. Figure 1.7 shows the formation of colloidal palladium from Pd / SiO₂ catalyst during the direct synthesis process and the catalytic cycle thought to be responsible for the production of hydrogen peroxide⁴³.

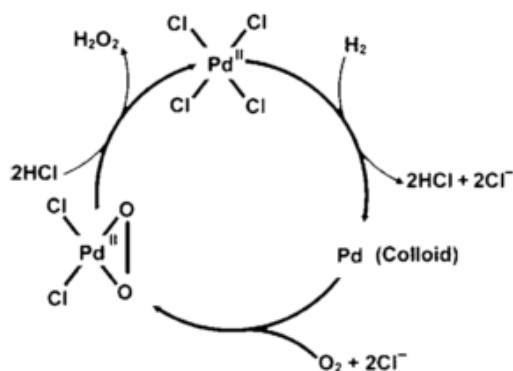
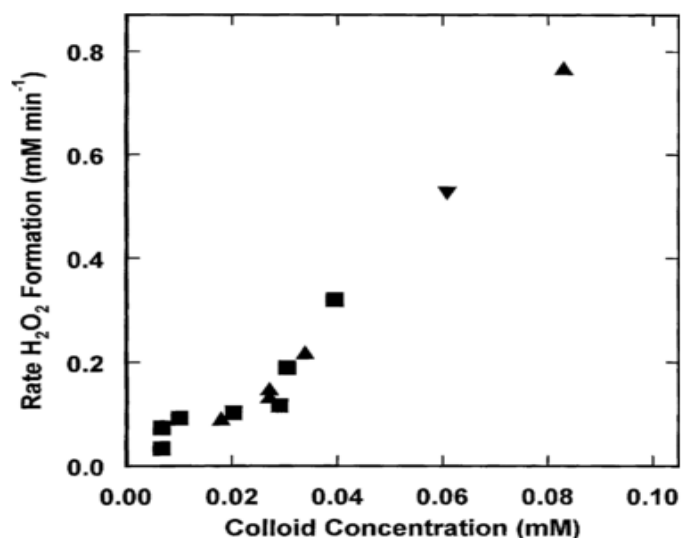


Figure 1.7. The formation of colloidal palladium from a Palladium tetrachloride species⁴³.

In the presence of hydrochloric acid supported metallic palladium has been shown to be initially oxidised to PdCl₄²⁻ ions, these ions are reduced back to metallic palladium by hydrogen, where some of the palladium that is not reduced being present in the colloidal form⁴³. The role of palladium colloids in the catalytic formation of hydrogen peroxide has arisen from two main observations. The first is that the rate of hydrogen peroxide formation did not change after the Pd / SiO₂ catalyst was removed and secondly faster rates were observed when no support was present, when palladium chloride was utilised as the catalyst⁴⁴.

Additionally Lunsford⁴⁴ has shown that the rate of H₂O₂ formation is 'approximately proportional' to the concentration of colloidal palladium, as seen in Figure 1.8. Dissanayke and Lunsford⁴⁴ reported that colloidal palladium is an active phase for the formation of H₂O₂ from H₂ and O₂ in an HCl acidified aqueous medium. As eluded to above the rate of H₂O₂ formation is almost constant for 3-5 hours but after this period the rate of formation and the concentration of H₂O₂ began to decrease. It is appropriate, therefore to consider colloidal palladium as a homogeneous catalyst for the direct synthesis of H₂O₂. This work by Dissanayke and Lunsford⁴⁴ and subsequent work by Chinta and Lusford⁴³ has suggested that the presence of HCl and O₂ facilitated the dissolution of Palladium from Pd / SiO₂ catalysts.



Variation in catalytic activity for H₂O₂ formation as a function of colloid concentration with the colloid being derived from: ■, 10⁻³ M PdCl₂; ▲, 5 wt% Pd/SiO₂(57); ▼, 5 wt% Pd/SiO₂(03).

Figure 1.8. The dependence of hydrogen peroxide rate of formation of colloidal Palladium concentration⁴⁴.

Although colloidal palladium is extremely interesting at a research level it is accepted that it is not suitable for commercial use as the management of the colloid is a difficult task. One of the major drawbacks of colloidal Pd is the short lifetime of the catalyst and a number of attempts to stabilize colloidal Pd, through the use of sodium citrate, poly(vinyl alcohol) and poly(ethylene glycol) have proved to be unsuccessful⁴⁴. In particular the use of PVP stabilized colloidal Pd has shown promise as a catalyst for the Heck coupling reaction⁴⁵.

Choudhary and co-workers^{3,46,47} have also studied palladium based catalysts for the direct synthesis of hydrogen peroxide and they and others have shown that the decomposition of hydrogen peroxide over supported palladium catalysts strongly depends on the oxidation state of the palladium. Supported PdO / C catalysts have been shown to have a much greater selectivity and much lower activity for hydrogen peroxide decomposition (approximately 70 %) than the corresponding Pd⁰ / C catalysts, with decomposition reported to be near 100 % in water^{47,48}. The tendency for H₂O₂ to adsorb onto the Pd⁰ surface rather than that of PdO has been suggested as the reason for the higher selectivity observed for the PdO catalyst⁴⁹.

It is possible to alter the hydrogen peroxide decomposition activity of the Pd⁰ catalysts via oxidative heat treatment, with the formation of PdO it is possible to a more selective catalyst through inhibition of the H₂O₂ decomposition pathway. Often the surface reduction of PdO to Pd⁰ due to the presence of H₂ in the reaction solvent has been attributed as the reason for

the increase in hydrogen peroxide decomposition for these catalysts, even in the presence of protons in the aqueous media, it is the ability of Pd⁰ to form Pd-H intermediate species which is suggested to assist in the decomposition of hydrogen peroxide⁵⁰.

Choudhary *et al.*⁵⁰ have claimed that a PdO catalyst is better suited to be used in hydrogen peroxide synthesis, many others including Lunsford and Chinta⁴³, and Burch and Ellis⁵¹ have claimed that higher hydrogen peroxide productivity and selectivity can be achieved with Pd⁰ catalysts. As PdO is typically reduced in the presence of H₂ it may be expected that, under reaction conditions a mixed oxidation state prevails, with both Pd⁰ and Pd²⁺ present, with both reduced and oxidized Pd providing different selectivity and activity towards H₂O₂. It is suggested that the ratio of these two Pd species is key in producing an active catalyst that is also selective towards H₂O₂.

Hutchings and co-workers have studied palladium catalysts on a variety of supports (Al₂O₃¹², SiO₂⁹, TiO₂¹⁵, Fe₂O₃¹³, MgO⁵², carbon⁵³) and these findings are summarised in Table 1.2. The decomposition and hydrogenation of H₂O₂ have been decoupled and are reported separately. The rate of catalytic decomposition is determined by utilising a known concentration of H₂O₂ (approximately 4 wt %) and a 25 % O₂ / CO₂ atmosphere, this prevents the hydrogenation reaction from occurring. By determination of the concentration of H₂O₂ post reaction it is possible to calculate the activity towards H₂O₂ decomposition. By then investigating the total degradation of H₂O₂ (in a similar manner to that described for H₂O₂ decomposition) through the use of a 5 % H₂ / CO₂ atmosphere it is possible to separate the individual degradation pathways. The carbon supported Pd catalyst was found to be the most effective, providing the greatest productivity (55 mol_{H₂O₂}Kg_{cat}⁻¹h⁻¹) and lowest rate of hydrogenation (135 mol_{H₂O₂}Kg_{cat}⁻¹h⁻¹) as well as a comparatively low rate of decomposition (118 mol_{H₂O₂} Kg_{cat}⁻¹h⁻¹). It is suggested by the authors that the catalytic selectivity is related to the isoelectric point of the supports, with the isoelectric point reported to follow the trend C > TiO₂ > Al₂O₃ > MgO. The relationship between isoelectric point of the support and the degradation of H₂O₂ generally holds with the MgO supported catalyst reported to have the greatest rates of H₂O₂ decomposition and hydrogenation and the greatest isoelectric point. It would be of interest to determine the stability of the MgO. The formation of Mg(OH)₂ may explain the greater rates of H₂O₂ degradation observed for Pd / MgO catalyst as⁵⁵ it is known that H₂O₂ is highly unstable under basic conditions¹¹.

Table 1.2. The efficiency of supported palladium catalysts in the direct synthesis of hydrogen peroxide.

Catalyst	H ₂ O ₂ hydrogenation / mol _{H₂O₂} Kg _{cat} ⁻¹ h ⁻¹ ^a	H ₂ O ₂ decomposition / mol _{H₂O₂} Kg _{cat} ⁻¹ h ⁻¹ ^b	H ₂ O ₂ productivity / mol _{H₂O₂} Kg _{cat} ⁻¹ h ⁻¹ ^c	H ₂ Selectivity / % ^d
Pd/Al ₂ O ₃ ¹²	200	24	9	<i>n.d</i>
Pd/TiO ₂ ¹⁵	288	247	30	21
Pd/MgO ⁵⁴	582	405	29	<i>n.d</i>
Pd/C ⁵⁴	135	118	55	34

Reaction conditions: **a** Rate of hydrogenation of H₂O₂ calculated from amount of H₂O₂ hydrogenated using standard reaction conditions: 2.9 MPa 5 % H₂ / CO₂, 8.5 g solvent (5.6 g MeOH, 2.22 g H₂O and 0.68 g 50 wt. % H₂O₂), 0.01 g catalyst, 2 °C, 1200 rpm, 30 min.

b Rate of decomposition of H₂O₂ calculated from H₂O₂ decomposed using standard reaction conditions: 2.9 MPa 25 % O₂ / CO₂, 8.5 g solvent (5.6 g MeOH, 2.9 g H₂O and 0.68 g 50 wt. % H₂O₂), 0.01 g catalyst, 2 °C, 1200 rpm.

c Rate of hydrogen peroxide production determined after reaction: 5 % H₂ / CO₂ and 25 % O₂ / CO₂, 1 : 2 H₂ / O₂ at 3.7 MPa, 5.6g MeOH, 2.9 g H₂O, 0.01 g catalyst and 1200 rpm).

d Hydrogen selectivity calculated by analysis of the reaction gases before and after reaction using the standard condition.

n.d. = not determined due to low reproducibility.

The dispersion of metal is often a critical aspect in a number of catalytic reactions, including the direct synthesis of H₂O₂. It has been observed by Menegazzo *et.al.*⁵⁶ that to produce an active, yet selective catalyst a compromise must be reached between high metal dispersion to increase catalytic activity and the presence of less energetic sites, where O₂ can adsorb without cleavage of the O-O bond. Further work by this group⁵⁴ has established that a Pd loading, on a SiO₂ support and under mild reaction conditions, of 1.5 wt. % is optimal for catalytic activity and selectivity. Furthermore they establish that the choice of support is key in controlling metal dispersion, with SiO₂ proven to be more efficient than a number of supports including CeO₂ and ZrO₂. It is observed that the mean size of the Pd nanoparticles in the highly selective (approximately 60 %) and active catalyst 1.5 wt. % Pd / SiO₂ catalyst is 5 nm, while the use of CeO₂ or ZrO₂ as a support produces nanoparticles with a mean size of 1 nm. The 1.5 wt. % Pd / CeO₂ and 1.5 wt. % Pd / ZrO₂ catalysts are observed to be much less selective (approximately 45 % for both catalysts). The authors suggest that the presence of smaller (1 nm) Pd nanoparticles, containing more energetic sites are able to chemisorb and dissociate O₂. The resultant atomic oxygen is then key in the formation of water and lowering of catalytic selectivity towards H₂O₂.

Further work by Abate and co-workers⁵⁶ was carried out investigating the effect of particle size on the direct synthesis of H₂O₂. Pd catalysts supported on ceramic asymmetric tubular alumina membranes were prepared by two distinct techniques (i) reduction with N₂H₄ in an ultrasonic bath and (ii) by impregnation deposition resulted in two catalysts with distinct differences in mean particle diameter. The former technique produces metal nanoparticles

with an average particle diameter of 11 nm, while the latter technique produces metal nanoparticles with an average particle diameter of 4nm. Investigation into catalyst selectivity towards H₂O₂ reveals that the samples with the larger Pd nanoparticles shows a higher pseudo-rate constant of direct synthesis of H₂O₂ in comparison to catalysts comprising smaller metal nanoparticles. In addition it is reported that the catalyst comprising larger metal nanoparticles are observed to offer a H₂O₂ combustion rate six times lower than the catalyst with a smaller average particle size.

Ouyang and co-workers⁵⁷ have investigated the role of Pd-PdO domains in the direct synthesis of H₂O₂, when utilising TiO₂ as a support. They report that the composition of surface Pd is a significant factor in determining catalytic selectivity and activity. It is reported that both total metal loading and pre-treatment of the catalyst are key parameters in catalyst design and may be utilised to tune catalyst performance. By lowering total Pd loading from 5 wt. % to 1 wt. % it is possible to improve both selectivity towards H₂O₂ (from 41 to 61 %) and H₂O₂ productivity (from 1.24 to 2.99 mol_{H₂O₂}g_{Pd}⁻¹h⁻¹). Interestingly the size of Pd nanoparticles is reported to stay relatively constant, at approximately 2.5 nm regardless of total metal loading. This improvement in catalytic performance is ascribed partly to the ratio of Pd : PdO. As metal loading is lowered the concentration of PdO on the surface of the nanoparticles is reported to increase. The authors suggest that O₂ preferentially adsorbs onto low co-ordination Pd sites and the presence of the Pd-PdO interface results in a weakening of the interaction between adsorbed O₂ and Pd. This is considered beneficial for improving catalytic selectivity towards H₂O₂.

1.7. Gold based catalysts in the synthesis of hydrogen peroxide.

The catalytic ability of gold has received an ever growing interest, its effectiveness as an oxidation⁵⁸ and hydrogenation⁵⁹ catalyst has found favour in various branches of chemistry. Its uses vary from low temperature oxidation of carbon monoxide⁵⁸ to hydrochlorination of acetylene⁶² and the epoxidation of propylene⁶¹.

Hutchings and co-workers¹² were the first to show that Au catalysts were effective in the direct synthesis of H₂O₂, they provide high selectivity, but relatively low formation rates. When compared to their palladium analogues, using supercritical carbon dioxide as a reaction medium (35 °C, 9.7 MPa) it was found that gold was active in the formation of

hydrogen peroxide. Subsequent experiments, using a water / methanol solvent showed that at lower temperatures (2 °C) hydrogen peroxide synthesis occurs at a higher rate over Au / Al₂O₃ in comparison to Pd / Al₂O₃ supported catalysts⁶², with values of catalytic productivity reported as 1530 mol_{H₂O₂} Kg_{cat}⁻¹h⁻¹ × 10⁻³ and 370 mol_{H₂O₂} Kg_{cat}⁻¹h⁻¹ × 10⁻³ for the Au and Pd / Al₂O₃ respectively. Subsequently Haruta and co-workers⁶³ have shown that Au/SiO₂ catalysts are effective for direct hydrogen peroxide synthesis. They concluded that catalyst activity was related to metal particle size, where calcination had increased Au particle size catalyst activity was found to have decreased. Ishihara⁴² has also demonstrated that gold is an effective catalyst for hydrogen peroxide formation, although the catalyst activity depends on the support used.

In view of these findings Hutchings and co-workers have investigated gold on a range of supports at low temperature using a CH₃OH / H₂O solvent, including Al₂O₃¹², Fe₂O₃¹³, SiO₂¹⁴, TiO₂¹⁵, carbon⁶⁴, zeolite Y and ZSM-5⁶⁵. In addition the use of Cs-exchanged tungstophosphoric acid has also been investigated as a support for Au⁶⁶. Comparison of gold on these various supports, summarized in Table 1.3, has shown that these catalysts have very little activity towards the synthesis of H₂O₂, compared to their palladium analogues, under the reaction conditions used. Furthermore gold supported catalysts have been shown to have lower hydrogen peroxide degradation rates than the analogous Pd catalysts.

Comparison of supported mono-metallic Au and Pd catalysts is observed in Table 1.4. Interestingly the 5 wt. % Au / Cs_{2.8}H_{0.2}PW₁₂O₄₀ catalysts offers lower H₂O₂ hydrogenation rates than the bare support, with the rate of H₂O₂ hydrogenation of the Cs_{2.8}H_{0.2}PW₁₂O₄₀ support reported as 162 mol_{H₂O₂}Kg_{cat}⁻¹h⁻¹ and that of the 5 wt. % Au / Cs_{2.8}H_{0.2}PW₁₂O₄₀ catalyst reported as 103 mol_{H₂O₂}Kg_{cat}⁻¹h⁻¹. This suggests that the incorporation of Au onto the support blocks sites responsible for this reaction.

Table 1.3. The efficiency of supported Gold catalysts in the direct synthesis of hydrogen peroxide.

Catalyst	H ₂ O ₂ Hydrogenation / mol _{H₂O₂} Kg _{cat} ⁻¹ h ⁻¹	H ₂ O ₂ decomposition / mol _{H₂O₂} Kg _{cat} ⁻¹ h ⁻¹	H ₂ O ₂ productivity / mol _{H₂O₂} Kg _{cat} ⁻¹ h ⁻¹
5 %Au/Al ₂ O ₃	229	18	2.6
5% Au/ TiO ₂ ⁶⁷	71	24	7
5% Au/MgO ¹⁶	100	12	0
5% Au / C ¹⁶	0	0	1
4.3 % Au / Zeolite Y ⁶⁶	<i>n.d.</i>	<i>n.d.</i>	2.99
4.3% Au / ZSM-5 ⁶⁸	<i>n.d.</i>	<i>n.d.</i>	1.75
5% Au / CS _{2.8} H _{0.2} PW ₁₂ O ₄₀ ⁶⁶	103	<i>n.d.</i>	14

Reaction conditions: As outlined in Table 1.2.**n.d.** = not determined.**Table 1.4.** Comparison of mono-metallic Au and Pd catalysts towards the direct synthesis and degradation of H₂O₂.

Catalyst	H ₂ O ₂ hydrogenation/ mol _{H₂O₂} Kg _{cat} ⁻¹ h ⁻¹	H ₂ O ₂ decomposition /mol _{H₂O₂} Kg _{cat} ⁻¹ h ⁻¹	H ₂ O ₂ productivity/ mol _{H₂O₂} Kg _{cat} ⁻¹ h ⁻¹
5 %Pd/TiO ₂ ⁶⁷	288	247	30
5% Au / TiO ₂ ⁶⁷	71	24	7
5% Pd / MgO ¹⁶	582	405	29
5% Au / MgO ¹⁶	100	12	0
5% Pd / C ¹⁶	135	118	55
5 % Au / C ¹⁶	0	0	1
5% Pd / CS _{2.8} H _{0.2} PW ₁₂ O ₄₀ ⁶⁶	281	<i>n.d.</i>	136
5% Au / CS _{2.8} H _{0.2} PW ₁₂ O ₄₀ ⁶⁶	103	<i>n.d.</i>	14

Reaction Conditions: As outlined in Table 1.2.**n.d.** = not determined.

Ishihara *et al.*⁶⁹ have studied various Au supported catalysts in the direct synthesis of hydrogen peroxide. It was concluded that the catalysts that offered the most promise were Au / SiO₂ and Au / Cu₂O, with Au / SiO₂ exhibiting the smallest decomposition activity, and

the greatest activity towards hydrogen peroxide synthesis. These findings are at odds somewhat with those of Hutchings and co-workers¹⁵ who have reported that TiO₂ is the most effective support for Au in the synthesis of hydrogen peroxide. However the reaction conditions of these studies were different and this may indicate the sensitivity of the reaction to the conditions in which it takes place.

1.8. Bimetallic catalysts for the direct synthesis of hydrogen peroxide.

The observation that Au-Pd bimetallic catalysts showed greater hydrogen peroxide productivity than either monometallic catalysts was initially reported by Hutchings and co-workers^{15, 53, 70} and subsequent work on Au-Pd on a range of supports has indicated that a synergistic effect is observed when both metals are combined on the same support. As noted by Hutchings and co-workers^{12, 13, 15} supported Au-Pd (1:1 by wt. %) catalysts produced significantly more H₂O₂ than the mono-metallic Au and Pd catalyst. With the surface ratio of Au : Pd reported to increase to 1 to 7 upon calcination, as determined by XPS⁷¹. This is associated with the development of Au-core PdO-shell nanoparticles

Further studies by Han *et.al*⁷² have reported that there is an optimum Au- Pd composition (Au : Pd ~ 1.5 : 1) where rate of formation is much greater than for either the gold only or palladium only supported catalysts. In this study the rate of H₂O₂ formation reaches a maxima at a Au : Pd ratio of 1.5 : 1 but then decreased by approximately 50 % as Au : Pd ratio increased to 3.4 : 1. However, selectivity towards H₂O₂ increases slightly as the catalyst becomes more Au-rich; from 59 to 62 % as the Au : Pd ratio increases from 1.5 : 1 to 3.4 : 1. The authors suggest that both the modification of the electronic structure of Pd by Au as well as reconstruction of the surface composition, for example, by tuning the Pd-Pd bond length are responsible for the enhanced selectivity towards H₂O₂. For the first case, it is suggested that there is a transfer of electrons from the s and p orbitals of the Au to the Pd d orbitals and the resulting transfer of negative charge alters the catalytic properties of Pd. For example by suppression of O-O bond cleavage, known to lead to the formation of H₂O. For the second case, there is a significant loss of surface Pd, resulting in an increase in selectivity towards H₂O₂ by inhibition of the various H₂O₂ degradation pathways.

Gudarzi *et al.*⁷³ have investigated the promotive effect of Au in Au-Pd bimetallic catalysts supported on activated carbon cloth for activity towards the synthesis of H₂O₂. They report that by increasing Au : Pd ratio from 1 : 4 to 1 : 2 it was possible to improve selectivity towards H₂O₂ from 47 % to 63 %. However catalytic activity toward H₂O₂ drops significantly from 1025 mol_{H₂O₂}Kg_{cat}⁻¹h⁻¹ for the Pd-rich catalyst to 514 mol_{H₂O₂}Kg_{cat}⁻¹h⁻¹ for the Au-rich catalyst.

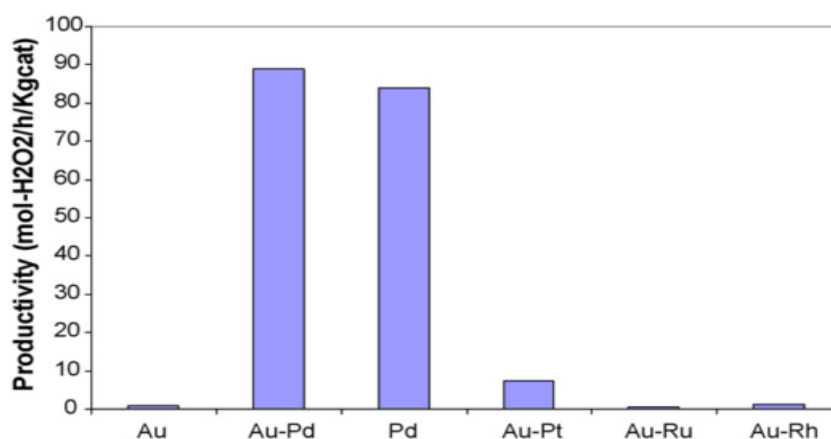
Interestingly it has been reported by Hutchings and co-workers¹² that Au-Pd supported catalyst are effective in the formation of hydrogen peroxide without the presence of acid and halide ions, in a water medium. This is due to the choice of reaction conditions, where CO₂ is utilized as the reaction gas diluent, initially in order to ensure that hydrogen is kept below its explosive limits but it has been discovered since that CO₂ acts as an in-situ acid promoter. It is suggested any commercial application of hydrogen peroxide is likely to favor a water medium in comparison to an organic one and so this is considered to be an important discovery in the development of bimetallic catalysts.

Choudhary and co-workers⁷⁴ have compared the effect that various noble metal additives have on supported palladium catalysts in the direct synthesis of hydrogen peroxide. It was reported that the addition of Au to Pd improved the conversion of hydrogen, from approximately 35 % (when no Au is present) to a maxima of 50 % when a Au : Pd ratio of 0.11 is investigated. As well as an improvement in H₂ conversion there is an increased rate of H₂O₂ synthesis, however the optimal Au : Pd ratio for H₂O₂ synthesis is observed to be approximately 0.02, beyond this ratio the yield of H₂O₂ decreases.

The investigation also established that platinum may also be used as an additive in palladium catalysts, with increasing platinum content the yield of H₂O₂ rose to a maxima of 15 % when a Pt : Pd ratio of approximately 0.02 was utilized. It is important to note that the initial increase in hydrogen peroxide yield was lower than that seen for the corresponding Au-Pd catalyst. In addition it is noteworthy to mention that hydrogen peroxide yield at higher platinum concentrations decreased below that of monometallic palladium catalysts and this was attributed to the increase in hydrogen peroxide decomposition activity and decreasing stability of the hydroperoxy precursor.^{51,74} The authors suggest that the improvement observed when Au is used in addition to Pd is due to the ability of Au to form stable hydroperoxy (OOH) species, which is considered to be the precursor for H₂O₂. This decreased stability has been linked to greater ability of platinum to catalyse O-O bond breaking⁵¹.

Finally it was reported by Hutchings⁶⁰ that the incorporation of ruthenium and rhodium into palladium supported catalyst was detrimental to hydrogen peroxide yield. These Ru-Pd and Rh-Pd catalysts show an increase in hydrogen conversion with increasing metal content, however there is also a corresponding rise in hydrogen peroxide decomposition.

As can be seen in Figure 1.9 the addition of both Pt and Pd to Au improves productivity over the monometallic Au catalyst, while the incorporation of Ru or Rh into a Au catalyst does not improve catalytic productivity.



Performance of 2.5 wt.% metal/Y for the synthesis of H₂O₂, the 2.5 wt.% Au and Pd catalysts are also shown. Reaction condition: Methanol 5.6 g, water 2.9 g, catalyst 10 mg, 5% H₂/CO₂ 420 psi, 25% O₂/CO₂ 150 psi, temperature 2 °C, reaction time 0.5 h.

Figure 1.9. The effect of metal additives in the productivity of catalyst towards H₂O₂.⁶⁰

Further comparison between Pd-Au and Pd-Pt catalysts supported on the macroreticular ion-exchange resin Lewatit K2621 has been conducted by Sterchele *et al.*⁷⁵. It is reported that the addition of Au to Pd to produce a 0.25 wt. % Au – 1 wt. % Pd / K2621 catalyst improves catalytic selectivity towards H₂O₂ from approximately 65 % for the 1 wt. % Pd / K2621 catalyst to approximately 75 % for the 0.25 wt. % Au – 1 wt. % Pd / K2621 catalyst. In comparison the addition of 0.25 wt % Pt to the 1 wt. % Pd / K2621 catalyst lowers catalytic selectivity towards H₂O₂ to approximately 38 %. The authors suggest that the improvement in catalytic selectivity observed for the 0.25 wt. % Au – 1 wt. % Pd / K2621 catalyst is a result of increased average nanoparticle size. It is reported that average nanoparticle diameter increases from 4.6 nm for the 1 wt. % Pd / K2621 catalyst to 11 nm for the 0.25 wt. % Au – 1 wt. % Pd / K2621 catalyst, while the addition of Pt to Pd decreases average nanoparticle diameter to 3.3 nm for the 0.25 wt. % Pt - 1 wt. % Pd / K2621 catalyst. It is suggested that these smaller metal nanoparticles have greater activity for the cleavage of the O-O bond resulting in the

formation of H₂O. As such catalytic selectivity towards H₂O₂ is greatest over the larger Au-Pd nanoparticles

Zhang and co-workers⁷⁶ have investigated Pd-Ag catalysts supported on activated carbon for the direct synthesis of H₂O₂, they demonstrate that the presence of Ag prevents the degradation of H₂O₂ and improves catalytic selectivity through increasing the concentration of surface PdO. The enhanced selectivity of PdO over Pd has previously been demonstrated by Choudhary et.al.⁴³ and is discussed in Section 1.6. In addition Zhang and co-workers⁷⁶ ascribed the increase in selectivity to electronic interactions between Pd and Ag in addition to inhibition of H₂ and O₂ adsorption by coverage of the Pd surface by Ag. By optimizing the ratio of Pd : Ag it is possible to improve catalytic selectivity towards H₂O₂ from 54 to 71 % for the monometallic Pd and the optimized Pd-Ag (PdAg₄₀, with Pd : Ag of approx. 40 : 1) supported catalyst respectively.

Gudarzi *et.al.*⁷⁷ have shown that the selectivity towards H₂O₂ as well as H₂O₂ yield of catalysts containing both Au and Pd on a carbon support is higher than Pd / C catalyst, however it has also been demonstrated that the Au / C catalyst offers greater selectivity than either the pure palladium or bimetallic catalysts. While on the basis of yield of hydrogen peroxide the Au-Pd / C catalyst is shown to be the most efficient.⁷⁸

For any large scale application of the direct synthesis process, catalyst cost is an important factor that must be considered and any reduction in cost, while maintaining efficiency would be of great benefit. The replacement of costly precious metals such as Au or Pd with readily abundant, less costly base metals would offer significant savings upon scaling of the process to an economically viable size. Hutchings and co-workers⁸⁰ have recently reported a series of Pd-base metal catalysts, which are completely selective towards the direct synthesis of H₂O₂. Through successive heat treatments it has been shown that the degradation of H₂O₂ can be completely inhibited. The detailed investigation of a 3 wt. % Pd – 2 wt. % Sn / TiO₂ catalyst that has been exposed to this optimized heat treatment cycle has yielded an approach that is believed to be applicable to a number of other Pd- base metal combinations, including Ni, Zn, Ga, In and Co.

Hutchings and co-workers⁷⁹ have provided much evidence that after an oxidation – reduction – oxidation (O-R-O) heat treatment the small Pd-rich nanoparticles responsible for H₂O₂

degradation are encapsulated into a SnOx layer limiting catalytic activity towards H₂O₂ destruction, possibly by reducing the availability of low coordination Pd edge sites. The larger uncovered Pd-Sn alloy nanoparticles are believed to be responsible for the formation of H₂O₂. Through this O-R-O treatment it is possible to produce a catalyst that is highly selective, stable and active; all key criteria for any possible industrial application. As can be seen in Figure 1.10 there is no loss of activity with sequential catalyst use; that is the replacement of reactant gas and it is possible to achieve relatively high concentrations of H₂O₂ through subsequent reactions. For any commercial application catalyst activity must be stable over multiple uses and offer high selectivity towards H₂O₂ and the 3 wt. % Pd – 2 wt. % Sn / TiO₂ catalysts reported by Hutchings and co-workers fulfill both of these requirements and may form the basis of any large scale development of the direct synthesis of H₂O₂.

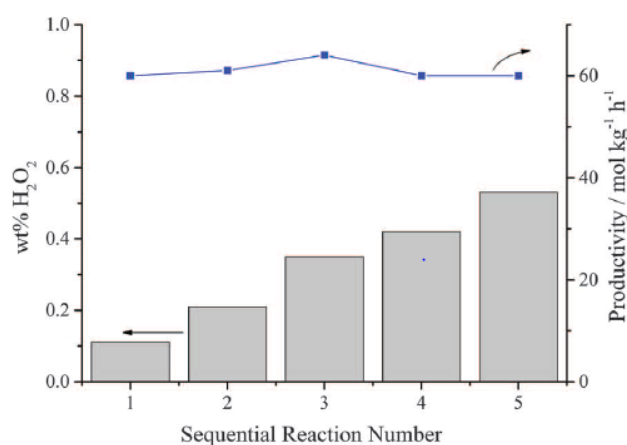
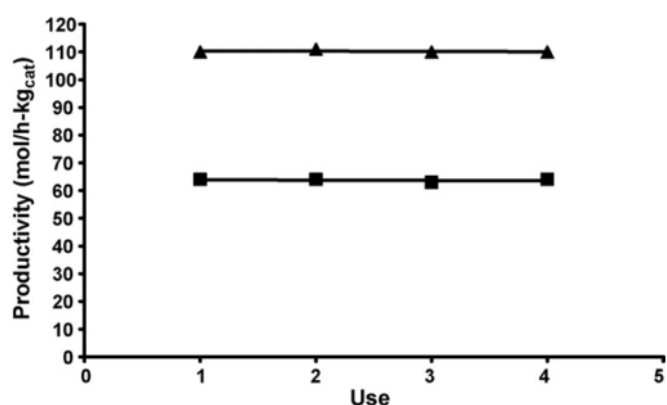


Figure 1.10. Sequential H₂O₂ synthesis reactions utilising a Sn-Pd / TiO₂ catalyst subjected to optimised O-R-O heat treatment.⁷⁹

1.9. The effect of the calcination process on the effectiveness of bimetallic catalysts in the direct formation of hydrogen peroxide.

It has been observed⁶² that the effect of calcination is vital for ensuring catalyst stability and re-usability, which is a key economic and environmental aspect. Uncalcined bimetallic catalysts offer greater activity towards hydrogen peroxide synthesis and high hydrogen conversions are observed for these catalysts. However these catalysts are intrinsically unstable and it is possible that the active metal components may leach from the catalyst support and reportedly approximately 90 % of the active metal component is lost upon a second use of the catalyst.⁸⁰ Interestingly this has been attributed as the reason for the higher activity of the uncalcined catalysts as a homogeneous catalyst is formed.¹⁶ In

comparison to their uncalcined counterparts those catalysts calcined at 400 °C offer greater stability and are still active after a number of uses as seen in Figure 1.11. Indeed it has been reported that catalysts have been used up to ten times without loss of performance and without leaching of any of the active metals. The role of calcination has been further investigated by Menegazzo *et.al.*⁵⁵ who report the calcination step is mandatory for the production of a stable catalyst.

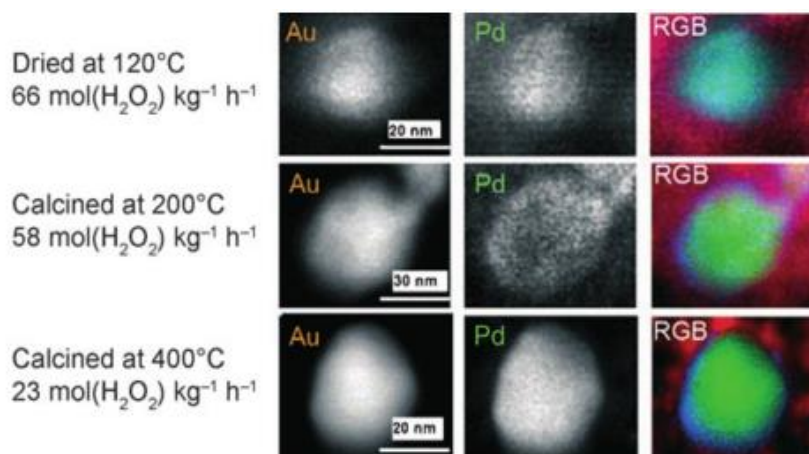


Productivity of hydrogen peroxide with the number of uses for catalysts calcined in air at 400 °C. TiO₂ (■), Aldrich G60 carbon (▲).

Figure 1.11. The effect of the calcination process in maintaining catalytic efficiency for 2.5 wt. % Au -2.5 wt. % Pd / TiO₂ (squares) / C (triangles) towards the direct synthesis of H₂O₂.¹⁶

Interestingly as calcination temperature increased the activity of the bimetallic Au-Pd catalysts supported on Al₂O₃ and TiO₂ decreased while the activity of the SiO₂ supported catalyst showed an increase with calcination temperature up to 300 °C. However at a calcination temperature of 400 °C the catalyst became drastically less active and this has been ascribed to the sintering of the nanoparticles,¹⁶ thus producing larger nanoparticles.

The development of larger metal nanoparticles has been suggested to be the attribute responsible for lower catalytic activity, with larger particles being associated with lower activity, both towards H₂O₂ synthesis and hydrogenation / decomposition.⁸¹ As can be seen from the HAADF image in Figure 1.12, of 2.5 wt. % Au - 2.5 wt. % Pd / Al₂O₃, as calcination occurs and then the temperature of calcination increase the morphology of the Au-Pd alloys moves from a homogeneous alloy, seen in the dried sample, to a core-shell structure when calcined, with a PdO-rich shell and an Au rich core. This morphology has been reported on a number of oxide supports, while it has been demonstrated that the metal nanoparticles on a carbon support exhibit a random alloying, rather than core-shell morphology.



HAADF (high angle annular dark field) image showing development of the core-shell structure in 2.5 wt% Au-2.5 wt% Pd/Al₂O₃ catalyst.

Figure 1.12. The development of core-shell morphology with calcination temperature.⁸¹

Cybula *et al.*⁸² have investigated the effect of calcination temperature on TiO₂ modified with Au-Pd, they report that as calcination temperature increased from 350 to 700 °C the surface Pd to Au ratio changes from 5 : 1 to 1 : 4, as well as led to an increase in nanoparticle size. This is particularly interesting as it suggests catalyst activity can be tuned through the use of calcination temperature. It is reported that as calcination temperature increases the nanoparticles move from a Au core – PdO shell morphology to an island like structure, with areas of different composition. Figure 1.13 follows the effect of calcination temperature on the Au-Pd nanoparticles via HAADF combined with elemental mapping. It is possible to observe the development of the Au-enriched surface as calcination temperature increases. It is suggested that the gold-enrichment in the shell region of the Au-PdO bimetallic nanoparticle observed by the authors may allow for the design of more selective catalysts for the direct synthesis of H₂O₂.

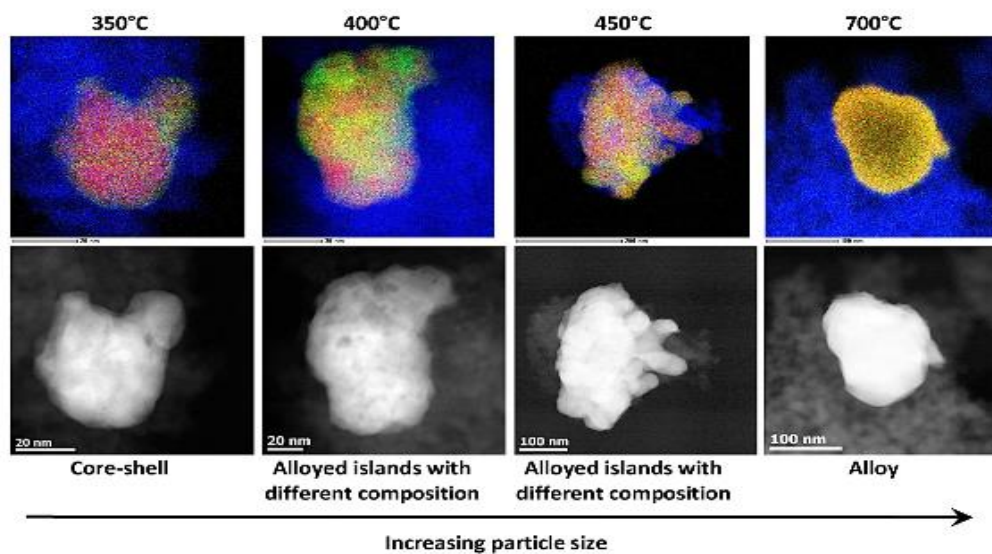


Figure 1.13. HAADF images combined with elemental mapping of Au-Pd modified TiO₂. Au (red), Pd (green) and Ti (blue) calcined at 350 400 and 700 °C.⁸²

1.10. Particle morphology in bimetallic Au-Pd supported catalysts.

It has been reported that the calcination process aids in the alloying of Au and Pd¹⁶ and so it was of interest to determine the nature of the metals in the Au - Pd supported catalysts, that is if the metal components existed separately or as an Au-Pd alloy and a number of studies have been undertaken to determine this.⁸¹

It is possible to collect the various supports into two groups; the metal oxides and carbon, with a difference in morphology of the metal nanoparticles seen between these two. The metal oxide supported catalysts have been shown to exhibit core-shell structures with PdO-rich shells and Au-rich cores^{16, 80, 83} upon calcination. Although it should be noted that the silica supported catalyst morphology is yet to be determined. Findings from Hutchings and co-workers have shown this to be the case when comparing 2.5 wt. % Au – 2.5 wt. % Pd / TiO₂ and 2.5 wt. % Au – 2.5 wt. % Pd / carbon catalysts and, further studies of Au-Pd nanoparticles supported on Fe₂O₃ and Al₂O₃ provide further evidence^{12,13,83,84}. They have shown that the effect of calcination and also calcination temperature on Au-Pd nanoparticle morphology. A systematic series of Au-Pd / Al₂O₃ samples, exposed to various heat treatments were studied by STEM-XEDS imaging. From this data it was possible to determine that the uncalcined (dried at 120 °C) catalyst shows homogeneous Au-Pd nanoparticles while the calcined samples indicate the development of the PdO rich shell, Au rich core morphology and this is seen in Figure 1.12. Hutchings suggests that the preferential

formation of Pd-O bonds at the alloy surface is responsible for palladium surface segregation within the alloy nanoparticles.⁸¹

The surface of these core-shell structures however will not consist entirely of palladium, as is the case with the 2.5 wt. % Au – 2.5 wt. % Pd / Al₂O₃ catalyst investigated. If this was true only the activity of the palladium will be observed and this does not occur. In comparison the carbon supported Au-Pd catalyst was shown to retain the random homogeneous alloy nature of the nanoparticles.⁸⁰

The dried only TiO₂ and SiO₂ supported catalysts exhibit an Au:Pd surface ratio (by weight) considerably different from the bulk value of 1:1, in comparison the surface ratio for the carbon and Al₂O₃ supported catalyst is similar to that of the bulk. It has been observed that upon calcination at 400 °C the surface of AuPd catalysts supported on SiO₂, TiO₂ and Al₂O₃ catalyst surface become enhanced in palladium in a manner consistent with the formation of core-shell structures. It has been suggested that the adoption of this core-shell morphology is responsible for the enhancement in the stability of the catalyst upon calcination at 400 °C⁵⁰ and the formation of core shell structures is believed to be due to the preferential formation of PdO over Au₂O₃ in temperatures of approximately 400 °C which in turn may be responsible for palladium surface segregation⁸⁵.

Hutchings and co-workers⁸¹ have suggested that the spontaneous formation of the core shell morphology of Au-Pd catalyst supported on oxide supports is due to the oxidation efficiency of the support surface. As carbon is a reducing support the process of core-shell formation, which is attributed to the formation of PdO species and subsequent surface segregation is deterred.

Figure 1.14 compares the morphology of the Au-Pd nanoparticles on oxide supports to that observed on carbon. It can be seen that upon calcination of the oxide supported catalysts at a temperature of 400 °C, in static air, the Au-core PdO-shell morphology develops. While when a carbon supported Au-Pd catalyst undergoes heat treatment the random homogeneous alloys present upon drying are retained⁸⁰.

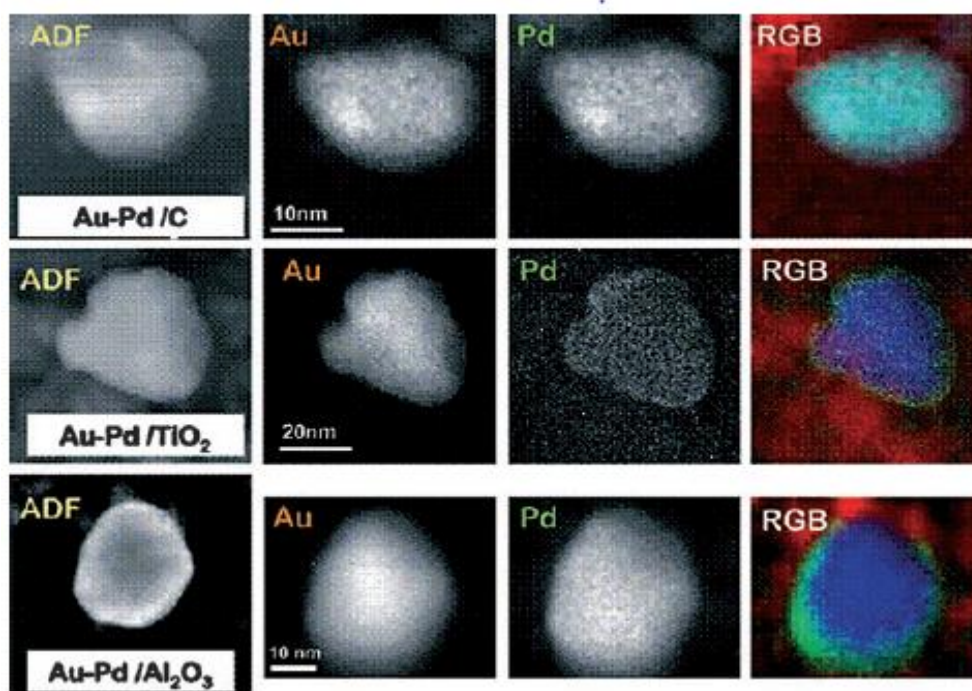


Figure 1.14. Montage of HAADF images (column 1) Au map (column 2), Pd map (column 3) and GF reconstructed overlay map (column 4; Au blue, Pd green) for calcined AuPd/C (row 1) calcined AuPd/TiO₂ (row 2) and calcined AuPd/Al₂O₃ (row 3).⁸⁰

Interestingly the carbon supported Au-Pd catalyst was shown to exhibit a tri-modal particle distribution⁸¹ although all particles were Au-Pd alloys. The smallest particles fell in the range 2-5 nm, the intermediary particles between 10 and 20 nm and the larger particles were greater than 100 nm in diameter, although particles of this size were uncommon. However, the particles do exhibit a change in the Au : Pd ratio, however as particle size increases the Pd : Au ratio decreases. The particles between 10-20 nm show the greatest similarity to the Au : Pd surface ratio exhibited by those supported on TiO₂ and SiO₂.⁸¹

Rossi and co-workers⁸⁶ have investigated the behavior of Au-Pd core-shell nanoparticles in the selective oxidation of benzyl alcohol. A significant improvement in catalytic conversion is observed when using a 10 : 1 (Au : Pd) ratio, a composition corresponding to the amount of Pd required to cover the existing Au cores with a monolayer of Pd. Density functional theory calculations indicate that both the number of active sites and the ease of product desorption is sensitive towards Pd content. It is suggested that these findings may prove significant for further development of Au-Pd catalysts for the direct synthesis of H₂O₂.

Further investigation into Au – Pd catalysts supported on SiO₂ by Strukul and co-workers⁸⁸ has revealed that the choice of catalyst preparation technique is able to improve selectivity

towards H₂O₂. Comparison of incipient wetness co-impregnation and consecutive incipient wetness impregnation reveals that the former technique is able to produce catalysts with greater activity and selectivity towards H₂O₂. Indeed catalytic selectivities for the co-impregnation and consecutive impregnation are reported as 53 % and 47 % respectively. The authors report that the choice of preparation technique can induce different metal interactions as well as different particle morphologies, with preparation via the co-impregnation technique providing mixed Au-Pd alloyed nanoparticles, where the presence of Au is able to enhance the formation of PdO. In comparison preparation of catalysts utilizing consecutive incipient wetness impregnation does not give rise to these mixed metal nanoparticles and as a result Pd is found to be present in the metallic Pd⁰ oxidation state. It is suggested that the presence of the AuPdO phase is able to ensure the availability of less energetic catalytic sites necessary to activate the O₂ molecule without cleavage of the O-O bond.

1.11. The role of the support in the direct synthesis of H₂O₂.

A variety of supports have been utilised in the direct synthesis of hydrogen peroxide from hydrogen and oxygen. The state of the support shows discernible influence on the formation of hydrogen peroxide as well as competing routes, particularly the hydrogenation of hydrogen peroxide and combustion of hydrogen. The performance of the supported catalyst is generally governed by several factors, including metal particle size, shape, morphology, the dispersion of the metal particles and the electronic state of the support¹¹. However Choudhary and co-workers⁷⁴ have shown that particle size and surface area of palladium-only catalyst are less important than the oxidation state in determining hydrogen peroxide selectivity.

The most common supports that have been studied for the direct synthesis of hydrogen peroxide are carbon, silica, alumina, silica-alumina and titanium dioxide has been studied.^{89,90} The reactivity of varying supports for Au-Pd supported catalysts has been investigated and the order of reactivity has been found to be carbon > TiO₂ > SiO₂ > Al₂O₃ > Fe₂O₃. Interestingly Ishihara *et.al.*⁹⁰ have demonstrated that gold-palladium catalysts supported on TiO₂ with the rutile structure offers greater selectivity and activity towards hydrogen peroxide synthesis than either the anatase-TiO₂ or mixed rutile and anatase P-25-TiO₂ support. It is also revealed that the surface composition of active components and metal

particle morphology play a more important role in governing catalysts activity and selectivity in comparison to surface area of the support. Evidence for this came from comparison of P-25-TiO₂ and rutile-TiO₂ as supports for gold-palladium catalysts. The rutile-TiO₂ has a significantly smaller surface area than the mixed analogue but was seen to be more active for hydrogen peroxide formation.

It has been shown that the presence of acidic reaction conditions has beneficial effects of the catalyst with regards to H₂O₂ yield.⁹¹ Furthermore it has been reported that accelerated reactor corrosion is a concern when using acidic additives. Therefore acidic supports, with lower isoelectric points, are receiving attention as a potential replacement for the more common supports.

The isoelectric point of the support has been shown to be an important factor for hydrogen peroxide synthesis⁸³, with supports with a lower isoelectric point offering the highest rate of H₂O₂ synthesis and lowest rate of hydrogen peroxide decomposition and hydrogenation. It is known that the support's isoelectric point controls its surface charge, and as basic supports favor the hydrogenation of hydrogen peroxide⁸³ it is preferential to utilize supports of a more acidic nature in the direct synthesis of hydrogen peroxide. Indeed the rate of H₂O₂ hydrogenation and decomposition has been reported at 206 and 217 molKg_{cat}⁻¹h⁻¹ for the MgO support alone, prior to the impregnation of metals, such as Pd and Au.⁸³ Table 1.5 compares the activity of various supports, with no metal incorporation towards H₂O₂ synthesis and degradation. According to these findings supports of carbon and silica should give catalyst that provides the greatest rate of synthesis of H₂O₂, with productivity values of 110 mol_{H₂O₂}Kg_{cat}⁻¹h⁻¹ reported for 2.5 wt. % Au – 2.5 wt. % Pd / C catalyst; while TiO₂, with an isoelectric point of approximately 6.5 is reported to have a productivity value of 64 mol_{H₂O₂}Kg_{cat}⁻¹h⁻¹.⁶⁸

Table 1.5. Comparison of the activity of various supports to the direct synthesis and degradation of H₂O₂.

Support	H ₂ O ₂ hydrogenation/ mol _{H₂O₂} Kg _{cat} ⁻¹ h ⁻¹	H ₂ O ₂ decomposition /mol _{H₂O₂} Kg _{cat} ⁻¹ h ⁻¹	H ₂ O ₂ productivity/ mol _{H₂O₂} Kg _{cat} ⁻¹ h ⁻¹
Al ₂ O ₃ ¹²	0	0	0
TiO ₂ ¹⁵	0	0	0
MgO ⁸²	206	217	0
Carbon ⁸²	94	24	0
CS _{2.8} H _{0.2} PW ₁₂ O ₄₀ ²²	162	<i>n.d.</i>	1

Reaction Conditions: As outlined in Table 1.2.**n.d.** = not determined

Hutchings initial discovery of the synergistic effect and subsequent advantages of Au-Pd supported catalysts has led to extensive study of this catalytic system in particular those catalysts on carbon⁸ and oxide supports have received much attention (Al₂O₃¹², SiO₂⁵³ TiO₂¹⁵ Fe₂O₃¹³ and MgO⁵²) as well as Zeolite-Y and HZSM-5⁶⁵, the results of which are summarized in Table 1.6. It was found that carbon⁵² was the best support, providing the highest hydrogen peroxide productivity and lowest rates of hydrogenation and decomposition.

Table 1.6. Effect of the support on hydrogenation, decomposition and synthesis over Au-Pd catalysts.

Catalyst, 5 wt. %	Hydrogenation / mol _{H₂O₂} Kg _{cat} ⁻¹ h ⁻¹ <i>a</i>	Decomposition / mol _{H₂O₂} Kg _{cat} ⁻¹ h ⁻¹ <i>b</i>	Productivity / mol _{H₂O₂} Kg _{cat} ⁻¹ h ⁻¹ <i>c</i>	H ₂ Selectivity / (%) ^d
1 : 1 (Au : Pd)				
Au-Pd/Al ₂ O ₃ ¹²	452	59	15	14
Au-Pd/TiO ₂ ¹⁵	235	129	64	70
Au-Pd/MgO ⁵²	817	535	29	38
Au-Pd/C ⁵	117	41	110	80
Au-Pd /γ ⁶⁵	<i>n.d.</i>	<i>n.d.</i>	89	<i>n.d.</i>
Au-Pd / HZSM- 5 ⁶⁵	<i>n.d.</i>	<i>n.d.</i>	52	<i>n.d.</i>

Reaction Conditions: As outlined in Table 1.2.**n.d.** = not determined.

Figure 1.15 compares the isoelectric point of the supports, catalytic productivity and hydrogenation activity for bimetallic 2.5 wt. % Au- 2.5 wt. % Pd supported catalysts. There is an inverse correlation between the rates of H₂O₂ production and hydrogenation and bimetallic catalysts that have a high rate of H₂O₂ synthesis have a low rate of hydrogenation and decomposition. From Figures 1.15 and 1.16 below it can be seen that the reason for the

poor catalytic performance of the MgO-supported bimetallic catalyst is related to the loss of catalyst selectivity due to the high rates of the subsequent hydrogenation and decomposition reactions.

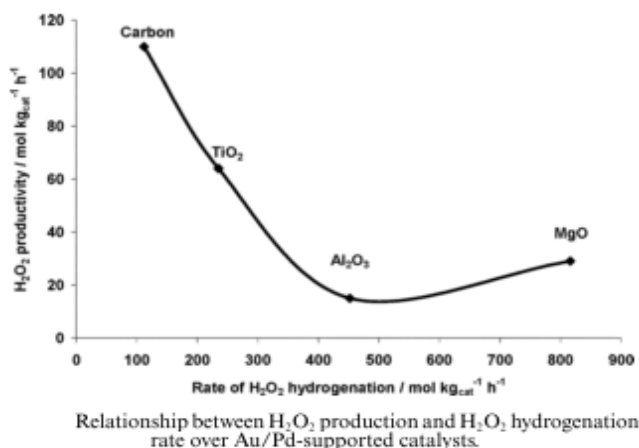


Figure 1.15. Comparison of catalytic activity of Au-Pd supported catalysts towards H₂O₂ synthesis and hydrogenation.⁵²

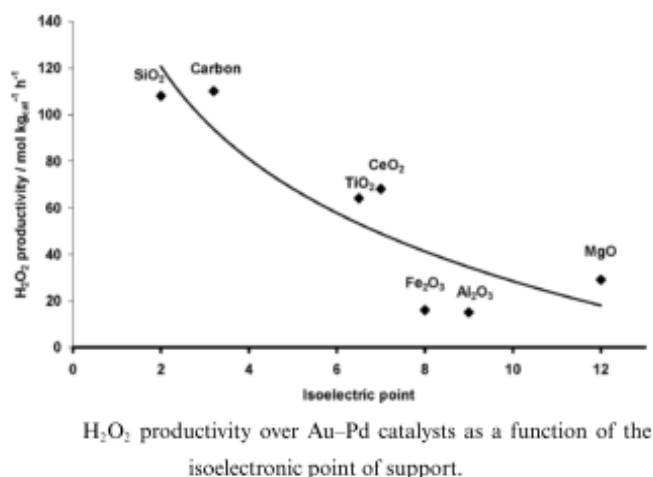


Figure 1.16 Comparison between the activity of bimetallic Au-Pd catalysts on various supports towards the formation of hydrogen peroxide and the isoelectric point of the support.⁵²

Hutchings and co-workers⁵² have shown that the support is critical in determining the performance of the catalyst for the direct synthesis of hydrogen peroxide as it controls the dispersion of the Au and Pd components as well as providing the sites that are responsible for the subsequent hydrogenation and decomposition of H₂O₂. As such it is possible to improve catalytic selectivity through the choice of catalyst support.

This has further been discussed by Menegazzo *et.al.*⁵⁵ who have reported that it is possible to control Pd nanoparticle size and in turn balance catalytic activity and selectivity towards

H₂O₂ through the choice of support. They report that the use of SiO₂ is superior to that of either ZrO₂ or CeO₂ in tuning these two parameters of catalytic efficiency. Again this may be related to the isoelectric point of the support, as seen in Figure 1.16 for the SiO₂ and CeO₂ supported AuPd catalysts.

The effects of acid additives in improvement of monometallic Pd supported catalysts, through inhibition of base-catalyzed decomposition and improvement in selectivity has been previously reported.⁵¹ In order to further improve catalytic selectivity Hutchings and co-workers⁸ have studied the effect of acid pre-treatment of carbon supported Au-Pd catalysts in the direct synthesis of hydrogen peroxide. It was found that acid treatment of the supports prior to metal dispersion is crucial in producing a catalyst that has low activity towards hydrogen peroxide hydrogenation and thus enhanced selectivity. It has been demonstrated that the process of acid pre-treatment of the support favors the formation of smaller, Pd rich, nanoparticles at the expense of those nanoparticles with larger Au content. Therefore gold dispersion is enhanced, as smaller nanoparticles form and these are then able to decorate support sites that are active for the hydrogenation of hydrogen peroxide.⁸ The observation that the smaller, Pd rich nanoparticles are associated with higher catalytic activity is in agreement with other investigations into bimetallic catalysts.⁷⁴

Interestingly the alteration in particle size distribution and subsequent inhibition of the hydrogenation sites of the support is only observed in bimetallic Au-Pd and monometallic Au-only supported catalysts. It has therefore been suggested that the alloying of Au is necessary to observe the redistribution of particle size. Hutchings⁸⁴ has attributed this to the electronic structure of Pd being influenced by Au in a manner that the hydrogenation activity is inhibited. This suggestion is in keeping with the work of Han *et.al.*⁷²

Hu and co-workers⁹² have demonstrated that a correlation exists between catalytic performance and the structure and physiochemical properties of the support. Through comparison of a number of carbon materials as supports for Pd they have demonstrated that the presence of an ordered graphitic structure, in addition to lower concentrations of surface carboxylic (-COOH) groups, favors catalytic selectivity towards H₂O₂. The presence of carboxylic groups on the support are shown to increase the rates of H₂O₂ hydrogenation and decomposition. It is suggested by the authors that the presence of these functional groups on the surface of the support increases the hydrophilicity of the catalyst and that H₂O₂

formed over this catalyst can be re-adsorbed onto the surface, leading to the subsequent degradation of H₂O₂.

Ao *et al.*⁹³ have reported that the selectivity of TiO₂ supported Pd catalysts can be improved if the TiO₂ support was doped with nitrogen before Pd deposition followed by treatment under different atmospheres. Investigation in to catalyst selectivity towards H₂O₂ is reported to increase from 61 % for the undoped 1 wt. % Pd / TiO₂ catalyst to 75 % for the 1 wt. % Pd / N-doped TiO₂ catalyst exposed to a N₂ atmosphere, while there is a slight decrease in selectivity upon exposure of the 1 wt. % Pd / N-doped TiO₂ catalysts to O₂ and H₂, to 59 and 55 % respectively. It is reported that there is no change in mean diameter of the Pd nanoparticles, with a particle size of approximately 2 nm reported for both the N-doped and unmodified TiO₂ supported catalysts. However, the atomic ratio of Pd⁰ : Pd²⁺ is reported to decrease from 1.1 for the 1 wt. % Pd / TiO₂ catalyst to 0.47 for the 1 wt. % Pd / N-doped TiO₂ catalyst exposed to a N₂ atmosphere, with a resulting increase in catalytic selectivity. In comparison exposure of the 1 wt. % Pd / N-doped TiO₂ catalyst to a H₂ or O₂ atmosphere increases the Pd⁰ : Pd²⁺ to 2.5 and 2.3 for the catalysts supported on N-doped TiO₂ exposed to H₂ and O₂ respectively with the resulting decrease in catalyst selectivity. The authors suggest that doping N into TiO₂ in different atmospheres can lead to the formation of oxygen vacancies, which are substituted by N_{ad} and O_{ad} species. The former favors the fixation of Pd atoms and the latter results in the adsorbed oxygen on TiO₂. The synergistic effects of the two factors are responsible for a volcano-like curve of the ratio of Pd⁰ : Pd²⁺ resulting in the different catalytic performances of the 1 wt. % Pd / N-doped TiO₂ catalysts. Likely more metallic Pd atoms on the surface of the catalyst favor the direct synthesis of H₂O₂ while side reactions are suppressed on Pd²⁺ rich surfaces.

1.12. The role of additives in the direct synthesis of hydrogen peroxide.

One of the major problems associated with the direct synthesis of H₂O₂ is that the catalysts used also show catalytic activity towards decomposition and hydrogenation of H₂O₂, as well as oxidation of hydrogen to water. These three unwanted side reactions cause a decrease in selectivity and yield of hydrogen peroxide and are therefore it is of great interest to inhibit these pathways.

Several studies^{19, 46,88,94-96} have reported that the presence of halides within the reaction medium; either as an alkali metal salt, halogen acid or conversely incorporated directly into the catalyst, cause an increase in the selectivity of catalysts towards H₂O₂. This is believed to be due to the halide acting as catalyst inhibitor for decomposition of H₂O₂ to water.

The effect of the halides in palladium catalysed, direct synthesis of H₂O₂ can be associated with their σ or π donation ability. The availability of halide electrons, and their capability to form σ bonds increases down the group. It is therefore expected that iodide will form the strongest bonds and donate the most electron density to the metal, if no other halide metal interactions were present. However it is also common for π interactions to occur between the halide lone pair of electrons and the metal d-orbitals. This results in the opposite trend for electron donation to that above. The intermediate halides in particular have been shown to be highly suitable in the promotion of hydrogen peroxide selectivity¹¹.

The nature of the palladium-halide interaction has been shown to be very important in controlling the selective oxidation of hydrogen to hydrogen peroxide.³¹ Catalysts where the palladium is oxidised and therefore have PdO-X interactions, where X is Cl⁻ or F⁻, have been shown to have lower activity for hydrogen peroxide decomposition than those catalysts that have Pd⁰-X interactions. It is worth noting that Br⁻ is a suitable promoter of hydrogen peroxide selectivity regardless of the oxidation state of palladium.⁷⁴

Choudhary and co-workers³ have demonstrated that bromination of various supported palladium catalysts provides an increase in selectivity and yield of hydrogen peroxide. Further investigation by Lunsford and Liu⁹⁷ suggested that the presence of Cl⁻ or Br⁻ inhibit hydrogen peroxide reduction, possibly due to the blocking of catalytic sites that would facilitate the breaking of O-O bonds.^{19,98} This prevents the non-selective combustion of hydrogen to water as well as decomposition and reduction of hydrogen peroxide. The work of Lunsford and co-workers⁹⁹ have also shown that Br⁻ is more effective than Cl⁻, on a molar basis, in promoting hydrogen peroxide formation. Bromide ions are known to block the active site of palladium catalysts responsible for the combustion of hydrogen to water and the disproportionation of hydrogen peroxide. However it has also been shown that an optimum amount of Br⁻ is required, when present in excess Br⁻ indiscriminately blocks

catalytically active sites thus inhibiting hydrogen conversion to hydrogen peroxide and in so doing decreases the net formation of hydrogen peroxide³.

Interestingly Choudhary *et.al.*⁹⁴ have revealed that the incorporation of two halides, when the first is bromine and the second is either chlorine or fluorine, offer greater hydrogen peroxide productivity than either of the halides alone. This is believed to be due to the synergistic effects of combining two halides, which interact to alter the electronic properties of palladium clusters in the catalyst. As eluded to above this synergistic effect is greatest when the two halides differ greatly in electronegativity. It is believed that the effect of the two halides is to inhibit O-O bond cleavage of oxygen and hydrogen peroxide and in doing so reducing the rate of hydrogen combustion, hydrogen peroxide decomposition and hydrogenation reactions.

X-ray absorption fine structure spectroscopy (EXAFS) characterization of Pd supported on the commercial resin K2621 under reaction conditions (*in-situ*) by Centomo *et.al.*⁷⁵ reveals that the role of bromide ions as enhancers of the selectivity of supported Pd catalysts cannot be limited to the selective blocking of active sites responsible for the degradation of H₂O₂ to water. The authors report that the inclusion of NaBr (10 ppm) to the reaction mixture is able to increase the atomic fraction of PdO from 62 to 76 % as well as promotes the leaching of Pd from the support and it is suggested that both of these factors contribute to the improved H₂O₂ selectivity observed when bromides (or chlorides) are used as additives for the direct synthesis process.

However it has been demonstrated that the presence of only halide ions is not sufficient for the promotion of the selective oxidation of hydrogen to hydrogen peroxide¹¹, particularly for palladium only catalysts. When present with H⁺ ions selectivity towards hydrogen peroxide is greatly enhanced. The presence of H⁺ in the reaction mixture has been found to be crucial for achieving higher hydrogen peroxide selectivity and productivity⁵¹ this is attributed to the pH of the reaction medium being lower than the catalyst support's isoelectric point. This ensures that it is only the halide anions, and not their associated cations, that are able to adsorb onto the palladium surface. The adsorption of the halides, as stated above alters the electronic environment of the catalyst surface. Choudhary¹⁰⁰ has shown that this modification occurs through the measurement of binding energies of the Pd 3d_{5/2} and Pd 3d_{3/2} electrons. These values decreased significantly after the catalysts (with a KBr promoter)

were used in hydrogen to hydrogen peroxide oxidation, indicating that the electronic nature of the palladium had been altered. In addition, these findings suggest that the adsorbed bromide anions are either close to the palladium particles in the catalyst or mobile on the catalyst surface during the reaction in order to interact with the palladium. It should also be noted that in the absence of protons it is possible that the halide promoter may cause an increase in hydrogen peroxide decomposition, particularly when the halide is iodine.¹⁰¹

Several studies^{62,100} have shown that when protons are present in the reaction medium, without the presence of halide, palladium catalysts show little selectivity for H₂O₂ formation. However, when both halide anions and protons are present in the reaction solution the catalyst shows both high selectivity and activity for H₂O₂ formation. Therefore both protons and halide are required in partnership in order for a catalyst to be efficient for the direct synthesis of hydrogen peroxide.

It is interesting to note that the presence of protons alone have been shown to inhibit H₂O₂ decomposition¹¹. These observations indicate that in the presence of protons, but the absence of halide anions the combustion reaction dominates, rather than hydrogenation or decomposition, as the major competitive reaction to H₂O₂ synthesis with these individual pathways outlined in Figure 1.1.

A number of classes of acids have been investigated as a proton source in the direct synthesis of hydrogen peroxide, including oxoacids (H₃PO₄, H₂SO₄, HNO₃) and haloacids (HCl, HBr, HI). It was discovered by Choudhary and Samanta⁸⁸ that the presence of an oxoacid did cause a small increase in hydrogen conversion however, very little H₂O₂ was produced. This result was found to be comparable for all oxoacids and clearly shows the importance of protons over their associated anions. However the presence of protons alone is not enough to encourage selective oxidation of H₂ to H₂O₂. For this to occur halo-acids must be utilized and many studies^{46,98} have shown that the presence of a halo-acid increases H₂O₂ yield and productivity to a far greater extent than non-halo acids. In addition to this the effect of acid concentration on hydrogen peroxide decomposition activity has been studied and it has been shown that as acid concentration increases so does the suppression of H₂O₂ decomposition.¹¹

However the use of high quantities of acid has been proposed to be responsible for the dissolution of the active phase from the catalyst, resulting in the formation of an unstable

catalyst and H₂O₂. In addition to this, it has been found that the presence of acid leads to an accelerated corrosion of the reactor¹¹. These drawbacks have led to the investigation of acidic supports in the direct synthesis of hydrogen peroxide as an alternative acid additive^{8,21,23,48} and the potential for the use of Cs- exchanged tungstophosphoric acid as a replacement for common haloacid additives are explored in Chapter 3.

1.11. Heteropolyacid based catalysts in the direct synthesis of hydrogen peroxide.

It has been reported that the presence of halide and acid prevent hydrogen peroxide decomposition. However the use of acids has been shown to have a detrimental effect on reactor longevity, accelerating the rate of reactor corrosion significantly. It has also been shown that acid additives can cause the leaching of the active metals from the support. In order to overcome these problems, acidic supports have been studied.

Heteropolyacids (HPAs) are inorganic acids with an acid strength stronger than other, solid acids³² this coupled with their precedence in large scale industrial processes as an oxidation and acid catalyst as well as the environmental benignity¹⁰¹ has led to HPAs being studied in the direct synthesis of hydrogen peroxide.^{102,103} It is known that the protons in Keggin-type tungstophosphoric acid (H₃PW₁₂O₄₀) are almost super-acidic¹⁰⁵. The high solubility in polar solvents as well as the low surface area (< 10 m²/g) of HPAs, including H₃PW₁₂O₄₀, has been overcome by the introduction of specific cations into the Keggin structure in exchange for protons. The use of large cations, such as Cs⁺, K⁺, Rb⁺ and NH₄⁺ has been shown to produce a water-insoluble structure with a considerably higher surface area (< 100 m²/g) than those HPAs which have not undergone cation exchange.¹⁰⁵

Park and co-workers¹⁰⁵ have reported that the separation of palladium-exchanged insoluble HPAs from a polar solvent is somewhat difficult owing to the small average size of the particles (approximately 10 nm). To overcome this insoluble HPAs have been immobilised on porous materials such as mesoporous silica.¹⁰⁶

Mesoporous silicas have large uniform pores, in the range of 10-50 nm and a large surface area and it is these attributes which have led to their use in catalysis science and engineering

alike. In particular mesostructured cellular foam (MCF) has been shown to be an efficient support for immobilisation of various large molecules.¹⁰³

Sun *et al.*²¹ have recently shown that Pd based supported heteropolyacid catalysts exhibit higher H₂O₂ productivity and selectivity than the conventional Pd only catalysts in the absence of promoters and the formation of H₂O₂ over a 4 hour period was almost one order of magnitude higher than that provided by other catalysts. Summarised in Table 1.7²¹

Table 1.7. Catalytic performance of Pd catalyst on various supports for the synthesis of H₂O₂ in the absence of promoters over a 4 hour period.

Catalyst	H ₂ Conversion / %	H ₂ O ₂ selectivity / %
Pd/SiO ₂	16	5.9
Pd/TiO ₂	15	9.4
Pd/Graphite	21	9.1
Pd/Cs _{1.5} H _{1.5} PW ₁₂ O ₄₀	21	67

Reaction Conditions: Catalyst (1 wt. % Pd loading, 0.05 g), T = 283 K, H₂ : O₂ : N₂ = 1 : 4 : 1, gas flow rate = 60 cm³ min⁻¹, solvent = ethanol (60 cm³), time = 4 h²¹

Again Sun and co-workers²¹ have demonstrated that the amount of Cs present in the polyoxometalate is crucial for the effective synthesis of H₂O₂. They have showed that as the amount of Cs increases from x = 0.5 to x = 1.5 in Cs_xH_{3-x}PW₁₂O₄₀ the selectivity and productivity of the catalyst towards H₂O₂ increased, while conversion of hydrogen decreased. However they have also shown that further increase in the amount of Cs (x > 1.5) decreased both the productivity and selectivity of the catalyst. Therefore they have reported that Pd / Cs_{1.5}H_{1.5}PW₁₂O₄₀ provides the highest H₂O₂ selectivity and productivity²¹. On the other hand it has also been reported by Okuhara *et al.*¹⁷⁸ that as Cs content is increased (from x = 2 to x = 3) the surface area and surface acidity of Cs_xH_{3-x}PW₁₂O₄₀ reaches a maximum and then falls. The effect in surface area can be explained when we consider that a relatively large cation, in this case Cs⁺, is replacing the much smaller H⁺. Surface acidity in this case represents the number of acid sites on the catalyst surface, therefore as surface area increases the number of acid surface sites increases to a point (x = 2.5) as Cs content increases however there is a decrease in proton concentration and so surface acidity decreases. This is an important aspect to consider when designing an effective catalyst as acidic supports have been shown to be effective in reduction of hydrogen peroxide decomposition and it is therefore of interest to utilise a support that is as acidic as possible. The alteration in surface area discovered by Park *et al.*¹⁰⁸, measured by BET, with increasing Cs content can be seen in Table 1.8.

Table 1.8. The variation of catalytic surface area with varying Cs content.¹¹⁰

Value of x in Pd _{0.15} Cs _x H _{2.7-x} PW ₁₂ O ₄₀	BET surface area (m ² /g)
2.0	30
2.2	57
2.5	105
2.7	125

It has been demonstrated that there is no correlation between catalytic activity and surface area Sun *et al.*²¹ have reported that those catalysts with the largest Cs content, and therefore greatest surface area have considerably lower selectivity towards H₂O₂ than those supported catalysts with lower Cs content and therefore smaller surface area. Therefore it is the acidity of the support that is expected to be critical in determining catalytic activity.

Park and co-workers¹⁰⁷ have also compared Pd_{0.15}Cs_{2.5}H_{0.2}W₁₂O₄₀ and Pd / Al₂O₃ catalysts in the presence and absence of an acidic promoter (H₂SO₄) and has shown that Pd_{0.15}Cs_{2.5}H_{0.2}W₁₂O₄₀ has greater selectivity for hydrogen peroxide, yield of hydrogen peroxide and conversion of hydrogen than the alumina supported palladium, in both the presence and absence of the promoter. This implies that Cs exchanged HPAs are an effective source of protons and offer an efficient alternative to the use of acidic additives.

Hutchings and co-workers^{23,66} have investigated Au-only, Pd-only and Au-Pd heteropolyacid supported catalysts in the direct synthesis of hydrogen peroxide. These catalysts with various Cs content were compared with a carbon supported Au-Pd catalyst which, under their chosen reaction conditions is the most effective catalyst for H₂O₂ synthesis. It was discovered that the Pd-only and bimetallic Au-Pd heteropolyacid supported catalysts showed higher H₂O₂ formation activity compared to the analogous carbon supported catalysts.

Interestingly the addition of Au by ion exchange to Pd only heteropolyacids did not change the catalytic performance, which disagrees with the synergistic effect shown where a more common support is used. In comparison the Au-Pd supported heteropolyacid catalysts showed higher catalytic performance which indicates that the method of preparation of the catalyst is crucial in formation of nanoparticles of varying size, location and morphology.

It is highly desirable for industry, from both an economic and environmental view point, that water be used in the direct synthesis of hydrogen peroxide, the use of toxic, environmentally unfriendly and more expensive organic solvents have contributed to the desire to develop an alternative to the indirect AO process. The ability to conduct catalysis at ambient

temperature is of course highly desired by industry and the production of a catalyst for the direct synthesis process that is able to be effective at ambient conditions is a commendable goal for research. To this end Hutchings and co-workers^{23,66} have demonstrated that heteropolyacid-based catalysts prepared by ion exchange offer much greater rates of formation of H₂O₂ than the Au-Pd- supported heteropolyacid and carbon- based supports prepared by impregnation, illustrated in Table 1.9. Additionally the rate of hydrogenation of the ion exchanged HPA catalysts is much smaller than that of the Pd-Au catalyst supported on heteropolyacid and has comparable hydrogenation rates to that shown by the carbon supported catalyst.

Table 1.9. H₂O₂ productivity and degradation using Au-Pd-exchanged heteropolyacid and Au-Pd supported catalysts at 20 °C using H₂O as a solvent.⁶⁶

Catalyst	H ₂ O ₂ Productivity / mol _{H₂O₂} kg _{cat} ⁻¹ h ⁻¹ ^a	H ₂ O ₂ Degradation / mol _{H₂O₂} kg _{cat} ⁻¹ h ⁻¹ ^b
2.5%Au-2.5%Pd/ Cs _{2.8} H _{0.2} PW ₁₂ O ₄₀	3	1310
2.5%Au-2.5% Pd / Cs _{2.5} H _{0.5} PW ₁₂ O ₄₀	11	1310
2.5%Au-2.5% Pd / Rb _{2.5} H _{0.5} PW ₁₂ O ₄₀	10	1205
Pd _{0.075} Au _{0.05} Cs _{2.5} H _{0.2} PW ₁₂ O ₄₀	61	776
Pd _{0.075} Au _{0.05} Rb _{2.5} H _{0.2} PW ₁₂ O ₄₀	49	2302
Pd _{0.1} Au _{0.0333} Cs _{2.5} H _{0.2} PW ₁₂ O ₄₀	58	793
2.5%Au-2.5%Pd/C (2% HNO ₃)	4	746

Reaction Conditions: As stated in Table 1.2.

In conclusion, the use of heteropolyacid based catalysts have been shown to be an effective for the direct synthesis of H₂O₂ under conditions that are attractive to industry. However, much research is still required in this area if these catalysts are to become mainstream in the direct synthesis route and lead to a viable alternative to the indirect auto-oxidation process.

1.12. The ammoximation of cyclohexanone to cyclohexanone oxime, utilising TS-1.

Titanium silicate-1 (TS-1) has widely been reported to offer high selectivity and efficiency in oxidation reactions alongside H₂O₂, such as aromatic hydroxylation^{109,110}, alkane oxidation¹¹¹⁻¹¹³, and alkene epoxidation,^{114,115} with the catalytic conversion of propylene to propylene oxide a key industrial process, with over 1.2 Mt of propylene oxide produced annually.¹¹⁶ Figure 1.18 highlights the versatility of TS-1 in a range of oxidation reactions when utilised alongside H₂O₂.

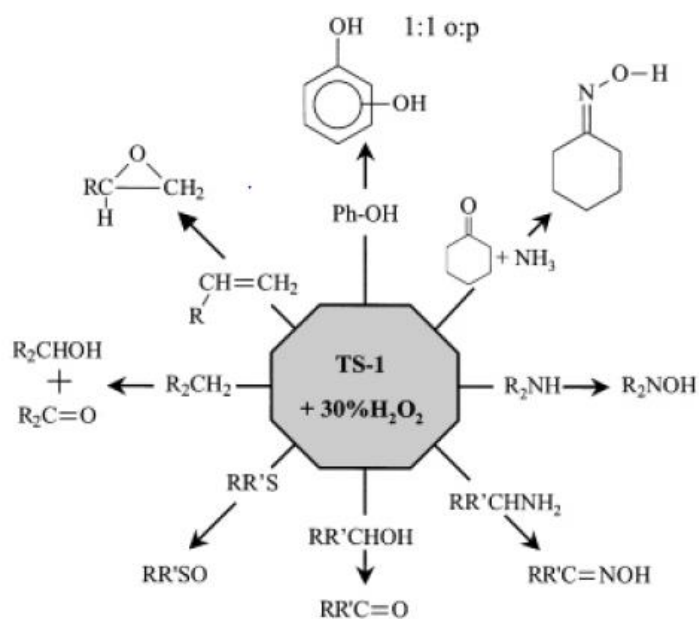


Figure 1.18. Schematic representation of oxidation reactions catalysed by TS-1.¹¹⁷

1.13. The structure of TS-1.

Analysis of the structure of TS-1 by Drago and co-workers¹¹⁸ has revealed the absence of strongly acidic sites on TS-1, in comparison to the zeolite HZSM-5, which they have ascribed as the reason for a lack of epoxide ring opening and the utility of TS-1 in epoxidation reactions. TS-1 has an MFI structure formed by three-dimensional systems of channels with dimensions of 0.53 x 0.56 nm and 0.51 x 0.51 nm. The structure of TS-1 prevents all molecules that have a cross-sectional area greater than 0.55 nm diffusing inside the pore structure of the zeolite, affording TS-1 remarkable shape selectivity. For example Hayashi and co-workers¹¹⁹ have shown that the oxidation of 2-propanol over TS-1 can be strongly retarded by the presence of one molar equivalent of 1-propanol, the linear alcohol is able to coordinate more strongly to the active site, followed by slow oxidation. In comparison the branched alcohol diffuses much slower but undergoes quicker oxidation.

The activity of TS-1 for has been closely related to morphology of the material. For example higher performance towards phenol hydroxylation has been observed for smaller crystals. These smaller crystals are reported to have greater Ti content within the lattice.¹¹⁵

The zeolite contains 1 wt % Ti, where the Ti(IV) atoms are incorporated into the framework in tetrahedral sites, substituting some non-adjacent Si atoms. Indeed the active sites for oxidation have been assigned to these isolated, tetrahedral Ti(IV) sites present in an –Si-O-Ti-O-Si- silica matrix, which does not contain Ti-O-Ti bonds. When H₂O₂ is present at low

temperatures solvolysis results in the formation of Ti-OOH and Si-OH, as seen in Figure 1.19, with the former giving rise to the active site responsible for catalytic oxidation.¹²⁰ The work by Limtrakul and co-workers¹²¹ supports these findings. They demonstrated that formation of hydroxylamine, the key step in the formation of cyclohexanone oxime, discussed in greater detail below, can be divided into two steps; firstly the decomposition of H₂O₂ over Ti sites to produce a peroxy-titanium species followed by the oxidation of NH₃. Interestingly their findings suggest that the decomposition of H₂O₂ occurs primarily on defective Ti sites.¹²¹

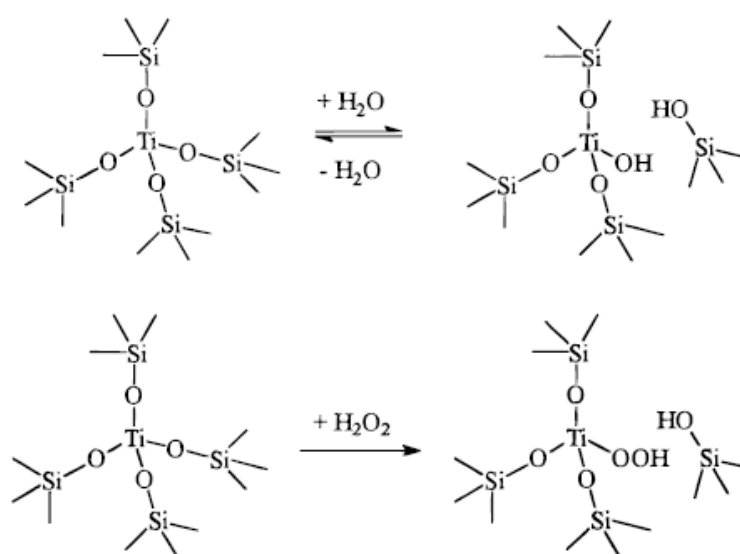


Figure 1.19. The formation of the catalytic sites responsible for the formation of hydroxylamine on TS-1.¹¹⁸

1.14. The ammoximation of cyclohexanone to cyclohexanone oxime.

The term ‘ammoximation’ describes the formation of an oxime through reaction of a ketone with ammonia and an oxidant, such as H₂O₂ or molecular oxygen. As exemplified in Figure 1.20.

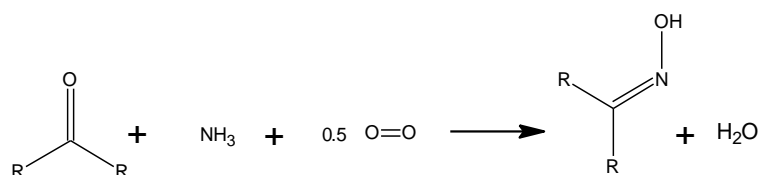
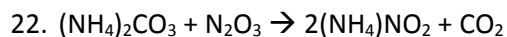
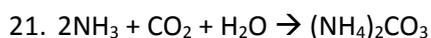
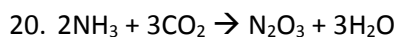


Figure 1.20. The conversion of a ketone to an oxime, through reaction with ammonia and oxygen.

The ammoximation reaction may be utilised to form a variety of oximes;¹²²⁻¹²⁴ acetone,¹²⁵ butanone,¹¹⁷ C₅-C₈ cyclic ketones¹¹⁷ as well as methyl- and dimethyl- substituted cyclohexanones¹²⁶ all yield the corresponding oxime. A key reaction that utilises ammoximation chemistry is the formation of cyclohexanone oxime, from cyclohexanone, a key precursor in the industrial production of ε-caprolactam the monomer of Nylon-6. As of 2010 worldwide production of ε-caprolactam is estimated at approximately 4 Mt / year, with the vast majority (approximately 70 %) utilised in the production of Nylon-6 and the remaining 30 % used in resins and films. In particular demand for Nylon resins has increased in recent years due to its growing use in the automotive industry as well as film-packaging for food and its use in electrical cables.

The industrial formation of ε-caprolactam has been dominated by the Raschig process, where cyclohexanone oxime is formed from cyclohexanone through use of hydroxylamine sulphate, this can then undergo Beckmann rearrangement to form ε-caprolactam. The formation of the hydroxylamine sulphate intermediate is carried out from combination of NH₃, CO₂ and SO₂ as outlined in Equations 20-23.



The formation of hydroxylamine sulphate results in the formation of a variety of undesired by-products including ammonium sulphate and NO_x. In particular the environmental issues associated with NO_x and sulphur oxide formation and co-formation of ammonium sulphate represents significant drawbacks to this process. Furthermore the formation of cyclohexanone oxime, utilising hydroxylamine sulphate, and the successive formation of ε-caprolactam by Beckmann rearrangement also result in the formation of ammonium sulphate, as can be seen in Figure 1.21.

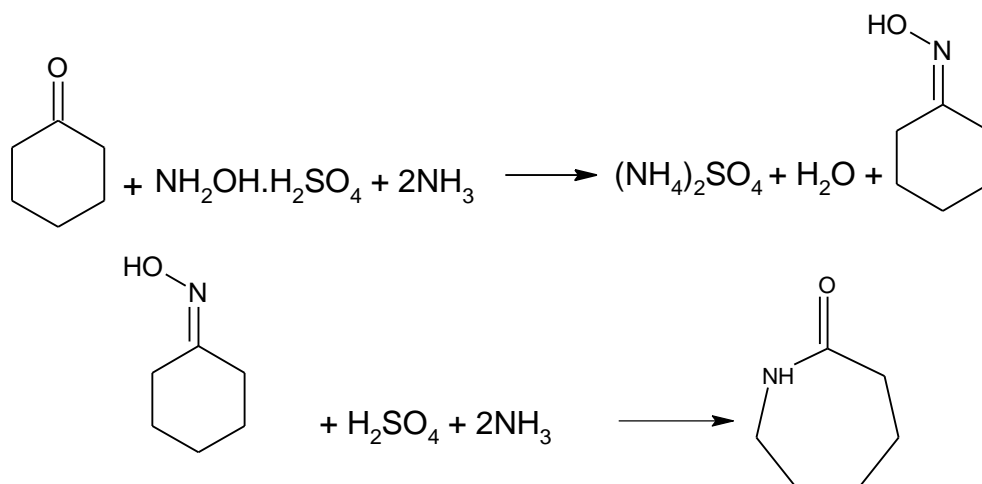


Figure 1.21. The formation of caprolactam from cyclohexanone oxime.

The formation of ammonium sulphate, in addition to NO_x , on a large scale is particularly unattractive, the commercial value of this by-product has declined rapidly in recent years and when coupled with the increasing legislation against NO_x production an alternative to the Raschig process is of great interest.

The use of TS-1 for the ammoxidation of cyclohexanone represented a breakthrough in the ammoxidation of cyclohexanone, when it was first reported in 1987 by Roffia and co-workers¹²⁷ and since then much interest has grown in the use of TS-1 as catalyst for the formation of cyclohexanone oxime and much research into utilising TS-1 as a catalyst for cyclohexanone ammoxidation has been conducted, with extremely high selectivity towards the oxime and conversion of cyclohexanone achieved.^{123, 128-131}

There have been two main mechanistic hypotheses proposed; the iminic route, widely accepted to occur in the gaseous phase, while in the liquid phase general consensus is now behind the hydroxylamine route, discussed below. The hydroxylamine route, shown in Figure 1.22, involves the formation of hydroxylamine via reaction between H_2O_2 and NH_3 on titanium centers, the basis of this hypothesis is the ability of TS-1 to catalyse the ammoxidation of ketones too large to enter inside the pores and on the ability of TS-1 to generate the hydroxylamine intermediate from NH_3 and H_2O_2 in the liquid phase. It has been reported by Dal Pozzo and co-workers¹³² that the formation of cyclohexanone oxime proceeds via the hydroxylamine route, in the liquid phase.

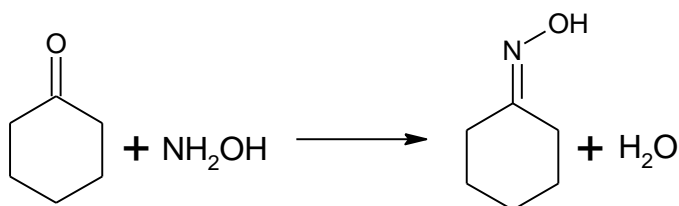


Figure 1.22. Schematic representation of the hydroxylamine route to cyclohexanone oxime formation.

As stated above the formation of cyclohexanone oxime in the gaseous phase is widely reported to proceed via the iminic route.^{124,133,134} Firstly the cyclohexanone reacts with NH_3 to form an unstable imine intermediate, which then adsorbs onto the catalyst surface to undergo oxidation to produce the oxime. In this case the role of Ti(IV) is to activate the oxygen, which then inserts into the imine. Figure 1.23 is a schematic representation of the iminic route to cyclohexanone oxime formation.

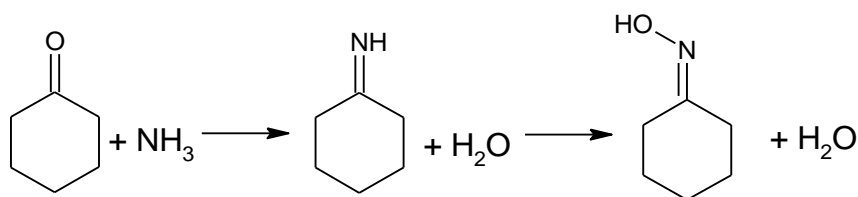


Figure 1.23. Schematic representation of the iminic route to cyclohexanone oxime formation.

Interestingly, recent work by Sooknoi¹³⁵ has shown that when acetic acid is used as the solvent the formation of cyclohexanone oxime tends to proceed through the oxidation of the imine, where the imine is formed through the condensation of cyclohexanone with NH_3 . This suggests that the solvent system can influence the route by which the ammoximation reaction proceeds. Interestingly they also report that, again, when acetic acid is used as the solvent it is possible to use a range of ammonium salts as the source of nitrogen. In particular ammonium acetate has been observed to provide a slightly greater yield of oxime when used as the source of nitrogen, in comparison to using ammonia solution.¹³⁵

However the use of TS-1 as a catalyst for the ammoximation of cyclohexanone does have some issues associated. Primarily the presence of high quantities of base results in the leaching of Ti from the zeolite framework. The Ti atoms removed from the framework accumulate on the remaining solid as a non-active hexacoordinated titanium species.¹³⁶ This is in stark comparison to the stability observed when TS-1 is utilised in a number of other

oxidation reactions. Activity of the catalyst trends with this loss of Ti from the framework and approaches that of supported Ti. Further issues with catalyst activity are also reported, with deactivation through coke-deposition and a decrease in adsorption capacity with increasing time on-stream reported.¹³⁷

The use of organic solvents such as methanol, toluene and t-butanol to improve catalyst stability have been investigated¹²⁸ and all have shown a remarkable ability to retard the loss of crystallinity in TS-1 when subjected to the presence of ammonia, in particular t-butanol is reported to provide the greatest stabilising effect, while also improving catalyst selectivity in comparison to methanol and toluene. However a variety of other solvents for this reaction has been investigated, including acetic acid and water.¹³⁵

1.15. Thesis Aims.

The aims of this thesis are outlined below:

1. It has been shown that the use of an acidic reaction medium may lead to an improvement in H₂O₂ yield and furthermore acidic supports can improve catalyst selectivity towards H₂O₂ synthesis. However, the use of high concentrations of acid can lead to reactor corrosion and the associated increase in maintenance costs and reactor downtime would be of significant concern to industry. While the use of ion exchanged tungstophosphoric acid, a Keggin-type heteropolyacid, as a support for precious metals active towards H₂O₂ synthesis reported within the literature. Investigation into the use of Cs-exchanged tungstophosphoric acid as an additive for catalyst known to be active towards the direct synthesis of H₂O₂ will be carried out with the aim of improving catalytic activity towards the direct synthesis process and in turn overall yield of H₂O₂.
2. The use of H₂O₂, as an oxidant, alongside TS-1, for the formation of cyclohexanone oxime, via the ammoximation of cyclohexanone has been investigated thoroughly in the literature. However the addition of H₂O₂ to the reaction mixture requires the concentration, transportation, storage and subsequent dilution of H₂O₂. All of which result in additional costs and have some significant risk attached. The *in-situ* formation of H₂O₂ and subsequent utilisation in the ammoximation of cyclohexanone, in a one pot approach, would offset many of these unwanted expenses and will be studied within this thesis.

1.17. References.

1. G. Pfeleiderer and H. J. Riedl, US Patent, 2,158,525, 1939.
2. W. W. H. Henkel, US Patent, US 1108752 A 1914.
3. V. R. Choudhary, C. Samanta and A. G. Gaikwad, *Chem. Commun.*, 2004, **10**, 2054-2055.
4. Y. F. Han and J. H. Lunsford, *Catal. Lett.*, 2005, **99**, 13-19.
5. D. P. Dissanayake and J. H. Lunsford, *J. Catal.*, 2003, **214**, 113-120.
6. Y.-F. Han and J. H. Lunsford, *J. Catal.*, 2005, **230**, 313-316.
7. Q. Liu, J. C. Bauer, R. E. Schaak and J. H. Lunsford, *Angew. Chem. Int. Ed.*, 2008, **47**, 6221-6224.
8. J. K. Edwards, B. Solsona, E. N. Ntainjua, F. Carley, A. A. Herzing, C. J. Kiely and G. J. Hutchings, *Science*, 2009, **323**, 1037-1041.
9. J. K. Edwards, S. F. Parker, J. Pritchard, M. Piccinini, S. J. Freakley, Q. He, A. F. Carley, C. J. Kiely and G. J. Hutchings, *Catal. Sci. & Technol.*, 2013, **3**, 812.
10. J. K. Edwards, E. N. Ntainjua, A. F. Carley, A. A. Herzing, C. J. Kiely and G. J. Hutchings, *Angew. Chem. Int. Ed.*, 2009, **48**, 8512-8515.
11. C. Samanta, *Appl. Catal. A. Gen.*, 2008, **350**, 133-149.
12. B. E. Solsona, J. K. Edwards, P. Landon, A. F. Carley, A. Herzing, C. J. Kiely and G. J. Hutchings, *Chem. Mater.*, 2006, **18**, 2689-2695.
13. J. K. Edwards, B. Solsona, P. Landon, A. F. Carley, A. Herzing, M. Watanabe, C. J. Kiely and G. J. Hutchings, *J. Mater. Chem.*, 2005, **15**, 4595-4600.
14. J. K. Edwards, A. Thomas, B. E. Solsona, P. Landon, A. F. Carley and G. J. Hutchings, *Catal. Today*, 2007, **122**, 397-402.
15. J. Edwards, B. Solsona, P. Landon, A. Carley, A. Herzing, C. Kiely and G. Hutchings, *J. Catal.*, 2005, **236**, 69-79.
16. J. K. Edwards, A. Thomas, B. E. Solsona, P. Landon, A. F. Carley and G. J. Hutchings, *Catal. Today*, 2007, **122**, 397-402.
17. J. K. Edwards, A. Thomas, A. F. Carley, A. A. Herzing, C. J. Kiely and G. J. Hutchings, *Green Chem*, 2008, **10**, 388-394.
18. T. A. Pospelova, N. I. Kobozev, *J. Phys. Chem.*, 1961, 262.
19. V. R. Choudhary, C. Samanta and P. Jana, *Appl. Catal. A. Gen.*, 2007, **317**, 234-243.
20. J. K. Edwards, E. N. Ntainjua, A. F. Carley, A. A. Herzing, C. J. Kiely and G. J. Hutchings, *Angew Chem. Int. Ed.*, 2009, **48**, 8512-8515.
21. M. Sun, J. Zhang, Q. Zhang, Y. Wang and H. Wan, *Chem. Commun.*, 2009, **39**, 5174-5176.
22. E. N. Ntainjua, M. Piccinini, S. J. Freakley, J. C. Pritchard, J. K. Edwards, A. F. Carley and G. J. Hutchings, *Green Chem.*, 2012, **14**, 170-181.
23. S. J. Freakley, R. J. Lewis, D. J. Morgan, J. K. Edwards and G. J. Hutchings, *Catal. Today*, 2015, **248**, 10-17.
24. G. Price, *Thermodynamics of chemical processes* Oxford University Press, United States, 1998.
25. M. Bowker, *The Basis and Applications of Heterogeneous Catalysis*, Oxford University Press, 1998.
26. J. M. Campos-Martin, G. Blanco-Brieva and J. L. Fierro, *Angew. Chem. Int. Ed.*, 2006, **45**, 6962-6984.
27. J. M. Campos-Martin, Blanco-Brieva, G. and Fierro, J. L. G., *Angew. Chem. Int. Ed.*, 2006, 6962-6984.
28. R. Meiers and W. F. Hölderich, *Catal. Lett.*, **59**, 1999, 161-163.

29. A. Thangaraj, R. Kumar, S. P. Mirajkar and P. Ratnasamy, *J.Catal.*, 1991, **130**, 1-8.
30. L. J. Thenard, *Ann. Chim. Phys*, 8, 1818, 306.
31. C. W. Jones, *Applications of hydrogen peroxide and its derivatives*, Royal Society of Chemistry, London, 1990.
32. N. Mizuno and M. Misono, *Curr.Opin.St.M.*, 1997, **2**, 84-89.
33. B. Liu, M. Qiao, J. Wang and K. Fan, *Chem. Commun.*, 2002, **11**, 1236-1237.
34. Y. Hou, Y. Wang, F. He, S. Han, Z. Mi, W. Wu and E. Min, *Mater.Lett.*, 2004, **58**, 1267-1271.
35. G. Centi, R. Dittmeyer, S. Perathoner and M. Reif, *Catal.Today*, 2003, **79–80**, 139-149.
36. A. Staykov, T. Kamachi, T. Ishihara and K. Yoshizawa, *J.Phys.Chem.C.*, 2008, **112**, 19501-19505.
37. H. C. Ham, G. S. Hwang, J. Han, S. W. Nam and T. H. Lim, *J.Phys.Chem.C.*, 2009, **113**, 12943-12945.
38. R. Todorovic and R. J. Meyer, *Catal. Today*, 2011, **160**, 242-248.
39. T. Deguchi and M. Iwamoto, *J.Phys.Chem.C*, 2013, **117**, 36, 18540-18548
40. J. Li and K. Yoshizawa, *Catal. Today*, 2015, **248**, 142-148.
41. J. Lunsford, *J.Catal.*, 2003, **216**, 455-460.
42. D. P. Dissanayake and J. H. Lunsford, *J Catal.*, 2002, **206**, 173-176.
43. S. Chinta and J. H. Lunsford, *J.Catal.*, 2004, **225**, 249-255.
44. D. Dissanayake, *J.Catal.*, 2003, **214**, 113-120.
45. A. Biffis, M. Zecca and M. Basato, *J.Mol.Catal.A-Chem.*, 2001, **173**, 249-274.
46. V. R. Choudhary, C. Samanta and P. Jana, *Ind.Eng.Chem.Res.*, 2007, **46**, 3237-3242.
47. V. R. Choudhary, A. G. Gaikwad and S. D. Sansare, *Catal.Lett.*, 2002, **83**, 235-239.
48. A. G. Gaikwad, S. D. Sansare and V. R. Choudhary, *J.Mol.Catal.A-Chem.*, 2002, **181**, 143-149.
49. S. D. Choudhary, A. G. Gaikwad V.R. Choudary, S.D. Sansare, US Patent No. 6,448,199 B1 (2002), assigned to Council of Scientific & Industrial Research – India.
50. V. R. Choudhary, C. Samanta and T. V. Choudhary, *Journal of Molecular Catalysis A: Chemical*, 2006, **260**, 115-120.
51. R. Burch and P. R. Ellis, *Appl.Catal.B-Environ.*, 2003, **42**, 203-211.
52. N. N. Edwin, J. K. Edwards, A. F. Carley, J. A. Lopez-Sanchez, J. A. Moulijn, A. A. Herzing, C. J. Kiely and G. J. Hutchings, *Green Chem.*, 2008, **10**, 1162-1169.
53. J. K. Edwards, A. F. Carley, A. A. Herzing, C. J. Kiely and G. J. Hutchings, *Faraday Discuss.*, 2008, **138**, 225-239.
54. F. Menegazzo, M. Signoretto, M. Manzoli, F. Boccuzzi, G. Cruciani, F. Pinna and G. Strukul, *J.Catal.*, 2009, **268**, 122-130.
55. F. Menegazzo, M. Signoretto, G. Frison, F. Pinna, G. Strukul, M. Manzoli and F. Boccuzzi, *J.Catal.*, 2012, **290**, 143-150.
56. S. Abate, K. Barbera, G. Centi, G. Giorgianni and S. Perathoner, *J. Energy Chem.*, 2016, **25**, 297-305.
57. L. Ouyang, P.-f. Tian, G.-j. Da, X.-C. Xu, C. Ao, T.-y. Chen, R. Si, J. Xu and Y.-F. Han, *J.Catal.*, 2015, **321**, 70-80.
58. R. W. J. Scott, C. Sivadinarayana, O. M. Wilson, Z. Yan, D. W. Goodman and R. M. Crooks, *J.Am.Chem.Soc.*, 2005, **127**, 1380-1381.
59. M. Contel, *Gold Chemistry. Applications and Future Directions in the Life Sciences*, John Wiley & Sons, Ltd 2010, p 104-109
60. G. J. Hutchings, *J.Catal.*, 1985, **96**, 292-295.
61. C. Qi, T. Akita, M. Okumura and M. Haruta, *Appl.Catal.A.Gen.*, 2001, **218**, 81-89.
62. P. Landon, P. J. Collier, A. F. Carley, D. Chadwick, A. J. Papworth, A. Burrows, C. J. Kiely and G. J. Hutchings, *Phys.Chem.Chem.Phys.*, 2003, **5**, 1917-1923.

63. Y. K. M. Okumura, K. Yamaguchi, T. Akita, S. Tsubota, and M. Haruta, *Chem. Lett.*, **32**, 2003, 822-823.
64. J. K. Edwards, A. F. Carley, A. A. Herzing, C. J. Kiely and G. J. Hutchings, *Faraday Discuss.*, 2008, **138**, 225-239.
65. G. Li, J. Edwards, A. F. Carley and G. J. Hutchings, *Catal.Today*, 2007, **122**, 361-364.
66. E. N. Ntainjua, M. Piccinini, S. J. Freakley, J. C. Pritchard, J. K. Edwards, A. F. Carley and G. J. Hutchings, *Green Chem.*, 2012, **14**, 170.
67. J. K. Edwards, B. E. Solsona, P. Landon, A. F. Carley, A. Herzing, C. J. Kiely and G. J. Hutchings, *J.Catal.*, 2005, **236**, 69-79.
68. J. Lin, F. Xin, L. Yang and Z. Zhuang, *Catal. Commun.*, 2013, **37**, 45-49
69. T. Ishihara, Y. Ohura, S. Yoshida, Y. Hata, H. Nishiguchi and Y. Takita, *Appl.Catal.A.Gen.*, 2005, **291**, 215-221.
70. J. K. Edwards and G. J. Hutchings, *Angew. Chem. Int. Ed.*, 2008, **47**, 9192-9198.
71. J. K. Edwards, Pritchard, J., Lu, L., Piccinini, M., Shaw, G., Carley, A. F., Morgan, D. J., Kiely, C. J. and Hutchings, G. J. , *Angew. Chem. Int. Ed.*, 2014, **53**, 2381-2384.
72. Y. F. Han, Z. Zhong, K. Ramesh, F. Chen, L. Chen, T. White, Q. Tay, S. N. Yaakub and Z. Wang, *J.Phys.Chem.C.*, 2007, **111**, 8410-8413.
73. D. Gudarzi, W. Ratchananusorn, I. Turunen, M. Heinonen and T. Salmi, *Catal.Today.*, 2015, **248**, 58-68.
74. V. R. Choudhary, C. Samanta and T. V. Choudhary, *Appl.Catal.A.Gen.*, 2006, **308**, 128-133.
75. S. Sterchele, P. Biasi, P. Centomo, S. Campestrini, A. Shchukarev, A.-R. Rautio, J.-P. Mikkola, T. Salmi and M. Zecca, *Catal.Today*, 2015, **248**, 40-47.
76. J. Gu, S. Wang, Z. He, Y. Han and J. Zhang, *Catal.Sci.Technol.*, 2016, **6**, 809-817.
77. D. Gudarzi, O. A. Simakova, J. R. H. Carucci, P. D. Biasi, K. Eränen, E. Kolehmainen, I. Turunen, D. Y. Murzin and T. Salmi, *Chem.Eng.J.*, 2010, **21**, 925-930.
78. J.K. Edwards, A.F. Carley, A. A. Herzing, M. Watanabe, C.J. Kiely and G. J. Hutchings, *J. Mater.Res.*, 2007, 831-837.
79. S. J. Freakley, Q. He, J. H. Harrhy, L. Lu, D. A. Crole, D. J. Morgan, E. N. Ntainjua, J. K. Edwards, A. F. Carley, A. Y. Borisevich, C. J. Kiely and G. J. Hutchings, *Science*, 2016, **351**, 965-968.
80. J. K. Edwards and G. J. Hutchings, *Angew.Chem.Int.Ed.*, 2008, **47**, 9192-9198.
81. J. K. Edwards, A. F. Carley, A. A. Herzing, C. J. Kiely and G. J. Hutchings, *Faraday Discuss.*, 2008, **138**, 225.
82. A. Cybula, J. B. Priebe, M.-M. Pohl, J. W. Sobczak, M. Schneider, A. Zielińska-Jurek, A. Brückner and A. Zaleska, *Appl.Catal.B-Environ.*, 2014, **152-153**, 202-211.
83. E. N. Ntainjua, J. K. Edwards, A. F. Carley, J. A. Lopez-Sanchez, J. A. Moulijn, A. A. Herzing, C. J. Kiely and G. J. Hutchings, *Green Chem.*, 2008, **10**, 1162.
84. J. K. Edwards, A. Thomas, A. F. Carley, A. A. Herzing, C. J. Kiely and G. J. Hutchings, *Green Chem.*, 2008, **10**, 388-394.
85. A. Molnár, C. Keresszegi and B. Török, *Appl.Catal.A.Gen.*, 1999, **189**, 217-224.
86. T. A. G. Silva, E. Teixeira-Neto, N. López and L. M. Rossi, *Sci.Rep.*, 2014, **4**, 5766.
87. F. Menegazzo, M. Manzoli, M. Signoretto, F. Pinna and G. Strukul, *Catal.Today*, 2015, **248**, 18-27.
88. C. Samanta and V. R. Choudhary, *Catal. Commun.*, 2007, **8**, 2222-2228.
89. P. Landon, P. J. Collier, A. F. Carley, D. Chadwick, A. J. Papworth, A. Burrows, C. J. Kiely and G. J. Hutchings, *Phys.Chem.Chem.Phys.*, 2003, **5**, 1917-1923.
90. Y. H. T. Ishihara, Y. Nomura, K. Kaneko, H. Matsumoto, *Chem.Lett.*, **36**, 7, 2007 878-879.
91. J. K. Edwards, A. Thomas, A. F. Carley, A. A. Herzing, C. J. Kiely and G. J. Hutchings, *Green Chem.*, 2008, **10**, 388.

92. B. Hu, W. Deng, R. Li, Q. Zhang, Y. Wang, F. Delplanque-Janssens, D. Paul, F. Desmedt and P. Miquel, *J.Catal.*, 2014, **319**, 15-26.
93. C. Ao, P. Tian, L. Ouyang, G. Da, X. Xu, J. Xu and Y.-F. Han, *Catal.Sci.Technol.*, 2016, **6**, 5060-5068.
94. V. R. Choudhary and C. Samanta, *J.Catal.*, 2006, **238**, 28-38.
95. E. N. Ntainjua, M. Piccinini, J. C. Pritchard, J. K. Edwards, A. F. Carley, J. A. Moulijn and G. J. Hutchings, *ChemSusChem*, 2009, **2**, 575-580.
96. E.N. Ntainjua, M. Piccinini, J. C. Pritchard, Q. He, J. K. Edwards, A. F. Carley, J. A. Moulijn, C. J. Kiely and G. J. Hutchings, *ChemCatChem*, 2009, **1**, 479-484.
97. Q. Liu and J. Lunsford, *J.Catal.*, 2006, **239**, 237-243.
98. C. Samanta and V. R. Choudhary, *Catalysis Communications*, 2007, **8**, 73-79.
99. Q. Liu and J. H. Lunsford, *Appl.Catal.A.Gen.*, 2006, **314**, 94-100.
100. V. Choudhary and C. Samanta, *J.Catal.*, 2006, **238**, 28-38.
101. S. Furuta, H. Matsushashi and K. Arata, *Catal.Comm.*, 2004, **5**, 721-723.
102. S. Park, D. R. Park, J. H. Choi, T. J. Kim, Y.-M. Chung, S.-H. Oh and I. K. Song, *J.Mol. Catal.A.Chem.*, 2010, **332**, 76-83.
103. S. Park, D. R. Park, J. H. Choi, T. J. Kim, Y.-M. Chung, S.-H. Oh and I. K. Song, *J. Mol. Catal. A. Chem.*, 2011, **336**, 78-86.
104. I. V. Kozhevnikov, *Chem.Rev.*, 1998, **98**, 171-198.
105. S. Park, T. J. Kim, Y.-M. Chung, S.-H. Oh and I. K. Song, *Res.Chem. Intermedi.*, 2010, **36**, 639-646.
106. S. Park, J. H. Choi, T. J. Kim, Y.-M. Chung, S.-H. Oh and I. K. Song, *Catal. Today*, 2012, **185**, 162-167.
107. T. Okuhara, T. Nishimura, H. Watanabe and M. Misono, *J.Mol.Catal.*, 1992, **74**, 247-256.
108. S. Park, J. H. Choi, T. J. Kim, Y.-M. Chung, S.-H. Oh and I. K. Song, *J.Mol.Catal.A. Chem.*, 2012, **353-354**, 37-43.
109. A. Corma, *J.Catal.*, 2003, **216**, 298-312.
110. L. Wang, G. Xiong, J. Su, P. Li and H. Guo, *The J.Phys.Chem.C*, 2012, **116**, 9122-9131.
111. W. Schuster, J. P. M. Niederer and W. F. Hoelderich, *Appl.Catal.A.Gen.*, 2001, **209**, 131-143.
112. M. G. Clerici, *Appl.Catal.*, 1991, **68**, 249-261.
113. D. R. C. Huybrechts, L. D. Bruycker and P. A. Jacobs, *Nature*, 1990, **345**, 240-242.
114. D. P. Serrano, R. Sanz, P. Pizarro, A. Peral and I. Moreno, *Micropor.Mesopor.Mat.*, 2013, **166**, 59-66.
115. C. Perego, A. Carati, P. Ingallina, M. A. Mantegazza and G. Bellussi, *Appl.Catal.A. Gen.*, 2001, **221**, 63-72.
116. O. A. K. Mario G. Clerici, *Liquid Phase Oxidation via Heterogeneous Catalysis: Organic Synthesis and Industrial Applications*, John Wiley & Sons, Inc, USA, 2003.
117. A. D. Silvia Bordiga, G. R. Francesca Bonino and A. Z. Carlo Lamberti, *Angew. Chem., Int. Ed.*, 2002, **24**, 4734-4737
118. R. S. Drago, S. C. Dias, J. M. McGilvray and A. L. M. L. Mateus, *J. Phys.Chem.B*, 1998, **102**, 1508-1514.
119. H. Hayashi, K. Kikawa, Y. Murai, N. Shigemoto, S. Sugiyama and K. Kawashiro, *Catal.Lett.*, 1996, **36**, 99-102.
120. G. Bellussi, A. Carati, M. G. Clerici, G. Maddinelli and R. Millini, *J. Catal.*, 1992, **133**, 220-230.
121. J. Sirijaraensre and J. Limtrakul, *Phys.Chem.Chem Phys.*, 2013, **15**, 18093-18100.
122. A. Zecchina, G. Spoto, S. Bordiga, F. Geobaldo, G. Petrini, G. Leofanti, M. Padovan, M. Mantegazza and P. Roffia, in *Studies in Surface Science and Catalysis*, eds. F. S. L. Guzzi and T. P, Elsevier, 1993, vol. Volume 75, pp. 719-729.

123. T. Tatsumi and N. Jappar, *J.Catal.*, 1996, **161**, 570-576.
124. J. Le Bars, J. Dakka and R. A. Sheldon, *Appl.Catal.A.Gen.*, 1996, **136**, 69-80.
125. X. Liang, Z. Mi, Y. Wang, L. Wang and X. Zhang, *React.Kinet.Catal.Lett.*, **82**, 1996, 333-337.
126. Y. Zhang, Y. Wang, Y. Bu, L. Wang, Z. Mi, W. Wu, E. Min, S. Fu, Zhu and Zehua, *React.Kinet.Catal.Lett.*, **87**, 2005, 25-32.
127. Roffia P., Padovan M., Moretti E., De Alberti G. EUR patent 208311, 1987.
128. C. Wu, Y. Wang, Z. Mi, L. Xue, W. Wu, E. Min, S. Han, F. He and S. Fu, *React.Kinet.Catal. Lett.* **77**, 2002, 73-81.
129. F. Song, Y. Liu, H. Wu, M. He, P. Wu and T. Tatsumi, *J.Catal.*, 2006, **237**, 359-367.
130. F. Song, Y. Liu, L. Wang, H. Zhang, M. He and P. Wu, *Appl.Catal.A.Gen.*, 2007, **327**, 22-31.
131. G. Liu, J. Wu and H. a. Luo, *Chinese. J.Chem.Eng.*, 2012, **20**, 889-894.
132. L. Dal Pozzo, G. Fornasari and T. Monti, *Catal.Comm.*, 2002, **3**, 369-375.
133. Y. Barbaux, D. Bouqueniaux, G. Fornasari and F. Trifirò, *Appl.Catal.A.Gen.*, 1995, **125**, 303-312.
134. D. P. Dreoni, D. Pinelli and F. Trifirò, *J.Mol. Catal.*, 1991, **69**, 171-190.
135. T. Sooknoi and V. Chitrannuwatkul, *J. Mol.Catal.A.Chem.*, 2005, **236**, 220-226.
136. G. Petrini, A. Cesana, G. D. Alberti, F. Genoni, G. Leofanti, M. Padovan, G. Papparatto and P. Roffia, in *Studies in Surface Science and Catalysis*, eds. H. B. Calvin and B. B. John, Elsevier, 1991, vol. Volume 68, pp. 761-766.
137. X. Zhang, Y. Wang and F. Xin, *Appl.Catal.A.Gen.*, 2006, **307**, 222-230.

2. Experimental

This Chapter outlines the experimental procedures followed during catalytic preparation, testing and material characterisation discussed in this Thesis.

2.1. Materials used

This Section outlines the chemicals used during the work contained within this thesis and the suppliers used with the purity of the various chemicals in parenthesis.

PdCl₂ – Johnson Matthey (99.99% trace metal basis)

HAuCl₄ - Johnson Matthey (99.99% trace metal basis)

H₂PtCl₆ - Johnson Matthey (99.99% trace metal basis)

Tungstophosphoric acid hydrate Sigma Aldrich (99.995 % trace metal basis)

CsNO₃ – Sigma Aldrich (99.99 % trace metal basis)

TS-1 – ACS Materials (≥ 99.0 %)

TiO₂ – Degussa p25 (99.5 % trace metal basis, 20-30 nm particle size)

SiO₂ – Fischer Scientific (60 A Particle size 35 – 70 micron, Silice 60A)

Carbon G60 – Sigma Aldrich (Darco powder – 100 mesh particle size)

MeOH – Sigma Aldrich (HPLC Grade)

EtOH - Sigma Aldrich (HPLC Grade)

t-BuOH - Sigma Aldrich (≥ 99.0 %)

Diethylene glycol monoethyl ether – Sigma Aldrich (≥99.0%)

Water – Fischer Scientific (HPLC Grade)

50 % H₂O₂ - Sigma Aldrich (Stabilised)

35 % H₂O₂ - Sigma Aldrich (Stabilised)

Cyclohexanone - Sigma Aldrich (99.8%)

Cyclohexanone oxime - Sigma Aldrich (97%)

28% NH₃ in water – Sigma Aldrich (≥ 99.99 % trace metals)

Ce(SO₄)₂ Sigma Aldrich (> 98 %)

(NH₄)₂Fe(SO₄)₂.6H₂O - Sigma Aldrich (> 98%)

2.2. Catalyst Preparation

2.2.1. Gold, Palladium and Gold-Palladium Catalysts prepared by wet impregnation.

Monometallic and bi-metallic gold, palladium catalysts were prepared by wet impregnation and co-impregnation of the appropriate support with solutions of HAuCl_4 , PdCl_2 , using an excess of solvent (in this case water). The catalysts were prepared to have a nominal metal content of 5 wt. %, unless otherwise stated.

A typical 1.0 g preparation procedure of a 2.5 wt. % Au- 2.5 wt. % Pd / support catalyst was carried out according to the following procedure which has been previously reported in the literature¹.

0.042 g of PdCl_2 was added to 2.04 ml of HAuCl_4 (12.25 g Au / 1000 ml) and heated to 80 °C with stirring and left until the PdCl_2 had completely dissolved. 0.95 g of the desired support was then added to the solution and the water allowed to evaporate until the mixture formed a paste like consistency. The samples were dried at 110 °C for 16 h and then calcined in static air at 400 °C for 3 h with a ramp rate of 20 °C min^{-1} .

2.2.2. Gold, Palladium, Platinum and Gold - Palladium - Platinum Catalysts prepared by wet impregnation.

Tri-metallic Au-Pd-Pt catalysts were prepared in a similar manner to Au-Pd catalysts, discussed in Section 2.2.1. The procedure for producing 1 g of 2 wt. % Au – 2 wt. % Pd -1 wt. % Pt supported catalyst is outlined below:

0.033 g of PdCl_2 was added to 1.63 ml of HAuCl_4 (12.25 g Au / 1000 ml) and 1 ml of H_2PtCl_6 (10 g Pt / 1000 ml) and heated to 80 °C with stirring and left until the PdCl_2 had completely dissolved. 0.95 g of the desired support was then added to the solution and the water allowed to evaporate until the mixture formed a paste like consistency. The samples were dried at 110 °C for 16 h and then calcined in static air at 400 °C for 3 h with a ramp rate of 20 °C min^{-1} .

2.2.3. Cs-exchanged tungstophosphoric acid.

The degree of Cs-incorporation into the structure of $\text{H}_3\text{PW}_{12}\text{O}_{40}$ was varied by varying the mass of CsNO_3 added to an aqueous solution of $\text{H}_3\text{PW}_{12}\text{O}_{40}$. A typical 1.0 g preparation

procedure of $\text{Cs}_{2.5}\text{H}_{0.5}\text{PW}_{12}\text{O}_{40}$ was carried out according to the following procedure which has been previously reported in the literature².

CsNO_3 (0.151 g) dissolved in 5.0 ml deionised water was added drop-wise to an aqueous solution of $\text{H}_3\text{PW}_{12}\text{O}_{40}$ (0.892 g) while stirring. The resulting solution was continuously stirred while heating (80°C). The water was allowed to evaporate until the mixture formed a paste like consistency. The samples were dried at 110 °C for 16 h and then calcined in static air at typically 300 °C for 2 h with a ramp rate of 20 °C min⁻¹.

2.3. Catalyst Testing

2.3.1. The Direct Synthesis of H_2O_2 .

Catalytic activity towards the direct synthesis of H_2O_2 from H_2 and O_2 was determined using a Parr Instruments stainless-steel autoclave (equipped with overhead stirrer and temperature/pressure sensors) with a nominal volume of 100 ml and maximum working pressure of 14 MPa, as shown in Figure 2.1 below. During a standard synthesis reaction the autoclave was charged with MeOH (5.6 g), HPLC standard H_2O (2.9 g) and catalyst (0.01 g). The autoclave was pressurised with 2.9 MPa 5 % H_2 / CO_2 and 1.1 MPa 25 % O_2 / CO_2 to give a total reaction pressure of 4 MPa. After cooling the autoclave to 2 °C (or reaching the given temperature) the reaction mixture is stirred at 1200 rpm for 0.5 h. The reaction starts when stirring begins, if stirring does not occur no H_2O_2 is observed, over the timescale of the reaction. After the reaction was completed a gaseous sample was collected and analysed by gas chromatography (discussed in Section 2.4.1) when necessary. After collection of the gaseous sample the remaining reactant gas was vented and the catalyst was removed from the solvent by filtration and two 0.5 g aliquots of the solvent were titrated against a $\text{Ce}(\text{SO}_4)_2$ solution acidified with 2% H_2SO_4 using ferroin as an indicator. The concentration of the $\text{Ce}(\text{SO}_4)_2$ solution was determined by titration of a known amount of $(\text{NH}_4)_2\text{Fe}(\text{SO}_4)_2 \cdot 6\text{H}_2\text{O}$, using ferroin as an indicator.¹

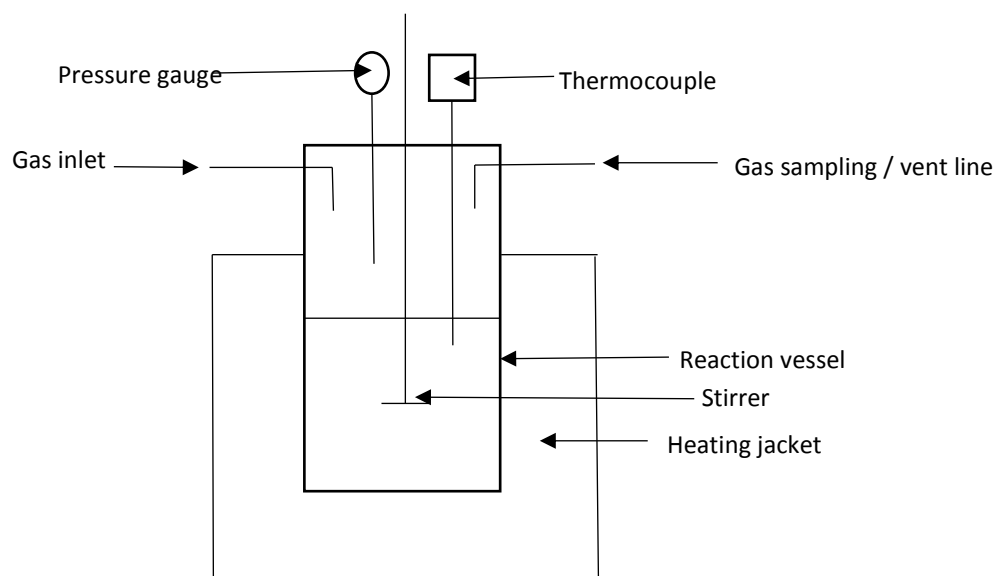


Figure 2.1. Schematic representation of a high pressure autoclave.

Catalytic performance was compared by determining the average rate of H_2O_2 formation, normalised for catalyst mass, to give a productivity value which is reported as $\text{mol}_{\text{H}_2\text{O}_2}\text{h}^{-1}\text{kg}_{\text{cat}}^{-1}$. The wt. % of H_2O_2 was also determined using the equations shown below:

$$\text{Ce}(\text{SO}_4)_2 \text{ to titrate whole reaction solution} = \frac{\text{Titre} \times 8.5 \text{ (total solution volume)}}{\text{Sample mass}}$$

$$\text{Moles Ce}(\text{SO}_4)_2 = \frac{\text{Vol. of Ce}(\text{SO}_4)_2 \text{ to titrate whole reaction solution} \times [\text{Ce}(\text{SO}_4)_2]}{1000}$$

$$\text{Moles H}_2\text{O}_2 = \frac{\text{Moles Ce}(\text{SO}_4)_2}{2}$$

$$\text{Productivity} = \frac{\text{Moles H}_2\text{O}_2}{\text{Catalyst Mass (Kg)} \times \text{Reaction Time (h)}}$$

$$\text{wt \% H}_2\text{O}_2 = \frac{\text{Moles H}_2\text{O}_2 \times \text{Molecular Mass H}_2\text{O}_2}{8.5 \text{ (total mass of solvent)}}$$

2.3.2. Degradation of H₂O₂.

The degradation activity of a catalyst towards H₂O₂ was determined in a manner similar to the direct synthesis activity of a catalyst. The autoclave was charged with MeOH (5.6 g), H₂O₂ (50 wt. % 0.69 g) HPLC standard H₂O (2.21 g) and catalyst (0.01 g). The solvent composition is equivalent to a 4 wt. % H₂O₂ solution; this allows for comparison to previous work conducted within the Hutching's research group. It is a larger concentration than that which can be produced in a standard synthesis reaction (outlined in Section 2.3.1 above) and allows for accurate determination of catalyst activity towards degradation. From the solution two aliquots were removed by pipette of between 0.04 g and 0.06 g +/- 1mg were removed and titrated with acidified Ce(SO₄)₂ solution using ferroin as an indicator to determine an accurate concentration of H₂O₂ at the start of the reaction. The autoclave was pressurised with 2.9 MPa 5 % H₂ / CO₂ and cooled to 2 °C, unless otherwise stated, and the reaction mixture was stirred at 1200 rpm for 0.5 h. The reaction starts when stirring begins, if stirring does not occur no H₂O₂ degradation is observed, over the timescale of the reaction. After the reaction was complete (0.5 h) the catalyst was immediately removed from the reaction solvents and as previously two aliquots of 0.05 g were titrated against the acidified Ce(SO₄)₂ solution using ferroin as an indicator. The degradation activity was calculated as mol_{H₂O₂} h⁻¹ kg_{cat}⁻¹ along with the percentage of H₂O₂ remaining after the reaction.

A 'blank' degradation test was carried out routinely to determine the contribution of the reactor to the degradation of H₂O₂. This followed the same procedure as that described in Section 2.3.2, however no catalyst was included. If any H₂O₂ degradation was observed the reactor was cleaned with aqua regia, to remove any metal deposited on the reactor vessel, followed by thorough cleaning with water. Once this was complete a second 'blank' reaction was carried out to ensure all deposited metal had been removed.

2.3.3. Direct synthesis of H₂O₂ under ammoximation conditions.

Catalytic activity towards H₂O₂ from H₂ and O₂ was determined under conditions approaching those used in the ammoximation process. A standard synthesis reaction, as outlined in Section 2.3.1. is carried out where MeOH is replaced by t-BuOH and a known volume of H₂O is replaced by cyclohexanone and /or NH₃, to ensure total volume remains constant. The choice of t-BuOH as a solvent stems from its use in literature investigating the ammoximation of cyclohexanone and this is discussed in greater detail in Chapter 1. Once the reaction was completed a gas sample undergoes analysis by gas chromatography to determine H₂

selectivity prior to analysing a liquid sample, for cyclohexanone conversion and cyclohexanone oxime selectivity, also by gas chromatography.

2.3.4. Degradation of H₂O₂ under ammoximation conditions.

The degradation activity of a catalyst towards H₂O₂ was determined in a manner similar to that described above in Section 2.3.2. However unlike above the autoclave was charged with t-BuOH (5.6 g), H₂O₂ (50 wt. % 2.07 g) HPLC standard H₂O (0.83 g) and catalyst (0.01 g). The solvent composition is equivalent to a 12 wt. % H₂O₂ solution. The higher concentration of H₂O₂ is required as the conditions utilised for the ammoximation of cyclohexanone are quite harsh and a smaller concentration would not allow for accurate determination of the contribution of the reaction conditions and the catalyst towards the degradation of H₂O₂.

2.3.5. The ammoximation of cyclohexanone to cyclohexanone oxime via H₂O₂ addition.

To determine the effect of metal impregnation on catalytic ability to produce cyclohexanone oxime the following procedure was followed:

Cyclohexanone (1.0 g, 10 mmol), catalyst (0.05 g), t-BuOH (2.5 g), H₂O (2.5 g) and 28 wt. % NH₃ (12 mmol, 0.73 g) were added into a two neck flask with condenser attached. The second flask neck is equipped with a H₂O₂ inlet line. The reaction mixture was heated, with stirring, to 80 °C and H₂O₂ (35 wt. %, 10 mmol, 0.89 g) was added over 1 h using a HPLC pump, at a rate of 0.0148 mlmin⁻¹. The reaction was allowed to continue for a further 0.5 h. After this time the reaction mixture was allowed to cool to room temperature and ethanol (10 ml) and internal standard (diethylene glycol monoethyl ether) (1.0 g) are added. The catalyst is removed by filtration and the mixture is analysed by gas chromatography.

2.3.6. Catalyst re-use for the ammoximation of cyclohexanone to cyclohexanone oxime via H₂O₂ addition.

Catalyst reusability was tested by running an ammoximation as outlined in Section 2.3.5 but increasing the catalyst mass to 0.1 g and using twice the standard reactant amounts. The addition rate of H₂O₂ (35 wt. %) was set to 0.297 mlmin⁻¹. After the reaction was complete the catalyst was removed by filtration and was allowed to dry at 110 °C for 16 h on the filter paper to ensure the sample was completely dry. Following this procedure an ammoximation test as described in Section 2.3.5 was conducted.

2.3.7. The ammoximation of cyclohexanone to cyclohexanone oxime via *in-situ* synthesis of H₂O₂.

Catalytic performance for the *in-situ* ammoximation of cyclohexanone was determined using a Parr Instruments stainless-steel autoclave (equipped with overhead stirrer and temperature/pressure sensors) with a nominal volume of 50 ml and maximum working pressure of 14 MPa. During a standard ammoximation reaction the autoclave was charged with cyclohexanone (0.13 g, 1.3 mmol), catalyst (0.05 g), t-BuOH (5.6 g), H₂O (2.69 g) and 28 wt. % NH₃ (0.08 g, 1.3 mmol). The autoclave was pressurised with 2.9 MPa 5 % H₂ / CO₂ and 1.1MPa 25 % O₂ / CO₂ to give a total reaction pressure of 4 MPa. The autoclave was then heated to the desired temperature and stirred at 1200 rpm for 1.5h.

After the reaction was complete, and the autoclave allowed to cool to room temperature, a gas sample was taken for analysis by GC. Following this, ethanol (1 ml) and internal standard (diethylene glycol monoethyl ether) (0.1 g) were added to the working solution. The catalyst was removed by filtration and the mixture was analysed by gas chromatography.

2.3.8. Hot filtration for the ammoximation of cyclohexanone to cyclohexanone oxime via *in-situ* synthesis of H₂O₂.

In order to establish the activity of leached metal towards the ammoximation of cyclohexanone a hot filtration test was carried out. This involves running a standard reaction, as outlined in Section 2.3.7. After the reaction was complete, and the autoclave allowed to cool to room temperature, a gas sample was taken for analysis. Following this the catalyst was removed by filtration and the reaction solution returned to the reactor which was pressurised with 2.9 MPa 5 % H₂ / CO₂ and 1.1MPa 25 % O₂ / CO₂ to give a total reaction pressure of 4 MPa. The autoclave was then heated to the desired temperature and stirred at 1200 rpm for 0.5 h.

After the reaction was complete analysis of both the reaction solution and reactant gas carried out, as outlined above in Section 2.3.7.

2.4. Gas Chromatography.

2.4.1. GC setup for analysis of gas from H₂O₂ direct synthesis reaction.

A Varian 3800 gas chromatogram fitted with a thermal conductivity detector was used to analyse the post reaction gas mixture from the direct synthesis reaction. In order to determine catalytic conversion of H₂ and H₂O₂ selectivity a gas sample from a 'blank' direct synthesis reaction (where no catalyst is present, but all other conditions are the same as those outlined above) is analysed by GC. This is to allow comparison of the gas composition after the catalysed direct synthesis reactions and calculation of H₂ conversion and H₂O₂ selectivity.

The column oven (containing a Porapak Q column) was held at 30 °C for 22 min which allows separation of H₂, O₂ and CO₂, using Argon as a carrier gas at a flow rate of 30 ml / min. The retention times of the components analysed during a H₂O₂ synthesis reaction is shown in Table 2.1.

Table 2.1. Retention times of components analysed during the direct synthesis of H₂O₂ from H₂ and O₂.

Component	Retention time / min
H ₂	1.63
O ₂	2.24
CO ₂	9.21

Hydrogen conversion was measured by calculating the difference between H₂: CO₂ ratio before and after the reaction. H₂ selectivity was calculated based on the rate of H₂O₂ synthesised at the end of the direct synthesis reaction.

2.4.2. GC set up for analysis of reaction mixture from ammoxidation of cyclohexanone.

A Varian 3800 gas chromatogram fitted with a flame ionisation detector was used to analyse the reaction mixture of the cyclohexanone ammoxidation process post reaction. In order to provide quantitative analysis of the reaction mixture, samples containing known concentrations of reactant, products, solvent and standard are first used to establish retention factors and allow the conversion of cyclohexanone, selectivity toward cyclohexanone oxime and overall yield to be calculated.

The column oven (containing a CP – Wax 52 CB column, with a polyethylene phase) temperature was held at 80 °C for 1 minute upon injection of the liquid sample. Secondly temperature was increased from 80 °C to 200 °C, at a ramp rate of 15 °C / min for a total ‘run time’ of 9 minutes. This allows for the elution of the analytes within the gaseous sample. Following from this the temperature is raised to 250 °C, at a ramp rate of 20 °C / min, this temperature is held for five minutes and ensures that no sample remains within the column, which may affect subsequent analysis.

Column pressure was maintained at 5 psi and the FID temperature was set to 270 °C. A carrier gas of He was utilised and a flow rate of 10 ml/min was chosen. In order to maintain sensitivity a splitless injection was utilised; the role of split injections is discussed below.

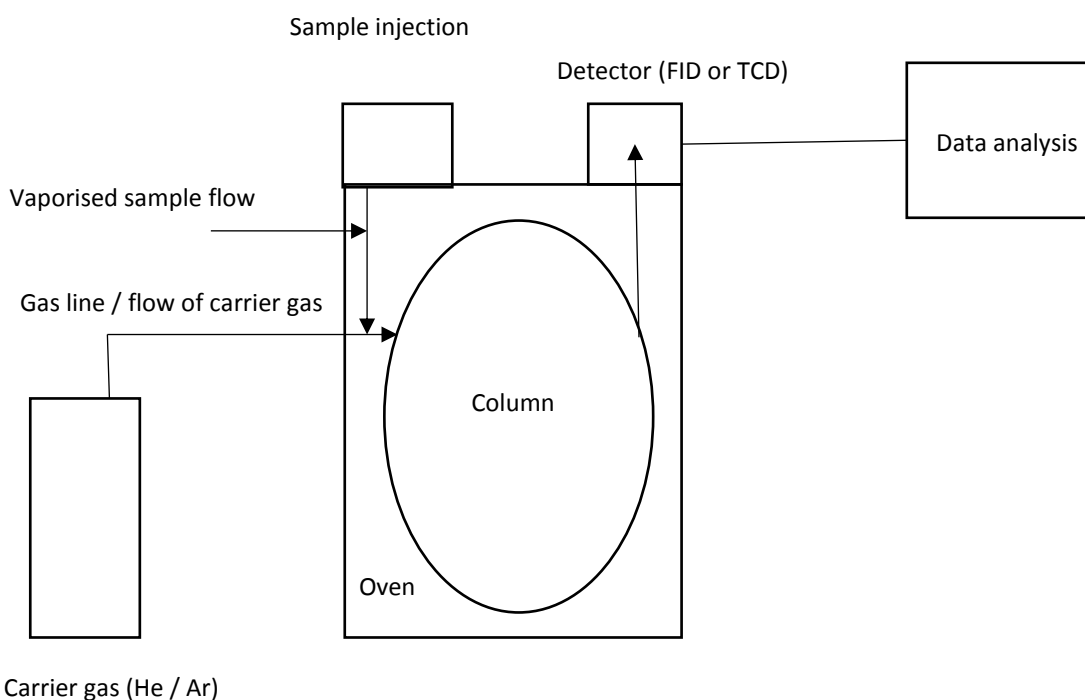


Figure 2.2. Schematic representation of a Gas Chromatograph.

Gas chromatography is a technique used to separate and analyse mixtures of chemical compounds, either liquid or gaseous. Liquid samples are first vaporised by an injector block, often set to a temperature higher than that of the column oven. Elution is brought about by a flowing of an inert gas for example He or N₂ termed the mobile phase. The mobile phase carries the vaporised sample through the column and does not interact with the analyte.

The stationary phase is an adsorbent or a high boiling point liquid on an inert material known as the stationary support, commonly used supports are diatomaceous earth, silica gel or alumina. The stationary phase is usually held in glass, quartz or stainless steel tubes.

There are generally two types of column: packed and capillary columns. These are enclosed in a thermostatically controlled oven, the temperature of which can range from ambient to over 400 °C and can remain constant during a separation or increase at a determined rate to increase elution.

There are a number of techniques for introducing the sample onto the column; split injection limits the amount of sample (approximately 2 %) allowed to pass onto the column and this can present issues with sensitivity. The splitting ratio can be altered using resistance to liquid sample flow. While a splitless injection overcomes this disadvantage.

There are many detectors available to monitor the carrier gas as it emerges from the column and act in response to changes in the gas composition as analytes are eluted. One of the most commonly used detectors is the Flame Ionisation Detector (FID). The effluent gas, once passed through the column is mixed with H₂ and air and is burned at a small metal jet. The jet forms the anode of an electrolytic cell and the cathode or collector anode is placed just above the flame tip. The pyrolysis of organic compounds often leads to the formation of ions and electrons and detection involves monitoring the current produced by the movement of these charge carriers from anode to cathode. The numbers of ions produced by pyrolysis of the organic analytes are proportional to the number of reduced carbon atoms in the flame and so quantitative analysis is possible³.

A thermal conductivity detector (TCD) is another common detector used in gas chromatography. The principle of operation is based on the relative change in the thermal conductivity of the gas passing across the detector filament, as the analytes elute from the column. Heat is lost continuously from the filament through the carrier gas to the wall of the detector. Through measuring the current required to maintain the temperature of the filament as the analytes pass over the filament a chromatographic signal is produced.

2.4.3. Quantitative Analysis by Gas Chromatography.

For quantitative analysis of how reactant concentration changes during a reaction ethanol is added to the reaction mixture (to ensure all product is dissolved) and an external standard (Diethylene glycol monoethyl ether) is added to the reaction mixture, post reaction and the catalyst is removed by filtration. A sample of this mixture is then injected into the GC. The

number of moles of reactant were determined from its mass pre-reaction and post reaction concentration is determined from the normalised area of the substrate signal from the FID. Cyclohexanone conversion, selectivity towards cyclohexanone oxime and cyclohexanone oxime yield are then calculated using the equations found in Appendix 2.1.

2.5. X-Ray Diffraction (XRD).

X-ray diffraction (XRD) is a bulk characteristic technique that allows the identification of crystallites and allows the detection of crystallite size greater than 5nm^4 . It is a non-destructive technique with a detection limit of approximately 5 wt%.

X-rays are formed by bombarding a metal target, usually Cu or Mo, with a high energy electrons emitted from a thermionic emission from a filament, usually W or Mo. The filament temperature can be varied in order to regulate generation of electrons. Collision of the incident electrons with the metal target produces a broad range of X-rays from the K-shell (1s) of the target atoms. X-rays are emitted as the resultant vacancies are filled with electrons from the L (2p) or M (3p) levels which have superimposed onto it characteristic narrow energies known as K_α and K_β . The X-rays produced are filtered to give a monochromatic source and the collision of these monochromatic X-rays with the atomic planes of the crystalline sample results in scattering of the X-rays, this can result in constructive interference (a 'reflection'), when the spacing between lattice planes (d) is equal to an integer number of wavelengths or when $AB + BC = n\lambda$. Figure 2.3 shows X-ray interaction with lattice planes of a crystalline sample.

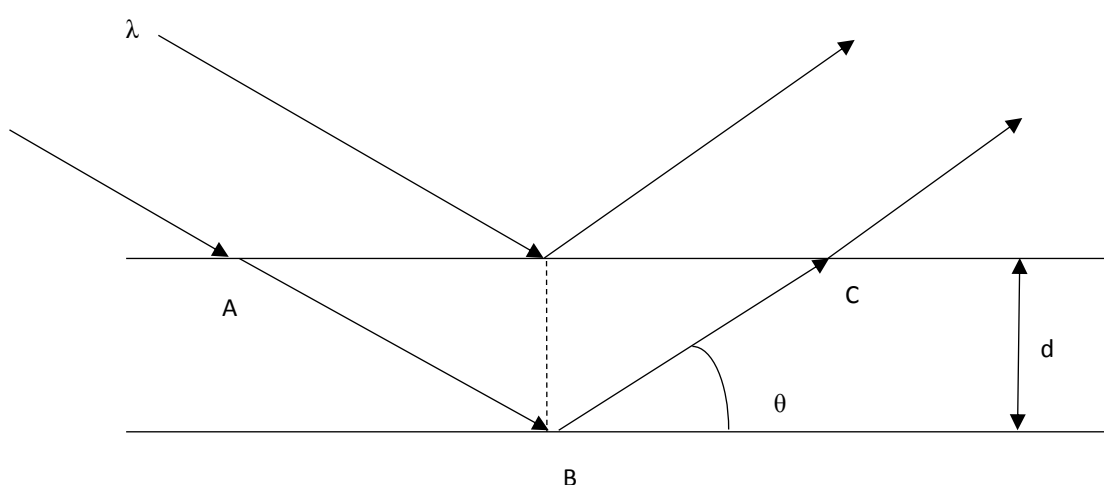


Figure 2.3. Diagram to show X-ray diffraction from lattice planes within a crystallite, where d represents lattice spacing and θ is the incident angle, normal to the plane.

Powder samples have an infinite number of randomly orientated crystallites, the collision of X-rays with the sample results in the scattering of these X-rays at the appropriate 2θ angle, as defined by Bragg's Law. It is possible to consider the crystallite as a stack of reflecting lattice planes, with separation between each plane denoted as d . When two X-rays are reflected by adjacent lattice planes, shown in Figure 2.3 the first X-ray strikes the upper lattice plane at a given point, however the second X-ray travels an additional distance (AB) before striking the second lattice plane. Once reflected by the respective lattice planes the two X-rays will differ in path length by a distance denoted as BC . It is therefore possible to describe the difference in net path length as:

$$AB + BC = 2d \sin \theta$$

For the majority of incident X-rays the incident angle or glancing angle (θ) the path-length difference will not equate to an integer of wavelengths, and these waves interfere destructively. However when the path-length difference is an integer number of the wavelengths the reflected X-rays are in-phase and interfere in a constructive manner and so it is possible to observe a reflection when the incident angle obeys Bragg's Law.

$$n\lambda = 2d \sin \theta$$

Where :

n = an integer,

λ = X-ray wavelength,

d = lattice spacing,

θ = angle between incident and normal to the plane.

Smaller crystallites, such as supported metallic nanoparticles, incomplete destructive interference can result in line broadening. This means that the shape of the reflection can provide information with regard to crystallite size. Larger crystallites, with more lattice planes will produce sharp, narrow peaks, while smaller crystallites will give rise to broader reflections. It is possible to estimate the crystallite size of a supported metallic nanoparticle using the Debye-Scherrer equation, shown below. Although this is limited to particles larger than 5 nm as below this limit the incident X-rays are not scattered to a great enough angle to be measured⁵.

$$n = \frac{k \lambda}{\beta \cos \theta}$$

Where: n = crystallite size

k = form factor,

λ = X-ray wavelength,

β = full width half maximum of the reflection

θ = diffraction angle.

Procedure:

Investigation of the bulk structure of the crystalline materials was carried out using a $(\theta-\theta)$ PANalytical X'pert Pro powder diffractometer using a Cu K_{α} radiation source, operating at 40 KeV and 40mA. Standard analysis was carried out using a 40 minute run with a back filled sample, between 2θ values of $10 - 80^{\circ}$. Phase identification was carried out using the International Centre for Diffraction Data (ICDD).

2.6. BET Surface Area Analysis.

The surface area of a powdered material can be determined by physical adsorption of a gas onto the surface of the solid, through weak Van der Waals forces between the adsorbate and the surface of the adsorbent.

The concept builds on Langmuir adsorption theory, which is a theory for monolayer adsorption, based on three assumptions:

1. Adsorption cannot exceed monolayer coverage.
2. The surface of the adsorbent is uniform, with all sites being equivalent.
3. The ability of an adsorbate molecule to adsorb on to a specific site is not dependent on the presence of pre-existing adsorbed molecules on neighbouring sites.

BET theory extends Langmuir theory to multilayer adsorption and assumes that gas molecules can physically adsorb to the surface of the sample infinitely, that there is no interaction between each adsorption layer and finally that Langmuir theory can be applied to each layer of adsorption. According to BET theory the rate of adsorption is equal to the rate of desorption once equilibrium has been reached.

The sample is first pre-treated in order to remove adsorbents, such as water or solvent from the sample surface. Following this physical adsorption of the adsorbate occurs, utilising varying pressures of N₂. The amount of N₂ adsorption can be related to pressure through the following adsorption isotherm equation.

$$\frac{P}{v(P_0 - P)} = \frac{1}{v_m C} + \frac{C - 1}{v_m C} \frac{P}{P_0}$$

Where:

P = equilibrium constant

P₀ = saturation pressure

v = volume

v_m = volume required to cover the surface in a monolayer

C = constant

The equation above can be linearised through a plot of $\frac{P}{v(P_0 - P)}$ versus $\frac{P}{P_0}$ where the intercept occurs at $\frac{1}{v_m C}$.

The surface area can then be determined using the following equation:

$$Surface\ area = \frac{v_m * N_A * S}{M}$$

Where v_m = volume required to cover the surface in a monolayer

N_A = Avagadro's Number (6.023x10²³)

S = cross sectional area of N₂ (0.162 nm²)

Procedure:

Surface area analysis was determined using a Micromeritics Gemini 2360 analyser. A known amount of sample, 100–200 mg was placed in a straight walled tube and degassed for 1 h at 120°C under a flow of N₂. The surface area was analysed using a single point analysis typically taking 5 points between P/P₀= 0.05–0.1.

2.7. Microwave Plasma Atomic Emission Spectroscopy (MP-AES).

MP-AES is an elemental analytical technique that is based on the principles of atomic emission. It utilises on a microwave and magnetically excited nitrogen plasma formed within a quartz torch. Samples analysis can range from examination of a reaction solution to determine leaching to digestion of metals from a support to determine accurate loadings. However this limits catalyst samples to those that are soluble or digestible, in comparison inductively coupled plasma (ICP) emission spectroscopy allows for solid analyse samples via laser ablation systems.

The nitrogen plasma is heated approximately 5000 Kelvin and causes atomisation of the sample and leads to the formation of a high population of excited states, providing MP-AES with a high sensitivity in comparison to those techniques which utilise a lower temperature, such as flame absorption spectroscopy.

Figure 2.4 outlines the principles of MP-AES, the uptake of the sample and introduction into the nitrogen plasma leads to excitation of electrons from the ground to the excited state. These electrons then relax to the lower quantised energy level, releasing photons of defined energy and wavelength as they do so. These energies and wavelengths are characteristic to each element and allow the use of a monochromator and mirror grating allows the analysis of individual wavelengths in a sequential manner. This, along with high intensities leads to low interference and a high sensitivity for each element.

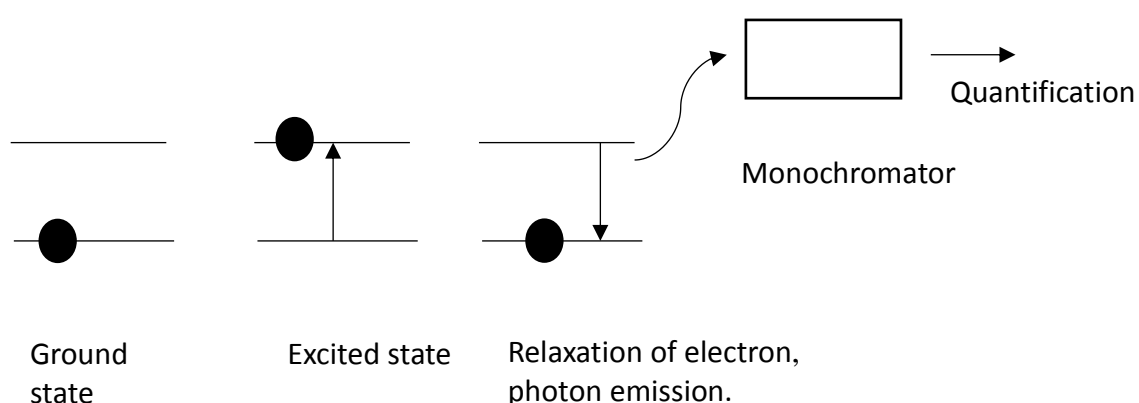


Figure 2.4. Schematic of basic principles of microwave plasma atomic emission spectroscopy.

Procedure:

Reaction solutions were first filtered to remove heterogeneous catalyst from the sample. Dilution of the sample with low chain alcohol such as ethanol was then conducted in order to avoid issues associated with the use of long chain organics utilised as the reaction medium, this dilution occurred in a 1 : 1 ratio, where 1 ml of ethanol was utilised for 1 ml of sample. Further filtration occurred using PTFE syringe filters (0.456 μm). Samples were then analysed using an Agilent MP-AES 4100, samples were investigated for the presence of precious metals (Au, Pd and Pt) using multiple wavelength calibrations for each individual element.

2.8. Electron Microscopy (EM).

2.8.1. Transmission electron microscopy (TEM).

Transmission electron microscopy (TEM) is a non-destructive technique that is utilised in heterogeneous catalyst characterisation, in particular it provides information with regards to particle size and dispersion as well as chemical composition, when coupled with Energy-dispersive X-ray spectroscopy (EDX). TEM has an approximate resolution of 5 \AA ⁵.

TEM utilises a high energy and high intensity electron beam, passed through a condenser which excludes high angle electrons to produce parallel rays, which are then impinge on the sample. Beam attenuation is dependent on the density and thickness of the sample under investigation and the transmitted electrons form a two-dimensional projection of the sample mass. As the electrons pass through the sample the electrostatic potential of the constituent elements within the sample cause the electrons to become scattered, subsequent magnification by electron optics lead to the formation of the bright-field image. The dark field image is obtained from the diffracted electron beams, which are slightly off angle from the transmitted beam. The position of the aperture it is possible to choose whether the diffracted beam (dark field) or the un-scattered electrons (bright field) are used to produce the image.

Typical operating procedures are 100-200keV electrons, 10^{-6} mbar vacuum, 0.3 nm resolution and a magnification of 3×10^5 to 10^6 . In general the identification of supported nanoparticles, such as supported metal nanoparticles requires that there is adequate contrast between the support and the particles themselves and that a thin sample, typically less than 100 nm, is utilised⁵.

2.8.2. Scanning Transmission Electron Microscopy (STEM).

STEM operates in a manner very similar to scanning electron microscopy (SEM), it can provide information about particle morphology at the atomic scale⁶. A focused, high energy, beam of electrons is scanned over a thin specimen through atomic interaction back-scattered electrons, secondary electrons and X-rays are produced as seen in Figure 2.5 all providing specific imaging modes.

Transmitted electrons, collected on axis give bright field signals. These are electrons that have not been scattered by the sample or have been inelastically scattered, through angles of milliradians, under specific conditions the bright field mode of STEM is identical to that in TEM. STEM is able to provide benefits in dark field operation, with a unique imaging mode, High Angle Annular Dark Field (HAADF) imaging. Here the images are derived from elastically scattered electrons that have passed very close to the atomic nuclei of the sample. High resolution is achieved, meaning that it possible to produce images that do not suffer from diffraction contrast, which can cause loss of structural information. The HAADF signal is proportional to $Z^{3/2}$, where Z is the atomic number.

Secondary electron imaging is an additional benefit of STEM, where backscattered and secondary electrons are collected in a manner similar to that seen in SEM. As such it is possible to correlate surface information, from secondary electrons, with bulk information from the STEM mode. Secondary electrons are produced by the primary electron beam entering the sample or when backscattered electrons leave the sample⁵.

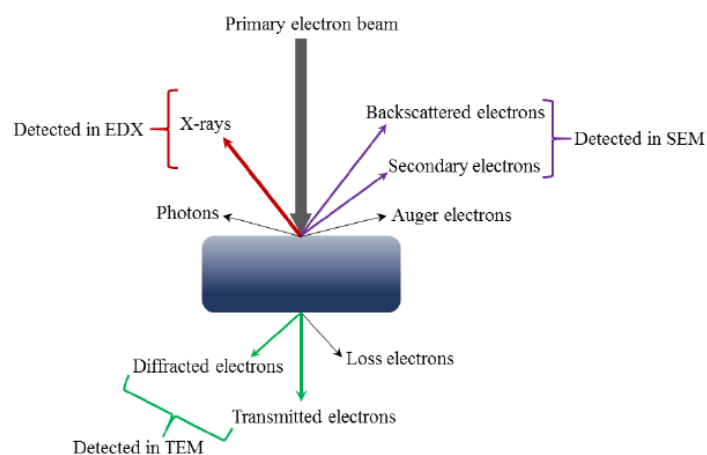


Figure 2.5. Schematic of detectable signals in electron microscopy, from a sample bombarded with a primary electron beam.

2.8.3. Energy Dispersive X-ray Spectroscopy (EDX).

EDX is a bulk characteristic technique that is used for elemental analysis. The interaction between an electron beam and an electron from within the atomic structure of the sample causes the emission of a core shell electron, producing a vacancy, this vacancy is filled by an outer shell electron and the excess energy is released in the form of an X-ray. The individual nature of the electronic structure of each element means that the energy of the emitted X-ray will be individual to each element and so it is possible to distinguish elements due to atomic number⁷.

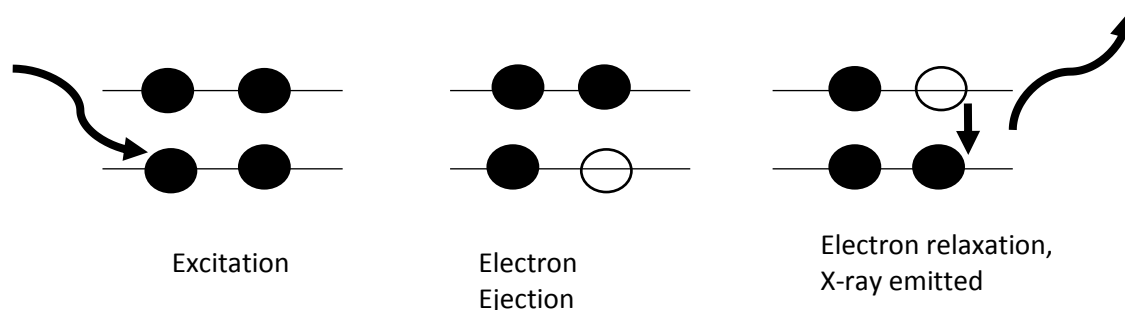


Figure 2.6. Energy dispersive X-ray spectroscopy schematic.

2.9. X-ray photoelectron spectroscopy (XPS).

X-ray photoelectron spectroscopy is a surface sensitive characterisation technique that provides information about the oxidation state of species as well as chemical composition of the catalyst surface, to a depth of approximately 10 nm⁴. XPS is based on the photoelectric effect, where the adsorption of high energy X-rays by a core electron results in its emission. The kinetic energy of the ejected electron is dependent on energy of the incident X-rays, the work function of the spectrometer as well as the binding energy of the core electron.

The binding energy of each core electron is specific to each element, which also depends on the oxidation state of the element; as the oxidation state of the sample increases so does the binding energy associated with the core electrons. For a core electron to be emitted the energy of the incident X-ray must be greater than the binding energy. Indeed to be able to detect an electron the energy of the incident X-ray must be greater than that of the binding energy combined with the work function of the spectrometer. The excess energy is measured

as the kinetic energy of the electron. The work function of the spectrometer is the energy required to eject an electron from the Fermi level into the vacuum. The equation below summarises the photoelectric effect.

$$E_K = h\nu - E_B - \varphi$$

Where E_K = Kinetic energy of the ejected electron

$h\nu$ = photon energy

E_B = binding energy

φ = work function of spectrometer

Figure 2.7. represents a simplified energy level diagram of the photoelectric effect equation above. This shows that to eject an electron from a core energy level the energy of the incident X-ray is equal to the binding energy and kinetic energy of the electron, combined with the work function.

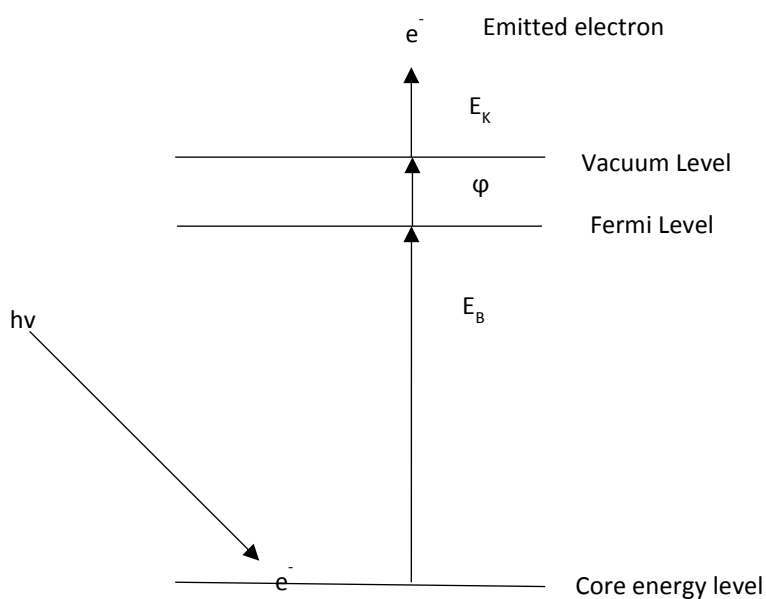


Figure 2.7. Energy level diagram to represent the energy barriers associated with the photoelectric effect.

As XPS is a sensitive technique it provides information about particle dispersion on a support. For a highly dispersed sample the intensity of the signal from the nanoparticles will be high, while in comparison the intensity of the signals associated with the support will be low.

Procedure : XPS analysis was carried out using a Kratos Axis Ultra-DLD spectrometer employing a monochromatic AlKa X-ray source (75-120 W) and analyzer pass energies of 160

eV (for survey scans) or 40 eV (for detailed scans). Samples were mounted using double sided adhesive tape and analysed under ultra-high vacuum (UHV) ($<5 \times 10^{-10}$ Torr). Binding energies were referenced to the C (1s) binding energy of adventitious carbon contamination which was taken to be 84.7eV.

2.10. Temperature Programmed Desorption (TPD).

TPD is an extremely powerful tool for measuring the desorption of adsorbed molecules from a surface with increasing temperature. In TPD studies a sample equilibrated with an adsorbate is heated in a controlled manner. Desorption of the previously adsorbed species occurs when the thermal energy exceeds the adsorption energy. The temperature of desorption therefore indicates the strength of the bond between the adsorbent and the substrate. Quantification of the desorbed species occurs through the use of a TCD. The variation in the thermal conductivity of the gas mixture is measured, to produce a plot of thermal conductivity as a function of sample temperature, allowing for the quantification of adsorbed species. Materials with acidic sites are probed for their acidity using a basis species, such as NH_3 , whilst basic materials are investigated using an acidic probe molecule, such as CO.

NH_3 -TPD was employed to probe the distribution of weak and strong acidic sites present (low and high temperature desorption respectively) and in turn allows for comparison of the acidity the materials investigated.

Procedure:

Temperature programmed desorption (TPD) was carried out using a Quantachrome Industries ChemBET TPR/TPD chemisorption analyser, fitted with a thermal conductivity detector (TCD). 50 mg of sample was pre-treated for 1 h at 130 °C ($15 \text{ }^\circ\text{Cmin}^{-1}$) in He (80 mlmin^{-1}). Ammonia was adsorbed at room temperature for 20 minutes to ensure saturation. Physisorbed ammonia was then removed at 100 °C (1h, $15 \text{ }^\circ\text{Cmin}^{-1}$) in He (80 mlmin^{-1}). Chemisorbed ammonia was subsequently desorbed by heating to 900 °C ($15 \text{ }^\circ\text{Cmin}^{-1}$) in a flow of He (80 ml min^{-1}) with the desorption monitored using a TCD with a current of 180 mV, and an attenuation of 1.

2.11. Infra-red Spectroscopy (IR).

Infra-red spectroscopy is an effective technique to clarify the structure of chemical compounds, it deals with the adsorption of light in the range of 0.8 – 1000 μm . The spectral range is divided into three regions; near-IR (14000-400 cm^{-1}), mid-IR (4000-400 cm^{-1}) and far-IR (400-10 cm^{-1}). IR spectroscopy measures the adsorption of different IR frequencies when a sample is placed in the path of an IR beam. The adsorption of a given frequency of IR-radiation corresponds to the energies involved in bond vibrations (stretching and bending) in the molecule being studied. However not all vibrations can be observed, a general selection rule for the adsorption of an IR photon is that the dipole moment of the molecule must alter during the vibration. The group frequency concept allows functional groups in a molecule to be treated as independent oscillators. The strength of a bond in a functional group can be determined by the position of the bands in the resulting IR spectra, which is derived from Hooke's law, below.

$$\nu = \frac{1}{2\pi c} \sqrt{\frac{k}{\mu}} \text{ where } \mu = \frac{m_A m_B}{m_A + m_B}$$

Where: ν = the wavenumber of the vibration (cm^{-1})

c = the speed of light = $2.998 \times 10^8 \text{ ms}^{-1}$

k = force constant of the bond

μ = reduced mass (g) with m_i = the mass of vibrating atom i (g)

Therefore, functional groups with stronger bonds or consisting of lighter atoms or stronger bonds absorb IR radiation of higher wavelength than those consisting of weaker bonds or heavier atoms.

Several forms of IR spectroscopy can be utilised and within this work both transmission and diffuse reflection forms are employed. The primary difference between these two techniques being that; transmission spectroscopy applies IR radiation through the sample, while in diffuse reflection IR radiation is reflected off the sample surface. These two techniques can therefore be described as bulk and surface techniques respectively.

2.12. CO Chemisorption.

Chemisorption can be thought of as the titration of surface sites by an adsorbate, usually H₂, O₂ or CO, which reacts only with the active phase to form a monolayer. Often it is used to determine metal dispersion, crystallite size and metal surface area on supported metal catalysts. From the experimentally measured adsorbed volume the number of adsorbed moles can be calculated as can the total number of surface atoms. It is then possible to calculate metal dispersion and surface area by knowing the loading of the metal on the support.

A relationship between the diameter of the metal cluster and its dispersion, which can be calculated through assumption that the cluster is spherical. The number of surface atoms can then be defined using the following equation.

$$N_s = \frac{\pi d^2}{S_M}$$

Where : N_s = number of surface atoms.

πd^2 = surface of the metal cluster.

S_M = Atomic cross sectional area.

Procedure:

CO chemisorption analysis was achieved on a Quantachrome ChemBet equipped with a cold trap. Samples (0.05 g) were pre-treated at 100 °C (ramp 20 °C min⁻¹) under helium for 1 hour prior to reduction in order to clean the surface. Analysis was performed by titrating 35 ul CO (BOC 99.99%, 25 ml min⁻¹) over the sample until the stable TCD signal was achieved. CO was pulsed through the apparatus by-passing the sample 3 times for calibration.

2.13. References

1. J.K. Edwards, B. Solsona, P. Landon, A.F. Carley, A. A. Herzing, C. J Kiely and G.J. Hutchings, *J.Catal.*, 2005, **236**, 69-79.
2. S. J. Freakley, R. J. Lewis, D. J. Morgan, J. K. Edwards and G. J. Hutchings, *Catal. Today*, 2015, **248**, 10-17.
3. G. Schwedt, *Essential Guide To Analytical Chemistry*, Wiley and Sons, 1997.
4. J. W. Niemantsverdriet, *Spectroscopy in Catalysis : An Introduction* Wiley VCH, 3 edn., 2000.
5. J. W. Niemantsverdriet, *Spectroscopy in Catalysis: An Introduction*, Wiley-VCH, Second Completely Revised Edition ed. edn., 2000.
6. D. V. D. S. Amelinckx, J. V. Landuyt, *Handbook of Microscopy – Applications in Materials Science, Solid State Physics and Chemistry Methods II.*, 1997.
7. C. Guozhong, *Nanostructures & Nanomaterials Synthesis, Properties & Applications.*, Imperial College Press., 2004.

Appendix. 2. 1

Analysis of reaction mixtures was conducted *via* gas chromatography. The following equations were used to determine cyclohexanone conversion (1, 2 and 3), selectivity towards cyclohexanone oxime (4) and yield of cyclohexanone oxime (5 and 6). Response factors were calculated for cyclohexanone (Figure A.1) and cyclohexanone oxime (Figure B.1) using diethylene glycol monoethyl ether as a standard.

$$(1) \text{ Cyclo. Conversion (\%)} = 100 - \text{Cyclo. Recovery (\%)}$$

$$(2) \text{ Cyclo. Recovery (\%)} = \left(\frac{\text{Final Mass of Cyclo. (g)}}{\text{Initial Mass of Cyclo.}} \right) \times 100$$

$$(3) \text{ Final Mass of Cyclo. (g)} = \left\{ \frac{\left(\frac{\text{GC counts of Cyclo.}}{\text{GC counts of STD-Y intercept from graph A}} \right)}{\left(\text{Slope from graph A} \times \text{Mass of STD (g)} \right)} \right\}$$

$$(4) \text{ Oxime Selectivity} = \frac{\text{Oxime Yield (\%)}}{\text{Cyclo. Conversion (\%)}} \times 100$$

$$(5) \text{ Oxime Yield (\%)} = \left\{ \frac{\left(\frac{\text{Mass of Oxime (g)}}{M_r \text{ Oxime}} \right)}{\left(\frac{\text{Initial Mass of Cyclo. (g)}}{M_r \text{ Cyclo.}} \right)} \right\} \times 100$$

$$(6) \text{ Mass of Oxime (g)} = \left\{ \frac{\left(\frac{\text{GC counts of Oxime}}{\text{GC counts of STD-Y intercept from graph B}} \right)}{\left(\text{Slope from graph B} \times \text{Mass of STD (g)} \right)} \right\}$$

Where:

Cyclo. = Cyclohexanone

Oxime = Cyclohexanone Oxime

STD = Standard (diethylene glycol monoethyl ether)

GC = Gas Chromatograph

M_r = Molar mass

Figure A.1 Obtained response factor for cyclohexanone with respect to diethylene glycol monoethyl ether standard

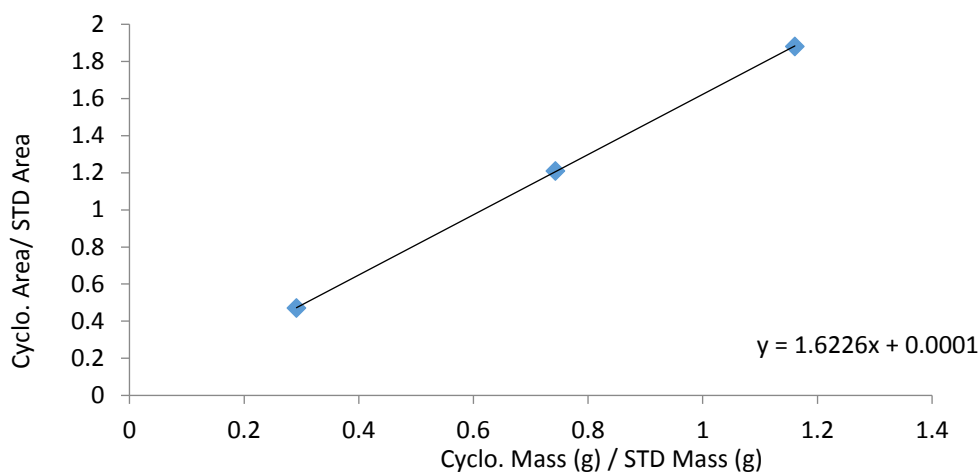
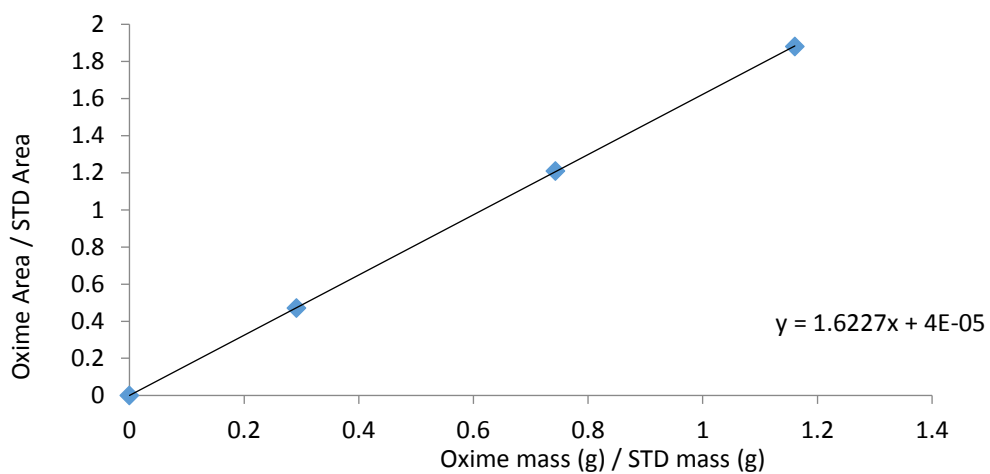


Figure B.1 Obtained response factor for cyclohexanone oxime with respect to diethylene glycol monoethyl ether standard.



3. The Direct Synthesis of H₂O₂ using supported Gold Palladium Catalysts and Heteropolyacid based additives.

3.1. Introduction.

Many studies have been carried out to produce heterogeneous catalysts with activity towards the direct synthesis of H₂O₂, from H₂ and O₂, with the use of supported Pd catalysts prevalent in the literature and largely based upon the seminal work by Pospelova and co-workers¹⁻³. However, these monometallic Pd catalysts, although highly active towards the direct synthesis of H₂O₂ also have activity to its subsequent degradation⁴. The introduction of Au into a Pd-only catalyst has been shown to produce a significantly more active catalyst, with superior selectivity to the monometallic Pd analogue.^{5,6} The utilisation of halides and acids, either as part of the reaction medium or incorporated into catalyst preparation are reported to limit the subsequent degradation pathways, in particular H₂O₂ decomposition.⁷⁻⁹ However the utilisation of halides and acidic reaction media can present some issues, in particular the cost of neutralising and replacing the promoters as well as corrosion caused to the reaction vessel and subsequent maintenance costs associated with such issues.

The almost super-acidic nature of heteropolyacids (HPAs) such as tungstophosphoric acid (H₃PW₁₂O₄₀) has been well studied¹⁰ and the ability to produce insoluble salts of these solid acids through the incorporation of cations such as Cs⁺, Rb⁺ and K⁺ has led to their investigation as acidic supports in the direct synthesis of H₂O₂. Indeed Park *et.al.* have studied Pd-exchanged heteropolyacids with varying Cs-content and shown that the most acidic catalyst (Pd_{0.15}Cs_{2.5}H_{0.5}PW₁₂O₄₀) was the most active towards the synthesis of H₂O₂¹¹. Sun *et.al.* have reported that Pd based catalysts utilising a heteropolyacid support show greater productivity and selectivity towards H₂O₂ when compared to more conventional supports¹². Hutchings and co-workers have investigated Au-Pd supported and exchanged heteropolyacids, under conditions deemed less conducive to H₂O₂ synthesis and shown that these catalysts afford superior activity compared to catalysts previously investigated under optimised reaction conditions^{13 14}. However both these studies do not investigate the extent of Cs incorporation into the H₃PW₁₂O₄₀ structure to a great extent, its effect on promoting catalytic activity towards the synthesis of H₂O₂ or the combination of Cs_xH₃.

$x\text{PW}_{12}\text{O}_{40}$ salts and catalysts already established as active towards the direct synthesis of H_2O_2 . Within this Chapter the extent of Cs incorporation in to $\text{H}_3\text{PW}_{12}\text{O}_{40}$ is explored in an attempt to improve catalytic activity towards H_2O_2 synthesis.

In an attempt to improve catalytic activity towards the direct synthesis of H_2O_2 the use of Cs-exchanged tungstophosphoric acid in addition to a well-established catalyst, known to be active towards H_2O_2 synthesis. In this case 2.5 wt. % Au – 2.5 wt. % Pd / TiO_2 is studied. The degree of Cs exchange and the amount of Cs-exchanged tungstophosphoric acid promotor used, as an additive with 2.5 wt. % Au – 2.5 wt. % Pd / TiO_2 were investigated. The effect of these two parameters on catalytic activity towards the direct synthesis of H_2O_2 and its subsequent degradation under standard reaction conditions, outlined in Chapter 2, were studied. Furthermore, reaction conditions were optimised, utilising the most effective Cs-exchanged additive and an investigation into the promotive role of Cs-exchanged tungstophosphoric acid on catalytic activity was carried out. Finally, reusability of these HPA-promoted catalyst systems was studied.

A supported Au-Pd catalyst was prepared using the standard wet impregnation technique using PdCl_2 and $\text{HAuCl}_4 \cdot 3\text{H}_2\text{O}$ as metal precursors and TiO_2 as the support, as outlined in Chapter 2, Section 2.2.1. While the metal exchanged heteropolyacids were produced via an ion exchange procedure, where the required metal nitrate and parent heteropolyacid were used as precursors.

All H_2O_2 synthesis and degradation testing was carried out according to the procedures discussed previously in Chapter 2, unless otherwise stated. For reference a summary of the testing conditions are given below. Blank degradation reactions, in the absence of a catalyst were carried out on a regular basis to determine reactor contribution to H_2O_2 degradation. If reactor contamination were determined to contribute to H_2O_2 degradation these were removed using aqua-regia followed by thorough cleaning with water. A subsequent blank reaction was then carried out subsequent to catalysed reactions.

Rate of H_2O_2 synthesis determined after reaction under standard reaction conditions:

5% H_2 / CO_2 (2.9 MPa) and 25% O_2 / CO_2 (1.1 MPa) , 8.5 g solvent (5.6 g methanol + 2.9 g H_2O), 0.01 g catalyst, 2 °C , 1200 rpm, 30 mins.

Rate of H₂O₂ degradation determined from the amount of H₂O₂ that is hydrogenated under standard reaction conditions:

2.9 MPa 5%H₂ / CO₂, 8.5 g solvent (5.6 g MeOH, 2.22 g H₂O and 0.68 g H₂O₂ (50 wt. %)), 0.01 g catalyst, 2 °C, 1200 rpm, 30 mins.

3.2. Results and discussion.

3.2.1. The direct synthesis of H₂O₂ using 2.5 wt. % Au – 2.5 wt. % Pd / TiO₂ catalyst and Cs-exchanged heteropolyacids.

To determine whether heteropolyacid additives show intrinsic activity towards the direct synthesis of H₂O₂, a range of free and Cs – exchanged tungstophosphoric acids were assessed and the results are shown in Table 3.1

Table 3.1. Productivity and degradation of catalysts, towards H₂O₂, under standard reaction conditions.

Catalyst	Productivity / mol _{H₂O₂} kg _{cat} ⁻¹ h ⁻¹	Degradation / mol _{H₂O₂} kg _{cat} ⁻¹ h ⁻¹
No catalyst	0	0
H ₃ PW ₁₂ O ₄₀	0	35
Cs _{0.1} H _{2.9} PW ₁₂ O ₄₀	0	39
CsH ₂ PW ₁₂ O ₄₀	0	63
Cs ₂ HPW ₁₂ O ₄₀	0	88
Cs _{2.5} H _{0.5} PW ₁₂ O ₄₀	0	124
Cs ₃ PW ₁₂ O ₄₀	0	187
2.5 wt. % Au – 2.5 wt. % Pd/TiO ₂	64	213

Reaction conditions: 2.5 wt. % Au – 2.5 wt. % Pd /TiO₂ (0.01g) or Cs_xH_{3-x}PW₁₂O₄₀ (0.01g), total pressure 580 psi, H₂ / O₂ = 0.525, 1200 rpm, 30 min, 5.6 g CH₃OH + 2.9 g H₂O (66 wt. % CH₃OH), 2°C .

It can be observed in Table 3.1 that there is no H₂O₂ formation or degradation in the absence of a AuPd catalyst or tungstophosphoric acid promotor. The productivity and degradation values observed for the 2.5 wt. % Au- 2.5 wt.% Pd / TiO₂ catalyst are 64 and 213 mol_{H₂O₂}kg_{cat}⁻¹h⁻¹ respectively. All Cs_xH_{3-x}PW₁₂O₄₀ salts with and without Cs exchanged into the Keggin structure are observed to have no activity towards H₂O₂ synthesis but are active towards its degradation. Indeed, the degradation activity for Cs₃PW₁₂O₄₀ is reported as 187 mol_{H₂O₂}kg_{cat}⁻¹h⁻¹ while the lower loaded Cs_{0.1}H_{2.9}PW₁₂O₄₀ has much less degradation activity, 39 mol_{H₂O₂}kg_{cat}⁻¹h⁻¹, comparable to the parent tungstophosphoric acid, with the activity of H₃PW₁₂O₄₀ towards H₂O₂ degradation observed to be 35 mol_{H₂O₂}kg_{cat}⁻¹h⁻¹. A correlation between the extent of Cs loading and the degree of H₂O₂ degradation can be made, with those additives with greater Cs-loading observed to be more active towards the degradation

of H₂O₂. It is known that H₂O₂ has greater stability under acidic reaction conditions and readily decomposes to H₂O in an alkaline medium. As such it is possible that by increasing the value of x in Cs_xH_{3-x}PW₁₂O₄₀, that is increasing Cs content, the surface acidity decreases and as such the extent of H₂O₂ degradation increases.

It has been suggested by Park *et.al*¹⁵, who investigated the direct synthesis of H₂O₂ using Pd exchanged tungstophosphoric acid, that by increasing Cs content it is possible to increase the surface acidity of the exchanged heteropolyacid, to a critical Cs loading; beyond this point surface acidity decreases. Dias and co-workers¹⁶ report that surface acidity follows the following trend H₃PW₁₂O₄₀ > Cs₂HPW₁₂O₄₀ ≈ Cs_{2.5}H_{0.5}PW₁₂O₄₀ > CsH₂PW₁₂O₄₀ >> Cs₃PW₁₂O₄₀. This suggests that the role of surface acidity may not be the critical factor in determining the activity of Cs-exchanged HPAs towards H₂O₂ degradation. However the general trend in the activity of the Cs_xH_{3-x}PW₁₂O₄₀ salts towards H₂O₂ degradation is very similar to the trend in surface acidity reported by Dias and co-workers¹⁶.

It is suggested that the introduction of Cs reduces the solubility of H₃PW₁₂O₄₀ through the formation of an insoluble Cs salt. Narasimharao *et.al*.¹⁷ report the formation of insoluble Cs-exchanged H₃PW₁₂O₄₀ for Cs_xH_{3-x}PW₁₂O₄₀ with values of x as little as 0.9. The ability of Cs-exchange into the Keggin unit to reduce the solubility of H₃PW₁₂O₄₀ is discussed below.

3.2.2. The effect of Cs-exchanged of tungstophosphoric acid on the promotion of 2.5 wt. % Au – 2.5 wt. % Pd / TiO₂ towards the direct synthesis of H₂O₂.

It is shown in Table 3.1 that decreasing the extent of Cs exchanged into the HPA structure results in a lower rate of H₂O₂ degradation, when the additive is not used in conjunction with a catalyst that is active towards H₂O₂ synthesis. The effect that the addition of Cs-exchanged HPAs (with varying Cs content) has on the direct synthesis of H₂O₂ is shown in Figure 3.1

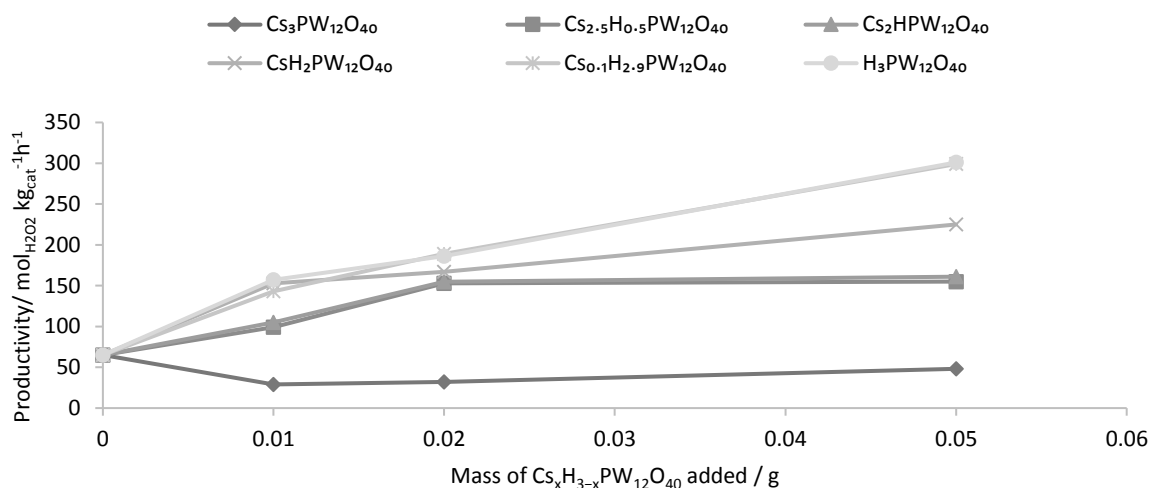


Figure 3.1. H_2O_2 Productivity for 2.5 wt. % Au – 2.5 wt. % Pd / TiO_2 and $Cs_xP_{3-x}W_{12}O_{40}$ as a function of additive loading.

Reaction conditions: 2.5 wt. % Au – 2.5 wt. % Pd / TiO_2 (0.01g), $Cs_xP_{3-x}W_{12}O_{40}$ (X g), total pressure 580 psi, $H_2 / O_2 = 0.525$, 1200 rpm, 30 min, 5.6 g CH_3OH + 2.9 g H_2O (66 wt. % CH_3OH), 2 °C.

It can be observed in Figure 3.1 that the addition of $Cs_xP_{3-x}W_{12}O_{40}$, with values of x ranging from 0 to 2.5, to 2.5 wt. % Au – 2.5 wt. % Pd / TiO_2 results in an increase in the rate of H_2O_2 formation. While the addition of $Cs_3PW_{12}O_{40}$ causes a decrease in productivity. Indeed with the addition of 0.01 g of $Cs_3PW_{12}O_{40}$ productivity drops to a minimum value of 29 $mol_{H_2O_2}Kg_{cata}^{-1}h^{-1}$, upon further addition of $Cs_3PW_{12}O_{40}$ productivity slowly increases to reach a value of 48 $mol_{H_2O_2}Kg_{cata}^{-1}h^{-1}$ when 0.05g of $Cs_3PW_{12}O_{40}$ is utilised. It is suggested that the increase in catalyst activity towards H_2O_2 observed with increasing addition of $Cs_3PW_{12}O_{40}$ is related to incomplete exchange of the protons within the Keggin structure. As such some promotional effect towards improving catalytic activity towards H_2O_2 synthesis remains. It is suggested that the exact composition of the $Cs_xP_{3-x}W_{12}O_{40}$ salts be investigated to determine the effectiveness of the ion exchange technique. However, it should be noted that regardless of the amount of $Cs_3PW_{12}O_{40}$ added catalytic activity is still significantly lower than the activity observed when only the 2.5 wt. % Au – 2.5 wt. % Pd / TiO_2 catalyst is utilised (64 $mol_{H_2O_2}Kg_{cat}^{-1}h^{-1}$). For all $Cs_xP_{3-x}W_{12}O_{40}$ additives investigated the rate of H_2O_2 synthesis increases with increasing additive mass.

The rate of H_2O_2 synthesis is observed to increase with the addition of $Cs_xP_{3-x}W_{12}O_{40}$ according to the following order: $H_3PW_{12}O_{40} = Cs_{0.1}PW_{12}O_{40} > Cs_1PW_{12}O_{40} > Cs_2PW_{12}O_{40} = Cs_{2.5}PW_{12}O_{40} > Cs_3PW_{12}O_{40}$. It is observed that $H_3PW_{12}O_{40}$ and $Cs_{0.1}PW_{12}O_{40}$ show approximately the same improvement towards H_2O_2 synthesis, regardless of the amount utilised in addition to the catalyst, which is in good agreement with the data previously

reported in Table 3.1. It can also be observed that the rate of H₂O₂ synthesis is comparable when Cs₂PW₁₂O₄₀ and Cs_{2.5}PW₁₂O₄₀ are employed as additives.

The effect that the addition of 0.05 g of Cs-exchanged and non Cs-exchanged H₃PW₁₂O₄₀ has on H₂ conversion and selectivity, when these additives are used in conjunction with 2.5 wt. % Au – 2.5 wt. % Pd / TiO₂ is shown in Table 3.2

Table 3.2. The effect of Cs exchanged HPAs on H₂ conversion and selectivity, under standard reaction conditions.

Cs _x P _{3-x} W ₁₂ O ₄₀ added	Productivity / mol _{H₂O₂} kg _{cat} ⁻¹ h ⁻¹	H ₂ conversion / %	H ₂ Selectivity / %
No Cs _x H _{3-x} PW ₁₂ O ₄₀	64	21	61
H ₃ PW ₁₂ O ₄₀	301	70	85
Cs _{0.1} H _{2.9} PW ₁₂ O ₄₀	299	69	86
CsH ₂ PW ₁₂ O ₄₀	225	66	63
Cs ₂ HPW ₁₂ O ₄₀	161	55	54
Cs ₃ PW ₁₂ O ₄₀	48	47	22

Reaction conditions: 2.5 wt. % Au – 2.5 wt. % Pd /TiO₂ (0.01g), Cs_xH_{3-x}PW₁₂O₄₀ (0.05g), total pressure 580 psi, H₂ / O₂ = 0.525, 1200 rpm, 30 min, 5.6 g CH₃OH + 2.9 g H₂O (66 wt. % CH₃OH), 2°C.

It is observed in Table 3.2 that the addition of Cs_xP_{3-x}W₁₂O₄₀, with or without the introduction of Cs into the Keggin structure, increases H₂ conversion, when compared to 2.5 wt. % Au – 2.5 wt. % Pd / TiO₂ catalyst alone. The highest rate of H₂ conversion is observed when H₃PW₁₂O₄₀ is utilised (70%) and this value is very similar to that observed for Cs_{0.1}H_{2.9}PW₁₂O₄₀ (69%). Measurement of H₂ selectivity shows that Cs_xH_{3-x}PW₁₂O₄₀ with values of x varying from 0 to 3 can be divided into two groups; those where Cs loading is greater than or equal to Cs_{2.0} and those with Cs loading equal to or lower than Cs_{1.0}. The former group is observed to lead to a decrease in H₂ selectivity, when compared to the 2.5 wt. % Au- 2.5 wt. % Pd/TiO₂ catalyst with a significant decrease observed when Cs₃PW₁₂O₄₀ is used alongside the catalyst, with H₂ selectivity falling to 22%. The latter group is observed to lead to a significant increase in H₂ selectivity with both H₃PW₁₂O₄₀ and Cs_{0.1}H_{2.9}PW₁₂O₄₀ reported to improve selectivity to above 80%.

To understand these trends the ability of the Cs_xH_{3-x}PW₁₂O₄₀ salts to promote the leaching of Au and Pd from the TiO₂ support as well as the solubility of the Cs_xH_{3-x}PW₁₂O₄₀ salt were determined by analysis of the post reaction solution by MP-AES. In particular the concentration of Cs and W in the post reaction solution were quantified and results of these studies are shown in Table 3.3. Furthermore the effect that the addition of Cs_xH_{3-x}PW₁₂O₄₀ of varying value of x has on the pH of the reaction solution prior to the reaction was measured and the results can be seen in Table 3.4.

Table 3.3. Leaching of Pd, Cs and W during the direct synthesis of H₂O₂ using 2.5 wt. % Au – 2.5 wt.% Pd/TiO₂ and Cs_xH_{3-x}PW₁₂O₄₀.

Catalyst	Pd / ppm	Au / ppm	Cs / ppm	W / ppm
H ₃ PW ₁₂ O ₄₀	9	0	0	1834
Cs _{0.1} H _{2.9} PW ₁₂ O ₄₀	8	0	0.05	1723
CsH ₂ PW ₁₂ O ₄₀	5	0	0.6	1096
Cs ₂ HPW ₁₂ O ₄₀	2	0	183	564
Cs _{2.5} H _{0.5} PW ₁₂ O ₄₀	1	0	150	359
Cs ₃ PW ₁₂ O ₄₀	1	0	95	240

Reaction conditions: 2.5 wt. % Au – 2.5 wt. % Pd / TiO₂ (0.01g), Cs_xH_{3-x}PW₁₂O₄₀ (0.05g), total pressure 580 psi, H₂ / O₂ = 0.525, 1200 rpm, 30 min, 5.6 g CH₃OH + 2.9 g H₂O (66 wt. % CH₃OH), 2°C.

Firstly it should be observed that no Au is detected in the post reaction solution, regardless of Cs content within the Cs_xP_{3-x}W₁₂O₄₀ salt. In comparison Pd is detected in all post reaction solutions, regardless of Cs content. These observations may be explained by the greater support – metal interaction for Au in comparison to Pd or the greater propensity for Pd to be oxidised.

It is observed that as the value of x in Cs_xH_{3-x}PW₁₂O₄₀ increases the amount of Pd detected in the post reaction solution decreases from 9 ppm when H₃PW₁₂O₄₀ is utilised to 1 ppm when Cs₃PW₁₂O₄₀ additive is used, as determined by analysis of the post reaction solution by MP-AES. It should be noted that the percentage of leached Pd when H₃PW₁₂O₄₀ is used as an additive is equivalent to 30 % of total Pd loading on the catalyst.

Investigation of the reaction solution by MP-AES shows that as the degree of Cs incorporation increases the solubility of Cs_xH_{3-x}PW₁₂O₄₀ decreases. H₃PW₁₂O₄₀, Cs_{0.1}PW₁₂O₄₀ and Cs₁PW₁₂O₄₀ are all highly soluble in the reaction solution, with the concentration of W particularly high for these three Cs_xH_{3-x}PW₁₂O₄₀ salts. The concentration of W is observed to decrease from 1843 ppm when H₃PW₁₂O₄₀ is utilised to 1096 ppm when CsH₂PW₁₂O₄₀ is utilised. Further addition of Cs decreases the concentration of W detected decreasing dramatically, reaching 240 ppm for the Cs₃PW₁₂O₄₀ additive. This suggests that incorporation of Cs is required to reduce the solubility of H₃PW₁₂O₄₀.

It is observed that the concentration of dissolved Cs within the reaction solution increases with the value of “x” in Cs_xH_{3-x}PW₁₂O₄₀, passing through a maximum, of 183 ppm with Cs₂HPW₁₂O₄₀. As Cs incorporation into the Keggin structure increases, as when Cs₃PW₁₂O₄₀ is used as an additive the concentration of Cs detected in the reaction solution decreases, to 95 ppm. This suggests that Cs incorporation is required to lower the solubility of the heteropolyacid. However, it is observed that even at the highest degree of Cs exchange, when the Cs₃PW₁₂O₄₀ additive is utilised, both Cs (95 ppm) and W (240 ppm) are detected in the reaction solution suggesting that these materials are still partially soluble.

The effect of the Cs content within the Keggin unit on pH of the reaction solution prior to the reaction was measured and the results are outlined in Table 3.4.

Table 3.4. The pH of the reaction solution for the direct synthesis of H₂O₂ using 2.5 wt. % Au – 2.5 wt.% Pd/TiO₂ and Cs_xH_{3-x}PW₁₂O₄₀

Catalyst	pH	Productivity/ mol _{H₂O₂} kg _{cat} ⁻¹ h ⁻¹
No catalyst	7	0
H ₃ PW ₁₂ O ₄₀	2.66	301
Cs _{0.1} H _{2.9} PW ₁₂ O ₄₀	2.68	299
CsH ₂ PW ₁₂ O ₄₀	3.33	225
Cs ₂ HPW ₁₂ O ₄₀	3.82	161
Cs _{2.5} H _{0.5} PW ₁₂ O ₄₀	3.90	155
Cs ₃ PW ₁₂ O ₄₀	6.30	48
Au Pd/TiO ₂	7	64

Reaction conditions: 2.5 wt. % Au – 2.5 wt. % Pd /TiO₂ (0.01g), Cs_xH_{3-x}PW₁₂O₄₀ (0.05g), total pressure 580 psi, H₂ / O₂ = 0.525, 1200 rpm, 30 min, 5.6 g CH₃OH + 2.9 g H₂O (66w. % CH₃OH), 2°C .

It is observed that the pH of the reaction solution decreases with the addition of all HPA additives. This is the most pronounced for the free Cs-acid H₃PW₁₂O₄₀ and Cs_{0.1}H_{2.9}PW₁₂O₄₀ (pH 2.66 and 2.68 respectively). Catalytic activity towards the direct synthesis of H₂O₂ is observed to correlate with the pH of the reaction solution, with the exception of Cs₃PW₁₂O₄₀. Interestingly the addition of Cs₃PW₁₂O₄₀ lowers the pH of the reaction solution but does not improve catalytic activity towards H₂O₂ formation. As Cs incorporation into the HPA structure decreases the pH of the reaction solution decreases. Through addition of Cs_{0.1}H_{2.9}PW₁₂O₄₀ the reaction solution pH is lowered to 2.68, this is very similar to that observed when the H₃PW₁₂O₄₀ additive is utilised (2.66) in addition to the 2.5 wt. % Au – 2.5 wt. % Pd / TiO₂ catalyst. It is known that acidic reaction conditions are beneficial to H₂O₂ stability¹⁸ and it is suggested that the incorporation of Cs exchanged HPAs and the resulting decrease in pH play a significant role in improving catalytic activity towards the formation of H₂O₂.

Table 3.5 shows the activity of the reaction solution towards H₂O₂ synthesis. After a standard reaction with 2.5 wt. % Au – 2.5 wt. % Pd / TiO₂ (0.01g) and Cs_xH_{3-x}PW₁₂O₄₀ (0.05g) the catalyst is removed by filtration. The reaction solution was then investigated for activity towards H₂O₂ synthesis.

Table 3.5. H₂O₂ Productivity for the reaction solution of 2.5 wt. % Au – 2.5 wt. % Pd / TiO₂ and Cs₃PW₁₂O₄₀.

Catalyst	Leached Pd / ppm	Leached Au / ppm	Net Productivity / mol _{H₂O₂} kg _{cat} ⁻¹ h ⁻¹	H ₂ conversion / %	H ₂ Selectivity / %
No Cs _x P _{3-x} W ₁₂ O ₄₀	n.d	0	0	0	0
H ₃ PW ₁₂ O ₄₀	9	0	19	7	75
Cs _{0.1} H _{2.9} PW ₁₂ O ₄₀	8	0	17	7	74
CsH ₂ PW ₁₂ O ₄₀	5	0	12	5	72
Cs ₂ HPW ₁₂ O ₄₀	1	0	3	2	73
Cs ₃ PW ₁₂ O ₄₀	1	0	3	2	71

Reaction conditions: 2.5 wt. % Au – 2.5 wt. % Pd / TiO₂ (0.01g), Cs_xP_{3-x}W₁₂O₄₀ (0.05 g), total pressure 580 psi, H₂ / O₂ = 0.525, 1200 rpm, 30 min, 5.6 g CH₃OH + 2.9 g H₂O (66 wt. % CH₃OH), 2 °C.

Where **n.d.** = none detected.

It is observed that when the 2.5 wt. % Au – 2.5 wt. % Pd / TiO₂ catalyst is used in the absence of a HPA promotor there is no leached metal detected and the reaction solution has no activity towards the formation of H₂O₂. Furthermore, it can be observed that only Pd is leached from the catalyst when it is used in addition to the Cs_xP_{3-x}W₁₂O₄₀ salt, regardless of the extent of Cs incorporation. It should be noted that no Au is detected within the reaction solution, possibly suggesting that the metal – support interaction for Au is greater than for Pd.

It is possible to report that there is some homogenous activity towards the direct synthesis of H₂O₂ for reaction solutions where heteropolyacid promoters were used in addition to 2.5 wt. % Au – 2.5 wt. % Pd / TiO₂. Indeed a general trend can be discerned whereby net activity towards H₂O₂ formation decreases as the value of “x” in Cs_xH_{3-x}PW₁₂O₄₀ increases, from 19 to 3 mol_{H₂O₂}kg_{cat}⁻¹h⁻¹ as Cs incorporation increases from H₃PW₁₂O₄₀ to Cs₃PW₁₂O₄₀. This activity can be related to Pd content within the reaction solution, regardless of Cs content, Pd is leached from the catalyst support. The extent of leaching decreases as the Cs content increases, with a maximum of 9 ppm Pd detected when the H₃PW₁₂O₄₀ additive is utilised. This correlates with the activity towards H₂O₂ synthesis. However, as stated previously 9 ppm Pd can be equated to approximately 30 % of the total Pd present on the catalyst. It may be expected that the activity of the leached metal in the reaction solution may be greater than that observed, it is suggested that the leached Pd is deposited on the liner of the reactor limiting activity towards the direct synthesis of H₂O₂. However further investigation into this is still required.

As expected given the relatively low values of productivities observed, the extent of H₂ conversion is particularly low, with the greatest H₂ conversion observed for the reaction solutions when both H₃PW₁₂O₄₀ and Cs_{0.1}H_{2.9}PW₁₂O₄₀ are utilised, with H₂ conversion of 7 %

reported when both of these additives are used. In comparison, when these two additives are used in addition to 2.5 wt. % Au – 2.5 wt. % Pd / TiO₂ in a standard reaction H₂ conversion is much greater, with values of 70 and 69 % reported for H₃PW₁₂O₄₀ and Cs_{0.1}H_{2.9}PW₁₂O₄₀ respectively .

Unlike for H₂ conversion H₂ selectivity is high, with values of over 70 % reported regardless of Cs content and this is expected as H₂ conversion is particularly low. Lunsford and co-workers¹⁹ have previously established the role of leached Pd for the direct synthesis, when 5 wt. % Pd / SiO₂ is utilised in addition to 1.0 M HCl and they attribute the loss of Pd to the presence of HCl in the reaction solution and the formation of PdCl₄²⁻. Indeed upon removal of the heterogeneous catalyst they report a net increase in H₂O₂ concentration of approximately 0.02 wt. % H₂O₂. This is similar to the net increase in wt. % H₂O₂ observed upon removal of the 2.5 wt. % Au – 2.5 wt. % Pd / TiO₂ catalyst when used in addition to H₃PW₁₂O₄₀.

These results demonstrate that the presence of H₃PW₁₂O₄₀, is able to promote the leaching of Pd from the catalyst support and that as Cs exchange into the Keggin structure increases the extent of Pd leaching decreases. Furthermore it has been shown that the leached Pd has some activity towards the direct synthesis of H₂O₂ and although this activity is limited when the reaction solution is investigated for activity towards the direct synthesis of H₂O₂ the contribution of the leached Pd may be greater during a standard reaction. That is when the 2.5 wt. % Au – 2.5 wt. % Pd / TiO₂ catalyst is used in addition with Cs_xH_{3-x}PW₁₂O₄₀.

Further analysis of the Cs-exchanged HPAs was carried out using NH₃-TPD and the results are seen in Figure 3.2.

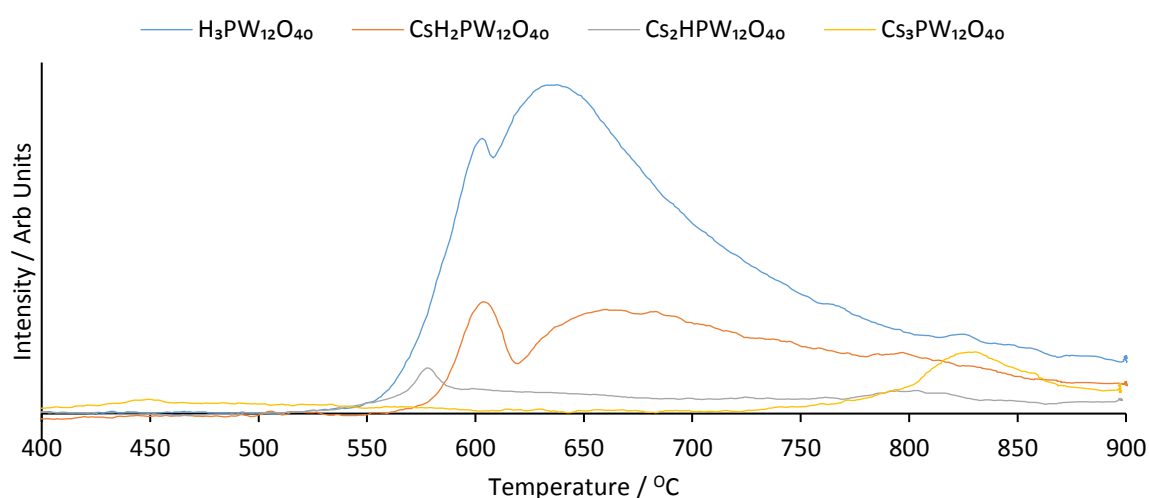


Figure 3.2. NH₃-TPD of in Cs_xH_{3-x}PW₁₂O₄₀ salts where x = 0, 1, 2 and 3.

It can be observed in Figure 3.2 that there is a correlation between acidity and Cs content. A trend is observed where acidity increases in the following order: $\text{H}_3\text{PW}_{12}\text{O}_{40} > \text{Cs}_1\text{PW}_{12}\text{O}_{40} > \text{Cs}_2\text{PW}_{12}\text{O}_{40} > \text{Cs}_3\text{PW}_{12}\text{O}_{40}$. These results are in good agreement with previous studies, which show a decrease of the acidity with an increase of the Cs content²⁰.

The Keggin structure of $\text{H}_3\text{PW}_{12}\text{O}_{40}$ has previously been reported to consist of a PO_4 tetrahedron surrounded by twelve WO_6 octahedra, which share edges in W_3O_{13} triad groups and corners between each triad through oxygen atoms²¹. From the structure it is possible to deduce four types of oxygen atoms, which are reported to provide for characteristic infrared bands in the range $1200 - 700 \text{ cm}^{-1}$. The exact position of these bands are known to depend upon the extent of hydration of the heteropolyacid²² and the nature of the counter cation present²³.

FTIR spectra of the $\text{Cs}_x\text{H}_{3-x}\text{PW}_{12}\text{O}_{40}$ salts were collected after preparation and calcination (300°C , 2h, static air). The spectra of the $\text{Cs}_x\text{H}_{3-x}\text{PW}_{12}\text{O}_{40}$ salts are shown in Figure 3.3.

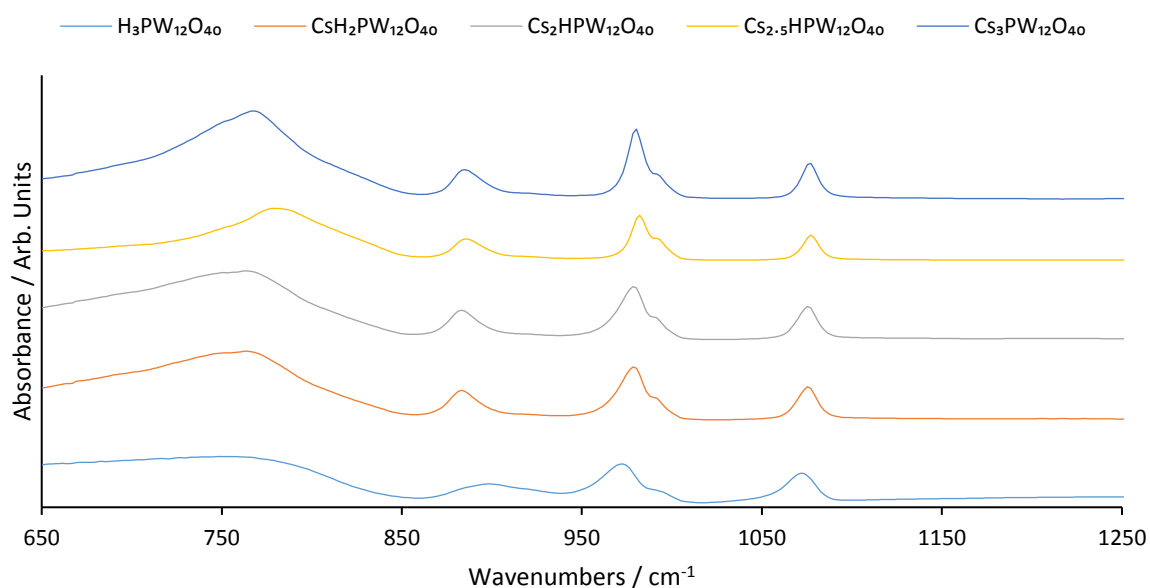


Figure 3.3. FTIR spectra of $\text{Cs}_x\text{H}_{3-x}\text{PW}_{12}\text{O}_{40}$ salts after calcination at 200°C , 3h, static air.

The Keggin structure of $\text{H}_3\text{PW}_{12}\text{O}_{40}$ has previously been reported to consist of a PO_4 tetrahedron surrounded by twelve WO_6 octahedra, which share edges in W_3O_{13} triad groups and corners between each triad through oxygen atoms. From the structure it is possible to deduce four types of oxygen atoms, which are reported to provide four characteristic bands in the range $1200- 700 \text{ cm}^{-1}$. The exact position of these bands are known to depend upon the extent of hydration of the heteropolyacid and the nature of the counter cation present²¹.

It is possible to observe four distinct infrared bands in Figure 3.3 and it possible to assign these as follows; $\nu(\text{P-O}) = 1080 \text{ cm}^{-1}$, $\nu(\text{W-O}_c\text{-W}) = 883 \text{ cm}^{-1}$, $\nu(\text{W-O}_e\text{-W}) = 784 \text{ cm}^{-1}$. However the typical vibration of $\nu(\text{W=O}) = 983 \text{ cm}^{-1}$ of $\text{H}_3\text{PW}_{12}\text{O}_{40}$ (HPA) can be observed to split into two components at 983 and 995 cm^{-1} . This splitting can be assigned to W=O associated with $\text{H}^+(\text{H}_2\text{O})_n$ species (983 cm^{-1}), as in hydrated $\text{H}_3\text{PW}_{12}\text{O}_{40}$ and W=O interacting with Cs^+ ions (995 cm^{-1}), this is in keeping with previous investigations reported by Essayem *et.al.*²² the weaker interactions of Cs^+ with W=O causes a strengthening of the latter bonds owing to its increase in double bond character, resulting in a higher frequency shift.

XRD patterns were also recorded for all the $\text{Cs}_x\text{H}_{3-x}\text{PW}_{12}\text{O}_{40}$ salts and are reported in Figure 3.4.

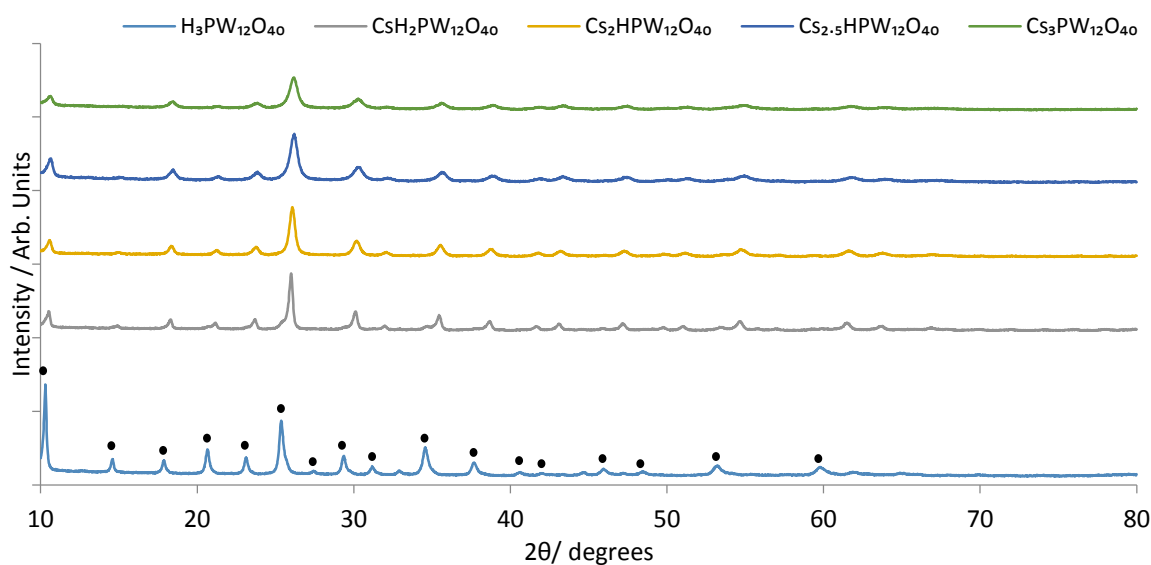


Figure 3.4. X-ray diffractogram of $\text{Cs}_x\text{H}_{3-x}\text{PW}_{12}\text{O}_{40}$ salts, where $x = 0-3$, calcined $200 \text{ }^\circ\text{C}$ in static air, ramp rate = $20 \text{ }^\circ\text{C min}^{-1}$. ●: $\text{H}_3\text{PW}_{12}\text{O}_{40}$

Figure 3.4 shows a sharp, intense diffraction pattern for the parent heteropolyacid indicating that the tungstophosphoric acid parent material is highly crystalline. Upon incorporation of Cs^+ the reflections broaden and decrease in intensity indicating a loss in crystallinity. The detected reflections of the $\text{Cs}_x\text{H}_{3-x}\text{PW}_{12}\text{O}_{40}$ salts are consistent with the cubic structure of $\text{H}_3\text{PW}_{12}\text{O}_{40}$ (ICDD number 00-050-0657) as the catalysts prepared have similar Cs^+ content. The main reflections associated with the $\text{H}_3\text{PW}_{12}\text{O}_{40}$ parent material are shifted towards higher 2θ values in the $\text{Cs}_x\text{H}_{3-x}\text{PW}_{12}\text{O}_{40}$ salts, consistent with an expansion of the tungstophosphoric acid unit cell upon introduction of Cs .

Surface area was measured using nitrogen adsorption for all the samples and is shown in Table 3.6.

Table 3.6. BET surface area of $\text{H}_3\text{PW}_{12}\text{O}_{40}$ with varied levels of Cs^+ incorporation.

Catalyst	Surface area / m^2g^{-1}
$\text{H}_3\text{PW}_{12}\text{O}_{40}$	0.52
$\text{Cs}_{0.1}\text{H}_{2.9}\text{PW}_{12}\text{O}_{40}$	0.47
$\text{CsH}_2\text{PW}_{12}\text{O}_{40}$	3.50
$\text{Cs}_{1.5}\text{H}_{1.5}\text{PW}_{12}\text{O}_{40}$	6.82
$\text{Cs}_2\text{HPW}_{12}\text{O}_{40}$	49.67
$\text{Cs}_{2.5}\text{H}_{0.5}\text{PW}_{12}\text{O}_{40}$	111.50
$\text{Cs}_3\text{PW}_{12}\text{O}_{40}$	121.13

Catalysts calcined 2 h, 300 °C, static air, ramp = 20 °C min^{-1}

A trend was observed where those samples with greater Cs^+ loading demonstrated greater surface areas. The $\text{Cs}_3\text{PW}_{12}\text{O}_{40}$ solid acid additive showed the highest surface area of 121 m^2g^{-1} . This correlates well with XRD analysis of these materials, which shows that with increasing degree of Cs^+ incorporation there is a decrease in crystallinity of the material. Interestingly the additives that provide the greatest promotion towards H_2O_2 synthesis have the lowest surface area, with the addition of $\text{Cs}_3\text{PW}_{12}\text{O}_{40}$ lowering catalytic activity towards H_2O_2 synthesis, from 64 to 48 $\text{mol}_{\text{H}_2\text{O}_2}\text{Kg}_{\text{cat}}^{-1}\text{h}^{-1}$. The addition of $\text{H}_3\text{PW}_{12}\text{O}_{40}$, with a surface area of 0.52 m^2g^{-1} improves catalytic activity by a factor of approximately 3.7 to 239 $\text{mol}_{\text{H}_2\text{O}_2}\text{Kg}_{\text{cat}}^{-1}\text{h}^{-1}$ suggesting that this characteristic is not important in improving catalytic activity towards H_2O_2 synthesis. This enhancement can be related to both the amount of Cs leached from the Keggin structure and the pH of the reaction solution when the $\text{Cs}_x\text{H}_{3-x}\text{PW}_{12}\text{O}_{40}$ salts are used in addition to the 2.5 wt. % Au – 2.5 wt. % Pd / TiO_2 catalyst with the salts containing less Cs offering greater acidity and therefore improved H_2O_2 stability in addition to a and a lower amount of Cs being introduced into reaction solution. As such the extent of H_2O_2 degradation is decreased in comparison to when the $\text{Cs}_x\text{H}_{3-x}\text{PW}_{12}\text{O}_{40}$ salts with greater Cs incorporation are utilised in addition to the catalyst.

It was observed in Figure 3.1 that the utilisation of $\text{Cs}_x\text{H}_{3-x}\text{PW}_{12}\text{O}_{40}$ salts in addition to 2.5 wt. % Au – 2.5 wt. % Pd / TiO_2 can dramatically enhance or hinder the formation of H_2O_2 . With catalytic activity seen to increase as Cs content decreases. Further investigation into the ability of $\text{Cs}_x\text{H}_{3-x}\text{PW}_{12}\text{O}_{40}$ salts to promote catalytic activity towards the degradation of H_2O_2 can be seen in Figure 3.5.

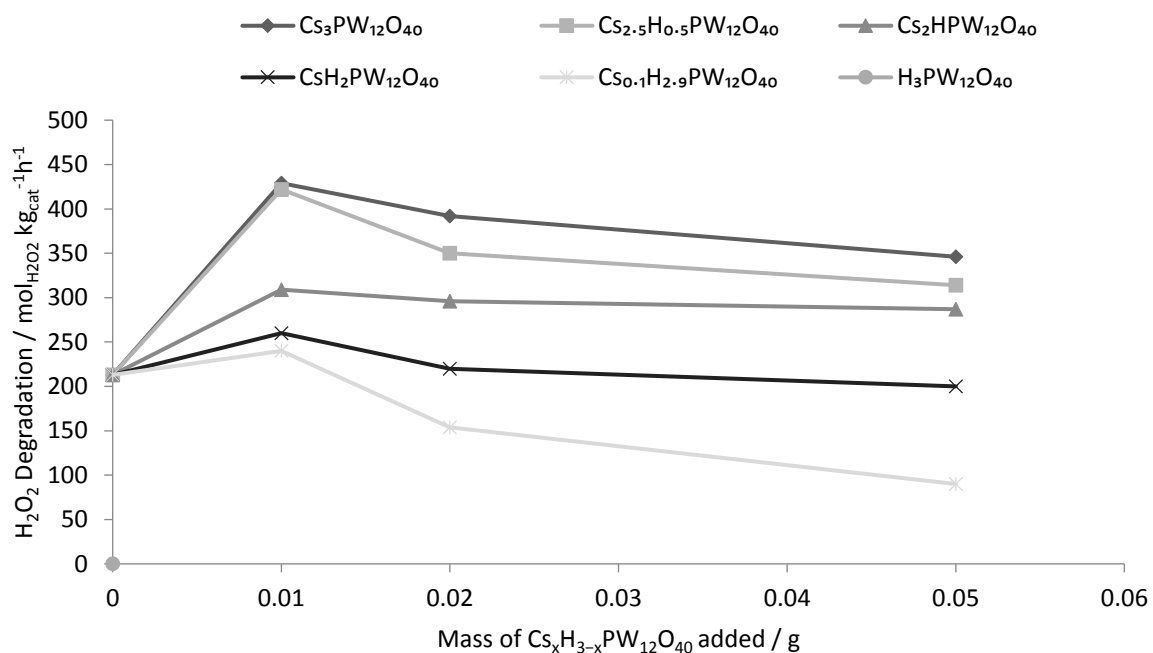


Figure 3.5. H_2O_2 Degradation for 2.5 wt. % Au – 2.5 wt. % Pd / TiO_2 and $\text{Cs}_3\text{PW}_{12}\text{O}_{40}$ as a function of additive loading.

Reaction conditions: 2.5 wt. % Au – 2.5 wt. % Pd / TiO_2 (0.01g), $\text{Cs}_x\text{P}_{3-x}\text{W}_{12}\text{O}_{40}$ (X g), total pressure 580 psi, $\text{H}_2 / \text{O}_2 = 0.525$, 1200 rpm, 30 min, 5.6 g CH_3OH + 2.9 g H_2O (66 wt. % CH_3OH), 2 °C.

It can be observed, in Figure 3.5, that the addition of 0.01g Cs-exchanged or non-exchanged tungstophosphoric acid results in an increase in the overall degradation of H_2O_2 , from 213 $\text{mol}_{\text{H}_2\text{O}_2} \text{kg}_{\text{cat}}^{-1}\text{h}^{-1}$ for the 2.5 wt. % Au – 2.5 wt. % Pd / TiO_2 catalyst only. This is expected as it has been shown (Table 3.1) that these materials have some activity towards the degradation of H_2O_2 . The increase in H_2O_2 degradation is observed to correlate with Cs loading, again as reported previously in Table 3.1, with the greatest increase reported when $\text{Cs}_3\text{PW}_{12}\text{O}_{40}$ is utilised in addition to the 2.5 wt. % Au – 2.5 wt. % Pd / TiO_2 catalyst. The rate of H_2O_2 degradation increases from 213 to 429 $\text{mol}_{\text{H}_2\text{O}_2} \text{kg}_{\text{cat}}^{-1}\text{h}^{-1}$ when 0.01g of $\text{Cs}_3\text{PW}_{12}\text{O}_{40}$ is combined with 2.5 wt. % Au – 2.5 wt. % Pd / TiO_2 . This increase in H_2O_2 degradation with HPA addition is observed regardless of Cs loading, when 0.01 g of the additive is utilised.

Further addition of HPA decreases the rate of H_2O_2 degradation. This decrease in H_2O_2 degradation correlates with Cs content; that is the lower the Cs content the greater the decrease in H_2O_2 degradation. It can be observed that with the addition of 0.05g of $\text{Cs}_{0.1}\text{H}_{2.9}\text{PW}_{12}\text{O}_{40}$ the rate of H_2O_2 degradation decreases to 90 $\text{mol}_{\text{H}_2\text{O}_2} \text{kg}_{\text{cat}}^{-1}\text{h}^{-1}$, this is very similar to that observed when the non Cs substituted $\text{H}_3\text{PW}_{12}\text{O}_{40}$ is used in addition to the 2.5 wt. % Au – 2.5 wt. % Pd / TiO_2 catalyst (83 $\text{mol}_{\text{H}_2\text{O}_2} \text{kg}_{\text{cat}}^{-1}\text{h}^{-1}$).

To understand the effect of Cs in the synthesis and degradation of H₂O₂ Cs has been added to 2.5 wt. % Au – 2.5 wt. % Pd / TiO₂ in the form of CsNO₃. The concentration of Cs used is equivalent to that present when 0.05g of the Cs substituted H₃PW₁₂O₄₀ is utilised as an additive for 2.5 wt. % Au – 2.5 wt. % Pd / TiO₂ and the results are shown in Figure 3.6.

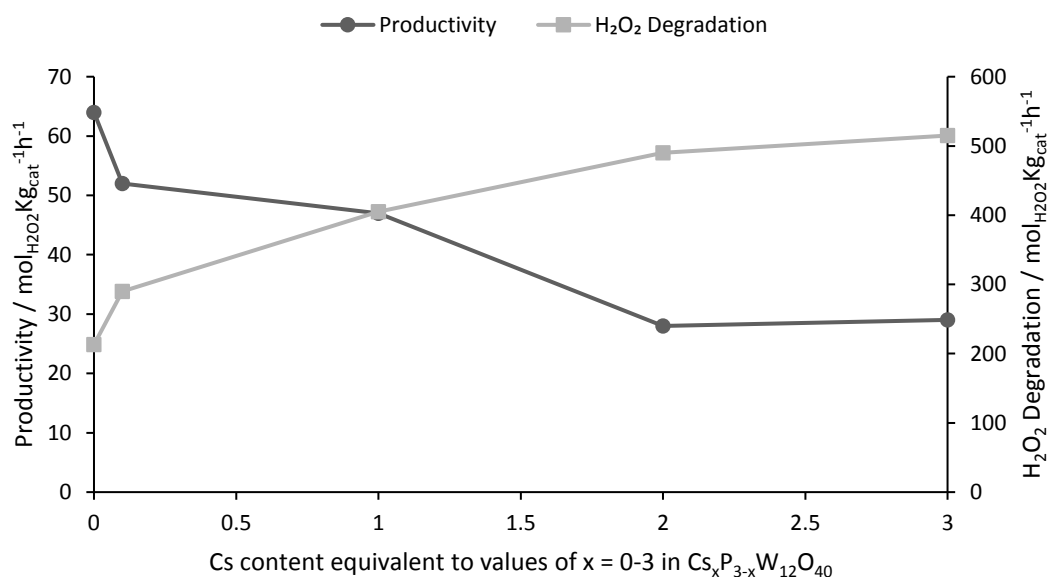


Figure 3.6. H₂O₂ Synthesis and Degradation for 2.5 wt. % Au – 2.5 wt. % Pd / TiO₂ and CsNO₃ as a function of CsNO₃ loading.

Reaction conditions: 2.5 wt. % Au – 2.5 wt. % Pd / TiO₂ (0.01g), CsNO₃ (X g), total pressure 580 psi, H₂ / O₂ = 0.525, 1200 rpm, 30 min, 5.6 g CH₃OH + 2.9 g H₂O (66 wt. % CH₃OH), 2 °C.

It is observed that as the Cs concentration increases the rate of H₂O₂ synthesis decreases, from 64 mol_{H₂O₂} kg_{cat}⁻¹ h⁻¹ to a minimum of 29 mol_{H₂O₂} kg_{cat}⁻¹ h⁻¹ when a concentration of Cs equivalent to that present in Cs₃PW₁₂O₄₀ is utilised. This correlates with an increase in the degradation of H₂O₂, which increases to a maximum of 515 mol_{H₂O₂} kg_{cat}⁻¹ h⁻¹ when Cs concentration is at a maximum. Further investigation was then conducted to determine the activity of Cs towards both the direct synthesis and degradation of H₂O₂ in the absence of the 2.5 wt. % Au – 2.5 wt. % Pd / TiO₂ catalyst. The results are shown in Table 3.7.

Table 3.7. The activity of CsNO₃ towards the direct synthesis and degradation of H₂O₂.

[Cs] equivalent to that in Cs _x P _{3-x} W ₁₂ O ₄₀	Productivity / mol _{H₂O₂} kg _{cat} ⁻¹ h ⁻¹	H ₂ O ₂ Degradation / mol _{H₂O₂} kg _{cat} ⁻¹ h ⁻¹
No catalyst	0	0
Cs _{0.1} H _{2.9} PW ₁₂ O ₄₀	0	26
CsH ₂ PW ₁₂ O ₄₀	0	125
Cs ₂ HPW ₁₂ O ₄₀	0	178
Cs ₃ PW ₁₂ O ₄₀	0	215

Reaction conditions for H₂O₂ degradation: CsNO₃ (X g), total pressure 420 psi, 5 %H₂ / CO₂, 1200 rpm, 30 min, 5.6 g CH₃OH + 2.22 g H₂O (66 wt. % CH₃OH), 0.68g H₂O₂ (50 wt. %) 2 °C.

It can be observed that Cs plays a significant role in the degradation of H₂O₂. Indeed, as the concentration of Cs in the reaction solution increases so does the activity towards the degradation of H₂O₂. It was shown in Table 3.1 that increasing the Cs content within the HPA structure results in an increase in the degradation of H₂O₂ and a general trend can be observed in Table 3.3; that as Cs content within the Keggin structure increases so does the amount of leached Cs. It is possible to conclude that the increase in H₂O₂ degradation observed with the addition of Cs_xP_{3-x}W₁₂O₄₀ salts may be related to the extent of Cs exchange.

The utilisation of tungstophosphoric acid with lower Cs incorporation as an additive to 2.5 wt. % Au – 2.5 wt. % Pd / TiO₂ leads to a greater improvement in catalytic activity towards H₂O₂ synthesis, than the utilisation of the Cs incorporated salts with greater Cs content. It has been demonstrated that as the amount of Cs introduced into the Keggin cage structure decreases there is an increase in surface acidity and a decrease in the pH of the methanol-water working solution. However reaction solution pH remains lower than that observed when no additive is present. The effect of Cs-heteropolyacids have on solvent pH is investigated in Section 3.2.5.2

3.2.3. The effect of adding Cs_{0.1}H_{2.9}PW₁₂O₄₀ to supported bimetallic catalysts.

The effectiveness of adding Cs_{0.1}H_{2.9}PW₁₂O₄₀ to 2.5 wt. % Au – 2.5 wt. % Pd / TiO₂ led to the investigation of adding this acid additive to other catalysts known for their activity towards H₂O₂ direct synthesis, namely 2.5 wt. % Sn – 2.5 wt. % Pd / TiO₂, 2.5 wt. % Au – 2.5 wt. % Pd / Acid washed Carbon and 2.5 wt. % Au – 2.5 wt. % Pd / ZrO₂. The results of this investigation are seen in Table 3.8.

Table 3.8. The effect of adding Cs_{0.1}H_{2.9}PW₁₂O₄₀ to supported bimetallic catalysts, 2.5 wt. % Sn – 2.5 wt. % Pd / TiO₂, 2.5 wt. % Au – 2.5 wt. % Pd / Acid washed Carbon and 2.5 Wt. % Au – 2.5 wt. % Pd / ZrO₂.

Catalyst	Productivity / mol _{H2O2} kg _{cat} ⁻¹ h ⁻¹	wt. % H ₂ O ₂
2.5 wt. % Au – 2.5 wt. % Pd / TiO ₂	64	0.13
2.5 wt. % Au – 2.5 wt. % Pd / TiO ₂ + Cs _{0.1} H _{2.9} PW ₁₂ O ₄₀	299	0.60
2.5 wt. % Sn – 2.5 wt. % Pd / TiO ₂	60	0.10
2.5 wt. % Sn – 2.5 wt. % Pd / TiO ₂ + Cs _{0.1} H _{2.9} PW ₁₂ O ₄₀	134	0.27
2.5 wt. % Au – 2.5 wt. % Pd / Acid washed Carbon	190	0.38
2.5 wt. % Au – 2.5 wt. % Pd / Acid washed Carbon + Cs _{0.1} H _{2.9} PW ₁₂ O ₄₀	348	0.70
2.5 wt. % Au – 2.5 wt. % Pd / ZrO ₂	76	0.15
2.5 wt. % Au – 2.5 wt. % Pd / ZrO ₂ + Cs _{0.1} H _{2.9} PW ₁₂ O ₄₀	210	0.43

Reaction conditions: Catalyst (0.01 g), Cs_{0.1}H_{2.9}PW₁₂O₄₀ (0.05 g), total pressure 580 psi, H₂ / O₂ = 0.525, 1200 rpm, 30 min, 5.6 g CH₃OH + 2.9 g H₂O (66 wt. % CH₃OH), 2 °C. Catalysts calcined 3 h, 400 °C, static air, ramp rate = 20 °C min⁻¹

As can be observed in Table 3.8 when adding 0.05g of $\text{Cs}_{0.1}\text{H}_{2.9}\text{PW}_{12}\text{O}_{40}$ to these catalysts a dramatic increase is observed in both productivity and Wt. % H_2O_2 , under standard reaction conditions. It can therefore be determined that the promotive effect first observed for the $\text{Cs}_{0.1}\text{H}_{2.9}\text{PW}_{12}\text{O}_{40}$ - 2.5 wt. % Au – 2.5 wt. % Pd / TiO_2 system is also present in other $\text{Cs}_{0.1}\text{H}_{2.9}\text{PW}_{12}\text{O}_{40}$ – catalyst systems, although the nature of this promotion requires further investigation before it is fully understood. The use of $\text{Cs}_{0.1}\text{H}_{2.9}\text{PW}_{12}\text{O}_{40}$ in addition to 2.5 wt. % Au – 2.5 wt. % Pd / Acid washed Carbon is observed to lead to a significant yield of H_2O_2 , with a concentration of 0.7 wt.%. Further investigation and optimisation of reaction conditions of this system may lead to a significant enhancement in yield of H_2O_2 .

It is suggested that some contribution to the increased catalytic activity towards H_2O_2 synthesis may be attributed to the leaching of active metals from the support and it is suggested that further work be conducted to determine the extent of leaching when $\text{Cs}_{0.1}\text{H}_{2.9}\text{PW}_{12}\text{O}_{40}$ is used in addition to the catalysts shown in Table 3.8. It has previously been shown (Table 3.3) that when using a TiO_2 support significant leaching of Pd can occur. It may be that with varying the support the extent of metal leaching changes and through catalyst design it may be possible to inhibit the leaching of metals from the support. For example it may be possible to limit the extent of leaching by exposing the catalyst to increased catalyst calcination temperature, although this is likely to decrease catalytic activity. It may be possible to reach a compromise between catalyst activity and stability.

3.2.4. The Effect of Reaction Conditions on the direct synthesis of H_2O_2 using $\text{Cs}_{0.1}\text{H}_{2.9}\text{PW}_{12}\text{O}_{40}$ as a solid acid additive for 2.5 wt. % Au – 2.5 wt. % Pd / TiO_2 .

Amongst other catalysts 2.5 wt. % Au - 2.5 wt. % Pd / TiO_2 has been established as a catalyst that is active towards the direct synthesis of hydrogen peroxide. It was decided to optimise the reaction conditions used when $\text{Cs}_{0.1}\text{H}_{2.9}\text{PW}_{12}\text{O}_{40}$ is added as an acid additive for this catalyst, in an attempt to increase overall yield of H_2O_2 . This additive has been observed to provide the greatest improvement in catalytic activity, when compared to higher loadings of Cs exchange.

Several reaction conditions are investigated including; reaction temperature, solvent composition and reaction time and the results will be presented in the following Sections.

It should be noted that a number of parameters can influence catalyst productivity and degradation and prevent a true representation of catalyst activity and selectivity being determined, including reaction time and catalyst mass. This is because both parameters are expressed in terms of moles of H₂O₂ produced / degraded per Kg of catalyst per hour. As such the overall yield of H₂O₂ (wt. %) and degradation of H₂O₂ (% degradation) are used throughout this section to allow for better normalisation of catalyst activity.

3.2.4.1. Effect of gas feed composition.

Figure 3.7 shows the effect of reactant gas ratio on the direct synthesis of H₂O₂. As H₂O₂ degradation is determined in the presence of H₂ / CO₂ only, it is not possible to determine the effect of H₂ : O₂ ratio on this parameter.

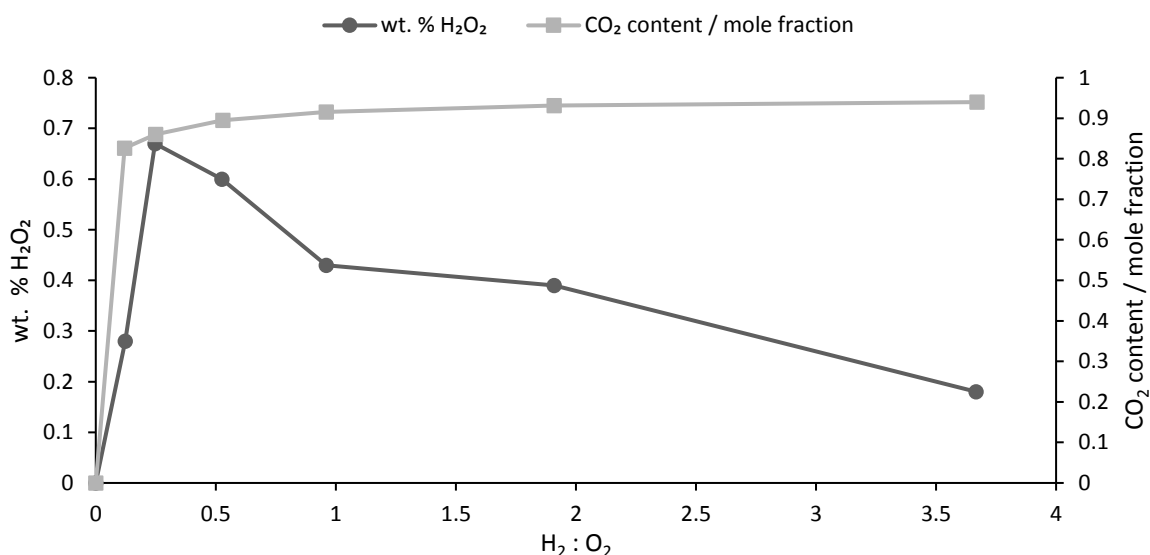


Figure 3.7 H₂O₂ wt. % for 2.5 wt. % Au – 2.5 wt. % Pd / TiO₂ and Cs_{0.1}H_{2.9}PW₁₂O₄₀ as a function of gas feed composition.

Reaction conditions: 2.5 wt. %Au – 2.5 wt. %Pd / TiO₂ (0.01 g), Cs_{0.1}H_{2.9}PW₁₂O₄₀ (0.05 g), total pressure 580 psi, 1200 rpm, 30 min, 5.6 g CH₃OH + 2.9 g H₂O (66 wt. % CH₃OH), 2 °C.

It is observed that at lower H₂ content (H₂ : O₂ ratio of 0.12) the observed H₂O₂ concentration is particularly low, with a concentration of 0.28 wt. % reported when the H₂ : O₂ ratio is 0.12. This concentration of H₂O₂ is twice that reported for the catalyst alone, under identical reaction conditions but a H₂ : O₂ ratio of 0.525²⁴. Given the relative expense of H₂ this may be of economic benefit to any large scale use of this reaction system for the direct synthesis of H₂O₂. By shifting the gas ratio slightly, to 0.25 it is possible to achieve extremely high concentrations of H₂O₂, with a total H₂O₂ concentration of 0.67 wt. % reported. Increasing H₂

content beyond this point is observed to result in a decrease in the total concentration of H_2O_2 produced, to a minimum of 0.18 wt. %, when a $\text{H}_2 : \text{O}_2$ ratio of 3.66 is employed.

The reaction gas consists of two components (5 % H_2 / CO_2 and 25 % O_2 / CO_2) as such as the $\text{H}_2 : \text{O}_2$ ratio changes so does the molar fraction of CO_2 . It has been previously shown that CO_2 , when used as the diluent for the reactant gasses is able to promote H_2O_2 selectivity through the formation of carbonic acid in the water-methanol solvent²⁵, lowering the solvent pH and stabilising H_2O_2 . Nevertheless, it can be presumed that the amount of CO_2 introduced is high enough to lead to complete saturation of the water-methanol solvent ensuring that the pH of the solution is constant regardless of the $\text{H}_2 : \text{O}_2$ ratio. It is observed in Figure 3.7 that the CO_2 content does not vary to a great extent with increasing O_2 content, as such the data in Figure 3.7 are likely to be representative of the effect of variation in the $\text{H}_2 : \text{O}_2$ ratio and not CO_2 content.

It may therefore be possible to explain the trend observed in Figure 3.7 in terms of limitation of reagent availability, in particular H_2 . Figure 3.8 shows how the shape of the experimental curve seems to correlate to the limiting reagent (H_2) concentration.

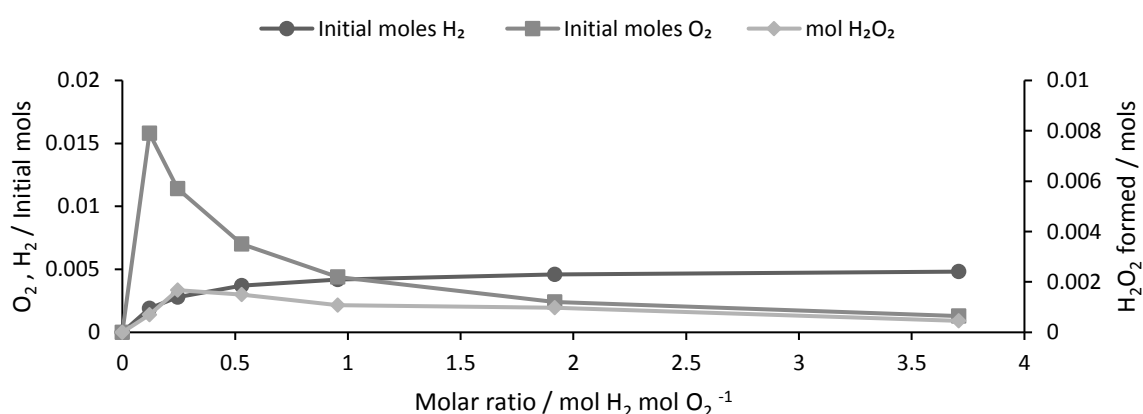


Figure 3.8. Comparison between total amount of moles H_2 and O_2 introduced to each experiment and H_2O_2 produced for 2.5 wt. % Au – 2.5 wt. % Pd / TiO_2 and $\text{Cs}_{0.1}\text{H}_{2.9}\text{PW}_{12}\text{O}_{40}$.

Reaction conditions: 2.5 wt. % Au – 2.5 wt. % Pd / TiO_2 (0.01 g), $\text{Cs}_{0.1}\text{H}_{2.9}\text{PW}_{12}\text{O}_{40}$ (0.05 g), total pressure 580 psi, 1200 rpm, 30 min, 5.6 g CH_3OH + 2.9 g H_2O (66 Wt. % CH_3OH), 2 °C.

For a simple model it may be expected that the synthesis of H_2O_2 is equally dependent on the $\text{H}_2 : \text{O}_2$ ratio as it is on the $\text{O}_2 : \text{H}_2$ ratio. Figure 3.9 suggests that this is not the case.

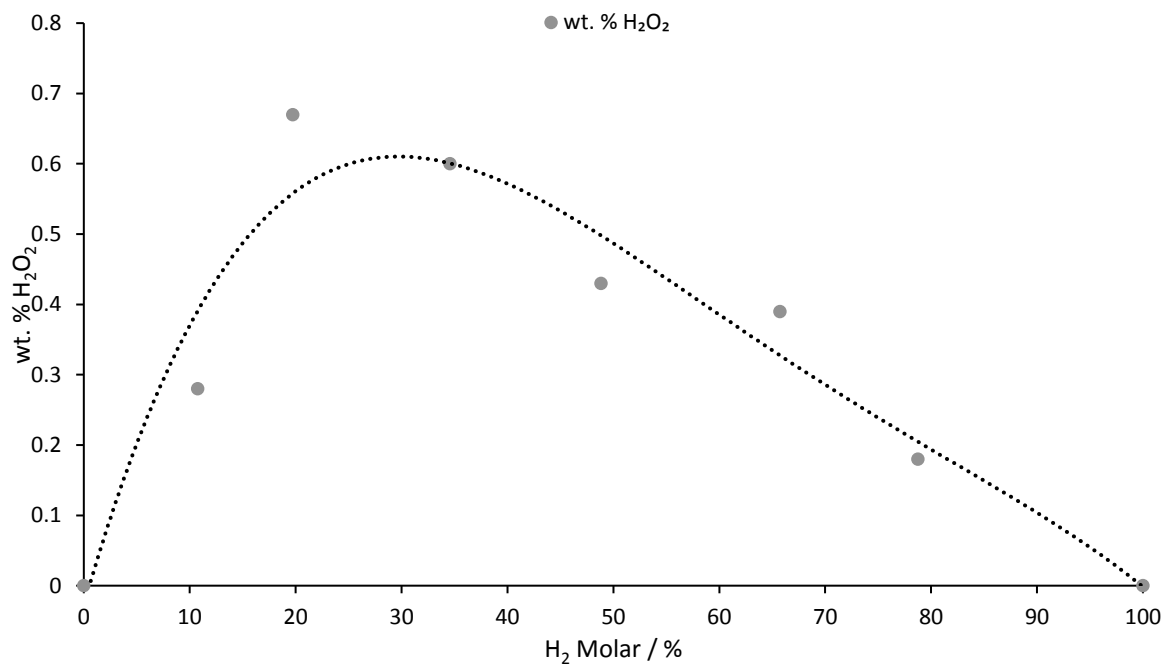


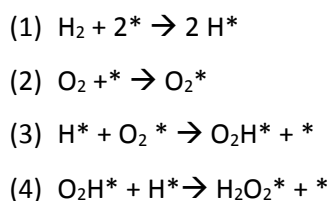
Figure 3.9. wt. % H₂O₂ produced for 2.5 wt. % Au – 2.5 wt. % Pd / TiO₂ and Cs_{0.1}H_{2.9}PW₁₂O₄₀ as a function of reactant gas composition.

Reaction conditions: 2.5 wt. %Au – 2.5 wt. %Pd / TiO₂ (0.01 g), Cs_{0.1}H_{2.9}PW₁₂O₄₀ (0.05 g), total pressure 580 psi, 1200 rpm, 30 min, 5.6 g CH₃OH + 2.9 g H₂O (66 wt. % CH₃OH), 2 °C.

The shape of the curve in Figure 3.9 is not symmetrical, it is observed that greater partial pressures of H₂ leads to a marked decrease in the yield of H₂O₂ in comparison to greater partial pressures of O₂. This can be explained by considering the competing reactions that take place over the surface of the catalyst during the direct synthesis of H₂O₂, namely:

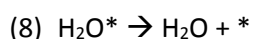
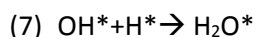
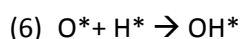
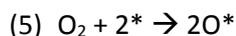
- Formation of H₂O₂ from H₂ and O₂.
- Formation of H₂O from H₂ and O₂ via combustion.
- Hydrogenation of H₂O₂ by H₂.
- Decomposition of H₂O₂ to H₂O.

It has been suggested by Ntainjua *et al.*²⁶ that these reaction pathways share the same surface intermediates and the formation of H₂O₂ occurs via the hydrogenation of O₂. The following kinetic scheme has been proposed with this in mind²⁶:

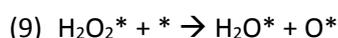


Where * denotes a vacant site.

It is therefore proposed that the formation of H₂O₂ takes place via a twostep hydrogenation of adsorbed O₂. The undesired, competing reactions leading to the formation of H₂O are proposed to involve the dissociation of O₂:



When two reaction sites are present in close proximity H₂O₂ can dissociate in the following manner:



With this in mind it is possible to understand why at higher partial pressures of H₂ the rate of H₂O₂ degradation is much greater than the rate of H₂O₂ synthesis, with an excess of H₂ there is increased scavenging of O* by atomic hydrogen. The contribution to H₂O₂ degradation is likely to be greatest from hydrogenation rather than decomposition. It would be of interest to decouple the two pathways that contribute to H₂O₂ degradation.

3.2.4.2. Effect of reaction temperature.

Reaction temperature was investigated while maintaining all other reaction conditions, the results of this experiment are shown in Figure 3.10.

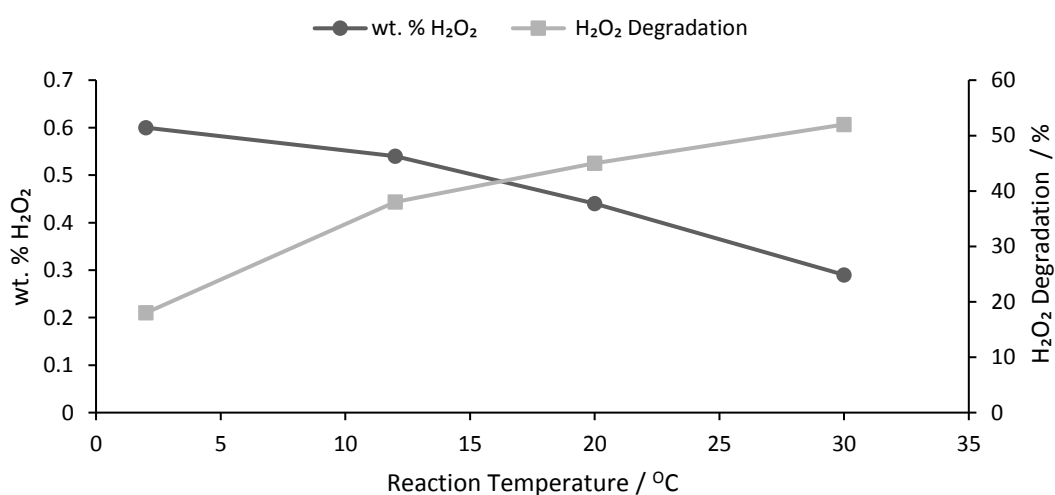


Figure 3.10. H₂O₂ concentration (wt. %) and H₂O₂ degradation (%) for 2.5 wt. % Au – 2.5 wt. % Pd / TiO₂ and Cs_{0.1}H_{2.9}PW₁₂O₄₀ as a function of temperature.

Reaction conditions: 2.5 wt. % Au – 2.5 wt. % Pd / TiO₂ (0.01 g), Cs_{0.1}H_{2.9}PW₁₂O₄₀ (0.05 g), total pressure 580 psi, H₂ / O₂ = 0.525, 1200 rpm, 30 min, 5.6 g CH₃OH + 2.9 g H₂O (66 wt. % CH₃OH).

As can be observed in Figure 3.10 as reaction temperature increases the concentration of H_2O_2 formed decreases with a corresponding increase in H_2O_2 degradation. This is similar to the findings of Crole *et.al.*²⁷ who have investigated the effect of temperature on the direct synthesis of H_2O_2 by 2.5 wt. % Au – 2.5 wt. % Pd / TiO_2 in a water only solvent.

It is known that as temperature increases the solubility of H_2 in methanol increases, conversely H_2 solubility in water decreases with increasing temperature¹⁸. Furthermore O_2 solubility in both water and methanol decreases with increasing temperature. It is therefore reasonable to propose that there is both a decrease in H_2O_2 synthesis and an increase in the rate of subsequent H_2O_2 hydrogenation, a significant component in H_2O_2 degradation. This assumption was investigated and indeed it is shown that as temperature increases so does H_2O_2 degradation. However the individual components of H_2O_2 degradation (decomposition and hydrogenation) have not been decoupled and therefore it is not possible to definitively state if the increase in degradation is due to decomposition or hydrogenation, or both.

The optimal temperature for this catalytic system is found to be 2 °C, where H_2O_2 concentration is reported to be greatest at 0.6 wt. % and the rate of degradation is at its lowest at 18 %. Although it should be noted that even at elevated temperatures high catalytic activity is still observed, indeed at 30 °C a H_2O_2 concentration of 0.29 wt. % is observed, even though the extent of H_2O_2 degradation is over 2.5 times that observed at 2 °C. The concentration of H_2O_2 synthesised is in excess of twice that reported for the 2.5 wt. % Au – 2.5 wt. % Pd / TiO_2 , under conditions optimised for this catalyst (0.128 wt.%). It is reasonable to assume that the observed rate of H_2O_2 synthesis, as with all systems studied for the direct synthesis of H_2O_2 , is lower than the true rate as at elevated temperatures the degradation of H_2O_2 becomes prevalent and as such not all the H_2O_2 formed is available at the end of the reaction.

This work is in finding with Crole *et.al.*²⁷ who have investigated 2.5 wt. % Au – 2.5 wt. % Pd / TiO_2 in a H_2O only solvent under a batch reaction conditions. In addition to this work Freakley *et.al.*¹⁴ have investigated 2.5 wt. % Au – 2.5 wt. % Pd / TiO_2 in a H_2O -MeOH solvent system, in a flow reactor. It is reported that increasing reaction temperature from 2 to 30 °C results in a decrease in productivity and this is ascribed to a decrease in the solubility of O_2 in both solvent components²⁷. Furthermore it is reported that the solubility of H_2 increases in methanol by approximately 30 % as temperature is raised from 2 to 30 °C, resulting in an increase in the rate of H_2O_2 hydrogenation and a decrease in H_2O_2 selectivity.

3.2.4.3. The effect of reaction time.

Figure 3.11 shows the effect of reaction time on the concentration of H₂O₂ formed and the extent of H₂O₂ degradation. Reactions were performed for systematically varied durations to study the effect of time on the amount of H₂O₂ formed and subsequently degraded. Separate reactions were performed as sampling from a single reaction in a time on line process would affect the reaction dynamics.

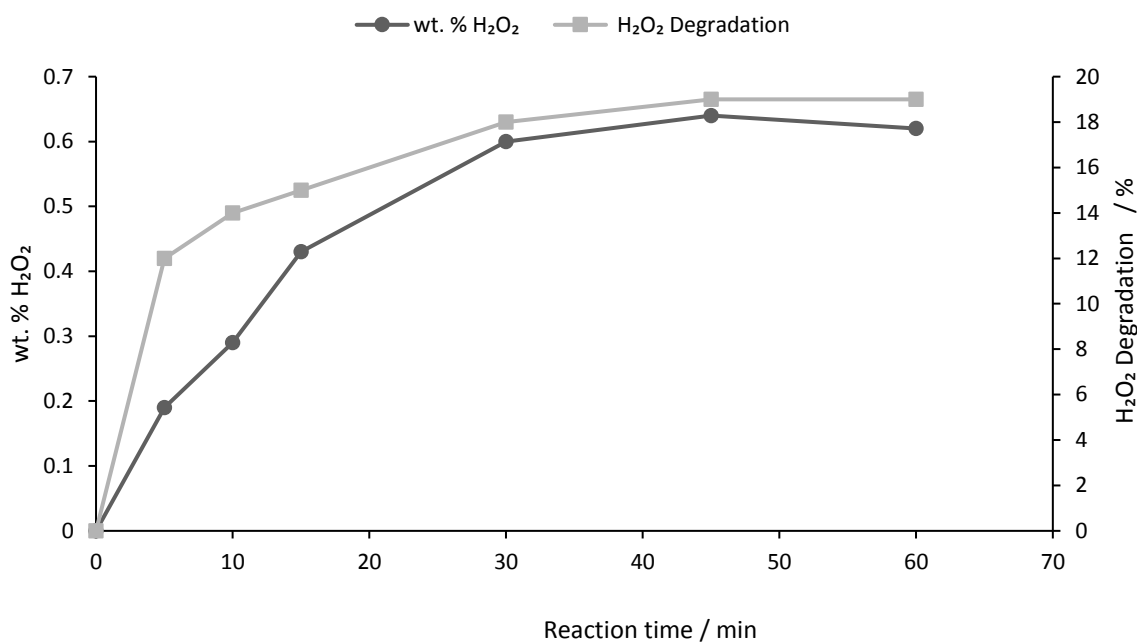


Figure 3.11. H₂O₂ concentration (wt. %) and H₂O₂ degradation (%) for 2.5 wt. % Au – 2.5 wt. % Pd / TiO₂ and Cs_{0.1}H_{2.9}PW₁₂O₄₀ as a function of time.

Reaction conditions: 2.5 wt. % Au – 2.5 wt. % Pd / TiO₂ (0.01 g), Cs_{0.1}H_{2.9}PW₁₂O₄₀ (0.05 g), total pressure 580 psi, H₂ / O₂ = 0.525, 1200 rpm, 2 °C, 5.6 g CH₃OH + 2.9 g H₂O (66 wt. % CH₃OH).

Initially, as reaction time increases so does the concentration of H₂O₂, to 0.19 wt. % at a reaction time of 5 minutes. Beyond this point H₂O₂ concentration increases to a maximum of 0.64 wt. % after 45 minutes. It may be expected that H₂O₂ concentration would increase continuously with time, however as time increases the availability of both H₂ and O₂ in the system decreases; the system is then limited by the availability of reactants.

The degradation of H₂O₂ is observed to increase sharply with reaction time; until 30 minutes where degradation is reported to be 18 %. Beyond this point the rate of degradation plateaus, as with the H₂O₂ yield, this is ascribed to decreasing availability of reactant gasses.

Both H₂O₂ degradation and H₂O₂ yield suggest that after a reaction time of 30 minutes the reaction becomes limited by the availability of reactants, it can be observed that at a time of 30 minutes H₂O₂ concentration is 0.6 wt% while after 30 minutes H₂O₂ concentration

plateaus. This is supported by data in Table 3.2, which shows that at a reaction time of 30 min H₂ conversion 69 %. However, it is possible that after 30 minutes the catalyst has become deactivated and this would explain the lack of variation in both the H₂O₂ yield and the extent of H₂O₂ degradation.

In an attempt to determine if at a reaction time of 30 minutes the catalyst has become deactivated or the system operates inside of mass transport limitation it was decided to investigate ‘top up’ reactions, where the reactant gas was replaced periodically. The length of time between gas replacements was studied in order to determine if this factor affects catalytic activity towards the direct synthesis of H₂O₂. A range of gas replacement times were chosen, ranging from 5 minute intervals to standard reaction length time, 30 minute intervals, to longer reaction times, 45 minute intervals, and the results are shown in Figure 3.12.

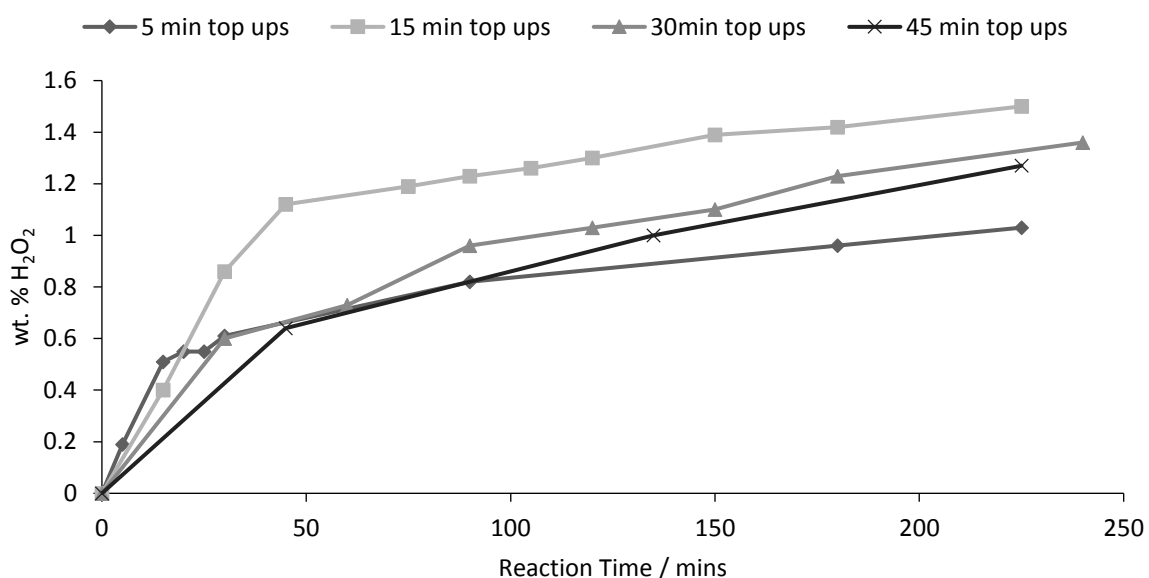


Figure 3.12. H₂O₂ concentration (wt. %) for 2.5 wt. % Au – 2.5 wt. % Pd / TiO₂ and Cs_{0.1}H_{2.9}PW₁₂O₄₀ as a function of reaction gas replacement.

Reaction conditions: 2.5 wt. % Au – 2.5 wt. % Pd / TiO₂ (0.01 g), Cs_{0.1}H_{2.9}PW₁₂O₄₀ (0.05 g), total pressure 580 psi, H₂ / O₂ = 0.525, 1200 rpm, 2 °C, 5.6 g CH₃OH + 2.9 g H₂O (66 wt. % CH₃OH).

It is observed that when replacement of the reactant gas occurs every 5 minutes, to give a total reaction time of 30 minutes (6 gas charges) the total H₂O₂ concentration is very similar to that observed when one 30 minute reaction is investigated, with no gas replacements, 0.6 and 0.61 wt. %. Again this is very similar to the H₂O₂ concentration reported for a 45 minute reaction, with one gas charge, with H₂O₂ yield reported to be 0.64 wt.%. Interestingly when the reactant gas is replaced at 15 minute intervals, to give a total reaction time of 30 minutes

(2 gas charges) the H_2O_2 concentration is much higher than gas replacements at either 5, 30 or 45 minute intervals. Indeed H_2O_2 concentration is reported to be 0.86 wt. %.

It is suggested that at shorter reaction times the reactant gas is unable to fully diffuse to the catalyst surface and so the reaction is limited by reactant availability. It is observed in Figure 3.12 that after 30 minutes, if the reactant gas is not replaced the formation of H_2O_2 becomes mass transport limited. As such when longer gas replacement times, 30 and 45 minutes, are employed the reaction becomes limited by the availability of H_2 or O_2 . However using a replacement time of 15 minutes ensures that both significant amounts of H_2 and O_2 are able to diffuse to the catalyst surface and the reaction remains outside of mass transport limitation.

It would be of great interest to investigate catalyst activity while maintaining reactant gas pressure, this would allow the system to be studied in a manner more similar to that likely used on a larger industrial scale and allow for the investigation of catalyst stability over time.

3.2.4.4. The effect of stirring speed.

Figure 3.13 shows the effect of the stirring speed on H_2O_2 yield and H_2O_2 degradation.

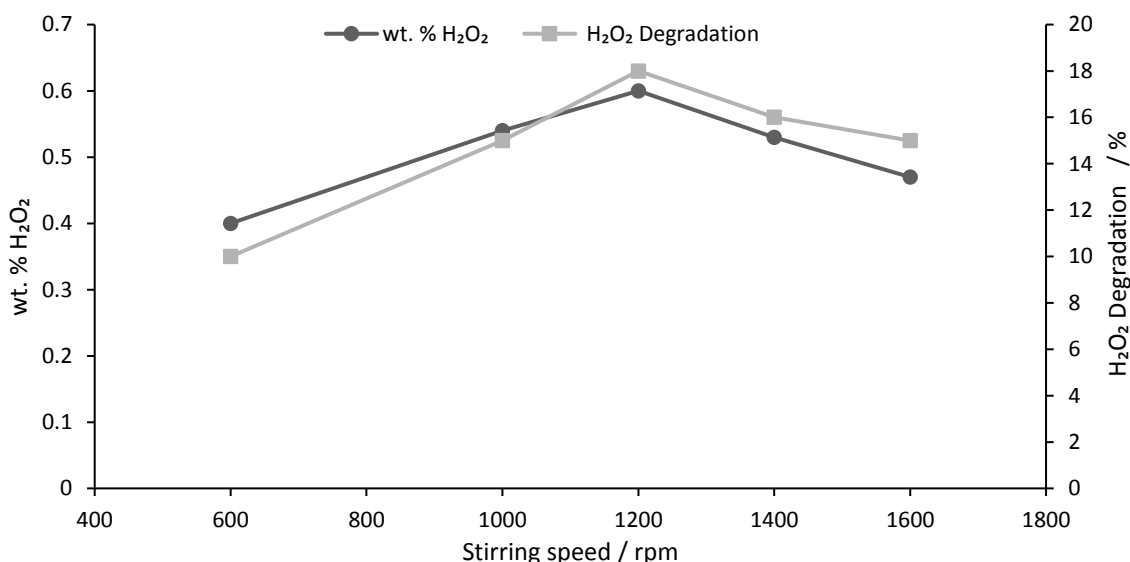


Figure 3.13. H_2O_2 concentration (wt. %) and H_2O_2 degradation (%) for 2.5 wt. % Au – 2.5 wt. % Pd/ TiO_2 and $\text{Cs}_{0.1}\text{H}_{2.9}\text{PW}_{12}\text{O}_{40}$ as a function of stirring speed.

Reaction conditions: 2.5 wt. % Au – 2.5 wt. % Pd / TiO_2 (0.01 g), $\text{Cs}_{0.1}\text{H}_{2.9}\text{PW}_{12}\text{O}_{40}$ (0.05 g), total pressure 580 psi, $\text{H}_2 / \text{O}_2 = 0.525$, 2 °C, 30 min, 5.6 g CH_3OH + 2.9 g H_2O (66 wt. % CH_3OH).

It could be assumed that an increase in stirring speed would be beneficial to the yield of H_2O_2 . It is likely that increasing stirring speed would result in an improvement in mass transfer of reactants to the catalyst. Likewise it would be expected that at lower stirring speeds that

mass transfer of reactants to the catalyst active sites would be reduced and conversion to the product, H_2O_2 , would be less than at higher speeds. The data shows that at stirring speeds below 1200 rpm, H_2O_2 concentration is considerably lower than that observed at 1200 rpm, with H_2O_2 yield observed to be 0.47 wt. % at a stirring speed of 600 rpm. While at a stirring speed of 1200 rpm H_2O_2 yield is reported to be 0.6 wt. %.

As with H_2O_2 yield, H_2O_2 degradation is observed to reach a maxima at a stirring speed of 1200, with a degradation of 18 % reported. When increasing stirring speed beyond 1200 rpm a decrease in H_2O_2 degradation, to 15 % is observed. It is suggested that, as both overall H_2O_2 yield and H_2O_2 degradation decreases beyond a stirring speed of 1200 rpm the reactants are unable to reach the active sites present on the catalyst responsible for these reaction pathways. As such this leads to a reduction in both the rate of H_2O_2 synthesis and subsequent degradation. It is possible that at higher stirring speeds the catalyst is forced on to the autoclave liner and so the number of catalytic sites available to catalyse either the synthesis or degradation of H_2O_2 decreases, as outlined in Figures 3.14 and 3.15.

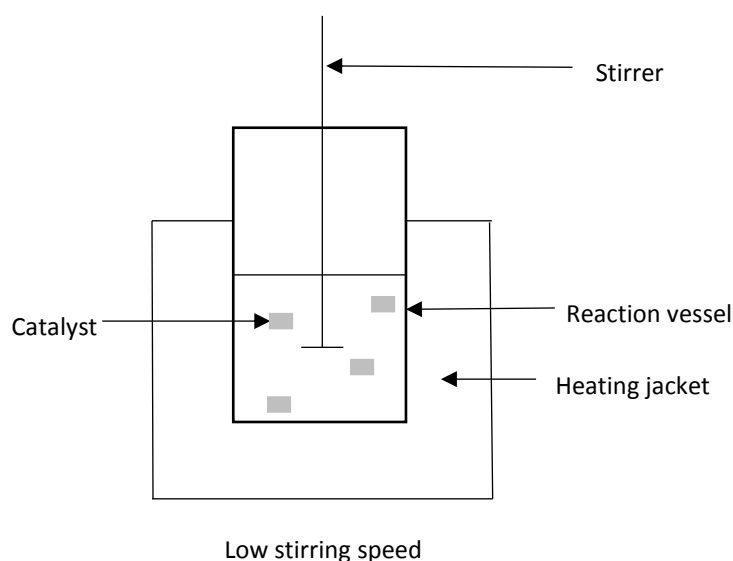


Figure 3.14. The effect of low reactor speed on catalyst distribution in a sealed autoclave.

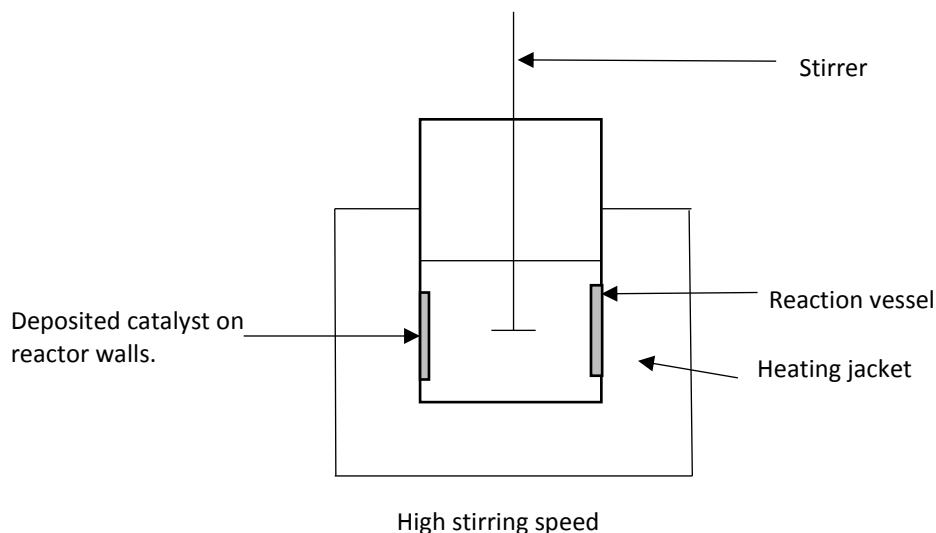


Figure 3.15. The effect of high reactor speed on catalyst distribution in a sealed autoclave.

3.2.4.5. The effect of catalyst mass.

Figure 3.16 show the effect of the catalyst mass on the concentration of H₂O₂ and its subsequent degradation.

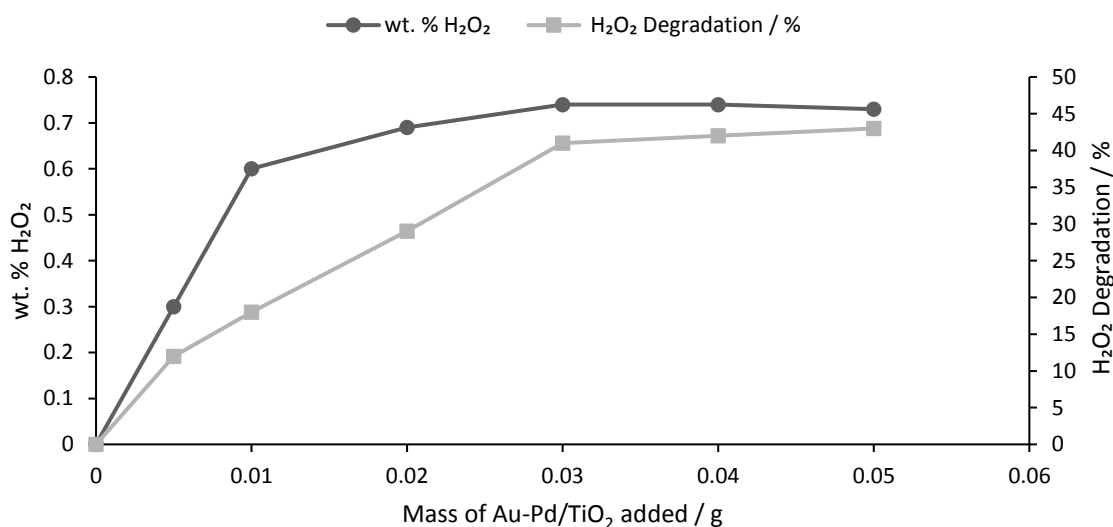


Figure 3.16. H₂O₂ concentration (wt. %) and H₂O₂ degradation (%) for 2.5 wt. % Au – 2.5 wt. % Pd / TiO₂ and Cs_{0.1}H_{2.9}PW₁₂O₄₀ as a function of 2.5 wt. % Au – 2.5 wt. % Pd / TiO₂ loading.

Reaction conditions: Cs_{0.1}H_{2.9}PW₁₂O₄₀ (0.05 g), total pressure 580 psi, H₂ / O₂ =0.525, 1200 rpm, 30 min, 5.6 g CH₃OH + 2.9 g H₂O (66 wt. % CH₃OH), 2 °C.

It can be seen that increasing the mass of the 2.5 wt. % Au – 2.5 wt. % Pd / TiO₂ catalyst increases the yield of H₂O₂, to a maximum of 0.74 wt. % when 0.03 g of catalyst is utilised. Beyond this point H₂O₂ concentration reaches a plateau. This is in agreement with the work conducted by Edwards *et al.*²³ who investigated the 2.5 wt. % Au – 2.5 wt. % Pd / TiO₂ catalyst under identical conditions, but in the absence of the Cs_{0.1}H_{2.9}PW₁₂O₄₀ additive. It should be

noted that Edwards and co-workers report a maximum H₂O₂ concentration of 0.32 Wt. % when the catalyst is used solely. The addition of the Cs_{0.1}H_{2.9}PW₁₂O₄₀ additive is reported to increase the yield of H₂O₂ to 0.74 Wt. %, more than twice that reported by Edwards *et.al*²⁴.

It is observed that by increasing catalyst mass it is possible to increase H₂O₂ concentration, to a maximum of 0.74 wt. % when 0.03 g of the catalyst is utilised. Beyond this point, further addition of catalyst does not result in an increase in H₂O₂ concentration.

As discussed above H₂O₂ concentration plateaus beyond the addition of 0.03 g of Au-Pd / TiO₂. It could be assumed that this may be due to the rate of either one or both H₂O₂ degradation pathways becoming greater than the rate of H₂O₂ synthesis. However investigation of the extent of H₂O₂ degradation with varied catalyst loadings shows a similar trend to that observed for H₂O₂ yield, with H₂O₂ degradation reaching a plateau as catalyst mass is increased beyond 0.03 g. It is suggested that this is due to limited availability of the reactants (H₂ and O₂). The system is now limited by mass transfer. Further addition of catalyst does not result in an increase in H₂O₂ yield. Furthermore it is suggested that when utilising greater masses of catalyst the high stirring speed forces a greater proportion of the catalyst onto the walls of the reactor, preventing access to active sites on the catalyst, in a manner similar to that described in Section 3.2.4.4. There may also be greater agglomeration of catalyst as total catalyst mass increases, which in turn reduces the availability of sites active towards the degradation and synthesis of H₂O₂.

3.2.4.6. Effect of Cs_{0.1}H_{2.9}PW₁₂O₄₀ mass.

Figure 3.17 shows the effect of increasing the mass of Cs_{0.1}H_{2.9}PW₁₂O₄₀ used in addition to 0.01 g of 2.5 wt. % Au – 2.5 wt. % Pd / TiO₂ for the direct synthesis and subsequent degradation of H₂O₂. The effect of Cs_{0.1}H_{2.9}PW₁₂O₄₀ content on the leaching of metals from the support during the direct synthesis reaction is also observed in Figure 3.18 as is the pH of the reaction solution prior to reaction.

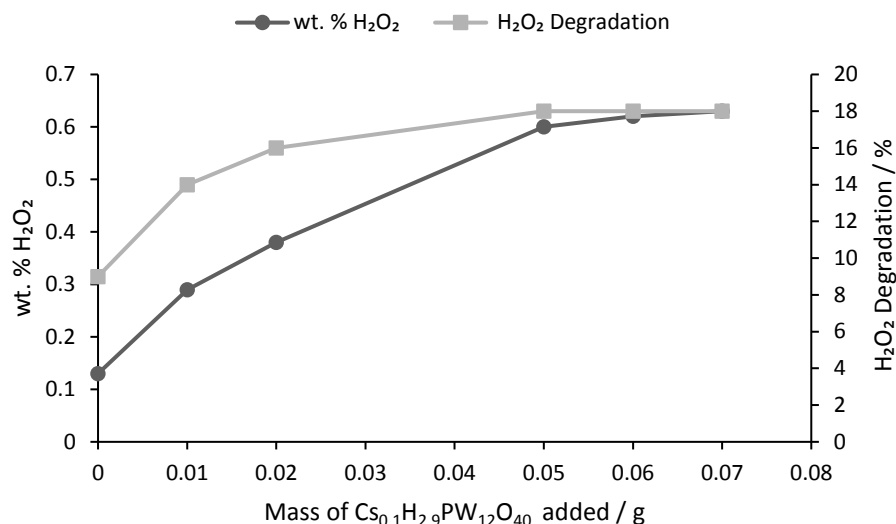


Figure 3.17. H_2O_2 concentration (wt. %) and H_2O_2 degradation (%) for 2.5 wt. % Au – 2.5 wt. % Pd / TiO_2 and $\text{Cs}_{0.1}\text{H}_{2.9}\text{PW}_{12}\text{O}_{40}$ as a function of $\text{Cs}_{0.1}\text{H}_{2.9}\text{PW}_{12}\text{O}_{40}$ loading.

Reaction conditions: 2.5 wt. % Au – 2.5 wt. % Pd / TiO_2 (0.01g), total pressure 580 psi, $\text{H}_2 / \text{O}_2 = 0.525$, 1200 rpm, 30 min, 5.6 g CH_3OH + 2.9 g H_2O (66 wt. % CH_3OH), 2 °C.

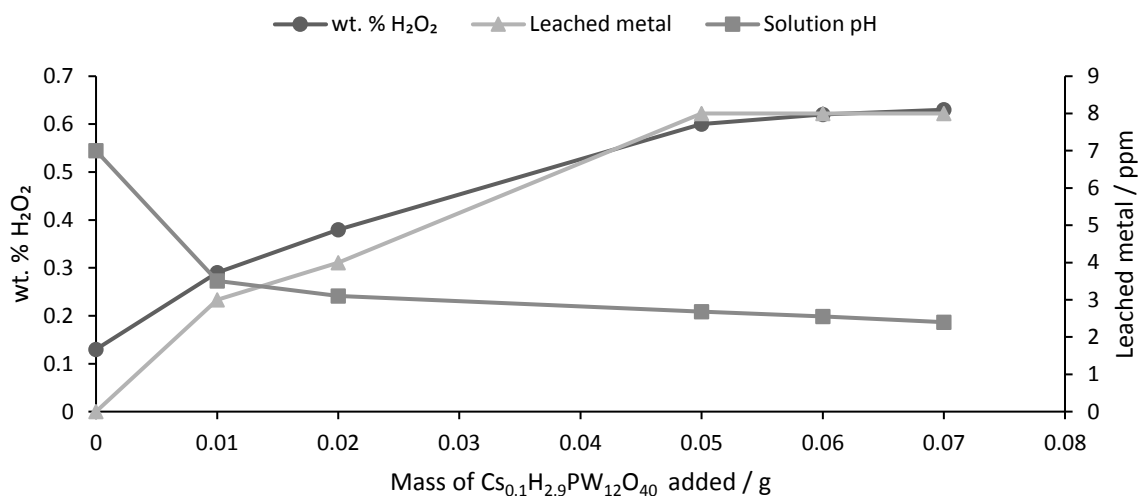


Figure 3.18. H_2O_2 concentration (wt. %), concentration of leached metal (ppm) and reaction solution pH for 2.5 wt. % Au – 2.5 wt. % Pd / TiO_2 and $\text{Cs}_{0.1}\text{H}_{2.9}\text{PW}_{12}\text{O}_{40}$ as a function of $\text{Cs}_{0.1}\text{H}_{2.9}\text{PW}_{12}\text{O}_{40}$ loading.

Reaction conditions: 2.5 wt. % Au – 2.5 wt. % Pd / TiO_2 (0.01g), total pressure 580 psi, $\text{H}_2 / \text{O}_2 = 0.525$, 1200 rpm, 30 min, 5.6 g CH_3OH + 2.9 g H_2O (66 wt. % CH_3OH), 2 °C.

It is observed, in Figure 3.17, that the addition of increasing amounts of $\text{Cs}_{0.1}\text{H}_{2.9}\text{PW}_{12}\text{O}_{40}$ leads to an increase in the concentration of H_2O_2 . Yield of H_2O_2 increases from 0.13 wt. % when only the 2.5 wt. % Au – 2.5 wt. % Pd / TiO_2 catalyst is present to 0.6 wt. % when 0.05 g of $\text{Cs}_{0.1}\text{H}_{2.9}\text{PW}_{12}\text{O}_{40}$ is utilised in addition to the catalyst. Beyond this point further addition of $\text{Cs}_{0.1}\text{H}_{2.9}\text{PW}_{12}\text{O}_{40}$ results in a very limited improvement in concentration of H_2O_2 , to a

maximum of 0.63 wt. % when 0.07 g of the additive is used. This can be related to the pH of the reaction solution, observed in Figure 3.18. It is observed that the pH of the reaction solution decreases dramatically with the addition of $\text{Cs}_{0.1}\text{H}_{2.9}\text{PW}_{12}\text{O}_{40}$, from a pH of 7 when only the catalyst is present to 3.51 when 0.01 g of $\text{Cs}_{0.1}\text{H}_{2.9}\text{PW}_{12}\text{O}_{40}$ is introduced also. This corresponds to an improvement in H_2O_2 yield, from 0.13 to 0.29 wt. %. Further addition of $\text{Cs}_{0.1}\text{H}_{2.9}\text{PW}_{12}\text{O}_{40}$ decreases the pH of the reaction solution slightly to 2.4 when 0.07 g of the additive is utilised, with a H_2O_2 concentration of 0.63 wt. % reported. It has previously been reported that acidic reaction conditions are favourable towards H_2O_2 formation, with a decrease in H_2O_2 degradation reported when using acidic conditions^{7 8 28}. It would therefore be reasonable to suggest that the improvement in H_2O_2 yield is related to a decrease in the pH of the reaction solution.

However as the mass of $\text{Cs}_{0.1}\text{H}_{2.9}\text{PW}_{12}\text{O}_{40}$ added increases so does the degradation of H_2O_2 , from 10 % when no $\text{Cs}_{0.1}\text{H}_{2.9}\text{PW}_{12}\text{O}_{40}$ is present to 18 % when 0.05 g of the additive is used. Increasing the mass of $\text{Cs}_{0.1}\text{H}_{2.9}\text{PW}_{12}\text{O}_{40}$ added further to 0.07g does not lead to an increase in the rate of H_2O_2 degradation. It has previously been shown in Table 3.7 that Cs can contribute to the degradation of H_2O_2 and that as Cs content increases so does the degradation of H_2O_2 . Furthermore, investigation into the stability of Cs-exchanged tungstophosphoric acid, Table 3.3, shows that a Cs loading equal to $\text{Cs}_{0.1}$ is not sufficient to produce a stable material, as inferred from the high concentration of W present in the reaction solution, 1723 ppm when $\text{Cs}_{0.1}\text{H}_{2.9}\text{PW}_{12}\text{O}_{40}$ is utilised in comparison to 1834 ppm when the non-substituted $\text{H}_3\text{PW}_{12}\text{O}_{40}$ is utilised. It is suggested that the increasing Cs content, as more $\text{Cs}_{0.1}\text{H}_{2.9}\text{PW}_{12}\text{O}_{40}$ is added, within the solvent system is the cause for the increase in degradation of H_2O_2 . This further correlates with the data observed in Table 3.1, which highlights the ability of $\text{Cs}_{0.1}\text{H}_{2.9}\text{PW}_{12}\text{O}_{40}$ to degrade H_2O_2 .

It is observed in Figure 3.18 that as the mass of $\text{Cs}_{0.1}\text{H}_{2.9}\text{PW}_{12}\text{O}_{40}$ added increases the concentration of leached Pd increases, from 0 ppm when the catalyst is used alone to a maximum of 9 ppm when 0.07g of $\text{Cs}_{0.1}\text{H}_{2.9}\text{PW}_{12}\text{O}_{40}$ is utilised. Investigation into the ability of free Pd towards the direct synthesis of H_2O_2 has been conducted in Table 3.5. It is shown that there is some activity towards the direct synthesis of H_2O_2 , with catalytic productivity reported as $19 \text{ mol}_{\text{H}_2\text{O}_2} \text{ kg}_{\text{cat}}^{-1} \text{ h}^{-1}$ corresponding to a H_2O_2 yield of 0.039 wt. %. However it is suggested that the contribution towards H_2O_2 synthesis from the leached Pd is minor and the increased H_2O_2 yield is due to the decrease in reaction solution pH and subsequent improvement in H_2O_2 stability.

3.2.4.7. Effect of solvent mass.

The role of solvent mass on the direct synthesis and degradation of H_2O_2 was investigated, while maintaining all other reaction conditions, the results of this investigation are observed, in Figure 3.19.

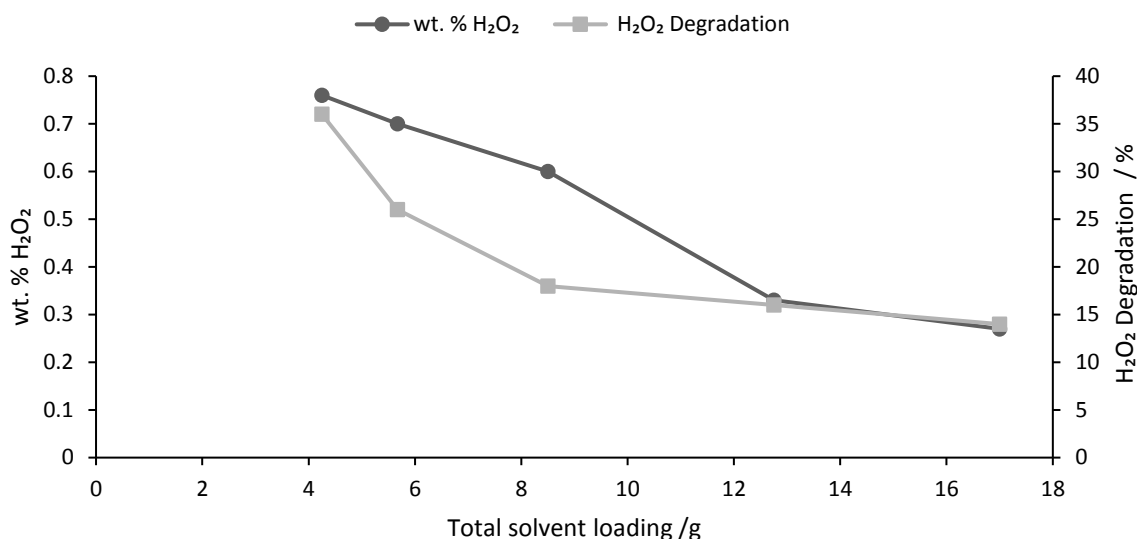


Figure 3.19. H_2O_2 Productivity and H_2O_2 wt. % for 2.5 wt. % Au – 2.5 wt. % Pd / TiO_2 and $\text{Cs}_{0.1}\text{H}_{2.9}\text{PW}_{12}\text{O}_{40}$ as a function of solvent loading.

Reaction conditions: 2.5 wt. % Au – 2.5 wt. % Pd / TiO_2 (0.01 g), $\text{Cs}_{0.1}\text{H}_{2.9}\text{PW}_{12}\text{O}_{40}$ (0.05 g), total pressure 580 psi, $\text{H}_2 / \text{O}_2 = 0.525$, 1200 rpm, 30 min, 66 wt. % CH_3OH , 2 °C.

It is observed that increasing total solvent loading results in a decrease in total concentration of H_2O_2 , with H_2O_2 concentration decreasing from 0.76 to 0.27 wt. % as total solvent loading increases from 4.25 to 17 g, while maintaining the ratio of water to methanol at 1 : 2. As with H_2O_2 yield H_2O_2 degradation decreases with total solvent loading, from a maxima of 36 % when 4.5 g of solvent to a minima of 14 % when 17 g of solvent is utilised. It is suggested that reactant availability may be responsible for the loss in activity towards. As total solvent loading increases so the available head space within the reactor decreases. This means that there is less H_2 and O_2 available for the synthesis of H_2O_2 and less H_2 present for the degradation of H_2O_2 . Furthermore it is suggested that increasing solvent loading results in a greater diffusion pathway from the boundary interphase between the gas – solvent boundary to the surface of the catalyst.

3.2.4.8. Effect of H₂O / CH₃OH ratio.

The effect that the ratio of methanol to water has on the direct synthesis and degradation of H₂O₂ was investigated, while keeping the total amount of solvent constant at 8.5 g. The results are shown in Figure 3.20.

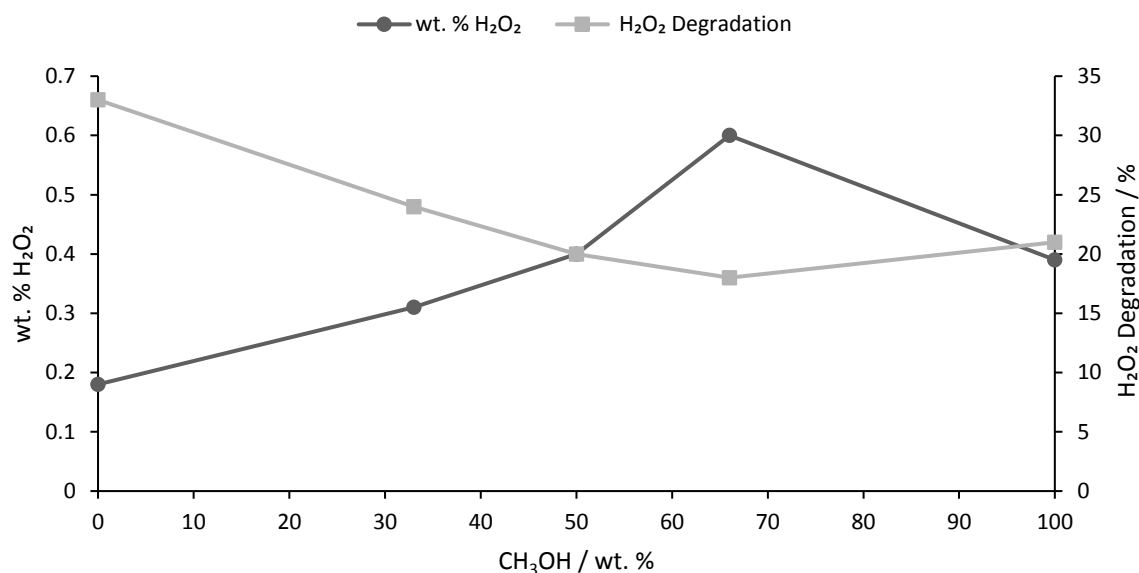


Figure 3.20. H₂O₂ Productivity and H₂O₂ wt. % for 2.5 Wt. % Au – 2.5 wt. % Pd / TiO₂ and Cs_{0.1}H_{2.9}PW₁₂O₄₀ as a function of solvent composition.

Reaction conditions: 2.5 wt. % Au – 2.5 wt. % Pd / TiO₂ (0.01 g), Cs_{0.1}H_{2.9}PW₁₂O₄₀ (0.05 g), total pressure 580 psi, H₂ / O₂ = 0.525, 1200 rpm, 30 min, 66 wt. % CH₃OH, 2 °C.

It is observed that as total methanol content increases to 66 wt. % catalytic activity towards H₂O₂ synthesis increases, with H₂O₂ concentration increasing to a maxima of 0.6 wt. %, when a water : methanol ratio of 1 : 2 is employed. Beyond this point H₂O₂ yield decreases to 0.39 wt. %, in a methanol only solvent and this can be ascribed to the improved solubility of H₂ in methanol in comparison to water. This is a similar observation to that reported by Crole *et.al.*²⁷ who have investigated the effect of solvent composition under similar reaction conditions, using a AuPd / TiO₂ catalyst. The decrease in H₂O₂ synthesis beyond a total methanol content of 66 wt. % is ascribed to the lower solubility of O₂ in methanol. As the solvent system becomes increasingly methanol rich the availability of O₂ decreases and in turn so does the rate of H₂O₂ formation.

Interestingly, the extent of H₂O₂ degradation decreases as methanol content increases, from 33 % when a water only solvent is employed to 18 % when a methanol-water solvent is used in a ratio of 2 : 1. It would be assumed that the rate of hydrogenation would increase as the

system becomes more methanol rich and as such the total amount of H₂O₂ degradation would increase. Indeed, Crole *et.al.*²⁷ have shown that as the solvent becomes more methanol rich the rate of H₂O₂ hydrogenation increase, however it is also reported that rate of H₂O₂ decomposition decreases drastically. It would therefore be of great interest to decouple the two degradation pathways and determine if a similar trend is observed; where hydrogenation increases but decomposition decreases as the solvent becomes increasingly methanol rich. Beyond a 2 : 1 ratio of methanol : water there is a slight increase in the rate of H₂O₂ degradation to 20 % in a pure methanol solvent.

It is known that H₂O₂ stability is improved by the presence of acidic reaction conditions¹⁸, and that the use of CO₂ as the reactant gas diluent has been shown to result in the formation of carbonic acid, improving H₂O₂ selectivity²⁵. It is known that CO₂ has greater solubility in methanol than H₂O²⁹ and so there may be greater stabilisation of H₂O₂ as the solvent system becomes more methanol rich, due to increased formation of carbonic acid. However as water content decreases so the extent of H₂O₂ degradation increases. As the presence of water is required for the formation of carbonic acid and subsequent stabilisation of H₂O₂ it is possible that when using a methanol only solvent there is no stabilisation of H₂O₂ from carbonic acid and as such H₂O₂ degradation increases.

Previous work by Edwards *et.al.*³⁰ investigating Au-Pd/ TiO₂ in a water-methanol solvent system has reported that a maximum catalytic activity towards H₂O₂ synthesis is observed when a water : methanol ratio of 1 : 4 is employed, beyond this ratio catalytic activity towards H₂O₂ synthesis decreases drastically, from 90 to 15 mol_{H₂O₂}kg_{cat}⁻¹h⁻¹ as the water : methanol ratio is increased to 1 : 4.5. In comparison when AuPd / TiO₂ is utilised in addition to Cs_{0.1}H_{2.9}PW₁₂O₄₀ it has been shown, in Figure 3.20, that a greater yield of H₂O₂ can be achieved when using a water methanol ratio of 1 : 2.

It would therefore be of interest to better optimise the solvent composition for the 2.5 wt. % Au – 2.5 wt. % Pd / TiO₂ – Cs_{0.1}H_{2.9}PW₁₂O₄₀ system to determine if an improvement in H₂O₂ yield can be achieved.

3.2.5.1. Variation in pH of the water-methanol working solution using common supports as an additive to 2.5 Wt. % Au – 2.5 Wt. % Pd / TiO₂

It has previously been shown (Table 3.4) that the addition of Cs_xH_{3-x}PW₁₂O₄₀ salts alter the pH of the reaction solution prior to reaction, with decreasing Cs incorporation resulting in a more acidic reaction solution. It can be seen that there is a strong relationship between the

pH of the reaction solution and catalytic productivity. The addition of the $\text{Cs}_{0.1}\text{H}_{2.9}\text{PW}_{12}\text{O}_{40}$ (0.05 g) lowers the pH from 7.0, when only 2.5 wt. % Au – 2.5 wt. % Pd / TiO_2 is present in the solution to 2.68 when the additive is used in conjunction with the catalyst. This coincides with an increase in catalytic activity towards H_2O_2 synthesis, from $64 \text{ mol}_{\text{H}_2\text{O}_2}\text{kg}_{\text{cat}}^{-1}\text{h}^{-1}$ for the 2.5 wt. % Au – 2.5 wt. % Pd / TiO_2 catalyst in the absence of the $\text{Cs}_x\text{H}_{3-x}\text{PW}_{12}\text{O}_{40}$ salt to $299 \text{ mol}_{\text{H}_2\text{O}_2}\text{kg}_{\text{cat}}^{-1}\text{h}^{-1}$ when the catalyst is used in addition to $\text{Cs}_{0.1}\text{H}_{2.9}\text{PW}_{12}\text{O}_{40}$. As Cs incorporation increases the promotional effect towards H_2O_2 synthesis decreases, to a minimum of $86 \text{ mol}_{\text{H}_2\text{O}_2}\text{kg}_{\text{cat}}^{-1}\text{h}^{-1}$ when $\text{Cs}_3\text{PW}_{12}\text{O}_{40}$ is utilised as an additive.

Furthermore Hutchings and workers have shown that the utilisation of acidic supports such as SiO_2 and carbon produces a catalyst that is more active in the direct synthesis of H_2O_2 than those where a basic support such as MgO is used³¹. For catalysts using supports with a lower isoelectric point, selectivity towards H_2O_2 is greater and the activity towards the subsequent hydrogenation and decomposition reactions are lower³². With this in mind it was decided to investigate the ability of common supports to promote the activity of 2.5 wt. % Au – 2.5 wt. % Pd / TiO_2 towards H_2O_2 synthesis with the results shown in Figure 3.21.

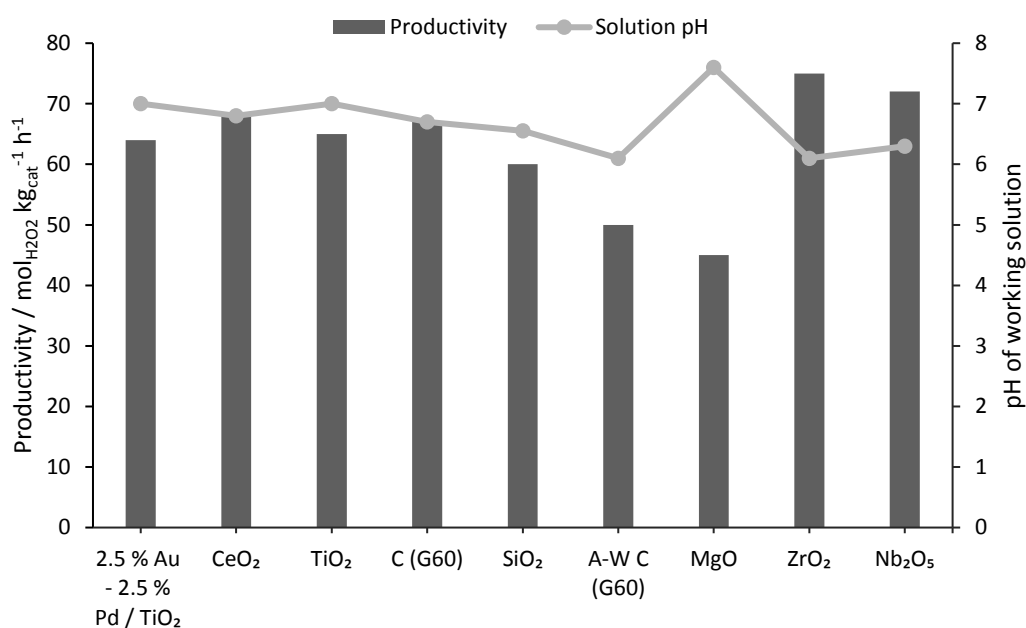


Figure 3.21. H_2O_2 Productivity and pH of reaction solution for 2.5 wt. % Au – 2.5 wt. % Pd / TiO_2 used in addition to common supports.

Reaction conditions: 2.5 wt. % Au – 2.5 wt. % Pd / TiO_2 (0.01 g), Support (0.05 g), total pressure 580 psi, $\text{H}_2 / \text{O}_2 = 0.525$, 1200 rpm, 30 min, 5.6 g CH_3OH + 2.9 g H_2O (66 wt. % CH_3OH), 2 °C.

A correlation between catalytic activity and the pH of the reaction solution pH, prior to reaction, can be observed (Figure 3.21). An increase in catalytic activity can be reported as the reaction solution becomes more acidic. The addition of ZrO_2 and Nb_2O_5 (0.05 g) are

observed to lead to an increase in catalytic activity to 75 and 72 mol_{H₂O₂}kg_{cat}⁻¹h⁻¹ when ZrO₂ and Nb₂O₅ are used respectively as an additive for 2.5 wt. % Au – 2.5 wt. % Pd / TiO₂. However the improvement in catalytic activity is minimal, especially compared to the increase observed when Cs_xH_{3-x}PW₁₂O₄₀ salts are utilised as additives for 2.5 wt. % Au – 2.5 wt. % Pd / TiO₂, regardless of Cs incorporation.

Furthermore it is noted that the use of MgO in addition to the 2.5 wt. % Au – 2.5 wt. % Pd / TiO₂ catalyst results in a significant increase in reaction solution pH, to 7.6, and a corresponding decrease in H₂O₂ formation, with catalytic activity decreasing from 64 mol_{H₂O₂}kg_{cat}⁻¹h⁻¹ for the 2.5 wt. % Au – 2.5 wt. % Pd / TiO₂ catalyst only to 45 mol_{H₂O₂}kg_{cat}⁻¹h⁻¹ when MgO is used in addition to the catalyst. The decrease in catalytic activity is ascribed to the formation of Mg(OH)₂ as MgO dissolves in the reaction solution, and a resulting decrease in the stability of H₂O₂. However, it is suggested that the decrease H₂O₂ yield observed is due to the greater degradation of H₂O₂ as a result of the increased pH of the reaction solution rather than a decrease in catalytic activity towards the synthesis of H₂O₂.

It is possible to conclude that the use of common supports as an additive for 2.5 wt. % Au – 2.5 wt. % Pd / TiO₂ can alter the pH of the reaction solution as well as catalytic activity towards H₂O₂, as a result of increasing or decreasing H₂O₂ stability.

3.2.5.2. Variation in pH of the water-methanol working solution using nitric and tungstic acid as an additive to 2.5 wt. % Au – 2.5 wt. % Pd / TiO₂.

In order to determine if the promotive effect observed when Cs-exchanged tungstophosphoric acid is used as a solid acid additive for the direct synthesis of H₂O₂ using a 2.5 wt. % Au – 2.5 wt. % Pd / TiO₂ catalyst is purely due to the change in the pH of the working solution, diluted tungstic or nitric acid were used to alter the pH of the water-methanol solvent. All other conditions remain as standard, with the acid replacing part of the water in the reaction solution. The results of this study can be seen in Figure 3.22.

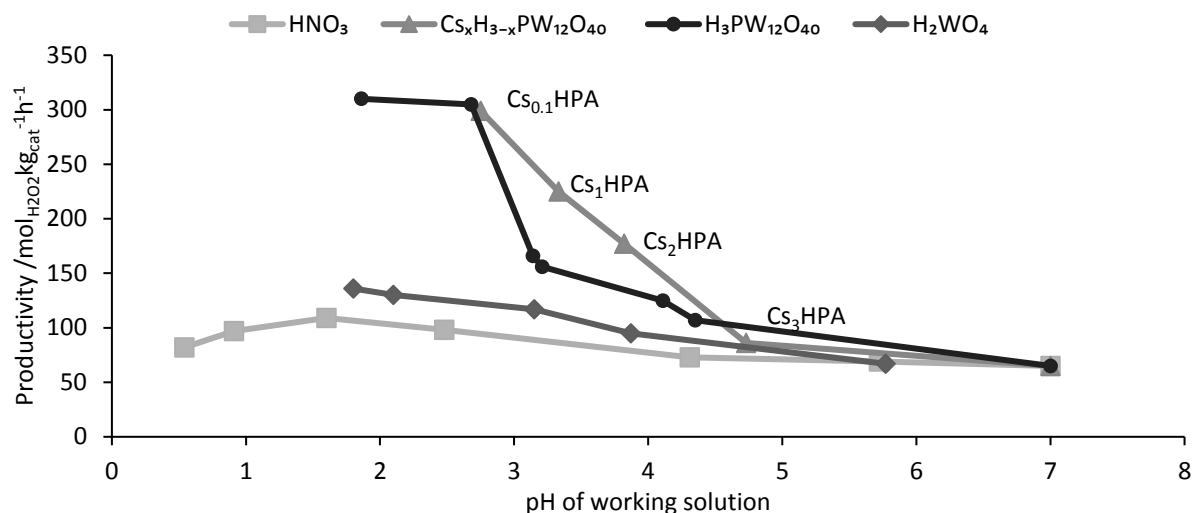


Figure 3.22. The effect that Cs-exchanged HPAs, dilute HNO₃ and H₂WO₄ has in promoting the direct synthesis of H₂O₂.

Reaction conditions: 2.5 wt. % Au – 2.5 wt. % Pd / TiO₂ (0.01g), Cs_xH_(3-x)PW₁₂O₄₀ (0.05 g) or dilute HNO₃, total pressure 580 psi, H₂ / O₂ = 0.525, 1200 rpm, , 5.6 g CH₃OH + 2.9 g H₂O (66 wt. % CH₃OH), 2 °C.

As can be seen in Figure 3.22 the addition of both nitric acid, tungstic acid, Cs-exchanged HPAs and the parent tungstophosphoric acid, with varying mass, lowers the pH of the water methanol working solution and results in an increase in the rate of H₂O₂ synthesis.

However the promotive effect observed when utilising either the Cs-exchanged tungstophosphoric acid or the parent, non-substituted, additive is observed to provide a greater catalytic activity when compared to the use of HNO₃. Using the Cs-exchanged material or the parent acid to set pH of the working solution at approximately 2.7 is reported to produce a much more active catalyst in comparison to when HNO₃ is used to produce a marginally lower pH, approximately pH 2.5. As can be seen in Figure 3.22. The utilisation of H₃PW₁₂O₄₀ or Cs-exchanged tungstophosphoric acid to set the pH of the working solution at approximately 2.7 results in an increase in catalytic activity from 64 mol_{H₂O₂} kg_{cat}⁻¹ h⁻¹ to 299 and 305 mol_{H₂O₂} kg_{cat}⁻¹ h⁻¹ for the Cs_{0.1}H_{2.9}PW₁₂O₄₀ salt and parent material respectively. However the use of HNO₃ only improves catalytic activity to 98 mol_{H₂O₂} kg_{cat}⁻¹ h⁻¹. This is particularly interesting as it suggests that the modification of the pH of the working solution by the Cs-exchanged or parent heteropolyacid is not the sole reason for the improvement in activity towards H₂O₂ synthesis. However further work using other, non-halide acids must be carried out to give a complete comparison of the role of conventional acids in comparison to heteropolyacids.

It is known that acidic conditions help to stabilise H_2O_2 ¹⁸ from its subsequent degradation and that the use of acid washed supports has been found to limit or 'switch off' H_2O_2 degradation.^{33,35} It is interesting to note that when HNO_3 or H_2WO_4 is used to alter the pH of the reaction solution the increase in catalytic activity is much smaller than the increase seen when both the $\text{Cs}_x\text{H}_{3-x}\text{PW}_{12}\text{O}_{40}$ salts and tungstophosphoric acid are utilised. This trend continues even when the pH of the working solution is reduced below that possible using the heteropolyacid additives either in the Cs-exchanged form or as the parent acid. It may therefore be reasonable to assume that the reduction of solution pH may not solely cause the increase in rate of synthesis of H_2O_2 . It has previously been shown in Table 3.3 that the use of $\text{Cs}_x\text{H}_{3-x}\text{PW}_{12}\text{O}_{40}$ salts result in the leaching of Pd from the support, with 30 % of total Pd observed to be leached from the support when $\text{H}_3\text{PW}_{12}\text{O}_{40}$ is used in addition to the catalyst. It is possible that the addition of excess nitric acid results in the leaching of metals active for the direct synthesis of H_2O_2 in particular Pd, in a manner similar to that observed when $\text{Cs}_x\text{H}_{3-x}\text{PW}_{12}\text{O}_{40}$ salts are used in addition to 2.5 wt. % Au – 2.5 wt. % Pd / TiO_2 .

It has previously been demonstrated (Table 3.3) that W is detected in the reaction solution regardless of Cs incorporation in the $\text{Cs}_x\text{H}_{3-x}\text{PW}_{12}\text{O}_{40}$ salts with a general trend reported where the amount of W detected decreases as Cs incorporation increases. This suggests that the solubility of the $\text{Cs}_x\text{H}_{3-x}\text{PW}_{12}\text{O}_{40}$ salt decreases with increasing Cs content. It is shown in Figure 3.22 that activity towards H_2O_2 synthesis increases with decreasing Cs content within the $\text{Cs}_x\text{H}_{3-x}\text{PW}_{12}\text{O}_{40}$ salt and furthermore it has been demonstrated that this is not solely due to the decrease in reaction solution pH.

It is known that the presence of phosphate in the reaction solution is able to stabilise H_2O_2 ³⁶ and that the stability of the Keggin structure can be related to Cs content. As the $\text{Cs}_x\text{H}_{3-x}\text{PW}_{12}\text{O}_{40}$ salt becomes less stable, with decreasing Cs content, the availability of phosphate ions (PO_4^{3-}) in the reaction solution increases and so H_2O_2 stability increases. It is therefore possible to conclude that the improvement in catalytic activity towards H_2O_2 synthesis is due to a combination of decreasing reaction solution pH and an increase in the availability of PO_4^{3-} . This correlates with the trend observed in Figure 3.22, where there is an apparent increase in catalytic activity as Cs content decreases. As such it is possible to suggest that the utilisation of Cs exchanged tungstophosphoric acid as an additive for 2.5 wt. % Au – 2.5 wt. % Pd / TiO_2 improves the stability of H_2O_2 rather than improving catalytic activity towards the synthesis of H_2O_2 .

3.2.7. Reusability of the Cs-exchanged HPAs in the direct synthesis of H₂O₂.

In order to produce a catalyst that may find industrial application it is important to ensure that the Cs-exchanged HPA additives are stable to re-use. Table 3.3 above shows that after reaction both Cs and W are detected in the reaction solution, regardless of Cs-content. The concentration of W within the solution decreases significantly as Cs loading into the Keggin structure increases. In comparison Cs content is observed to pass through a maximum of 183 ppm, when Cs loading is equal to Cs_{2.0}. As Cs content is increased further to Cs_{2.5} the concentration of Cs detected in the reaction solution decreases to 150 ppm. Further investigation into the reaction solution shows that Pd is present within the reaction solution when the catalyst is used in addition to the Cs_xH_{3-x}PW₁₂O₄₀ salt, regardless of Cs content.

Table 3.9 shows the reusability of 2.5 wt. % Au – 2.5 wt. % Pd / TiO₂ - Cs_xH_{3-x}PW₁₂O₄₀ with varying values of x. The experimental procedure is similar to that reported in Chapter 2 Section 2.3.1 for the direct synthesis of H₂O₂, however upon completion of the first reaction the solid is removed from the reaction solution by filtration followed by drying (110 °C, 16 h, static air). The resultant solid was then weighed to determine the extent of material lost during recovery and investigated for its activity towards the direct synthesis of H₂O₂.

Table 3.9. The reusability of 2.5 wt. % Au – 2.5 wt. % Pd / TiO₂ - Cs_xH_{3-x}PW₁₂O₄₀.

Reaction conditions: Catalyst (0.01 g), Cs_x H_{3-x}PW₁₂O₄₀ (0.05 g), total pressure 580 psi, H₂ / O₂ =0.525, 1200 rpm, 30 min, CH₃OH + 2.9 g H₂O (66 Wt. % CH₃OH), 2 °C.

Catalyst system	Catalyst mass post reaction / g	Productivity Fresh / mol _{H₂O₂} kg _{cat} ⁻¹ h ⁻¹	Productivity Reuse / mol _{H₂O₂} kg _{cat} ⁻¹ h ⁻¹
2.5 wt. % Au – 2.5 wt. % Pd / TiO ₂ + Cs _{2.5} H _{0.5} PW ₁₂ O ₄₀	0.058	188	188
2.5 wt. % Au – 2.5 wt. % Pd / TiO ₂ + Cs ₂ HPW ₁₂ O ₄₀	0.053	239	207
2.5 wt. % Au – 2.5 wt. % Pd / TiO ₂ + Cs _{0.1} H _{2.9} PW ₁₂ O ₄₀	0.01	299	n.d.

Where n.d. = not able to determine

Firstly it should be noted that after reaction, filtration and recovery not all of the solid mixture of catalyst and Cs_xH_{3-x}PW₁₂O₄₀ salt was recovered and for calculation of catalyst activity it was assumed that total catalyst recovery was possible. That is, any mass loss was due to the loss of Cs_xH_{3-x}PW₁₂O₄₀ salt.

It is reported that the Cs_xH_{3-x}PW₁₂O₄₀ salts with values of x lower than 2.5 were not stable upon re-use with the activity of the 2.5 wt. % Au – 2.5 wt. % Pd / TiO₂ - Cs₂HPW₁₂O₄₀ physical

mixture decreasing from 239 to 207 mol_{H₂O₂} kg_{cat}⁻¹h⁻¹. This is partly explained by the incomplete recovery of the physical mixture after its first use. Secondly it was shown in Table 3.3 that there is significant loss of both Cs and W from the Keggin unit upon use of the Cs₂HPW₁₂O₄₀ additive, with 183 ppm of Cs and 564 ppm of W detected in the reaction solution in addition to 2 ppm Pd. While reusability studies utilising Cs_{0.1}H_{2.9}PW₁₂O₄₀ in addition to 2.5 wt. % Au – 2.5 wt. % Pd / TiO₂ were not possible due to the inability to separate Cs_{0.1}H_{2.9}PW₁₂O₄₀ from the reaction solution post reaction. Although it has previously been shown (Table 3.3) that a significant amount of Pd is leached from the catalyst support when Cs_{0.1}H_{2.9}PW₁₂O₄₀ is used in addition to the 2.5 wt. % Au – 2.5 wt. % Pd / TiO₂ catalyst.

Re-use of the catalytic system utilising Cs_{2.5}H_{0.5}PW₁₂O₄₀ as an acid additives shows no loss in activity towards the direct synthesis of H₂O₂ and a significant increase in activity compared to the catalyst alone, with an activity of 188 mol_{H₂O₂} kg_{cat}⁻¹h⁻¹ reported when Cs_{2.5}H_{0.5}PW₁₂O₄₀ is used in addition to 2.5 wt. % Au – 2.5 wt. % Pd / TiO₂. While the catalyst alone has been shown to offer an activity of 64 mol_{H₂O₂} kg_{cat}⁻¹h⁻¹. However it has previously been shown in Table 3.3. that Pd, Cs and W are detected in the reaction solution after reaction, with a Pd concentration of 1 ppm observed. This suggests that over multiple uses catalyst activity may decrease due to the loss of Pd from the support.

It would be of great interest to investigate the stability of 2.5 wt. % Au – 2.5 wt. % Pd / TiO₂, when Cs_{2.5}H_{0.5}PW₁₂O₄₀ is used as an additive, over longer reaction times. It may be possible to stabilise the loss of Pd and maintain the high activities reported. It is suggested that future investigation concentrates on increasing the stability of 2.5 wt. % Au – 2.5 wt. % Pd / TiO₂ in the presence of Cs-exchanged tungstophosphoric acid, as well as decreasing the solubility of Cs_{2.5}H_{0.5}PW₁₂O₄₀ as this material has shown the most promise in reusability.

3.3. Conclusion.

Cs-exchanged heteropolyacids have been investigated as additives for 2.5 wt. % Au – 2.5 wt. % Pd / TiO₂ in the direct synthesis of H₂O₂. It has been shown that the addition of Cs_xH_{3-x}PW₁₂O₄₀ salts where x is less than 2.5 results in the promotion of catalytic activity towards the direct synthesis of H₂O₂ with a maximum productivity of 301 mol_{H₂O₂} kg_{cat}⁻¹h⁻¹ reported when 0.05 g of the unsubstituted H₃PW₁₂O₄₀ is utilised in addition to the 5 wt. % Au – 2.5 wt. % Pd / TiO₂ catalyst. While the addition of 0.05 g of Cs₃PW₁₂O₄₀ causes a decrease in the rate of H₂O₂ formation, to a minimum of 48 mol_{H₂O₂} kg_{cat}⁻¹h⁻¹, which is ascribed to the ability of Cs to degrade H₂O₂. A general trend is observed where the amount of leached Cs increases as the value of x in Cs_xH_{3-x}PW₁₂O₄₀ increases, to a maximum of 180 ppm for Cs₂HPW₁₂O₄₀. Increasing the value of x beyond Cs_{2.0} decreases the total amount of leached Cs to 95 ppm when the Cs₃PW₁₂O₄₀ additive is utilised, suggesting that although Cs incorporation into the Keggin cage structure is key in reducing the solubility of tungstophosphoric acid it is not possible to completely inhibit the dissolution of the Cs_xH_{3-x}PW₁₂O₄₀ salt. This is supported by the detection of W within the reaction solution, regardless of the extent of Cs exchanged.

It has been demonstrated that as the extent of Cs exchanged in to the Keggin decreases so does the pH of the reaction solution prior to the reaction occurring and it is suggested that this is partly responsible for the improvement in catalyst activity towards H₂O₂ formation. In addition it has been reported that the use of Cs_xH_{3-x}PW₁₂O₄₀ salts as additives for 2.5 wt. % Au – 2.5 wt. % Pd / TiO₂ results in the leaching of Pd from the support, with leaching of up to 30 % observed when H₃PW₁₂O₄₀ is utilised in addition to the 2.5 wt. % Au – 2.5 wt. % Pd / TiO₂ catalyst. Both of these factors are considered to be responsible for the increase in H₂O₂ synthesis observed when Cs_xH_{3-x}PW₁₂O₄₀ salts are used in addition to 2.5 wt. % Au – 2.5 wt. % Pd / TiO₂. Furthermore, it has been demonstrated that the presence of Cs in the reaction solution is able to degrade H₂O₂ and a general trend is reported, where the amount of Cs detected in the reaction solution increases with increasing value of x in Cs_xH_{3-x}PW₁₂O₄₀.

Catalyst reusability has been investigated and it is shown that retention of catalytic activity towards H₂O₂ synthesis can only be achieved when the value of x in Cs_xH_{3-x}PW₁₂O₄₀ is greater than 2.5. Despite the high extent of Cs exchange required a substantial increase in activity of the catalyst towards H₂O₂ synthesis is observed with productivity reported to increase from 64 to 188 mol_{H₂O₂}kg_{cat}⁻¹h⁻¹. This is viewed as a meaningful step forward in the

development of the direct synthesis of H₂O₂ process. However it should be noted that Cs, W and Pd are all detected within the reaction solution after use and as such it is highly likely that catalyst activity will decrease with subsequent uses.

Comparison between catalytic activity towards H₂O₂ synthesis when either HNO₃, H₂WO₃ or Cs_xH_{3-x}PW₁₂O₄₀ salts are used in addition to 2.5 wt. % Au – 2.5 wt. % Pd / TiO₂ suggests that the decrease in the reaction solution pH is not the only reason for improved H₂O₂ synthesis activity. It is suggested that the presence of phosphate ions within the reaction solution, through the dissolution of the Keggin cage structure, increases H₂O₂ stability and is responsible for the observed increase in catalytic activity towards H₂O₂. As Cs content within the Cs_xH_{3-x}PW₁₂O₄₀ salt increases so does the stability of the Keggin structure and as a result the availability of PO₄³⁻ decreases.

3.4. References

1. T. A. Pospelova, N.I. Kobozev, *Russ. J. Phys. Chem.*, 1961, **35**, 1192-1197.
2. T. A. Pospelova, N.I. Kobozev, *Russ. J. Phys. Chem.*, 1961, 535-542.
3. T. A. Pospelova, N.I. Kobozev, E. N. Eremin, *Russ. J. Phys. Chem.*, 1961, 298-305
4. Y.-F. Han and J. H. Lunsford, *J.Catal.*, 2005, **230**, 313-316.
5. P. Landon, P. J. Collier, A. F. Carley, D. Chadwick, A. J. Papworth, A. Burrows, C. J. Kiely and G. J. Hutchings, *Phys.Chem.Chem. Phys.*, 2003, **5**, 1917-1923.
6. P. Landon, P. J. Collier, A. J. Papworth, C. J. Kiely and G. J. Hutchings, *Chem. Commun.*, 2002, **18**, 2058-2059.
7. V. Choudhary and C. Samanta, *J.Catal.*, 2006, **238**, 28-38.
8. V. R. Choudhary, C. Samanta and T. V. Choudhary, *J.Mol.Catal.A.Chem.*, 2006, **260**, 115-120.
9. C. Samanta and V. R. Choudhary, *Catal. Commun.*, 2007, **8**, 2222-2228.
10. T. Okuhara, T. Nishimura, H. Watanabe and M. Misono, *J.Mol.Catal.*, 1992, **74**, 247-256.
11. S. Park, T. J. Kim, Y.-M. Chung, S.-H. Oh and I. K. Song, *Res.Chem.Intermedi.*, 2010, **36**, 639-646.
12. M. Sun, J. Zhang, Q. Zhang, Y. Wang and H. Wan, *Chem Commun*, 2009, **34**, 5174-5176.
13. E. N. Ntainjua, M. Piccinini, S. J. Freakley, J. C. Pritchard, J. K. Edwards, A. F. Carley and G. J. Hutchings, *Green Chem.*, 2012, **14**, 170.
14. S. J. Freakley, R. J. Lewis, D. J. Morgan, J. K. Edwards and G. J. Hutchings, *Catal Today*, 2015, **248**, 10-17.
15. S. Park, S. Lee, S. Song, D. Park, S. Baeck, T. Kim, Y. Chung, S. Oh and I. Song, *Catal. Commun.*, 2009, **10**, 391-394.
16. J. A. Dias, E. Caliman and S. C. Loureiro Dias, *Micropor.Mesopor.Mater.*, 2004, **76**, 221-232.
17. K. Narasimharao, D. R. Brown, A. F. Lee, A. D. Newman, P. F. Siril, S. J. Tavener and K. Wilson, *J.Catal.* 2007, **248**, 226-234.
18. C. Samanta, *Appl.Catal.A.Gen.*, 2008, **350**, 133-149.
19. D. P. Dissanayake and J. H. Lunsford, *J.Catal.*, 2002, **206**, 173-176.
20. J. Lee, S. Hwang, D. R. Park, J. G. Seo, M. H. Youn, J. C. Jung, S.-B. Lee, J. S. Chung and I. K. Song, *KoreanJ.Chem.Eng.* 2010, **27**, 807-811.
21. M. T. Pope, *Angew.Chem.Int.Ed.* 1983, **96**, 730.
22. N. Essayem, *Journal of Catalysis*, 2001, **197**, 273-280.
23. C. Rocchiccioli-Deltcheff, M. Fournier, R. Franck and R. Thouvenot, *Inorg. Chem.*, 1983, **22**, 207-216.
24. J.K Edwards, B.E. Solsona, P. Landon, A. Carley, A. A. Herzing, C.J. Kiely and G.J. Hutchings, *J.Catal.* 2005, **236**, 69-79.
25. E. N. Ntainjua N, M. Piccinini, J. C. Pritchard, J. K. Edwards, A. F. Carley, J. A. Moulijn and G. J. Hutchings, *ChemSusChem*, 2009, **2**, 575-580.
26. E. N. Ntainjua N, J. K. Edwards, A. F. Carley, J. A. Lopez-Sanchez, J. A. Moulijn, A. A. Herzing, C. J. Kiely and G. J. Hutchings, *Green Chem.* 2008, **10**, 1162.
27. D. A. Crole, S. J. Freakley, J. K. Edwards and G. J. Hutchings, *Proc. R. Soc. A*, 2016, **472**, 20160156.
28. V. R. Choudhary, C. Samanta and P. Jana, *Appl.Catal.A.Gen*, 2007, **317**, 234-243.
29. I. Urukova, J. Vorholz and G. Maurer, *J.Phys.Chem.B*, 2006, **110**, 14943-14949.
30. J. K. Edwards, A. Thomas, B. E. Solsona, P. Landon, A. F. Carley and G. J. Hutchings, *Catalysis Today*, 2007, **122**, 397-402.
31. J. K. Edwards, A. Thomas, A. F. Carley, A. A. Herzing, C. J. Kiely and G. J. Hutchings, *Green Chem.*, 2008, **10**, 388.

32. E. N. Ntainjua, J. K. Edwards, A. F. Carley, J. A. Lopez-Sanchez, J. A. Moulijn, A. A. Herzing, C. J. Kiely and G. J. Hutchings, *Green Chem.*, 2008, **10**, 1162-1169.
33. J. K. Edwards, B. Solsona, E. N. N, A. F. Carley, A. A. Herzing, C. J. Kiely and G. J. Hutchings, *Science*, 2009, **323**, 1037-1041.
34. J. K. Edwards, E.N Ntainjua, A. F. Carley, A. A. Herzing, C. J. Kiely and G. J. Hutchings, *Angew.Chem. Int.Ed.*, 2009, **48**, 8512-8515.
35. J. K. Edwards, S. F. Parker, J. Pritchard, M. Piccinini, S. J. Freakley, Q. He, A. F. Carley, C. J. Kiely and G. J. Hutchings, *Catal.Sci.Technol.*, 2013, **3**, 812.
36. P. Wegner, *US patent number US20030151024 A1*, 2003, Hydrogen peroxide stabilizer and resulting product and applications.

4. Ammoximation of cyclohexanone via *in-situ* H₂O₂ synthesis.

4.1. Introduction.

TS-1 has been well reported as an efficient, selective catalyst for many oxidation reactions, when used alongside H₂O₂, such as alkane oxidation¹, alkene epoxidation² and the formation of propylene oxide³. The ammoximation of cyclohexanone to cyclohexanone oxime is a key industrial process that utilises the excellent selectivity of TS-1 along with H₂O₂. The formation of cyclohexanone oxime is crucial in the formation of caprolactam the monomer of Nylon-6, a highly commercialised polymer that is used in a wide range of sectors, from automotive to food packaging and electrical cables.

Current production of cyclohexanone oxime is reliant on the transportation and storage of large quantities of H₂O₂, with which comes inherent risk and cost. By producing H₂O₂ *in-situ* it is suggested that large economic savings could be made to the industrial production of cyclohexanone oxime.

In order to investigate the feasibility of producing cyclohexanone oxime through the *in-situ* synthesis of H₂O₂ catalysts utilising commercial TS-1 as a support have been prepared by impregnation. Their activity towards the direct synthesis of H₂O₂, at sub-ambient and elevated temperatures using conditions established from literature⁴⁻⁶, have been investigated and following on from this the activity of a model 5 % Pd / TS-1 catalyst towards H₂O₂ synthesis and subsequent degradation under conditions similar to those used for the ammoximation reaction, via the addition of H₂O₂, was also examined.

Following this mono- and bi-metallic Au-Pd catalysts supported on TS-1 were evaluated for their activity towards the ammoximation of cyclohexanone to cyclohexanone oxime via addition of pre-formed H₂O₂, in a manner to that already reported within the literature⁷. Finally using a model 5 wt. % Pd / TS-1 reaction conditions were established for the ammoximation of cyclohexanone via the *in-situ* synthesis of H₂O₂ from H₂ and O₂.

Figure 4.1 is a proposed reaction scheme for the ammoximation of cyclohexanone to cyclohexanone oxime via the *in-situ* generation of H₂O₂. It is known that many catalysts that are active towards the direct synthesis of H₂O₂ are also active towards the degradation of

H₂O₂. However it is suggested that due to the use of elevated temperatures and presence of basic conditions, in the form of NH₃, the development of a catalyst that is inactive towards H₂O₂ degradation would have minimal impact on limiting overall breakdown of H₂O₂. Furthermore it has been reported that a number of minor organic by-products may be formed, either through the reaction of cyclohexanone oxime with H₂O₂ to form nitrocyclohexane or the homogeneous reaction of cyclohexanone to yield cyclohexenylcyclohexanone and cyclohexanone azine ⁸.

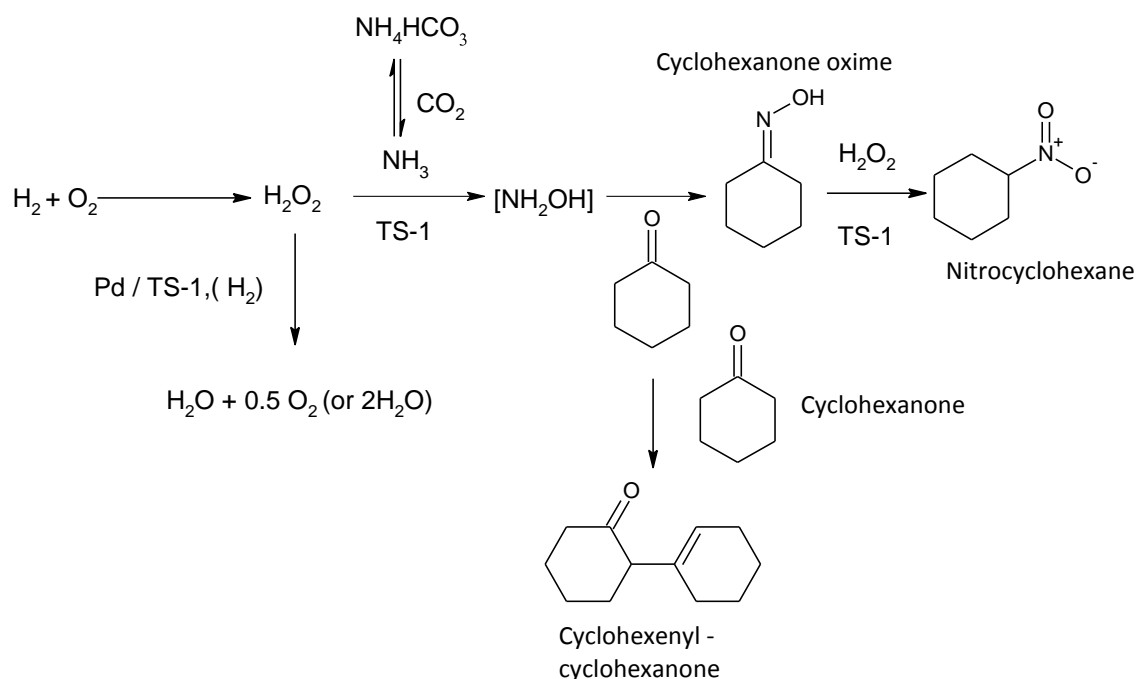


Figure 4.1. Proposed reaction scheme for the ammoxidation of cyclohexanone via *in-situ* generation of H₂O₂.

4.2. Results.

Supported Au / Pd as well as bi-metallic catalysts were prepared on TS-1 by the standard impregnation methods as outlined in Chapter 2 using PdCl₂ and HAuCl₄. All H₂O₂ synthesis and degradation testing as well as cyclohexanone oxime synthesis, via *in-situ* formation of H₂O₂ or the addition of pre-formed H₂O₂ were carried out according to the procedures outlined in Chapter 2.

A summary of the standard testing conditions is outlined below:

1. H₂O₂ direct synthesis reaction conditions: Catalyst (0.01 g), MeOH (5.6 g), H₂O (2.9 g), 5 % H₂ / CO₂ (2.9 MPa) and 25 % O₂ / CO₂ (1.1 MPa), 30min, 2 °C, 1200 rpm.

2. H₂O₂ degradation reaction conditions: Catalyst (0.01 g), MeOH (5.6 g), H₂O (2.22g), H₂O₂ (0.68 g 50 wt. %) 5 % H₂/CO₂ (2.9 MPa) 30min, 2 °C, 1200 rpm.
3. Ammoximation of cyclohexanone via the addition of pre-formed H₂O₂ reaction conditions: Catalyst (0.05 g), cyclohexanone (10 mmol), NH₃ (28 wt. % 12 mmol), H₂O (2.5 g), t-BuOH (2.5 g), 80 °C, 35 wt. % H₂O₂ (10 mmol, 0.89 mlhr⁻¹ then 0.5 h stir).
4. Cyclohexanone ammoximation reaction conditions: Catalyst (0.05 g), t-BuOH (5.6 g), H₂O (2.69 g), cyclohexanone (0.13 g), NH₃ (28 Wt. %, 0.079 g), 5 % H₂/ CO₂ (2.9 MPa) and 25 % O₂/CO₂ (1.1 MPa), 30 min, 80 °C, 1200 rpm.

4.2.1. H₂O₂ synthesis activity of monometallic and bimetallic Au-Pd catalysts supported on TS-1.

Monometallic catalysts were prepared by impregnation containing 5 wt. % Au or 5 wt. % Pd using TS-1 as a support material. These catalysts were calcined at 400 °C for 3h in static air. Bi-metallic catalysts were prepared containing 5 wt. % Pd - Au on TS-1 in a 1 : 1 ratio and calcined in a similar manner.

Initial studies were conducted to determine the ability of Au, Pd and Au-Pd catalysts to synthesise H₂O₂, using standard reaction conditions, outlined in Chapter 2, Section 2.3.1. Further work was then conducted at higher temperatures (30 °C). Table 4.1 compares H₂O₂ synthesis rates at 2 and 30 °C using a water (H₂O) / methanol (MeOH) solvent system.

Table 4.1 Catalytic activity towards the direct synthesis of H₂O₂, in a H₂O / MeOH solvent system.

Catalyst	H ₂ O ₂ productivity / mol _{H₂O₂} kg _{cat} ⁻¹ h ⁻¹ (2 °C)	H ₂ O ₂ productivity/ mol _{H₂O₂} kg _{cat} ⁻¹ h ⁻¹ (30 °C)
5 wt. % Au / TS-1	2	0
2.5 wt. % Au- 2.5 wt. % Pd / TS-1	100	19
5 wt. % Pd / TS-1	116	26
2.5 wt. % Au- 2.5 wt. % Pd / Al ₂ O ₃	15 ⁹	0
2.5 wt. % Au- 2.5 wt. % Pd / TiO ₂	64 ¹⁰	36
2.5 wt. % Au- 2.5 wt. % Pd / SiO ₂	108 ¹¹	51
2.5 wt. % Au- 2.5 wt. % Pd / C	110 ¹²	55

Reaction conditions: Catalyst (0.01 g), 580 psi, H₂ / O₂ = 0.525, 1200 rpm, 30 min, 5.6 g MeOH + 2.9 g H₂O (66 wt. % CH₃OH), X °C.

Catalysts calcined 3 h, 400 °C, static air, 20 °C min⁻¹

It is observed that the TS-1 supported Au, Pd, Au-Pd, catalysts are active towards the direct synthesis of H₂O₂ and at sub-ambient temperatures the bi-metallic Au-Pd catalysts are observed to have greater rates of H₂O₂ synthesis than analogous catalysts supported on TiO₂ (64 mol_{H₂O₂} kg_{cat}⁻¹ h⁻¹)¹³ and Al₂O₃ (15 mol_{H₂O₂} kg_{cat}⁻¹ h⁻¹)⁹ and have comparable activity to the corresponding SiO₂ (108 mol_{H₂O₂} kg_{cat}⁻¹ h⁻¹)¹⁴ and carbon supported catalyst (110 mol_{H₂O₂} kg_{cat}⁻¹ h⁻¹)¹¹.

As expected when higher temperatures are investigated the rate H₂O₂ synthesis decreases for all catalysts investigated. Both the 5 wt. % Pd and 2.5 wt. % Au – 2.5 wt. % Pd / TS-1 catalysts are observed to lose approximately 80 % of their activity toward H₂O₂ synthesis, with productivity values of 26 and 19 mol_{H₂O₂} kg_{cat}⁻¹ h⁻¹ reported for the 5 wt. % Pd and 2.5 wt. % Au – 2.5 wt. % Pd / TS-1 catalysts respectively. This is ascribed to an increase in the rate of H₂O₂ degradation, it is known that H₂O₂ stability decreases as temperature increases. It has previously been reported by Hutchings and co-workers¹⁵ that raising reaction temperature results in an increase in the conversion of H₂, from 20 % at 2 °C to 30 % at 30 °C, but a corresponding decrease in selectivity towards H₂O₂. It has been reported by Freakley *et.al.*¹⁵ that as reaction temperature is increased the solubility of O₂ in both water and methanol decreases, resulting in a decrease in the rate of H₂O₂ synthesis. In addition

Freakley *et.al.*¹⁵ report that an increase in temperature results in an increase in H₂ solubility in methanol, as such the rate of hydrogenation of H₂O₂ is expected to be greater at elevated temperatures and these two factors combined result in a decrease in H₂O₂ selectivity.

Interestingly, the activity of the 5 wt. % Pd / TS-1 catalyst is observed to be greater than that of the 2.5 wt. % Au- 2.5 wt. % Pd / TS-1 when investigated at both 2 and 30 °C. This is somewhat at odds with previous work conducted by Hutchings and co-workers, who have shown that, on a range of supports the incorporation of Au onto a Pd-only catalyst improves catalytic activity towards H₂O₂ synthesis beyond that of the monometallic catalysts^{13 9 16}. This has been ascribed to the formation of core-shell metal nanoparticles and the electronic modification of Pd by Au¹⁷. It would be of great interest to investigate particle morphology and the extent of alloying of Au and Pd on a TS-1 support to determine if a similar particle morphology is adopted when utilising this support. It has previously been demonstrated that when utilising a carbon support¹⁷ Au-Pd nanoparticles adopt a random alloy, unlike when oxide supports such as TiO₂ are used¹⁷. It may be that in a similar manner to when carbon is used as a support the metal nanoparticles adopt a random alloy morphology, rather than a Au-core PdO-shell morphology.

4.2.2. The direct synthesis of H₂O₂, using 5 wt. % Pd/ TS-1 as a model catalyst, moving towards ammoximation conditions.

The direct synthesis of H₂O₂ has been well studied by Hutchings *et.al.*^{4,13} using a H₂O - MeOH solvent system, due to the high solubility of H₂ in MeOH and conversely the high solubility of O₂ in H₂O. Wu *et.al.*¹⁸ has shown that when tertiary / t- butanol (t-BuOH) is used as a solvent superior levels of both cyclohexanone conversion and oxime selectivity are observed when compared to H₂O, toluene and MeOH when TS-1 is used as the catalyst for the ammoximation of cyclohexanone. Further investigation by Francesconi and co-workers¹⁹ have shown that the solubility of hydrogen increases with alcohol chain length. Therefore, in order to find a balance between high solubility of H₂ and O₂ and superior selectivity towards cyclohexanone oxime a mixed H₂O / t-BuOH solvent system was chosen to investigate the ammoximation reaction via *in-situ* H₂O₂ generation and firstly for the direct synthesis of H₂O₂ from H₂ and O₂. Further investigation on the role of solvent composition is carried out below in Section 4.3.4.

Table 4.2 compares the H₂O₂ synthesis rates of 5 wt. % Pd / TS-1 in a H₂O / t-BuOH solvent system under various temperatures (30 - 80 °C) and in the presence of cyclohexanone and NH₃.

Table 4.2. Direct synthesis of H₂O₂ from H₂ and O₂ in H₂O/t-BuOH solvent system.

Temperature / °C	Solvent only		Cyclohexanone present ^(a)		NH ₃ present ^(b)	
	H ₂ O ₂ productivity / mol _{H₂O₂} kg _{cat} ⁻¹ h ⁻¹	H ₂ Conversion / %	H ₂ O ₂ productivity / mol _{H₂O₂} kg _{cat} ⁻¹ h ⁻¹	H ₂ Conversion / %	H ₂ O ₂ productivity / mol _{H₂O₂} kg _{cat} ⁻¹ h ⁻¹	H ₂ Conversion / %
30	60	10	55	9	0	10
50	12	13	10	12	0	12
80	7	17	5	15	0	16

Reaction conditions: 5 wt. %Pd / TS-1 (0.01 g), 580 psi, H₂ / O₂ =0.525, 1200 rpm, 30 min, 5.6 g t-BuOH + 2.9 g H₂O (66 Wt. % t-BuOH), X °C. ^(a) cyclohexanone (0.13 g 1.3 mmol), ^(b) NH₃ (28 wt. %, 0.08 g 1.3 mmol).

It has been shown that the solubility of H₂ in alcohols increases with chain length¹⁹, and as such it is likely that the rate of H₂O₂ synthesis is linked to the number of carbon atoms present in the solvent chain. This is demonstrated when the rate of H₂O₂ synthesis using a H₂O / MeOH and H₂O / t-BuOH solvent system are compared. H₂O₂ productivity for the 5 wt. % Pd / TS-1 catalyst increases from 26 to 60 mol_{H₂O₂} kg_{cat}⁻¹ h⁻¹ with increasing alcohol chain length, at 30 °C.

As can be seen in Table 4.2 the catalytic activity towards H₂O₂ decreases from 60 to 7 mol_{H₂O₂} kg_{cat}⁻¹ h⁻¹ as temperature increases to 80 °C. This is as expected, as H₂O₂ productivity is determined at the end of the reaction and is therefore not a measure of total H₂O₂ synthesis but of how much is remaining post reaction. It is known that H₂O₂ is unstable at elevated temperatures²⁰ and as such it is expected that lower rates of H₂O₂ synthesis would be observed.

When cyclohexanone is incorporated into the system there is a small decrease in the synthesis rate of H₂O₂, from 60 to 55 mol_{H₂O₂} kg_{cat}⁻¹ h⁻¹. This may be due to partial inhibition of active sites responsible for H₂O₂ synthesis, a decrease in H₂ solubility when cyclohexanone is present or the use of H₂ in the reduction of cyclohexanone resulting in less H₂ available for H₂O₂ synthesis.

The presence of NH₃ results in no H₂O₂ being detected at the end of the reaction. Again this is unsurprising as it is known that H₂O₂ is unstable in the presence of basic conditions²¹. It is possible that under the conditions utilised some NH₃ utilised in the formation of NH₂OH and it is suggested that the extent of hydroxylamine formation could be quantified via the addition of cyclohexanone and measurement of the resultant yield of cyclohexanone oxime.

4.2.3. The degradation of H₂O₂ using 5 wt. % Pd / TS-1 as a model catalyst, moving towards ammoximation conditions.

For a catalytic system to be efficient towards H₂O₂ synthesis the rate of catalytic breakdown of H₂O₂ must be limited as much as possible. Furthermore the ability of the solvent, cyclohexanone and NH₃ to contribute to H₂O₂ degradation must also be understood. The conditions utilised for the ammoximation of cyclohexanone via *in-situ* synthesis of H₂O₂ are quite challenging as H₂O₂ readily decomposes at elevated temperatures and in basic conditions, it is therefore important to determine how effective these reaction conditions are at decomposing H₂O₂. Table 4.3 outlines the effect of the reaction conditions towards the degradation of 12 wt. % H₂O₂ in a t-BuOH / H₂O solvent mixture in the presence of cyclohexanone and / or NH₃ and a 5 wt. % Pd / TS-1 catalyst. Standard H₂O₂ degradation testing, as outlined in Chapter 2, Section 2.3.2, utilises a lower concentration of H₂O₂ (4 wt. %). However as the reaction conditions are known to be unfavourable towards H₂O₂ stability it was decided to use a greater concentration of H₂O₂ (12. wt. %).

Table 4.3. Comparison of H₂O₂ degradation at 30 °C in the presence and absence of 5 Wt. % Pd / TS-1.

	H ₂ O ₂ degradation /	
	%	
	No catalyst	Catalyst
Solvent system only	0	35
Solvent + Cyclohexanone	14	38
Solvent + NH ₃	71	82
Solvent + Cyclohexanone + NH ₃	76	85

Reaction conditions: 5 wt. % Pd / TS-1 (0.01 g), 580 psi, H₂ / O₂ =0.525, 1200 rpm, 30 min, 5.6 g t-BuOH + 0.86 g H₂O, 2.04 g H₂O₂ (50 Wt. %), 28 wt. % NH₃ (0.08 g 1.3 mmol), cyclohexanone (0.13 g 1.3mmol), 30 °C.

It is observed that the solvent system does not contribute to the degradation of H₂O₂, in the absence of catalyst, cyclohexanone or ammonia. This is particularly interesting as it is expected that some degradation of H₂O₂ would be observed at an elevated temperature. Upon introduction of the 5 wt. % Pd / TS-1 catalyst a dramatic increase in H₂O₂ degradation is observed, with 35 % degradation reported.

The introduction of cyclohexanone leads to a slight increase in the rate of H₂O₂ degradation. With degradation reported to be 14 % in the absence of catalyst and 38 % when the catalyst

is present and this correlates with the slight decrease in the rate of H₂O₂ synthesis observed when cyclohexanone is present, shown in Table 4.2.

Unsurprisingly the introduction of NH₃ to the solvent system leads to a rise in the breakdown of H₂O₂, to 71 % in the absence of the catalyst respectively. This is expected due to the low stability of H₂O₂ under basic conditions. Upon addition of the catalyst a rise in H₂O₂ degradation is observed, to 82 %. It is suggested that the relatively small increase in H₂O₂ degradation with catalyst addition is due to limitations in mass transfer of the H₂O₂ to the catalyst, the NH₃ present in solution readily decomposes H₂O₂ before it can reach catalytic sites responsible for its degradation. Combination of both cyclohexanone and NH₃ results in a further increase in H₂O₂ degradation, to 76 % when no catalyst is present and 85 % when a catalyst is introduced.

The data shown in Table 4.3 demonstrates the ability of the reaction conditions to contribute to H₂O₂ degradation and highlights the difficulties associated with the in-situ synthesis of H₂O₂ in the ammoximation reaction. However it is suggested that by improving catalyst selectivity towards H₂O₂ it is possible to more efficiently utilise the reactants, in particular H₂, and reduce costs to any future industrial application.

4.2.4. The ammoximation of cyclohexanone to cyclohexanone oxime via H₂O₂ addition.

The monometallic and bimetallic Au-Pd catalysts prepared by impregnation were tested for the ammoximation of cyclohexanone via the addition of pre-formed H₂O₂. These catalysts were compared to the bare TS-1 material, following the procedure is outlined in Chapter 2. But is shown below for clarity:

Cyclohexanone (1.0 g, 10 mmol), catalyst (0.05 g), t-BuOH (2.5 g), H₂O (2.5 g) and 28 wt. % NH₃ (12 mmol, 0.73 g) were added into a two neck flask with condenser attached. The second flask neck is equipped with a H₂O₂ inlet line. The reaction mixture was heated, with stirring, to 80 °C and H₂O₂ (35 wt. %, 10 mmol, 0.89 g) was added over 1 h using a HPLC pump, at a rate of 0.0148 mlmin⁻¹. The reaction was allowed to continue for a further 0.5 h. After this time the reaction mixture was allowed to cool to room temperature and ethanol (10 ml) and internal standard (diethylene glycol monoethyl ether) (1.0 g) are added. The catalyst is removed by filtration and the mixture is analysed by gas chromatography.

The ability of the catalyst to convert cyclohexanone and catalyst selectivity towards the oxime was determined by gas chromatography. Catalytic re-use was also investigated in a manner similar to that outlined above. The results are summarised in Table 4.4.

Table 4.4. Comparison of fresh Au, Pd, and Au-Pd loaded TS-1 and non-metal loaded TS-1 for the ammoximation of cyclohexanone via the addition of H₂O₂.

Unused Catalyst		
Catalyst	Cyclohexanone Conversion / %	Oxime Selectivity / %
TS-1	40	70
5 wt. % Au / TS-1	39	72
2.5 wt. % Au- 2.5 wt. % Pd / TS-1	34	67
5 wt. % Pd / TS-1	36	64
Used Catalyst		
Catalyst	Cyclohexanone Conversion / %	Oxime Selectivity / %
TS-1	40	30
5 wt. % Au / TS-1	39	14
2.5 wt. % Au- 2.5 wt. % Pd / TS-1	33	24
5 wt. % Pd / TS-1	33	18

Reaction Conditions: Catalyst (0.05 g), cyclohexanone (10 mmol), NH₃ (28 wt. % 12 mmol), H₂O (2.5 g), t-BuOH (2.5 g), 80 °C, 35 wt. % H₂O₂ (10 mmol, 0.89 mlhr⁻¹ then 0.5 h stir).

It is reported that the monometallic and bimetallic Au-Pd catalysts show similar levels of cyclohexanone conversion and selectivity towards cyclohexanone oxime as the bare TS-1. The non-metal containing TS-1 material is reported to offer 70 % selectivity towards the oxime, and conversion rates of 40 %, while both of these measures vary slightly when Au and Pd are incorporated onto the support. This suggests that the introduction of these metals do not adversely effect the activity of the support towards the ammoximation of cyclohexanone to a great extent and that the presence of the metal on the support does not block availability to the Ti(IV) sites, believed to be key in the formation of hydroxylamine. These catalysts may show promise for the ammoximation of cyclohexanone via *in-situ* H₂O₂ synthesis.

Catalytic reusability was investigated, where the material were dried at 110 °C for 16 h prior to re-use. Upon re-use a similar extent of conversion of cyclohexanone to the fresh materials was observed, whereas a dramatic decrease in selectivity towards cyclohexanone oxime was determined. The use of basic reaction conditions are known to lead to the loss of Ti from the framework of TS-1 resulting in the deactivation of TS-1²². It is believed that this may partially explain the loss in selectivity towards cyclohexanone oxime. Furthermore, it is known that the formation of organic by-products such as; nitrocyclohexane, cyclohexenylcyclohexanone and cyclohexanone azine, seen in Figure 4.2, can all contribute to catalyst deactivation via

blocking of the pore system within TS-1, preventing access to Ti(IV) sites¹⁸ required to activate H₂O₂. It may be that the formation of these un-wanted by-products become more dominant upon catalyst re-use and a further investigation into the products formed upon catalyst re-use would be beneficial. As would investigation into catalyst regeneration. However as this study is primarily an investigation into the ability of precious metals supported on TS-1 to catalyse the ammoximation of cyclohexanone via *in-situ* H₂O₂ synthesis, that is in the presence of a reducing atmosphere and dilute carbonic acid present in the reaction solution due to the use of CO₂ as a diluent for the reactant gasses (H₂ and O₂) it was not thought prudent to heavily characterise the catalysts described in this section of work. It is possible to conclude that the incorporation of Au and Pd onto TS-1 does not adversely affect the ability of the support to catalyse the formation of cyclohexanone oxime. Furthermore the work of Wu *et.al.* has demonstrated that the use of high temperatures, 80 °C, is able to negate the formation of unwanted by-products during the ammoximation of cyclohexanone¹⁸, via the addition of pre-formed H₂O₂. As such it is the extent of pore blocking by by-products may be minimal.

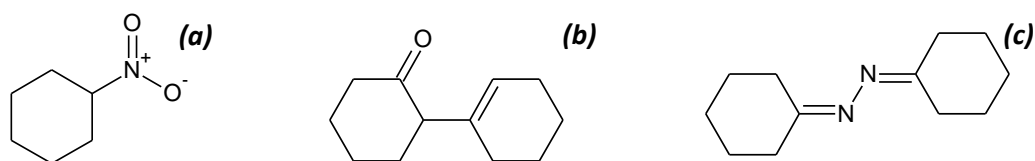


Figure 4.2. Unwanted by-products reported during the ammoximation of cyclohexanone to cyclohexanone oxime. ^(a) Nitrocyclohexane, ^(b) Cyclohexenylcyclohexanone, ^(c) Cyclohexanone azine.

4.3. Optimisation of Reaction Conditions for the Ammoximation of Cyclohexanone to Cyclohexanone Oxime.

Previously it has been shown that Au / Pd / Au – Pd / TS-1 catalysts are active for both the direct synthesis of H₂O₂ and the ammoximation of cyclohexanone through the addition of H₂O₂ (Sections 4.2.1 and 4.2.4).

The ability of these materials to catalyse the ammoximation of cyclohexanone via *in-situ* H₂O₂ synthesis is evaluated below using 5 wt. % Pd / TS-1 as a model catalyst. Further investigation in to the role of catalyst design in improving this approach to the ammoximation of cyclohexanone is outlined in the following Chapter.

As discussed above the reaction conditions utilised in the ammoximation of cyclohexanone are not conducive H₂O₂ stability, in particular the use elevated temperatures and presence

of base can lead to high rates of H₂O₂ degradation. Furthermore it has been shown that the ratio of reactants (H₂O₂ : NH₃ : cyclohexanone) is key in producing a highly selective process for the ammoximation reaction utilising addition of H₂O₂^{23, 24}. It is therefore important to use reaction conditions that find a balance between optimal cyclohexanone conversion and selectivity towards cyclohexanone oxime as well as H₂O₂ synthesis and overall stability of the catalyst. To this end the reaction conditions utilised in the ammoximation of cyclohexanone to cyclohexanone oxime via *in-situ* H₂O₂ synthesis were investigated. For any process to be industrially feasible catalyst stability is very important, to this end the leaching of Pd from the support was measured as a function of solvent composition as well as cyclohexanone and NH₃ concentration.

4.3.1. Reaction temperature optimisation.

The optimal temperature for the industrial ammoximation process has been reported to be between 80-90 °C, with excess temperatures suggested to limit the availability of both H₂O₂ and NH₃, due to degradation or vaporisation²⁵. While H₂O₂ direct synthesis has been shown to favour sub-ambient temperatures^{13, 20}, as H₂O₂ rapidly decomposes to H₂O at elevated temperatures. Finding a balance between these two processes offers a major initial challenge, rapid H₂O₂ decomposition may limit the synthesis of NH₂OH as H₂O₂ is unable to reach the Ti (IV) sites present on the TS-1. The formation of this intermediate is believed to be key in the ammoximation of cyclohexanone²⁶.

As has been shown in Section 4.2.2 above it is possible to make H₂O₂ in a H₂O/ t-BuOH solvent at elevated temperatures. It is highly likely that at temperatures as high as 80 °C H₂O₂ can be synthesised, however H₂O₂ 'lifetime' may be very short due to the high decomposition rate at such a high temperature and as H₂O₂ concentration is determined at the end of the reaction it is not possible to determine true values for catalytic activity towards H₂O₂ synthesis. Figure 4.3 shows the effect of reaction temperature on the ammoximation of cyclohexanone via *in-situ* H₂O₂ synthesis.

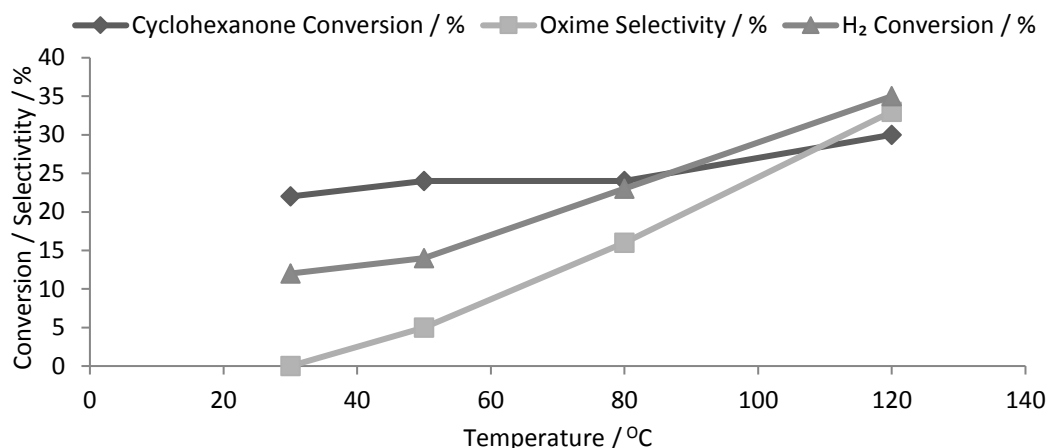


Figure 4.3. The effect of reaction temperature on the ammoximation of cyclohexanone.

Reaction conditions: 5 wt. % Pd / TS-1 (0.05 g), cyclohexanone (0.13 g, 1.3mmol), NH₃ (0.08 g, 28 wt %, 1.3 mmol), total pressure 580 psi, H₂ / O₂ =0.525, 1200 rpm, 90 min, 5.6 g t-BuOH + 2.69 g H₂O (66 wt. % t-BuOH), X °C.

It can be seen that for any significant oxime synthesis to be observed a temperature of 80 °C (where selectivity and cyclohexanone conversion are reported as 16 and 24 % respectively) is required. This is found to correlate well with temperatures reported in literature for the ammoximation process via the addition of H₂O₂¹⁸ below this temperature it is found that the formation of un-wanted organic by-products can dominate²⁷. Further increasing temperature to 120 °C causes a rise in conversion to 33 %, while selectivity increases to 30 %. It has been suggested by Dal Pozzo and co-workers²⁶ that at higher temperatures the formation unwanted inorganic by-products, in particular nitrites and nitrates, occurs less readily as the competitive catalytic formation of hydroxylamine is kinetically predominant to the oxidation of ammonia by H₂O₂.

It can be observed that as reaction temperature increases so does the extent of H₂ conversion, increasing from 12 to 35 % as the reaction temperature increases from 30 to 120 °C. It has been reported by Freakley *et.al.*¹⁵ that increasing reaction temperature in a water – methanol solvent system leads to a decrease in the solubility of oxygen in both water and methanol, while the solubility of H₂ increases in methanol. This results in an increase in the rate of hydrogenation of H₂O₂ and a decrease in the rate of H₂O₂ synthesis. It is suggested that a similar effect is observed in Figure 4.2. That is at increased temperatures the solubility of H₂ is greater in the solvent and with more H₂ present in the system the rate of H₂O₂ hydrogenation is increased. However as O₂ solubility decreases the rate of H₂O₂ formation decreases, by decreasing the rate of H₂O₂ formation it is possible to ensure that the available Ti(IV) sites of the TS-1 support are able to readily activate H₂O₂ to allow for hydroxylamine formation.

Furthermore, the formation of ammonia salts, such as ammonium carbonate at ambient temperatures, when the autoclave is charged with reactant gases (O_2/CO_2 and H_2/CO_2) will result in a decrease in the rate of hydroxylamine formation. As temperature increases so does the rate of ammonium carbonate decomposition, and it may be that this causes the ratio of reactants to be closer to 1 : 1 : 1 and as such an improvement in selectivity is observed.

Finally increased temperature may result in improvement in reactant diffusion, this means that there is increased diffusion of NH_3 to Ti (IV) sites present on the support as well as diffusion of hydroxylamine from the support to cyclohexanone and as such conversion of cyclohexanone is improved. However as the reaction solution is stirred at 1200 rpm the effect of increased temperature on diffusion is believed to be minimal at best.

4.3.2. Catalyst mass optimisation.

Figure 4.4 shows the effect of catalyst mass on the ammoximation of cyclohexanone to cyclohexanone oxime.

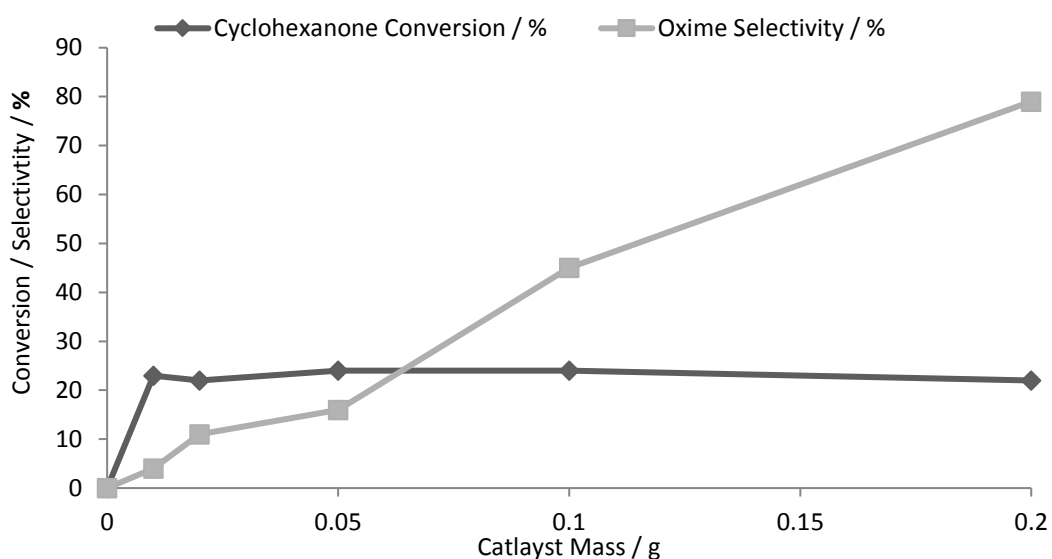


Figure 4.4. The effect of catalyst mass on the ammoximation of cyclohexanone.

Reaction conditions: 5 wt. % Pd / TS-1 (X g), cyclohexanone (0.13 g, 1.3 mmol), NH_3 (0.08 g, 28 wt. %, 1.3 mmol), total pressure 580 psi, $H_2/O_2=0.525$, 1200 rpm, 90 min, 5.6 g t-BuOH + 2.69 g H_2O (66 wt. % t-BuOH), 80 °C.

Firstly it should be noted that in the absence of catalyst there is no conversion of cyclohexanone and no oxime is detected. Furthermore it can be seen that increasing catalyst mass leads to improvement in catalytic selectivity but not conversion, by increasing catalyst mass from 0.01g to 0.2 g selectivity increases by almost 20 times from 4 to 79 %. It is

reasonable to expect that by using more catalyst there is greater availability of Ti (IV) sites and so conversion of H_2O_2 to hydroxylamine is likely to increase.

The utilisation of more 5 Wt. % Pd / TS-1 is likely to lead to an increase in the concentration of H_2O_2 , however it is known that many catalysts active for the direct synthesis of H_2O_2 are also active for its subsequent degradation and as such it is unclear if the net H_2O_2 synthesis is increased with increasing catalyst amount. In this case it is possible that the net synthesis of H_2O_2 changes very little as the increase in synthesis rate is offset by increasing catalytic degradation of H_2O_2 . However, it may also be possible that the formation of H_2O_2 is limited by diffusion of H_2 and O_2 to the active sites present on the catalyst. But the increased availability of Ti(IV) sites means that once H_2O_2 is formed it is utilised more selectively in the formation of hydroxylamine and not degraded to water by the reaction conditions or catalyst.

The presence of more Ti(IV) sites may mean that the conversion of H_2O_2 and NH_3 to NH_2OH is increased, that is selectivity towards hydroxylamine based on H_2O_2 increases, and so the selectivity towards the oxime is increased as catalyst mass utilised rises. In comparison to selectivity conversion remains fairly static regardless of total catalyst loading.

4.3.3. Solvent composition optimisation

It has been reported that the presence of t-butanol (t-BuOH) improves both catalytic stability, conversion of cyclohexanone and selectivity towards the oxime for the ammoximation process with the addition of pre-formed H_2O_2 ¹⁸. While the direct synthesis of H_2O_2 has been highly studied using a H_2O / MeOH mixture as this offers high solubility of both H_2 and O_2 and furthermore aids in stabilising H_2O_2 . However from an environmental and economic perspective the use of H_2O as a solvent may be beneficial.

Figure 4.5 shows the effect of solvent composition on cyclohexanone conversion, selectivity towards cyclohexanone oxime as well as H_2 conversion and the leaching of Pd from the catalyst during the reaction.

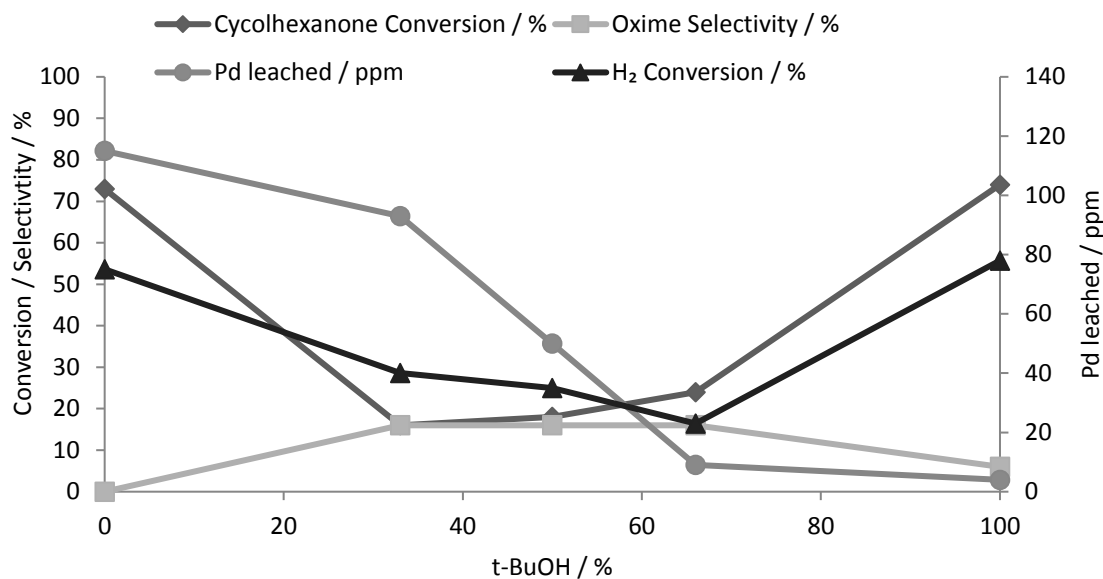


Figure 4.5. The effect of solvent composition on the ammoxidation of cyclohexanone.

Reaction conditions: 5 wt. % Pd / TS-1 (0.05 g), cyclohexanone (0.13 g), NH₃ (0.08 g, 28 wt. %), total pressure 580 psi, H₂ / O₂ = 0.525, 1200 rpm, 90 min, total solvent mass 8.5 g, 80 °C.

It can be observed that in a pure H₂O system rates of cyclohexanone conversion are extremely high, 73 %, while no oxime is observed. This can be explained when the amount of Pd leached from the support is considered. A pure H₂O solvent system results in a high amount of leaching of Pd into the solvent (115 ppm). It has been shown by Lunsford and co-workers²⁸ that colloidal Pd is active for the direct synthesis of H₂O₂. As Pd is present in the solution it is suggested that diffusion of reactant gas to those active sites responsible for H₂O₂ synthesis present on the unsupported Pd is quicker than diffusion to Pd supported on TS-1. H₂O₂ formed by colloidal Pd will have a greater diffusion pathway to Ti(IV) sites present on the support than that formed by supported Pd. This increased diffusion pathway means that decomposition of H₂O₂, due to high temperatures and presence of NH₃ as well as catalytic breakdown of H₂O₂ may be greater than when H₂O₂ is synthesised by supported Pd.

When a pure t-BuOH solvent system is utilised conversion of cyclohexanone is 74 % while selectivity to the oxime is very low (6 %), while measurement of H₂ conversion shows that in a 100 % t-BuOH system H₂ conversion is high (78 %). It is believed that the solubility of H₂ is much higher than that of O₂ and so conversion of cyclohexanone to the corresponding alcohol by hydrogenation is high accounting for both the high conversion and low selectivity rates. Furthermore another reason for the low selectivity towards cyclohexanone oxime may be due to an increase in the hydrogenation of H₂O₂, as H₂ availability is increased. It is therefore suggested that by manipulation of the solvent system it would be possible to optimise H₂ : O₂ ratio in a manner that improves selectivity towards cyclohexanone oxime.

4.3.4. Cyclohexanone concentration optimization.

It has been shown above that it is possible to synthesise H_2O_2 in the presence of cyclohexanone from H_2 and O_2 in a H_2O / t-BuOH solvent mixture. However catalytic activity decreased slightly upon incorporation of cyclohexanone. Figure 4.6 shows the effect of cyclohexanone concentration on conversion of cyclohexanone and selectivity towards the oxime.

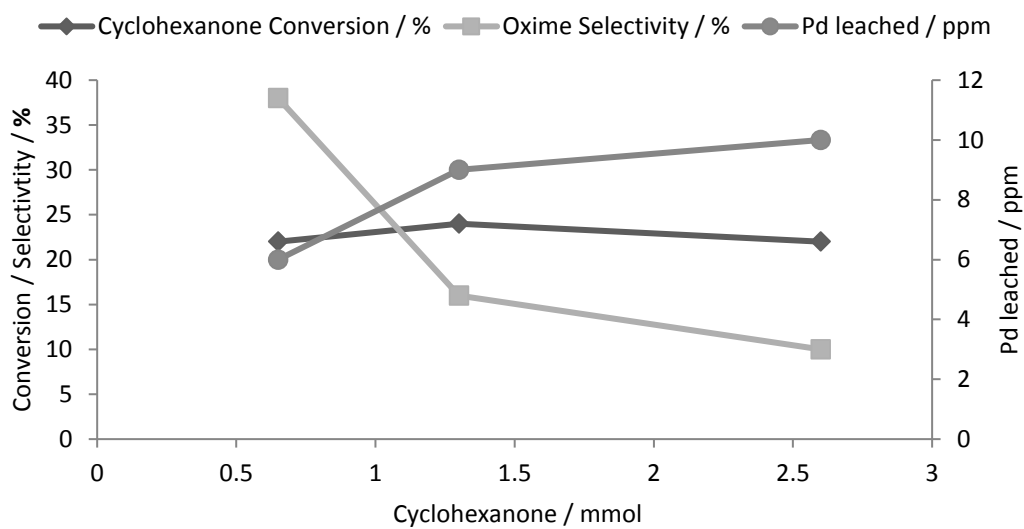


Figure 4.6. The effect of cyclohexanone concentration on the ammoxidation of cyclohexanone. **Reaction conditions:** 5 wt. % Pd / TS-1 (0.05 g), cyclohexanone (X g), NH_3 (0.08 g, 28 wt. %, 1.3 mmol), total pressure 580 psi, $\text{H}_2 / \text{O}_2 = 0.525$, 1200 rpm, 90 min, 5.6 g t-BuOH + 2.69 g H_2O (66 wt. % t-BuOH), 80°C .

It is observed that as cyclohexanone concentration increases selectivity towards the oxime decreases, from 38 to 10 % as cyclohexanone concentration rises from 0.65 to 2.6 mmol. There is little change in conversion of cyclohexanone with increasing concentration of this reactant, with conversion remaining in the range of 22 – 26 % regardless of concentration. It can also be observed that as cyclohexanone concentration increases the amount of Pd leached from the catalyst increases, suggesting that it is not just the presence of H_2O in the system that can contribute to the loss of catalyst stability, although Pd leaching is observed to be much less than that observed when a H_2O only solvent is utilised, with only 10 ppm of Pd detected. Further work investigating methods to increase catalyst stability is investigated in Chapter 5.

It can be assumed that not all H_2 present in the system (approximately 1.3 mmol) is converted to H_2O_2 and it has been shown above that reaction conditions can cause H_2O_2 degradation. This means that H_2O_2 concentration within the system may be much lower than that of NH_3

and cyclohexanone. The selectivity towards cyclohexanone oxime, during the ammoximation reaction, when pre-formed H_2O_2 is added to the reaction mixture has been shown to be linked to the ratio of reactants (H_2O_2 : NH_3 : cyclohexanone) and it has been observed that a 1 : 1 : 1 ratio is optimal²³. If this is true for the ammoximation process via *in-situ* H_2O_2 synthesis lowering the cyclohexanone concentration may cause the concentration of cyclohexanone to become similar to that of H_2O_2 and in turn results in an improved selectivity.

4.3.5. Ammonia concentration optimization.

It is well known that the presence of basic conditions leads to rapid degradation of H_2O_2 ²⁹. This offers a particular challenge to the synthesis of cyclohexanone oxime via the *in-situ* synthesis of H_2O_2 , especially when considering the high temperatures required for significant oxime formation, which also presents issues to H_2O_2 stability. The formation of hydroxylamine is believed to require H_2O_2 co-ordination to the Ti (IV) sites of TS-1, however the highly basic conditions within the reaction solution, as well as high temperature, means that H_2O_2 degradation is a considerable issue and that not all the H_2O_2 formed is able to diffuse to the Ti (IV) sites on the support without undergoing degradation to H_2O .

Figure 4.7 shows the effect of NH_3 concentration on conversion of cyclohexanone and selectivity towards the oxime.

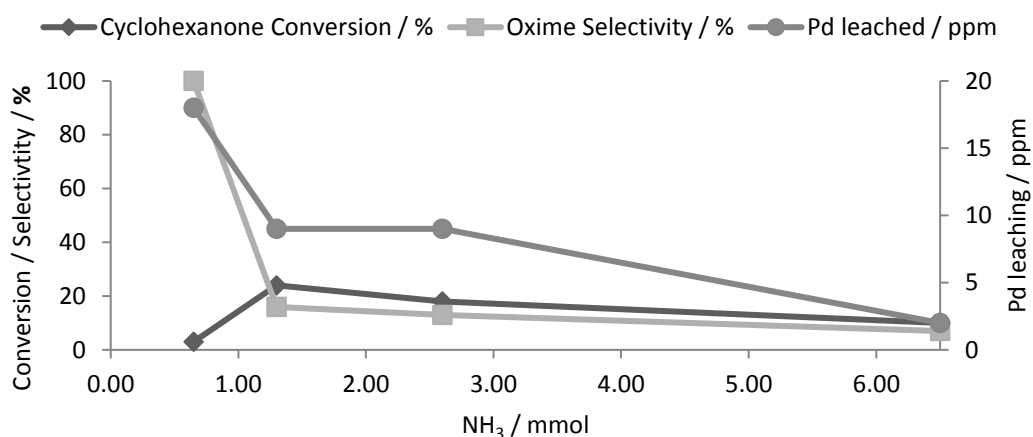


Figure 4.7. The effect of ammonia concentration on the ammoximation of cyclohexanone.

Reaction conditions: 5 wt. % Pd / TS-1 (0.05 g), cyclohexanone (0.13 g, 1.3 mmol), NH_3 (X g, 28 wt. %), total pressure 580 psi, $\text{H}_2 / \text{O}_2 = 0.525$, 1200 rpm, 90 min, 5.6 g t-BuOH + 2.69 g H_2O (66 wt. % t-BuOH), 80 °C.

It can be seen that selectivity towards the oxime decrease as NH_3 concentration rises, from 100 to 7 %. This decrease is unsurprising, as previously discussed the presence of NH_3 in the reaction solution is detrimental to H_2O_2 , as H_2O_2 is stabilised by the presence of acidic reaction conditions. With more NH_3 in the reaction solution it is likely that rates of H_2O_2 degradation will increase due to the higher pH of the solution. It has previously been shown in Section 4.2.2 above that no H_2O_2 is detected when catalyst activity towards H_2O_2 synthesis in the presence of NH_3 is investigated. However this does not mean that no H_2O_2 is formed, and the detection of cyclohexanone oxime indicates that H_2O_2 is indeed formed. Interestingly the amount of Pd leached from the support decreases with increasing NH_3 concentration, from 18 to 2 ppm. It is suggested that as some H_2O from the reaction solution is replaced with NH_3 it is possible this contributes to some reduction in the overall leaching of Pd from the catalyst.

4.3.6. Reaction time optimisation.

Figure 4.8 shows the effect of reaction time on the ammoximation of cyclohexanone. It should be noted that reactions were performed for varied durations of time rather than sampling from a continuous experiment and this would affect the reaction dynamics.

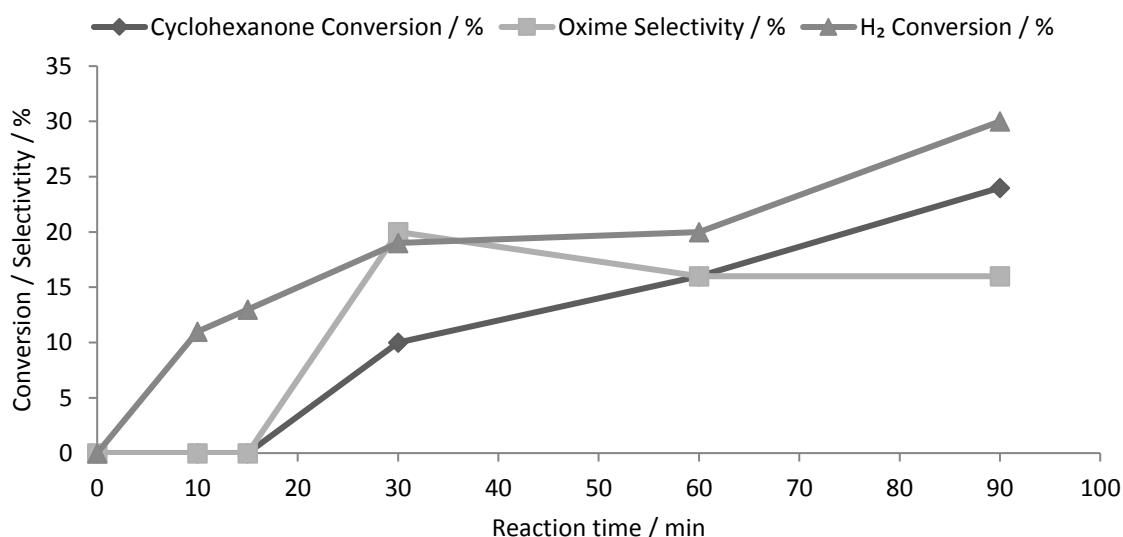


Figure 4.8. The effect of reaction time on the ammoximation of cyclohexanone.

Reaction conditions: 5 wt. % Pd / TS-1 (0.05 g), cyclohexanone (0.13 g), NH_3 (0.08 g, 28 wt. %), total pressure 580 psi, $\text{H}_2/\text{O}_2=0.525$, 1200 rpm, X min, 5.6 g t-BuOH + 2.69 g H_2O (66 wt. % t-BuOH), 80 °C.

As can be seen an induction period is required for any oxime to be detected. Even though H_2 conversion is measured at 13 % at a reaction time of 15 min no oxime is detected. It is

suggested that at short reaction times the concentration of H_2O_2 synthesised is minor and the degradation of H_2O_2 due to reaction conditions ensures that no H_2O_2 is able to diffuse to the Ti(IV) sites present on the support to result in the formation of cyclohexanone oxime. It may also be possible that a proportion of NH_3 is removed from the system while the reaction is reaching reaction temperature. The formation of $(\text{NH}_4)_2\text{CO}_3$ or NH_4HCO_3 , through reaction between the CO_2 , used as a diluent for the reactant gasses, and NH_3 may contribute to the lack of oxime detected at short reaction times. It may be that the lack of oxime formation is due to the unavailability of a proportion of NH_3 . It is not until the ammonia salt decomposes and the NH_3 is free to produce hydroxylamine that the oxime can be formed.

It is observed that as reaction time increases so does the conversion of cyclohexanone, to a maximum of 24 % at a reaction time of 90 mins. As with cyclohexanone conversion the conversion of H_2 increases with time to a maximum of 30 % at a reaction time of 90 mins. Selectivity remains stable between a reaction time of 30 and 90 minutes, at approximately 20 %. Although this is a relatively low value it is suggested that through catalyst design it is possible to improve selectivity as well as conversion and this is discussed in Chapter 5.

4.3.7. Reactant gas composition optimization.

The effect that the ratio of $\text{H}_2 : \text{O}_2$ has on the ammoxidation of cyclohexanone is shown in Figure 4.9.

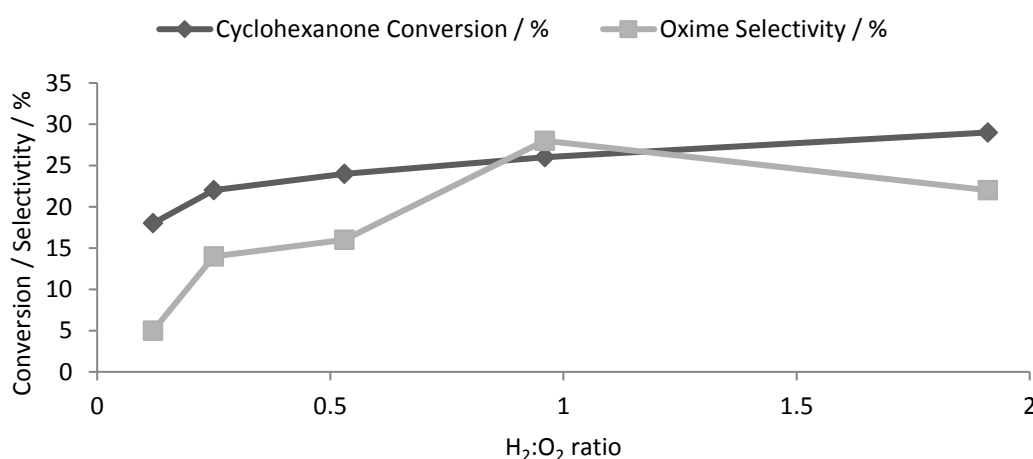


Figure 4.9. The effect of $\text{H}_2:\text{O}_2$ ratio on the ammoxidation of cyclohexanone, while maintaining total pressure. **Reaction conditions:** 5 wt. % Pd / TS-1 (0.05 g), cyclohexanone (0.13 g), NH_3 (0.08g, 28 wt. %), total pressure 580 psi, 1200 rpm, 90 min, 5.6 g t-BuOH + 2.69 g H_2O (66 wt. % t-BuOH), 80 °C.

Hutchings and co-workers have shown that the optimal ratio of $H_2 : O_2$ for the direct synthesis of H_2O_2 , under their reaction conditions, in a H_2O - MeOH solvent system is 1 : 2 in favour of O_2 ^{9, 13, 16}. It was theorised that the high hydrogenation activity of Pd would mean that the use of lower H_2 pressures would result in less hydrogenation of cyclohexanone to unwanted by-products, such as cyclohexanol, and in turn greater selectivity towards the oxime.

However this was not observed, as can be seen in Figure 4.9 selectivity towards cyclohexanone oxime remains fairly low when an excess of O_2 is present selectivity is particularly low, with selectivity towards the oxime observed to reach a minimum of 5 % when a $H_2 : O_2$ ratio of 1 : 8 is utilised. It is suggested that at low H_2 content little H_2O_2 is synthesised and so the formation of the oxime is limited. However it has been shown that cyclohexanone is able to undergo homogeneous reaction to produce cyclohexenylcyclohexanone and cyclohexanone azine and it is suggested that at low H_2O_2 synthesis rates the propensity of these homogeneous reactions to occur increases and so low catalytic selectivity is observed.

As the ratio of reactant gases becomes close to 1 : 1 selectivity towards the oxime increases and peaks at 28 %. It is suggested that at this ratio catalytic selectivity towards H_2O_2 is greatest and in turn the net rate of H_2O_2 synthesis is greatest. Beyond a 1:1 ratio, selectivity towards the oxime decreases to 22%, while conversion continues to rise. It is suggested that the excess H_2 , in the presence of a hydrogenation catalyst such as Pd, leads to unwanted formation of cyclohexanol as well as other unwanted by-products when H_2 is present at a high concentration. It is also likely that the contribution towards H_2O_2 degradation from hydrogenation, rather than decomposition, is higher and it is possible that the net H_2O_2 synthesis rate decreases allowing for an increase in the formation of cyclohexenylcyclohexanone and cyclohexanone azine.

4.3.8. Total reactant gas pressure, while maintaining H₂ : O₂.

Figure 4.10 shows the effect of total gas pressure on the ammoximation of cyclohexanone, while maintaining H₂ : O₂ at 1 : 2.

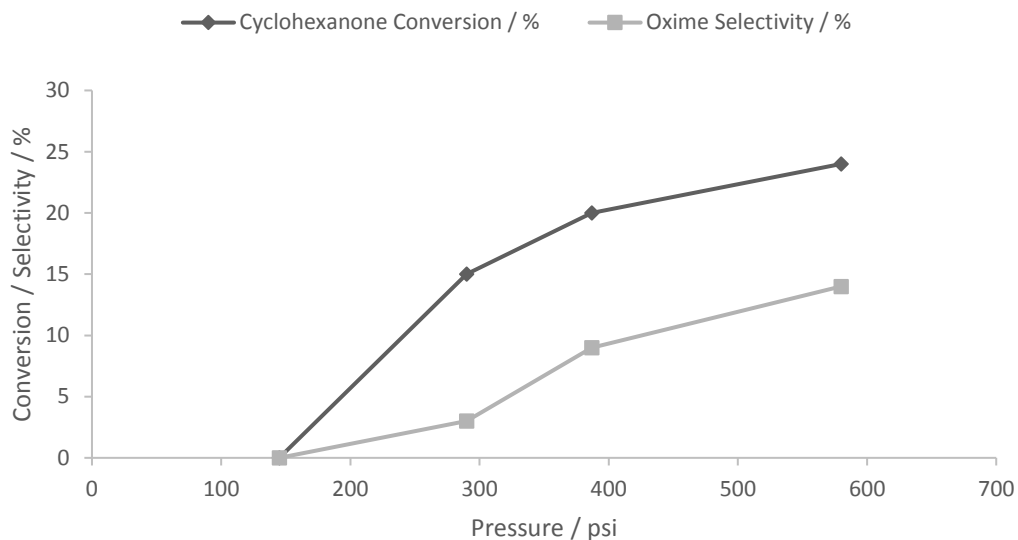


Figure 4.10. The effect of total reactant gas pressure, while maintaining H₂ : O₂, on the ammoximation of cyclohexanone.

Reaction conditions: 5 wt. % Pd / TS-1 (0.05 g), cyclohexanone (0.13 g, 1.3 mmol), NH₃ (0.08 g, 28 wt. %), total pressure X psi, H₂ / O₂ = 0.525, 1200 rpm, 90 min, 5.6 g t-BuOH + 2.69 g H₂O (66 wt. % t-BuOH), 80 °C.

It is observed that as total pressure rises both cyclohexanone conversion and oxime selectivity increases. By increasing total pressure more H₂ and O₂ dissolves in the solvent and so the total concentration of H₂O₂ produced is likely to increase with total reactant gas pressure. This in turn leads to an increase in the formation of NH₂OH and conversion of cyclohexanone to the oxime. At low pressures of reactant gas, it is likely that some H₂O₂ will be formed, however the reaction conditions used mean that H₂O₂ degradation is high and subsequently NH₂OH formation is low. This may explain why no oxime is detected when a total gas pressure of 145 psi is utilised. As total pressure rises both the selectivity towards the oxime and the conversion of cyclohexanone, to 14 and 24 % for selectivity and conversion respectively when a total pressure of 580 psi is applied.

4.3.9. Stirring speed optimization.

Figure 4.11 shows the effect of stirring speed on the ammoximation of cyclohexanone.

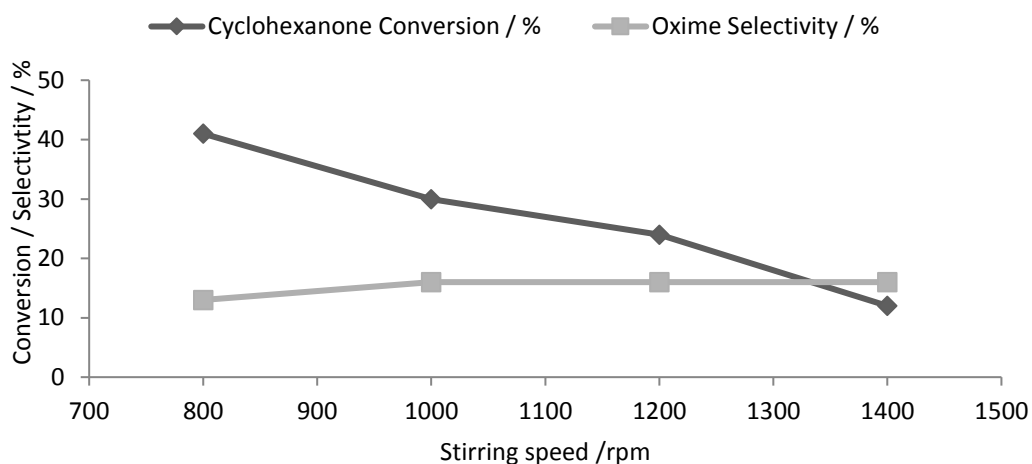


Figure 4.11. The effect of stirring speed on the ammoximation of cyclohexanone.

Reaction conditions: 5 wt. % Pd / TS-1 (0.05 g), cyclohexanone (0.13 g), NH₃ (0.08 g, 28 wt. %), total pressure 580 psi, H₂ / O₂ = 0.525, X rpm, 90 min, 5.6 g t-BuOH + 2.69 g H₂O (66 wt. % t-BuOH), 80 °C.

As can be seen in Figure 4.11 conversion of cyclohexanone to the oxime decreases with stirring speed. It was initially believed that improving stirring speed would cause greater dissolution of the reactant gasses and in turn be beneficial to enhancing H₂O₂ concentration. If this was the case it would be expected that both cyclohexanone conversion and selectivity towards the oxime would improve. Instead very little change in selectivity is observed, while conversion of cyclohexanone decreases dramatically, from 41 to 12 % as stirring speed increases from 800 to 1400 rpm.

It may be that the decrease in conversion is a result of the catalyst being forced onto the wall of the reactor liner at higher speeds, in a manner similar to that seen in Figures 4.12 and 4.13. This would result in a decrease in the availability of the active sites responsible for the direct synthesis of H₂O₂ and in turn formation of the hydroxylamine intermediate decreases. As hydroxylamine is utilised in the formation of cyclohexanone oxime it is possible to use the yield of cyclohexanone oxime as an indication of the concentration of hydroxylamine produced through the course of a reaction.

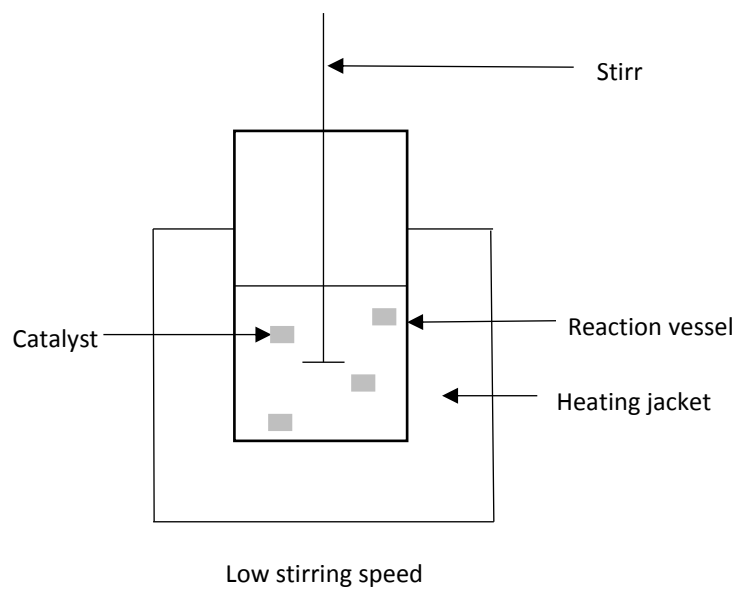


Figure 4.12. The effect of low reactor speed on catalyst distribution in a sealed autoclave.

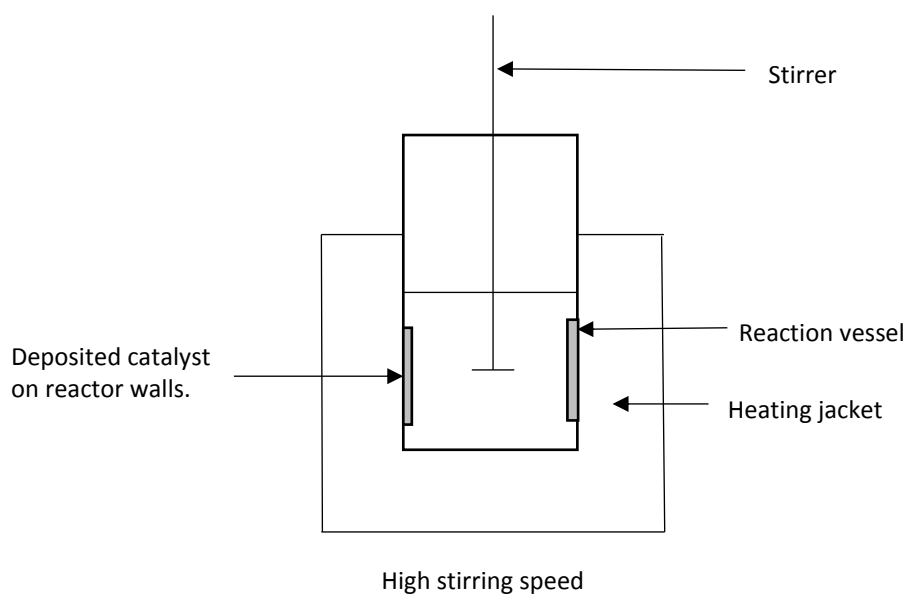


Figure 4.13. The effect of high reactor speed on catalyst distribution in a sealed autoclave.

4.4. Determining the activity of leached metal towards the ammoximation of cyclohexanone via *in-situ* synthesis of H₂O₂.

It has previously been determined in Sections 4.3.4 and 4.3.6 that leaching of Pd from the support can be a significant issue and is one that must be addressed through catalyst and process design. To determine the activity of the leached metal towards the ammoximation of cyclohexanone a hot filtration was carried out, the procedure for which is outlined in Chapter 2 Section 2.3.8. but is briefly discussed below. Finally the activity of 2.5 wt. % Au – 2.5 wt. % Pd / TiO₂ when used in addition to TS-1, as a physical mixture, towards the ammoximation of cyclohexanone was investigated.

Due to the reactor availability the hot filtration reaction was carried out in a 100 ml stainless steel Parr autoclave in comparison all previous data was determined using a 50 ml stainless steel Parr autoclave.

After a standard reaction the catalyst is removed by filtration, the reactor cleaned to ensure no contamination and the filtrate returned to the reactor, which is re-pressurised with reactant gas (5% H₂ / CO₂ and 25 % O₂ / CO₂) and allowed to come to the desired temperature (80 °C). The reaction is allowed to run for a further 0.5 h after which the reactor is cooled to room temperature and analysis of the reaction solution and reactant gas is carried out as outlined in Chapter 2 Section 2.3.8. Table 4.5 shows the results of this study for a 5 wt. % Pd / TS-1 catalyst.

Table 4.5. The activity of leached Pd on the ammoximation of cyclohexanone.

	Cyclohexanone Conversion / %	Oxime Selectivity / % ^e	Oxime Yield / %	H ₂ Conversion / %	Pd leached / ppm
Catalyst present ^a	20	42	8	36	11
Filtrate ^b	23	35	8	6	11
Filtrate + TS-1 ^c	22	37	8	8	11
Au-Pd / TiO ₂ + TS-1 ^d	3	0	0	25	6

^a **Reaction conditions:** 5 wt. % Pd / TS-1 (0.05 g), cyclohexanone (0.13 g, 1.3 mmol), NH₃ (0.08 g, 28 wt. %, 1.3 mmol), total pressure 580 psi, H₂ / O₂ = 0.525, 1200 rpm, 90 min, 5.6 g t-BuOH + 2.69 g H₂O (66 wt. % t-BuOH), 80 °C.

^b **Reaction conditions:** Cyclohexanone (0.13 g, 1.3 mmol), NH₃ (0.08 g, 28 wt. %, 1.3 mmol), total pressure 580 psi, H₂ / O₂ = 0.525, 1200 rpm, 30 min, 5.6 g t-BuOH + 2.69 g H₂O (66 wt. % t-BuOH), 80 °C.

^c **Reaction conditions:** TS-1 (0.05 g), Cyclohexanone (0.13 g, 1.3 mmol), NH₃ (0.08 g, 28 wt. %, 1.3 mmol), total pressure 580 psi, H₂ / O₂ = 0.525, 1200 rpm, 30 min, 5.6 g t-BuOH + 2.69 g H₂O (66 wt. % t-BuOH), 80 °C.

^d **Reaction conditions:** 2.5 wt. % Au – 2.5 wt. % Pd / TiO₂ (0.05 g), TS-1 (0.05 g), Cyclohexanone (0.13 g, 1.3 mmol), NH₃ (0.08 g, 28 wt. %, 1.3 mmol), total pressure 580 psi, H₂ / O₂ = 0.525, 1200 rpm, 30 min, 5.6 g t-BuOH + 2.69 g H₂O (66 wt. % t-BuOH), 80 °C.

Investigation into the activity of a 5 wt. % Pd / TS-1 catalyst towards the ammoximation of cyclohexanone is observed to result in an oxime yield of 8 %. It has been found that after the reaction 11 ppm of leached Pd is detected in the reaction solution. Investigation into the activity of the filtrate (with the catalyst removed) shows no additional formation of the oxime suggesting that leached Pd has no activity towards the ammoximation of cyclohexanone. However cyclohexanone conversion is observed to increase from 20 to 23 % it is suggested that the increase in cyclohexanone conversion may be a result of hydrogenation of cyclohexanone to cyclohexanol or uncatalysed homogeneous side reactions of cyclohexanone, as reported by Cesana *et.al.*⁸ It is observed that upon investigation of the filtrate there is some H₂ conversion (6 %) this may be attributed to one or combination of the following possibilities; the formation of H₂O₂, hydrogenation of cyclohexanone or error in analysis of the reactant gas post reaction by gas chromatography. It is suggested that if any H₂O₂ is formed by the homogeneous Pd it is unable to diffuse to the Ti (IV) sites present on the support and be involved in the formation of hydroxylamine.

Further investigation into the activity of the leached Pd towards the ammoximation of cyclohexanone was conducted, with the addition of bare TS-1 to the filtrate. It is observed that again there is no activity towards the formation of cyclohexanone oxime. However an

increase in cyclohexanone conversion is observed from 20 to 22 %, as is some H₂ conversion (8 %). This suggests that again there may be some homogeneous side reactions of cyclohexanone or hydrogenation of cyclohexanone.

Finally it was decided to determine the activity of 2.5 wt. % Au – 2.5 wt. % Pd / TiO₂ when used in addition to TS-1 towards the ammoximation of cyclohexanone. It can be seen that there is no oxime produced from this physical mixture, despite some conversion of cyclohexanone (3 %), this is attributed to the hydrogenation of cyclohexanone to cyclohexanol or uncatalysed homogeneous side reactions of cyclohexanone. It is known that 2.5 wt. % Au – 2.5 wt. % Pd / TiO₂ is active towards the direct synthesis of H₂O₂, as shown in Table 4.1. It has further been shown that for a 5 wt. % Pd / TS-1 catalyst there is an improvement in catalytic activity towards the direct synthesis of H₂O₂ when using a t-BuOH / water solvent mixture in comparison to a MeOH / water solvent, as seen in Table 4.2. It is therefore suggested that an improvement in catalytic activity towards H₂O₂ synthesis may also be observed for the 2.5 wt. % Au – 2.5 wt. % Pd / TiO₂ catalyst, when using a t-BuOH / water solvent. It is suggested that the lack of oxime formation is due to the degradation of H₂O₂ as it diffuses from the 2.5 wt. % Au – 2.5 wt. % Pd / TiO₂ catalyst to the Ti (IV) sites on the TS-1.

As such future investigation into catalyst design will focus on the use of TS-1 supported catalysts.

4.5. Conclusion.

In this Chapter it has been shown that the impregnation of Au, Pd and Au-Pd onto a commercial TS-1 results in the production of catalysts that are active towards H₂O₂ synthesis at sub-ambient temperatures. As seen in Table 4.6 productivity values of 5 wt. % Pd / TS-1 are observed to be greater than the bi-metallic 2.5 wt. % Au – 2.5 wt. % Pd / TS-1 catalyst. This trend is inconsistent with previous work conducted by Hutchings and co-workers who have observed a synergistic effect when both Au and Pd are supported on a variety of supports including TiO₂¹³, SiO₂¹⁴ and carbon¹⁴. Possibly this is due to the extent of alloying between Au and Pd when utilising TS-1 as a support. This is investigated further in Chapter 5. Interestingly the 5 wt. % Pd / TS-1 catalyst is seen to offer much greater productivity values than a number of bi-metallic Au-Pd catalysts including 2.5 wt. % Au - 2.5 wt. % Pd / TiO₂ and shows similar activity towards H₂O₂ synthesis as 2.5 wt. % Au - 2.5 wt. % Pd / C.

Table 4.6. Comparison of catalytic activity towards H₂O₂ synthesis.

Catalyst	Productivity / mol _{H₂O₂} kg _{cat} ⁻¹ h ⁻¹
5 wt. % Au / TS-1	2
2.5 % Au – 2.5 wt. % Pd / TS-1	100
5 wt. % Pd / TS-1	116
5 wt. % Au / TiO ₂	7
2.5 % Au – 2.5 wt. % Pd / TiO ₂	64
5 wt. % Pd / TiO ₂	30
5 wt. % Au / C	1
2.5 % Au – 2.5 wt. % Pd / C	110
5 wt. % Pd / C	55

Reaction conditions: Catalyst (0.01 g), 580 psi, H₂ / O₂ = 0.525, 1200 rpm, 30 min, 5.6 g MeOH + 2.9 g H₂O (66 Wt. % CH₃OH), 2 °C.

Further investigation into the activity of 5 wt. % Pd / TS-1 utilising a water - alcohol solvent system shows that when t-BuOH is utilised as the solvent in a 2 : 1 ratio with water a greater productivity is observed when compared to a MeOH – water solvent system, at 30 °C. The productivity of the 5 wt. % Pd / TS-1 catalyst is observed to be 60 and 26 mol_{H₂O₂}kg_{cat}⁻¹ h⁻¹ for a t-BuOH – water and MeOH – water solvent system and this is ascribed to increased H₂ solubility in t-BuOH compared to MeOH.

The use of elevated temperatures has been shown to be deleterious towards H₂O₂ stability when using a water-methanol solvent system, as outlined in Section 4.2.1. It is observed that catalyst activity decreases from 116 to 26 mol_{H₂O₂} kg_{cat}⁻¹ h⁻¹ for the 5 wt. % Pd / TS-1 catalyst and this is attributed to an increase in the degradation of H₂O₂ via hydrogenation, although this hypothesis must be investigated further. In addition the presence of basic conditions, *i.e.* NH₃, has been shown to result in the total degradation of highly concentrated H₂O₂ (12 wt.%) when using a water-t-butanol solvent system. However it is not possible to determine if the decrease in H₂O₂ concentration is a result of H₂O₂ degradation or the formation of hydroxylamine. It may be of interest to determine the extent of hydroxylamine produced and it is suggested that quantification may be possible through the addition of cyclohexanone and determination of the yield of cyclohexanone oxime. However, the conditions utilised for the ammoximation of cyclohexanone to cyclohexanone oxime are considered to be harsh towards H₂O₂ stability, in particular the presence of base and the utilisation of elevated temperatures as such in the absence of the catalyst it is suggested that total degradation of H₂O₂ will occur.

Further investigation into the activity of Au, Pd and Au-Pd supported TS-1 catalysts towards the ammoximation of cyclohexanone to cyclohexanone oxime in the presence of pre-formed H₂O₂ has shown that the impregnation of Au and Pd does not adversely affect the activity of the catalyst towards the ammoximation of cyclohexanone. The monometallic Au catalyst supported on TS-1 provides a similar yield of cyclohexanone oxime as the bare TS-1 support (28 %), while the monometallic 5 wt. % Pd / TS-1 and 2.5 wt. % Au – 2.5 wt. % Pd / TS-1 catalysts are observed to offer a slightly smaller yield of cyclohexanone oxime, with a yield of 23 % observed for both the Pd / TS-1 and Au-Pd / TS-1 catalysts as shown in Table 4.7.

Table 4.7. Comparison of catalytic activity towards the ammoximation of cyclohexanone via the addition of pre-formed H₂O₂.

Catalyst	Cyclohexanone oxime yield / %
TS-1	28
5 wt. % Au / TS-1	28
2.5 wt. % Au – 2.5 wt. % Pd / TS-1	23
5 wt. % Pd / TS-1	23

Reaction Conditions: Catalyst (0.05 g), cyclohexanone (10 mmol), NH₃ (28 wt. % 12 mmol), H₂O (2.5 g), t-BuOH (2.5 g), 80 °C, 35 wt. % H₂O₂ (10 mmol, 0.89 mlhr⁻¹ then 0.5 h stir).

It is shown through the formation of the oxime that H₂O₂ synthesis is possible under these conditions even though H₂O₂ stability may be an issue. The ability to produce cyclohexanone oxime via *in-situ* H₂O₂ synthesis may open up a number of other oxidation processes that involve TS-1 and preformed H₂O₂ to this one pot approach, in particular the ammoximation of other ketones.

Reaction conditions have been investigated and optimised for the ammoximation of cyclohexanone using a model 5 wt. % Pd / TS-1 catalyst. It has been shown that the utilisation of increased reaction temperatures in particular is a key requirement to improve yield of cyclohexanone oxime, with oxime yield increasing from 0 to 10 % as reaction temperature increases from 30 to 120 °C. This is in agreement with the work of Wu *et.al*¹⁸. who have report that increasing reaction temperature results in an increase in an increased yield of cyclohexanone oxime. Furthermore it is observed that by improving H₂ solubility, through manipulation of reactant gas ratios (Section 4.3.8), total reactant gas pressure (Section 4.3.9) and solvent composition (Section 4.3.4) it is possible to improve yield of cyclohexanone oxime. It is suggested that by increasing H₂ solubility it is possible to ensure that the rates of H₂O₂ synthesis and hydroxylamine formation are similar and oxime yield is improved.

The improved cyclohexanone oxime yield at temperatures considered detrimental towards H₂O₂ stability suggests that rate of hydroxylamine formation is much greater than that of H₂O₂ degradation. It is suggested that investigation into the rates of these two reactions form the basis of further study.

Finally it is observed that the activity of leached metal towards the ammoximation of cyclohexanone is minimal, with no additional formation of cyclohexanone oxime upon removal of the heterogeneous catalyst. It is suggested that the reaction conditions utilised (80 °C and presence of basic reaction conditions) result in the degradation of H₂O₂ synthesised by homogeneous Pd before it is able to be activated by the Ti(IV) sites present on the TS-1 support. As such any H₂O₂ synthesised by the homogeneous Pd is not utilised in the formation of cyclohexanone oxime. Furthermore it has been demonstrated that the physical mixture of a catalyst known to be active towards the direct synthesis of H₂O₂ with TS-1 again shows no formation of cyclohexanone oxime and again this is attributed to the degradation of any synthesised H₂O₂ before activation by Ti (IV) sites present on the TS-1 support.

It is suggested that the results obtained within this Chapter prove the feasibility of a one-pot approach to the ammoximation of cyclohexanone via *in-situ* H₂O₂ generation and call for further investigation into the this approach to the synthesis of cyclohexanone oxime.

4.6. References.

1. W. Schuster, J. P. M. Niederer and W. F. Hoelderich, *Appl.Catal.A. Gen.*, 2001, **209**, 131-143.
2. D. P. Serrano, R. Sanz, P. Pizarro, A. Peral and I. Moreno, *Micropor.Mesopor. Mat.*, 2013, **166**, 59-66.
3. O. A. K. Mario G. Clerici, *Liquid Phase Oxidation via Heterogeneous Catalysis: Organic Synthesis and Industrial Applications*, John Wiley & Sons, Inc, USA, 2003,101-103.
4. J. K. Edwards, B. E. Solsona, E. N. N, A. F. Carley, A. A. Herzing, C. J. Kiely and G. J. Hutchings, *Science*, 2009, **323**, 1037-1041.
5. J. K. Edwards, A. F. Carley, A. A. Herzing, C. J. Kiely and G. J. Hutchings, *Faraday Discuss.*, 2008, **138**, 225-239.
6. J. K. Edwards and G. J. Hutchings, *Angew. Chem. Int. Ed.*, 2008, **47**, 9192-9198.
7. F. Song, Y. Liu, H. Wu, M. He, P. Wu and T. Tatsumi, *J.Catal.*, 2006, **237**, 359-367.
8. A. Cesana, M. A. Mantegazza and M. Pastori, *J. Mol. Catal.A. Chem* 1997, **117**, 367-373.
9. B. E. Solsona, J. K. Edwards, P. Landon, A. F. Carley, A. Herzing, C. J. Kiely and G. J. Hutchings, *Chem. Mater*, 2006, **18**, 2689-2695.
10. J. K. Edwards, B. E. Solsona, P. Landon, A. F. Carley, A. Herzing, C. J. Kiely and G. J. Hutchings, *J.Catal.* 2005, **236**, 69-79.
11. E. Ntainjua N, J. K. Edwards, A. F. Carley, J. A. Lopez-Sanchez, J. A. Moulijn, A. A. Herzing, C. J. Kiely and G. J. Hutchings, *Green Chem.*, 2008, **10**, 1162.
12. J. K. Edwards, J. Pritchard, M. Piccinini, G. Shaw, Q. He, A. F. Carley, C. J. Kiely and G. J. Hutchings, *J.Catal.*, 2012, **292**, 227-238.
13. J. Edwards, B. Solsona, P. Landon, A. Carley, A. Herzing, C. Kiely and G. Hutchings, *Journal of Catalysis*, 2005, **236**, 69-79.
14. J. K. Edwards, A. Thomas, A. F. Carley, A. A. Herzing, C. J. Kiely and G. J. Hutchings, *Green Chem.*, 2008, **10**, 388.
15. S. J. Freakley, M. Piccinini, J. K. Edwards, E. N. Ntainjua, J. A. Moulijn and G. J. Hutchings, *ACS Catal.*, 2013, **3**, 487-501.
16. J. K. Edwards, B. Solsona, P. Landon, A. F. Carley, A. Herzing, M. Watanabe, C. J. Kiely and G. J. Hutchings, *J. Mater. Chem.*, 2005, **15**, 4595.
17. J. K. Edwards, A. F. Carley, A. A. Herzing, C. J. Kiely and G. J. Hutchings, *Faraday Discuss.*, 2008, **138**, 225.
18. C. Wu, Y. Wang, Z. Mi, L. Xue, W. Wu, E. Min, S. Han, F. He and S. Fu, *React. Kinet. Catal.Lett.*,2002, **77**, 73-81.
19. J. V. H. d'Angelo and A. Z. Francesconi, *J. Chem.Eng. Data*, 2001, **46**, 671-674.
20. C. Samanta, *Appl. Catal. A. Gen.*, 2008, **350**, 133-149.
21. J. K. Edwards and G. J. Hutchings, *Angew. Chem. Int. Ed.*, 2008, **47**, 9192-9198.
22. G. Petrini, A. Cesana, G. D. Alberti, F. Genoni, G. Leofanti, M. Padovan, G. Papparatto and P. Roffia, *Stud. Surf. Sci.Catal.*, 1991, **68**, 761-766.
23. G. Liu, J. Wu and H. a. Luo, *Chinese J. Chem. Eng.*, 2012, **20**, 889-894.
24. S. Zhao, W. Xie, J. Yang, Y. Liu, Y. Zhang, B. Xu, J.-g. Jiang, M. He and P. Wu, *Appl. Catal. A. Gen.*, 2011, **394**, 1-8.
25. A. Thangaraj, R. Kumar, S. P. Mirajkar and P. Ratnasamy, *J. Catal.*, 1991, **130**, 1-8.
26. L. Dal Pozzo, G. Fornasari and T. Monti, *Catal.Commun.* 2002, **3**, 369-375.
27. A. Thangaraj, S. Sivasanker and P. Ratnasamy, *J. Catal.*, 1991, **131**, 394-400.
28. D. Dissanayake, *J. Catal*, 2003, **214**, 113-120.
29. J. K. Edwards, S. J. Freakley, R. J. Lewis, J. C. Pritchard and G. J. Hutchings, *Catal. Today*, 2015, **248**, 3-9.

5. Catalyst Design in the ammoximation of cyclohexanone via the *in-situ* synthesis of H₂O₂.

5.1. Introduction.

The previous Chapter outlined the ability of Pd supported on TS-1 to catalyse the ammoximation of cyclohexanone to cyclohexanone oxime, via *in-situ* synthesis of H₂O₂. The current Chapter investigates the role of catalyst design in improving selectivity towards cyclohexanone oxime as well as cyclohexanone conversion for this reaction.

Both the role of metal weight loading and heat treatment temperature on catalytic activity towards cyclohexanone formation are explored. Additionally, a variety of supported metal catalysts previously reported as active for direct H₂O₂ synthesis are now assessed for activity towards the ammoximation of cyclohexanone. Rates of cyclohexanone ammoximation and H₂O₂ synthesis / degradation are then studied and compared.

In order to screen catalysts efficiently a reaction time of 30 minutes was chosen (unless otherwise stated), other reaction conditions remained consistent with those previously studied in Chapter 4 and are shown for clarity:

Cyclohexanone ammoximation reaction conditions: Catalyst (0.05 g), t-BuOH (5.6 g), H₂O (2.69 g), cyclohexanone (0.13 g), NH₃ (28 Wt. %, 0.079 g), 5 % H₂ / CO₂ (2.9 MPa) and 25 % O₂/CO₂ (1.1 MPa), 30 min, 80 °C, 1200 rpm.

H₂O₂ direct synthesis reaction conditions: Catalyst (0.01 g), MeOH (5.6 g), H₂O (2.9 g), 5 % H₂ / CO₂ (2.9 MPa) and 25 % O₂ / CO₂ (1.1 MPa), 30min, 2 °C, 1200 rpm.

H₂O₂ degradation reaction conditions: Catalyst (0.01 g), MeOH (5.6 g), H₂O (2.22 g), H₂O₂ (50 wt. % 0.68 g), 5 % H₂/CO₂ (2.9 MPa) 30min, 2 °C, 1200 rpm.

5.2. Results and discussion

5.2.1. Effect of Pd loading on the ammoxidation of cyclohexanone to cyclohexanone oxime via direct synthesis of H₂O₂ from H₂ and O₂.

It is well known that Pd is highly active for the direct synthesis of H₂O₂ from H₂ and O₂, however it has been reported that Pd is also active towards the subsequent degradation of H₂O₂ by hydrogenation to H₂O¹⁻³. Thus, catalyst design to improve selectivity towards H₂O₂ is considered essential. It is suggested that for a catalyst to be selective towards cyclohexanone oxime whilst also showing high selectivity in H₂ usage, the rate of H₂O₂ synthesis must be similar to that of the ammoxidation. This is to ensure that H₂ is used selectively in oxime formation and not in the formation of H₂O, via H₂O₂ degradation.

Figure 5.1 compares the activity of TS-1 supported Pd catalysts towards the ammoxidation of cyclohexanone via *in-situ* H₂O₂ synthesis.

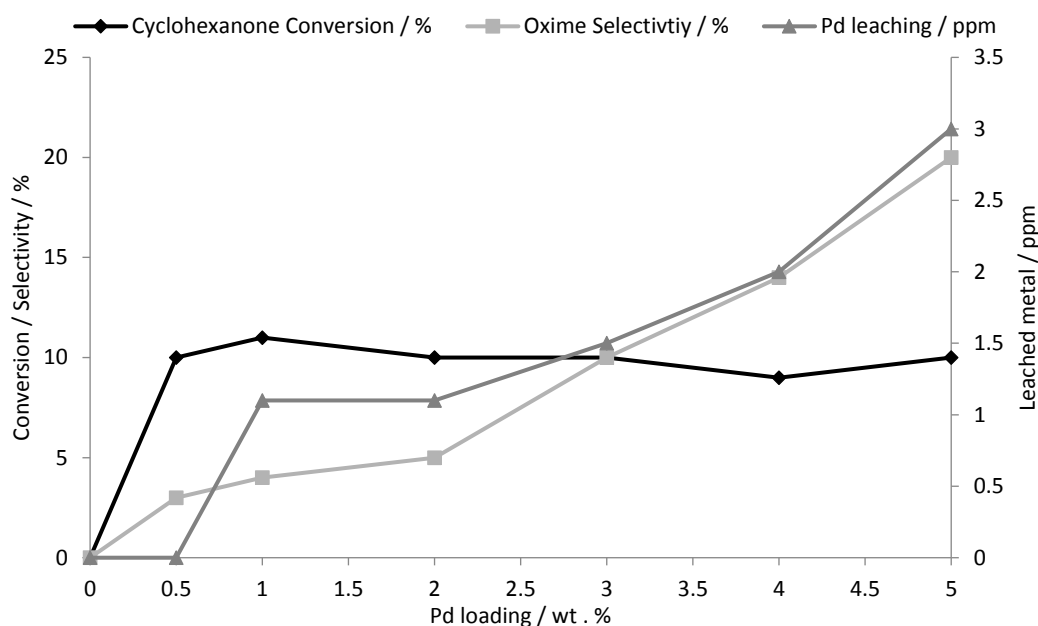


Figure 5.1. The effect of Pd loading on the ammoxidation of cyclohexanone.

Reaction conditions: X wt. % Pd / TS-1 (0.05 g), cyclohexanone (0.13 g, 1.3 mmol), NH₃ (28 wt. %, 0.08g, 1.3mmol), total pressure 580 psi, H₂ / O₂ = 0.525, 1200 rpm, 30 min, 5.6 g t-BuOH + 2.69 g H₂O (66 wt. % t-BuOH), 80 °C.

Firstly, it is observed that the presence of Pd is required to result in the formation of cyclohexanone oxime, no oxime is detected when non-metal supported TS-1 is utilised. It has been reported by Cesena *et.al* that the formation of minor organic by-products, such as cyclohexenylcyclohexanone and cyclohexanone azine can occur through uncatalysed, homogeneous reactions of cyclohexanone. However, it can be observed in Figure 5.1 that in

the absence of Pd, that is when just TS-1 is utilised, no cyclohexanone conversion is measured, over the time period investigated.

It can be observed from Figure 5.1 that there is little change in cyclohexanone conversion, regardless of Pd loading. It is observed that conversion shows low sensitivity to increasing Pd loading over a range of 0.5 – 5 wt. % Pd. On the other hand, oxime selectivity increases greatly with Pd content, from 3 to 20 %, as Pd loading increases from 0.5 to 5 wt. %. The amount of leached Pd correlates well with total metal loading. The 5 wt. % Pd catalyst shows the highest degree of Pd leaching (3 ppm) whilst, no apparent leaching is detected for the 0.5 wt. % Pd catalyst.

To rationalise the trends observed in Figure 5.1, these catalysts were assessed for H₂O₂ synthesis and degradation under standard conditions, the results of which are shown in Figure 5.2.

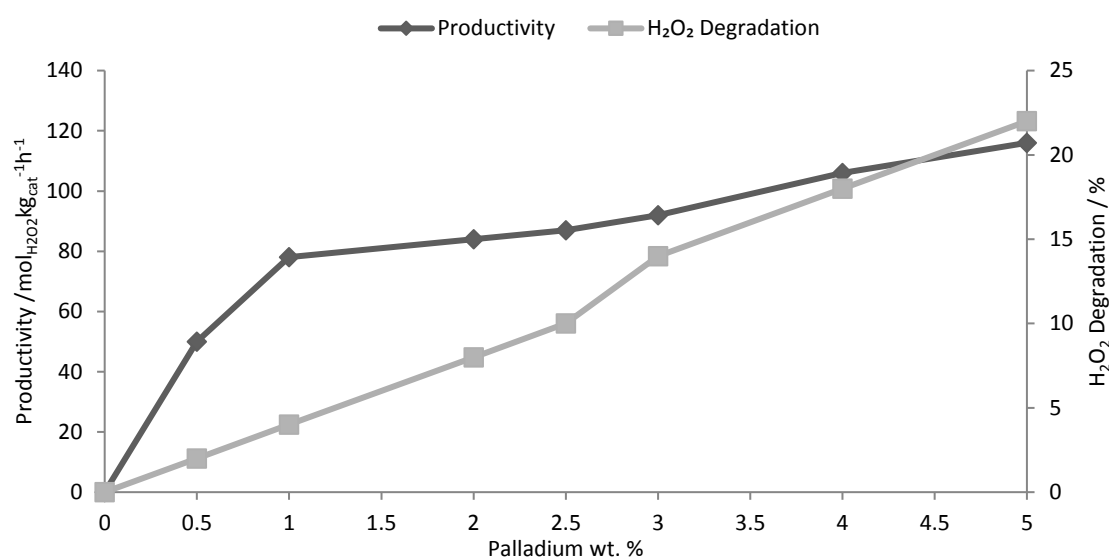


Figure 5.2. The effect of Pd loading on the direct synthesis and degradation of H₂O₂.

Reaction conditions: X wt. % Pd / TS-1 (0.01 g), total pressure 580 psi, H₂ / O₂ = 0.525, 1200 rpm, 30 min, 5.6 g MeOH + 2.9 g H₂O (66 wt. % MeOH), 2 °C.

It can be observed that the rates of H₂O₂ synthesis and degradation increase with Pd loading, with the 5 wt. % Pd / TS-1 offering the greatest productivity (116 mol_{H₂O₂}kg_{cat}⁻¹h⁻¹). The reaction conditions utilised in the ammoxidation of cyclohexanone (high reaction temperature of 80 °C and presence of NH₃) have been shown to result in high H₂O₂ degradation rates (Chapter 4, Section 4.2.3). It is now possible to conclude that Pd loading also influences activity towards H₂O₂ degradation, as well as synthesis, although it is considered that the reaction conditions are more significant in this regard.

It is possible to conclude that catalyst activity towards H_2O_2 synthesis and degradation, as well as selectivity towards cyclohexanone oxime is dependent on Pd loading. Interestingly the extent of cyclohexanone conversion shows little variation, regardless of Pd loading. However the rate of H_2O_2 synthesis is seen to increase as total Pd loading rises. It is possible that the conversion of cyclohexanone may be limited by lack of available NH_3 . It is suggested that the formation of NH_4HCO_3 , through the reaction of NH_3 and carbonic acid (H_2CO_3), formed from the CO_2 reactant gas diluent, results in the removal of NH_3 from the system. The reaction may therefore be limited by reactant availability. It is suggested that the use of N_2 as a reactant gas diluent may prevent the formation of NH_4HCO_3 and as such overcome this issue.

5.2.2. Effect of calcination temperature on catalyst activity for the ammoximation of cyclohexanone to cyclohexanone oxime via direct synthesis of H_2O_2 from H_2 and O_2 .

Previous work by Hutchings and co-workers has shown that calcination of supported Au-Pd catalysts at $400\text{ }^\circ\text{C}$ in static air produces a stable, re-useable catalyst for the direct synthesis of H_2O_2 in a H_2O -MeOH solvent system at $2\text{ }^\circ\text{C}$ ⁴.

As demonstrated in Chapter 4 leaching of supported metals, which are active for H_2O_2 synthesis, can be an issue when utilising a solvent system that includes H_2O . In an attempt to produce a more stable and re-usable catalyst the role of calcination temperature on catalyst activity and stability was investigated. 5 wt. % Pd / TS-1 catalysts were calcined (static air, 3 h, $20\text{ }^\circ\text{C min}^{-1}$ ramp rate) at temperatures ranging from $400 - 800\text{ }^\circ\text{C}$. The effect on catalytic activity for the ammoximation of cyclohexanone as well as catalyst stability is shown in Figure 5.3.

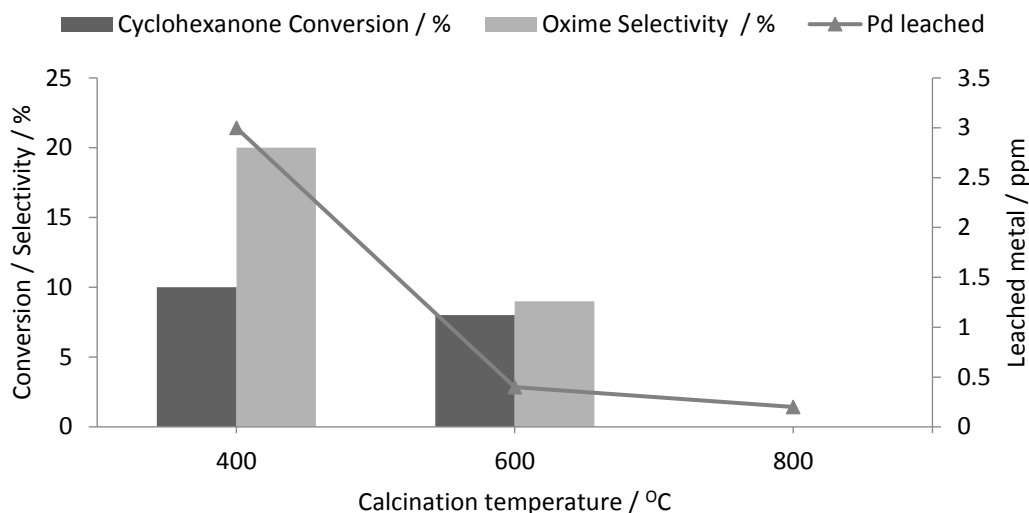


Figure 5.3. The effect of calcination temperature on the catalytic activity of 5 wt. % Pd / TS-1 towards the ammoxidation of cyclohexanone.

Reaction conditions: 5 wt. % Pd / TS-1 (0.05 g), cyclohexanone (0.13 g, 1.3 mmol), NH₃ (28 wt. %, 0.08g, 1.3mmol), total pressure 580 psi, H₂/ O₂ = 0.525, 1200 rpm, 30 min, 5.6 g t-BuOH + 2.69 g H₂O (66 wt. % t-BuOH), 80 °C.

It is observed in Figure 5.3 that increasing the calcination temperature from 400 to 800 °C, caused cyclohexanone conversion to decrease from 10 to 0 % and oxime selectivity to fall from 20 to 0 %. Indeed a 3 h calcination in static air, at 800 °C, effectively deactivated the catalyst towards cyclohexanone ammoxidation. In contrast with catalyst activity trends, an increase in calcination temperature led to a lower degree of Pd leaching, from 3 and 0.2ppm for calcinations at 400 and 800 °C respectively.

The effect of calcination temperature on the dispersion of Pd was investigated via CO chemisorption, the results of this study are shown in Table 5.1

Table 5.1. The effect of calcination temperature on Pd dispersion, as determined by CO chemisorption.

Calcination temperature / °C	Pd Surface area / m ² g ⁻¹	Average Crystallite Size / nm	Dispersion / %
400	7.37	23	1.65
600	6.55	26	1.45
800	5.67	31	1.21

It is clear that as calcination temperature increases so the Pd surface area decreases, from 7.73 m²g⁻¹ for the sample calcined at 400 °C to 5.67 m²g⁻¹ for the sample calcined at 800 °C. This coincides with a decrease in dispersion of the metal on the support from 1.65 to 1.21 % and an increase in average crystallite size suggesting that an increase in calcination temperature leads to sintering of the metal nanoparticles. This increase in particle size is

suggested to a significant cause to the loss in catalyst activity towards both the ammoxidation of cyclohexanone and the synthesis of H₂O₂.

The effect that calcination temperature has on the crystallinity of the TS-1 support was determined by XRD and the results are shown in Table 5.2. Assigned diffractograms are shown in Appendix 5.1, Figures A1, A2 and A3.

Table 5.2. The effect of metal impregnation and calcination temperature upon the physical properties of TS-1 catalysts as determined by XRD and N₂ physisorption.

Catalyst	Calcination temperature / °C	TS-1 Crystallinity / %	Pd particle size / nm ^[a]	Au particle size / nm ^[a]	Pt particle size / nm ^[a]	BET surface area / m ² g ⁻¹ ^[b]
TS-1	Uncalcined	100	-	-	-	
5 wt. % Pd/ TS-1	400	85.6	15.2	-	-	340
	800	59.7	66.0	-	-	310
2.5 wt. % Au – 2.5 wt. % Pd/ TS-1	400	83.0	-	17	-	302
	800	56.3	17	32	-	292
2 wt. % Au – 2 wt. % Pd – 1 wt. % Pt/ TS-1	400	68.0	-	46.7	-	299
	800	33.8	-	50.3	28.7	280

^[a] Determined using the Scherrer equation, ^[b] Determined via N₂ physisorption.

Using the principle reflections associated with TS-1 ($\theta = 23.1^\circ$, 24.4° and 24.5°) it is possible to determine that impregnation of TS-1 with Pd, followed by calcination at 400 °C leads to a 14.6 % decrease in crystallinity of TS-1 with metal impregnation and heat treatment. By increasing the calcination temperature to 800 °C the crystallinity of the TS-1 decreases further, reaching 59.7 %. Across the same temperature range the BET surface area of the 5 wt. % Pd / TS-1 catalyst falls from 340 to 310 m²g⁻¹. The observed decrease in catalyst activity towards the ammoxidation of cyclohexanone may partly be attributed to a structural change in the TS-1 support. However it has already been shown in Chapter 4 that comparable rates of cyclohexanone conversion and oxime selectivity are observed for both the bare and metal loaded TS-1 (calcined, static air, 3 h, 400 °C), when *ex-situ* H₂O₂ is utilised, so the decrease in catalytic activity may not be solely attributed to this loss in crystallinity.

To determine the effect of increasing calcination temperature upon the active phase, responsible for H₂O₂ synthesis, the Pd nanoparticle size was determined using the PdO reflection at 35° (Appendix 5.1 Figure A1). As shown in Table 5.2, upon increasing the calcination temperature from 400 °C to 800 °C, the calculated PdO nanoparticle size increases from 15.2 to 66 nm. However it should be noted that the detection limit of XRD is

approximately 5 nm and as such it would not be possible to observe Pd nanoparticles below this limit. Investigation of Pd nanoparticle size by XRD is therefore qualitative only.

Further investigation, by XPS is shown in Appendix 5.3 Table A1. It is observed Pd is present as Pd²⁺, which agrees with the observation of PdO in the XRD analysis. It can further be observed that as calcination temperature increases, the dispersion of Pd on the support decreases, with atomic concentration of Pd decreasing from 1.14 % at a calcination temperature of 400 °C to 1.01 % at 800 °C, this correlates with analysis by XRD, which shows increasing peak intensity of the Pd reflection at 35° and CO chemisorption which shows decrease dispersion of Pd on the support.

It can also be seen that as calcination temperature rises the Si : Ti ratio decreases, from 103.9 at 400 °C to 79.7 when calcined at 800 °C. This suggests that at elevated temperatures the concentration of Ti at the surface increases, which again correlates with the loss of crystallinity from analysis.

Analysis of the 5 wt. % Pd / TS-1 catalysts exposed to increasing calcination temperature by Transmission Electron Microscopy (TEM) can be seen in Figure 5.4

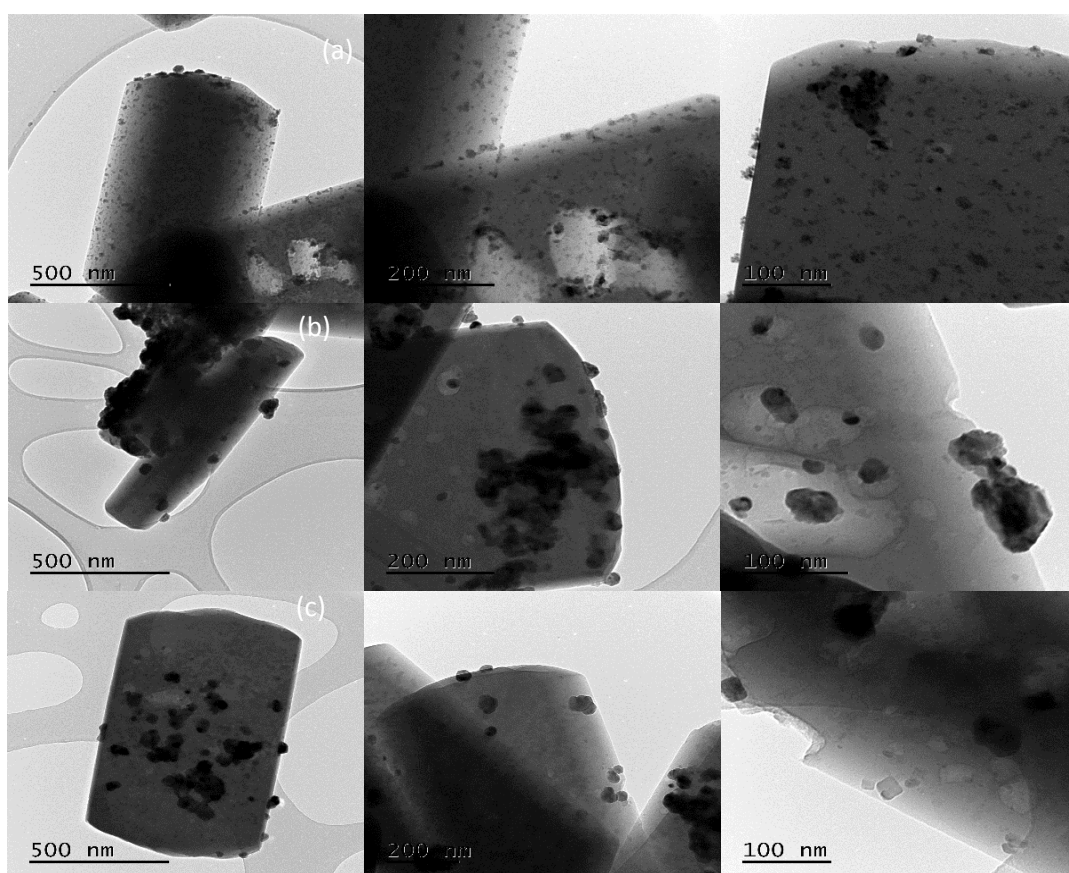


Figure 5.4. Transmission Electron Microscopy of 5 wt. % Pd / TS-1 exposed to calcination temperatures of ^(a) 400 °C, ^(b) 600 °C, ^(c) 800 °C (3 h, 20 °C min⁻¹, static air).

It can be observed from Figure 5.4, that metal nanoparticle size increases dramatically with increasing calcination temperature, however particle size distribution could not be carried out due to particle boundary deformation. As nanoparticles agglomerate, with increasing calcination temperature, it is not possible to differentiate one nanoparticle from its neighbours. However, it is clear to see from Figure 5.4 that as calcination temperature increases the nanoparticles agglomerate. This is in agreement with investigation by CO chemisorption (Table 5.1), XPS (Appendix 1.3 and XRD (Table 5.2). In addition to this investigation by STEM – EDX, Figure 5.5, reveals that Pd nanoparticles becomes less disperse with increasing calcination temperature.

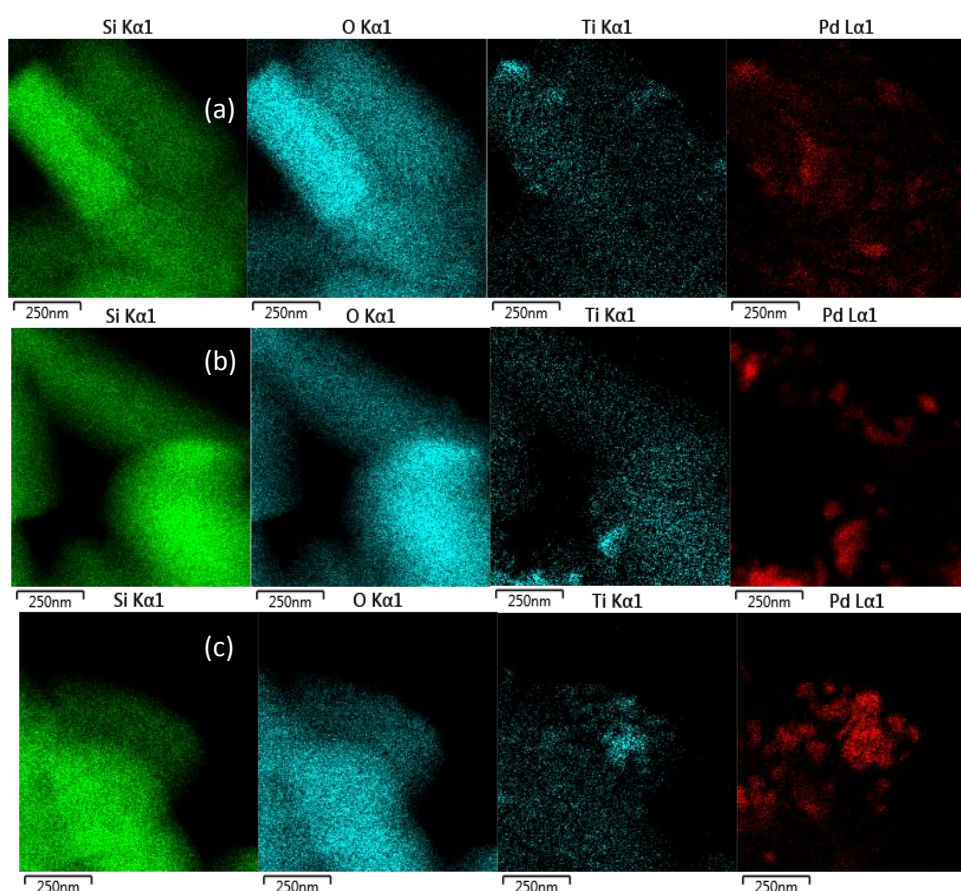


Figure 5.5. STEM – EDX analysis of 5 wt. % Pd / TS-1 exposed to calcination temperatures of (a) 400 °C, (b) 600 °C, (c) 800 °C (3 h, 20 °C min⁻¹, static air). Si (Green), O (Blue), Ti (Blue), Pd (Red).

The increase in Pd nanoparticle size may contribute to the observed decrease in catalyst activity for both H₂O₂ synthesis and cyclohexanone ammoxidation reactions. It is suggested that ‘small’ nanoparticles (those below 5nm in diameter), are highly active for the synthesis of H₂O₂ while larger nanoparticles are less active. By increasing the calcination temperature, the Pd particle size increases and in turn catalyst activity for H₂O₂ synthesis decreases.

These two factors; the loss in TS-1 crystallinity and Pd nanoparticle growth may both lead to lower rates of cyclohexanone oxime formation by (a) decreasing the rate of H₂O₂ synthesis through Pd particle growth and (b) lowering the rate of H₂O₂ activation on the TS-1 support through loss of framework Ti (IV) sites. Both of these would decrease the rate of hydroxylamine formation and the subsequent synthesis of cyclohexanone oxime.

Finally investigation of the 5 wt. % Pd / TS-1 catalysts exposed to increasing calcination temperature (400 – 800 °C) by FTIR can be seen in Figure 5.6.

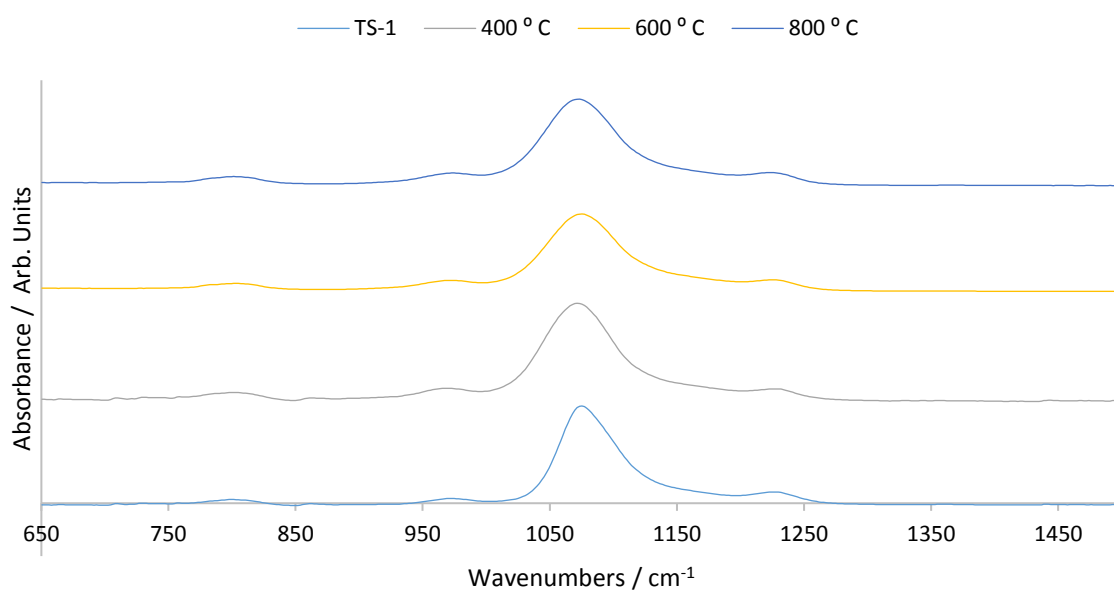


Figure 5.6. FTIR spectra of 5 wt. % Pd / TS-1 catalysts calcined at 400 – 800 °C (3 h, static air, 20 °C min⁻¹)

It can be observed that no discernible change can be observed in the structure of TS-1, upon impregnation of Pd and subsequent calcination at increasing temperatures when investigated by FTIR. This it is possible to observe four distinct infrared bands in Figure 5.6 at 800 cm⁻¹ and 1100 cm⁻¹ assigned to lattice modes associated with internal linkages in tetrahedral SiO₄, at 990 cm⁻¹ assigned to stretching vibrations of SiO₄ tetrahedra bound to Ti atoms as Si-O-Ti linkages and at 1240 cm⁻¹ assigned to tetrahedral Ti present in the TS-1 framework.

The activities of 5 wt. % Pd / TS-1 catalysts for H₂O₂ synthesis following calcination at 400, 600 and 800 °C are shown in Figure 5.7. These studies were carried out using standard H₂O₂ synthesis and degradation procedures, as outlined in Section 5.1.

It was shown in Figure 5.3 that as the calcination temperature increases activity towards cyclohexanone ammoxidation decreases. Based upon the data in Figure 5.4 it is possible to

conclude that this is due to a decrease in productivity for H₂O₂ synthesis at elevated calcination temperatures.

Figure 5.7 shows the effect of calcination temperature on the catalytic activity of 5 wt. % Pd towards the direct synthesis of H₂O₂ and its subsequent degradation.

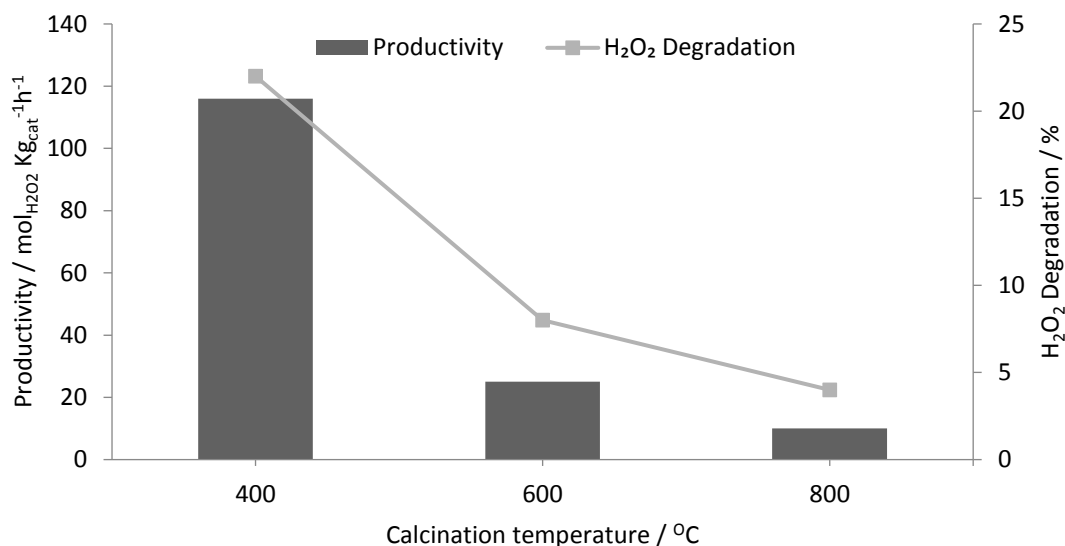


Figure 5.7. The effect of calcination temperature on the activity of 5 wt. % Pd / TS-1 towards the direct synthesis and degradation of H₂O₂.

Reaction conditions: 5 wt. % Pd / TS-1 (0.01 g), total pressure 580 psi, H₂ / O₂ = 0.525, 1200 rpm, 30 min, 5.6 g MeOH + 2.9 g H₂O (66 wt. % MeOH), 2 °C.

It is observed in, Figure 5.7, that catalytic activity for H₂O₂ synthesis decreases substantially with increasing calcination temperature, from 116 to 10 mol_{H₂O₂} Kg_{cat}⁻¹ h⁻¹ for calcinations at 400 °C and 800 °C respectively (a percentage loss of approx. 90 %). As with the ammoximation of cyclohexanone, catalytic activity towards the synthesis of H₂O₂, also decreases with increasing calcination temperature, to a minimum of 6 % when a calcination temperature of 800 °C is employed. This can be attributed to an increase in size of Pd particles with increasing temperature, as shown via XRD (Table 5.2) and TEM analyses (Figure 5.4).

5.2.3. The effect of Au-Pd metal ratio on the ammoximation of cyclohexanone to cyclohexanone oxime via direct synthesis of H₂O₂ from H₂ and O₂

It has been shown that bi-metallic Au-Pd/ TS-1 catalysts are active for the direct synthesis of H₂O₂ in a H₂O / MeOH system, at both 2 °C and elevated temperatures (Chapter 4 Section 4.2.1). It has furthermore been demonstrated (Chapter 4 Section 4.2.4) that these catalysts are active for the ammoximation of cyclohexanone via the addition of H₂O₂ and that when compared to TS-1 alone there is little difference in either selectivity towards the oxime or cyclohexanone conversion. Mono- and bi-metallic Au – Pd / TS-1 catalysts (of varying Au: Pd ratio) were investigated for the ammoximation of cyclohexanone with H₂O₂ synthesised *in situ* and the results of these studies are shown in Figure 5.8.

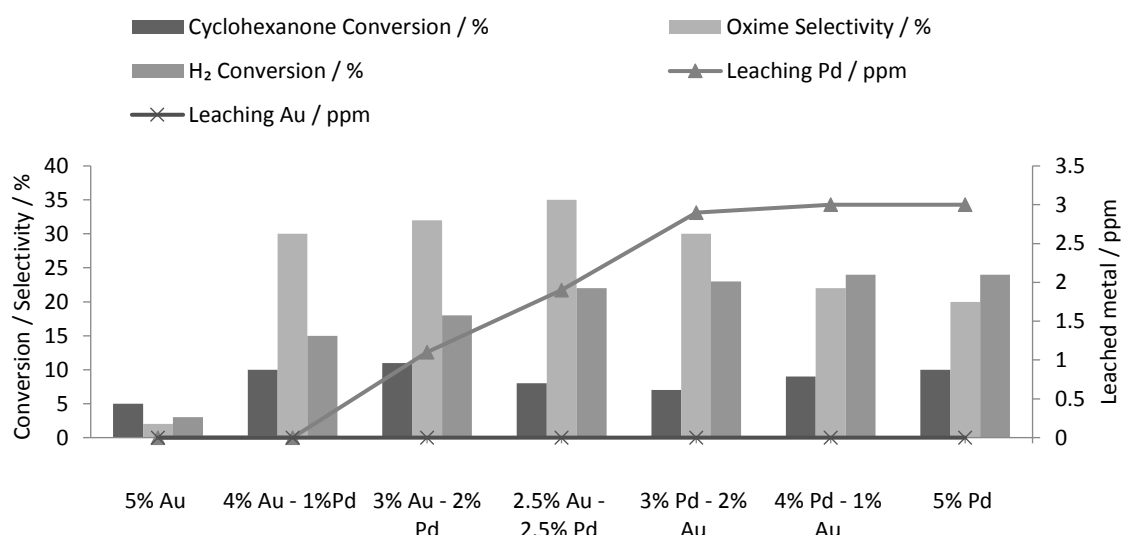


Figure 5.8. The effect of Au : Pd ratio on the ammoximation of cyclohexanone. Total metal loading on TS-1 is 5 wt. %.

Reaction conditions: Catalyst (0.05 g), cyclohexanone (0.13 g, 1.3 mmol), NH₃ (28 wt. %, 0.08g, 1.3mmol), total pressure 580 psi, H₂ / O₂ = 0.525, 1200 rpm, 30 min, 5.6 g t-BuOH + 2.69 g H₂O (66 wt. % t-BuOH), 80 °C.

It is observed, Figure 5.8, that bimetallic Au-Pd catalysts show consistently low cyclohexanone conversion of 5 – 11% under the reaction conditions used. However the introduction of Pd to a Au-only catalyst improves oxime selectivity dramatically, from 2 % for 5 wt. % Au / TS-1 to 30% for 4 wt. % Au - 1 wt. % Pd / TS-1. Selectivity towards cyclohexanone oxime follows a volcano-like trend that correlates with Pd content until Au : Pd ratio of 1:1 is reached, where selectivity towards the oxime is seen to be 35 %. This is particularly interesting as the mono-metallic Au catalyst shows very little activity towards the ammoximation of cyclohexanone and this can be related to its low activity towards the direct synthesis of H₂O₂, as shown in Figure 5.9. However by incorporating Au into a Pd

catalyst so that the ratio of the two metals is 1 : 1 by wt. % it is possible to dramatically improve the selectivity towards cyclohexanone oxime. Beyond a 1:1 ratio of Au: Pd, further increasing the Pd content leads to a decrease in oxime selectivity.

H₂ conversion is also observed to increase with Pd content, reaching a maximum at a Au: Pd ratio of 1:1. Beyond this point H₂ conversion remains fairly constant. This correlates with H₂O₂ synthesis rates over the same catalyst series, which do not differ greatly. Indeed, 2.5 wt. % Au – 2.5 wt. % Pd / TS-1 and 5 wt. % Pd / TS-1 show comparable H₂O₂ productivities, at 100 and 116 mol_{H₂O₂} Kg_{cat}⁻¹h⁻¹ respectively, as seen in Figure 5.9.

It is known that upon calcination, Au-Pd particles on a range of oxide supports form a core-shell morphology consisting of a Au-rich core surrounded by a PdO shell⁵. These bi-metallic systems show superior activity and selectivity towards H₂O₂ when compared to monometallic counterparts and enhancement in the activity of Au-Pd oxide supported catalysts towards H₂O₂ synthesis has been attributed to electronic modification of the metals⁶. In these studies particle size has been related to the Au: Pd ratio, with smaller particles containing higher concentrations of Pd. It is possible that upon calcination of the bi-metallic TS-1 supported catalysts a degree of alloying is induced and this may explain the enhancement in selectivity towards the oxime observed for bimetallic catalysts in Figure 5.8. It is suggested that further investigation into the morphology of the metal nanoparticles is required to determine the extent of alloying between Au and Pd and to determine if a core shell morphology is adopted as it is on oxide supports, such as P25 TiO₂.

Leaching studies reveal no loss of Au regardless of total content. In contrast Pd leaching increases with the total Pd loading, to a maximum of 3 ppm for the 5 wt. % Pd / TS-1 catalyst which is consistent with trends observed in Figure 5.1.

Investigation of these Au-Pd catalysts supported on TS-1 for the direct synthesis and degradation of H₂O₂ is shown in Figure 5.9.

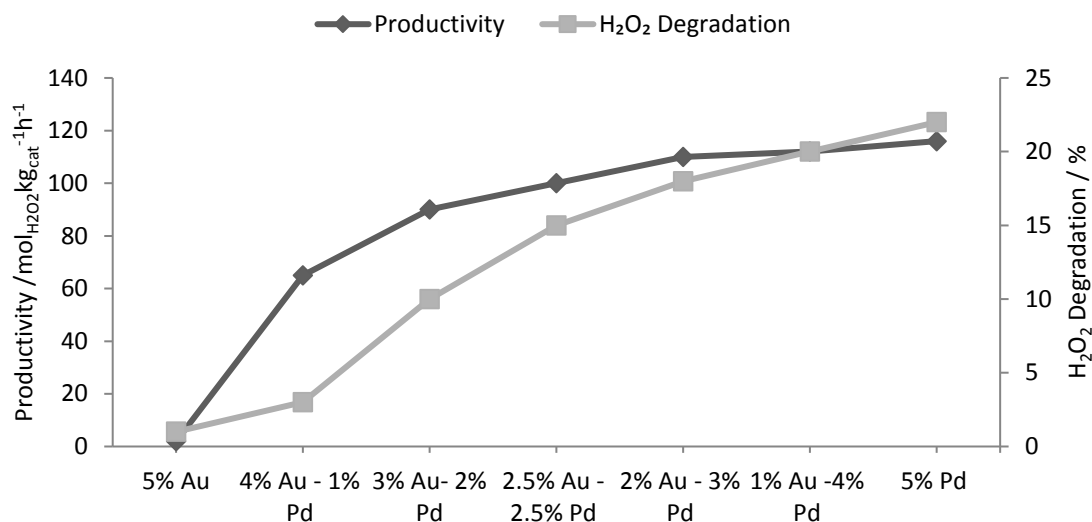


Figure 5.9. The effect of the Au : Pd ratio on the direct synthesis and degradation of H₂O₂. Total metal loading on TS-1 is 5 wt. %. **Reaction conditions:** Catalyst (0.01 g), total pressure 580 psi, H₂ / O₂ = 0.525, 1200 rpm, 30 min, 5.6 g MeOH + 2.9g H₂O (66 wt. % MeOH), 2 °C.

It is observed in Figure 5.9 that catalytic activity towards H₂O₂ synthesis is correlated to Pd content, with the rate of H₂O₂ synthesis increasing with Pd content. Catalytic activity towards the synthesis of H₂O₂ increases from 2 mol_{H₂O₂}kg_{cat}⁻¹h⁻¹ for 5 wt. % Au / TS-1 to 116 mol_{H₂O₂}kg_{cat}⁻¹h⁻¹ for 5 wt. % Pd / TS-1. Unlike the ammoxidation of cyclohexanone, activity towards H₂O₂ synthesis does not show a volcano-like trend.

It is suggested that at higher Pd content the rate of H₂O₂ synthesis exceeds that of hydroxylamine formation by the Ti (IV) active sites within the TS-1 support's pores and as such degradation of H₂O₂ formed but not involved in hydroxylamine synthesis increases. This degradation may either be catalytic or as a result of the reaction conditions utilised. As Au is shown to have limited activity towards the ammoxidation of cyclohexanone and no improvement in activity towards H₂O₂ synthesis is observed when both Pd and Au are incorporated onto the same support it may be that the role of Au, when incorporated into a Pd / TS-1 catalyst is to limit the rate of H₂O₂ synthesis. By ensuring the rate of H₂O₂ synthesis does not exceed the rate of hydroxylamine formation it is possible to ensure greater oxime selectivity.

It is suggested that catalyst design to ensure the rate of H₂O₂ synthesis is equal to the rate of hydroxylamine formation is key in producing a highly selective catalyst.

Investigation of these bi-metallic Au – Pd / TS-1 catalysts by XRD shows an increase in the intensity of the reflections associated with Au metal nanoparticles at 38 ° (Appendix 5.1, Figure A4) with increasing Au loading, suggesting the presence of Au nanoparticles of larger

than 5 nm. No peaks that can be attributed to Pd species are observed, regardless of Pd loading, which suggests that the particle size of the Pd nanoparticles is below the detection limit of this technique, approximately 5nm.

Au-Pd catalysts prepared using a variety of oxide supports such as P25 TiO₂ are reported to show the greatest activity towards H₂O₂ synthesis at a Au : Pd ratio of 1: 1. As such a 2.5 wt. % Au - 2.5 wt. % Pd catalyst would be expected to show a higher rate of H₂O₂ synthesis than monometallic 5 wt. % Pd or 5 wt. % Au catalysts^{6,7} following calcination in static air, catalysts comprising of Au-Pd impregnated on certain oxide supports, such as P25 TiO₂, present alloyed nanoparticles core-shell morphology, where the core is Au-rich and the shell Pd-rich. Investigation of the Au-Pd catalysts used in Figure 5.7 by STEM- EDX mapping of Au and Pd or regions within the same catalysts shown in Figure 5.10.

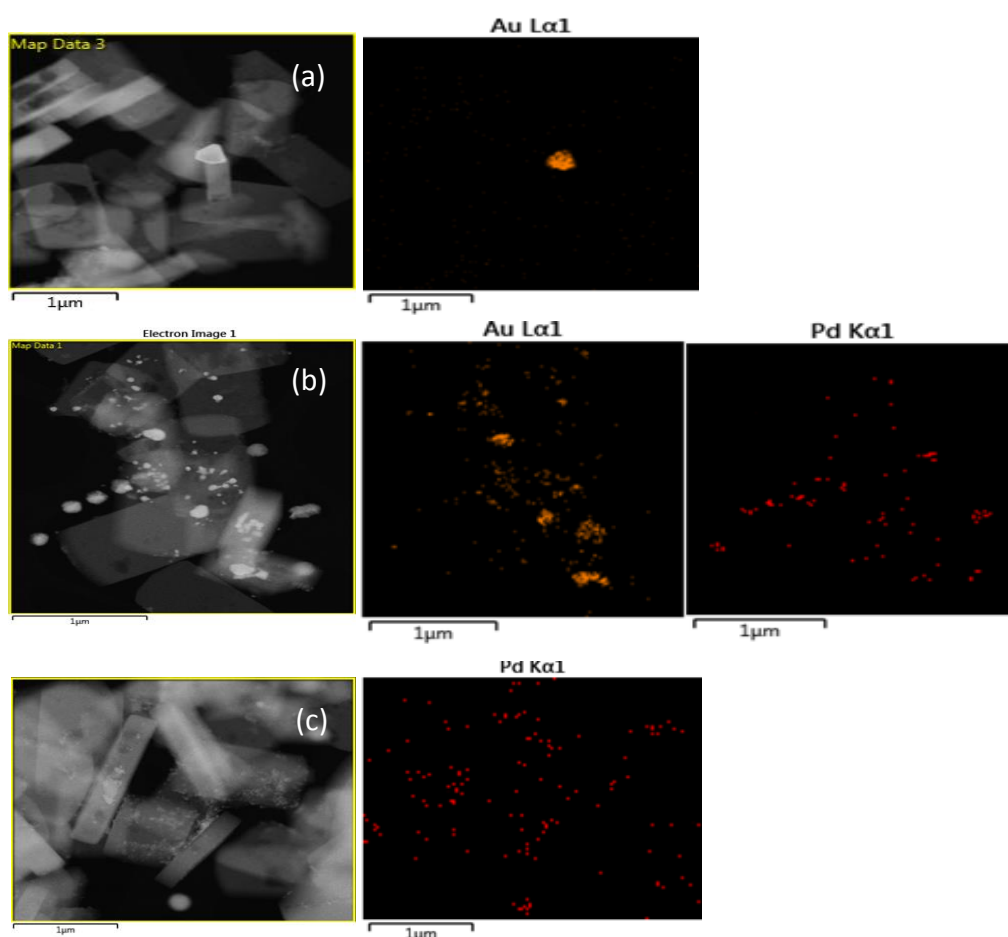


Figure 5.10 STEM-EDX mapping of regions in (a) 5 wt. % Au/ TS-1, (b) 2.5 wt. % Au -2.5 wt. % Pd / TS-1 and (c) 5 wt. % Pd/ TS-1

STEM-EDX, shown in in Figure 5.10 show the presence of large, poorly dispersed Au particles for 5 wt. % Au/ TS-1 (a). This is in agreement with XRD data in Table 5.2. Meanwhile the

mono-metallic Pd catalyst (5 wt. % Pd/ TS-1, (c)) is observed to contain much smaller metal nanoparticles that are highly dispersed, again in agreement with XRD data, where no characteristic PdO peaks are observed (Appendix 5.1, Figure A1). The combination of both Au and Pd onto the same support (b) is shown to improve the dispersion of Au. This is found to be consistent with previous reports by Hutchings and co-workers⁸. Following metal impregnation and calcination, there is some loss in total surface area (Table 5.2), from 340 m²g⁻¹ for unmodified TS-1 to a minimum of 302 m²g⁻¹ for 2.5 wt. % Au – 2.5 wt. % Pd / TS-1. This loss in surface area is not deemed significant to overall catalytic activity. It was shown in Chapter 4 (Section 4.2.4) that there is very little difference in activity of the mono- and bi-metallic Au-Pd catalysts towards the ammoximation of cyclohexanone via the addition of preformed H₂O₂ and so the slight loss in total surface area, possibly through the blocking of pores by metal incorporation, does not adversely affect the activity of TS-1.

It has previously been reported by Hutchings and co-workers that the alloying of Au and Pd on a range of oxide supports results in electronic modification of the Pd, producing a more selective catalyst⁶. A lack of complete alloying between Au and Pd, when supported on TS-1, may be responsible for the correlation between Pd loading and increased H₂O₂ synthesis and degradation rates.

5.2.4. Investigating the role of Au in improving catalytic selectivity towards cyclohexanone oxime.

As previously shown in Figure 5.8 addition of Pd to a Au/ TS-1 increases cyclohexanone oxime selectivity. Contrasting this, the activity towards the direct synthesis and subsequent degradation of H₂O₂ increases as the catalyst becomes more Pd-rich (Figure 5.9).

It is well known that upon calcination, Au-Pd alloyed nanoparticles can form on a variety of oxide supports as well as carbon and the resulting catalysts have been reported to offer improved activity towards H₂O₂ synthesis compared to the mono-metallic analogues⁹. To investigate whether such a synergistic effect is in operation for bimetallic Au-Pd/ TS-1 catalysts during cyclohexanone ammoximation, the selectivity and conversion observed over bi-metallic 2.5 wt. % Au- 2.5 wt. % Pd / TS-1 were compared to those observed when monometallic 2.5 wt. % Au / TS-1 and 2.5 wt. % Pd / TS-1 were used separately and in combination as a physical mixture. The results are shown in Figure 5.11.

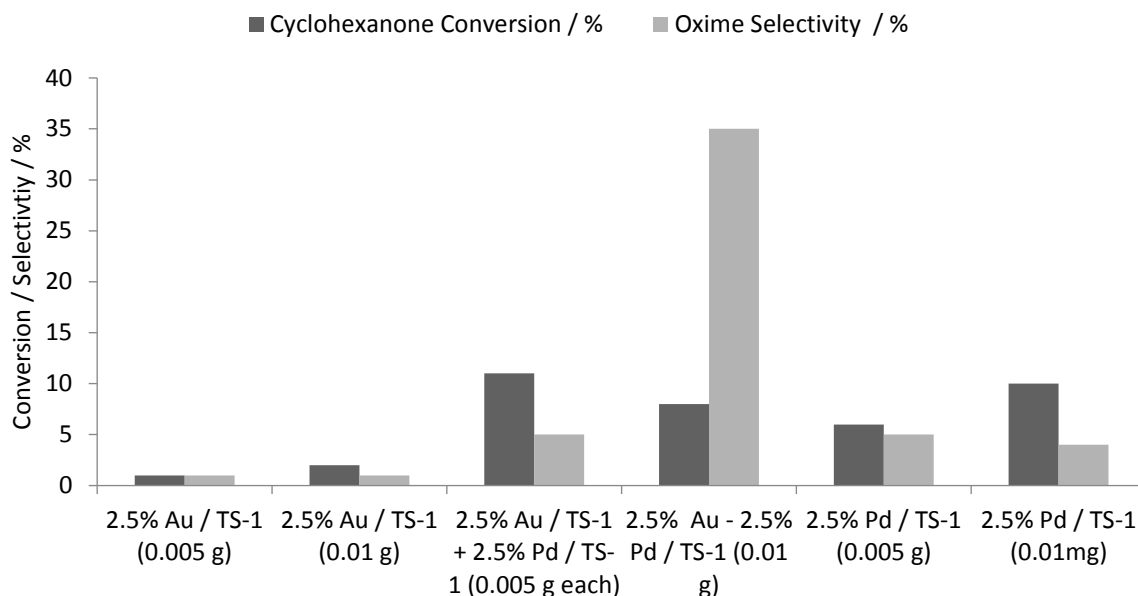


Figure 5.11 Effect of combining Au and Pd on the same support and as a physical mixture towards the ammoxidation of cyclohexanone.

Reaction conditions: Catalyst, cyclohexanone (0.13 g, 1.3 mmol), NH₃ (0.08g, 28 wt. %, 1.3 mmol), total pressure 580 psi, H₂ / O₂ = 0.525, 1200 rpm, 30 min, 5.6 g t-BuOH + 2.69 g H₂O (66 wt. % t-BuOH), 80 °C.

Figure 5.11 demonstrates the beneficial effect of co-impregnating Au and Pd onto the same TS-1 support. As shown in Figure 5.8 it is only when both Au and Pd are incorporated onto the TS-1 support that an improvement in selectivity is observed. As in Figure 5.8 monometallic Au catalysts show poor cyclohexanone conversion and selectivity towards the oxime when compared to analogous Pd- only catalysts. This is again observed when comparing 2.5 wt. % Au / TS-1 and 2.5 wt. % Pd / TS-1, with the Pd-only catalyst showing 5 times the rate of cyclohexanone conversion when compared with the Au-only analogue (10 % and 2 % respectively). When physical mixtures of the two catalysts are assessed (0.005 g of each catalyst) conversion rates and selectivity towards the oxime are comparable to those observed for the Pd-only catalyst, which is consistent with the low cyclohexanone conversion rate observed for 5 wt. % Au / TS-1 in Figure 5.8.

When a bi-metallic 2.5 wt. % Au - wt. 2.5% Pd / TS-1 catalyst is investigated a dramatic increase in selectivity towards the oxime is observed, from 5% when a physical mixture of the two catalysts is utilised to 35% for the bi-metallic catalyst. The improvement in catalytic selectivity towards the oxime may be attributed to the formation of Au-Pd nanoparticles on the surface of the TS-1 support. The formation of these Au-Pd bi-metallic nanoparticles on various oxide supports has previously been shown to lead to improved catalytic activity for the direct synthesis of H₂O₂ in comparison to the monometallic catalysts⁹. The effect of

combining both metals on the same support for the direct synthesis of H_2O_2 is discussed later. As the rate of H_2O_2 synthesis is increased the concentration of H_2O_2 available to be activated by the Ti (IV) sites present in TS-1 increases. This leads to an increase in the concentration of Ti-OOH sites, thereby increasing the rate of hydroxylamine formation and thus oxime formation. It may therefore be that the incorporation of both metals on to the same support is key in producing a catalyst where the rate of H_2O_2 synthesis is closer to the rate of hydroxylamine formation. This would result in greater oxime selectivity based on H_2 . That is more H_2 is utilised in the formation of cyclohexanone oxime, rather than in the formation of H_2O , via the degradation of H_2O_2 , or unwanted by-products such as cyclohexanol. Further work is needed to determine whether optimisation of the rates of H_2O_2 and hydroxylamine synthesis is a key factor in further enhancing catalyst selectivity. It has been demonstrated previously in Figure 5.8 that the addition of Au to a Pd / TS-1 catalyst improves selectivity towards cyclohexanone oxime at comparable cyclohexanone conversion.

Figure 5.12 shows the improvement in the rate of H_2O_2 synthesis, observed when Au and Pd are co-impregnated onto the same support.

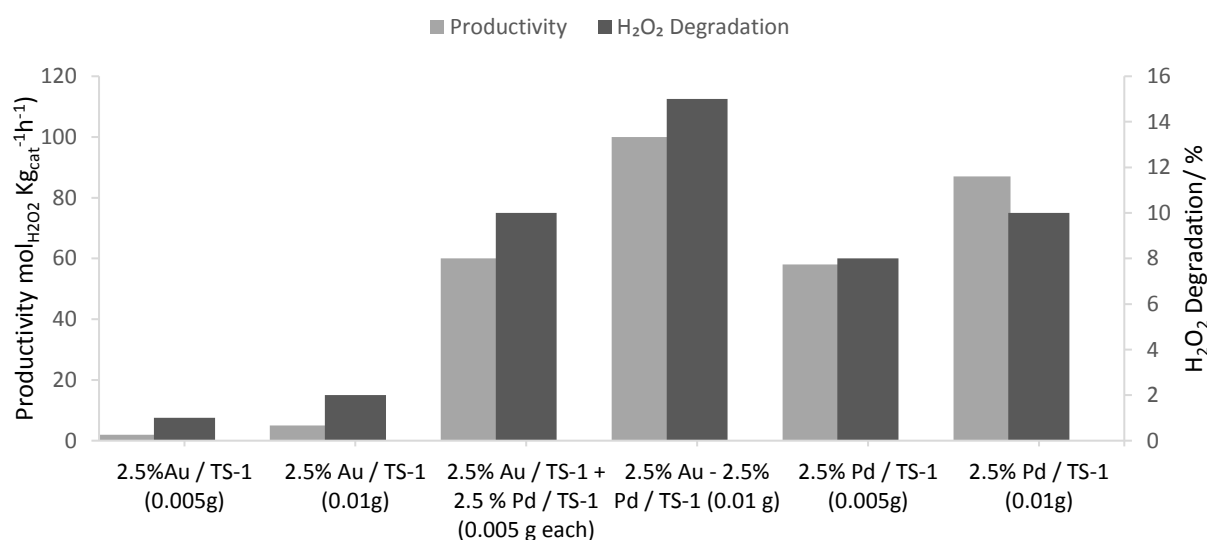


Figure 5.12. Effect of combining Au and Pd on the same support towards the direct synthesis and degradation of H_2O_2 .

Reaction conditions: 5 wt. % Pd / TS-1 (0.01 g), total pressure 580 psi, $\text{H}_2 / \text{O}_2 = 0.525$, 1200 rpm, 30 min, 5.6 g MeOH + 2.9 g H_2O (66 wt. % MeOH), 2 °C.

Figure 5.12 shows a similar trend for H_2O_2 synthesis as that observed in Figure 5.11 for the ammoxidation of cyclohexanone. Indeed, a catalyst prepared by co impregnation of Au and Pd onto the TS-1 support shows a higher H_2O_2 synthesis rate than the analogous physical

mixture of monometallic catalysts (100 and 60 mol_{H₂O₂} Kg_{cat}⁻¹h⁻¹ respectively). It is clear from Figure 5.11 that the monometallic 2.5 wt. % Pd/ TS-1 catalyst is far more active for the direct synthesis of H₂O₂ than the analogous Au-only catalyst and that a physical mixture of the two mono-metallic catalysts offers H₂O₂ synthesis rates comparable to the sum of the two catalysts. Impregnation of Au and Pd onto the same support produces a catalyst that shows significantly higher activity for H₂O₂ synthesis than a physical mixture of the two mono-metallic catalysts. This suggests that the incorporation of the two metals is key for H₂O₂ synthesis, as reported previously by Hutchings and co-workers¹⁰. It has been suggested that the alloying of these two metals results in electronic modification of the Pd and that this results in the formation of a more active H₂O₂ synthesis catalyst¹¹.

5.2.5. The effect of calcination temperature on 2.5 wt. % Au – 2.5 wt. % Pd / TS-1 activity towards the ammoximation of cyclohexanone.

It has previously been shown for 5 wt. % Pd / TS-1 catalyst, that catalytic activity for both cyclohexanone ammoximation and direct H₂O₂ synthesis of decreases as the calcination temperature increases. However stability of the catalyst, in the ammoximation reaction, improves.

Comparison of 5 wt. % Pd/ TS-1 and 2.5 wt. % Au-2.5 wt. % Pd / TS-1 (both calcined at 400 °C, 3 h, static air, 20 °C min⁻¹) has shown that the bi-metallic Au-Pd catalyst shows higher catalytic activity towards cyclohexanone ammoximation than the monometallic Pd catalyst. The effect of varying the calcination temperature on the catalytic performance of 2.5 wt. % Au - 2.5 wt. % Pd / TS-1 catalyst was investigated to determine if the deleterious effect of a high calcination temperature, observed for the Pd mono-metallic, can be offset through the incorporation of Au. The results of this study are shown in Figure 5.13.

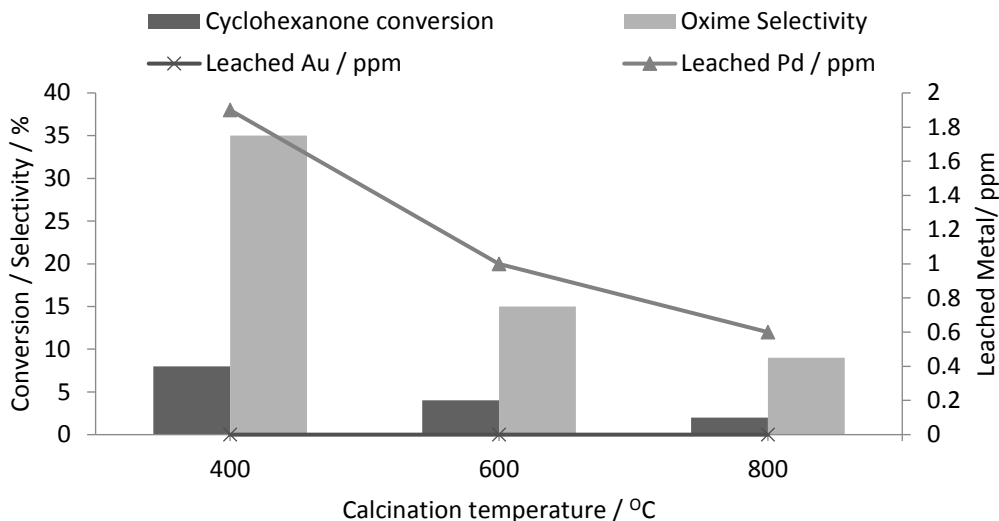


Figure 5.13. Effect of calcination temperature on the catalytic performance of 2.5 wt. % Au- 2.5 wt. % Pd/ TS-1 for cyclohexanone ammoximation.

Reaction conditions: Catalyst (0.05 g), cyclohexanone (0.13 g, 0.13 mmol), NH₃ (0.08g, 28 wt. %, 1.3 mmol), total pressure 580 psi, H₂ / O₂ = 0.525, 1200 rpm, 30 min, 5.6 g t-BuOH + 2.69 g H₂O (66 wt. % t-BuOH), 80 °C.

It is observed that, as with the 5 wt. % Pd / TS-1 catalyst, the calcination temperature increases there is a substantial decrease in catalyst activity, with both cyclohexanone conversion and oxime selectivity decreasing, from 8 and 35 % when calcined at 400 °C to 2 and 9 % when the catalyst is calcined at 800 °C. Unlike the mono-metallic Pd catalyst, some activity is retained following calcination at 800 °C. In a similar manner to the Pd only catalyst a decrease in leached Pd is observed as calcination temperature increases. Interestingly, no leached Au is observed regardless of calcination temperature. Some activity towards the ammoximation of cyclohexanone is retained suggesting that the introduction of Au into a Pd-only catalyst is able to off-set the deleterious effects of increased calcination temperature on catalyst activity towards the ammoximation of cyclohexanone.

Figure 5.14 shows the effect of calcination temperature on the direct synthesis and degradation of H₂O₂ by 2.5 wt. % Au – 2.5 wt. % Pd / TS-1.

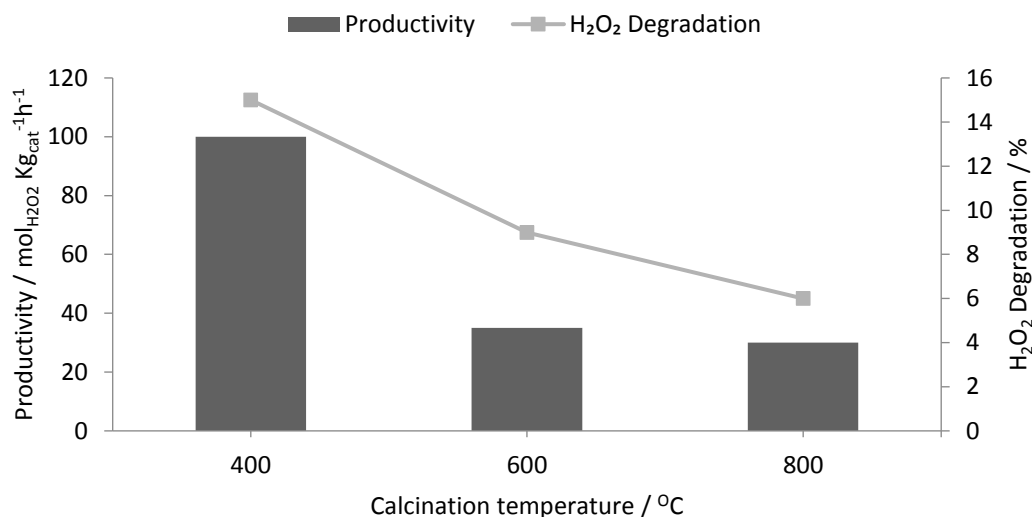


Figure 5.14. Effect of calcination temperature on the catalytic activity of 2.5 wt. % Au-2.5 wt. % Pd/ TS-1 for the direct synthesis and degradation of H₂O₂.

Reaction conditions: 2.5 wt.% Au- 2.5 wt. % Pd / TS-1 (0.01 g), total pressure 580 psi, H₂ / O₂ =0.525, 1200 rpm, 30 min, 5.6 g MeOH + 2.9 g H₂O (66 wt. % MeOH), 2 °C.

It is observed that, as with 5 wt. % Pd / TS-1 (Section 5.2.2), increasing the calcination temperature causes a decrease in the activity of the catalyst for direct H₂O₂ synthesis. Indeed, when calcined at 400 °C the rate of H₂O₂ synthesis is 100 mol_{H₂O₂}Kg_{cat}⁻¹h⁻¹, whilst by increasing the calcination temperature to 800 °C productivity decreases to 30 mol_{H₂O₂}Kg_{cat}⁻¹h⁻¹. Further investigation has shown that catalytic activity towards the degradation of H₂O₂ also decreases with calcination temperature. This is attributed to the development of larger metal nanoparticles, as confirmed by XRD analysis (Table 5.2). In particular the increased intensity of peaks at 2θ values characteristic of Au (38° and 45°)(Appendix 5.1, Figure A2) suggests growth of Au particles with increasing calcination temperature.

Table 5.2 shows that as the calcination temperature increases the crystallinity of TS-1 decreases. Upon calcination at 400 °C crystallinity decreases to 83 % and this further decreases to 56.3 % upon calcination at 800 °C. This loss in crystallinity follows a similar trend to that observed for 5 wt. % Pd / TS-1, discussed in Section 5.2.2. Further investigation by XRD (Table 5.2), shows that a contrast with the monometallic Pd / TS-1 catalyst, no Pd reflections are observed for the bimetallic 2.5 wt. % Au – 2.5 wt.% Pd/ TS-1 catalyst (Appendix 5.1, Figure A2) following calcination at 400 °C. However, increasing the calcination temperature to 600 and 800 °C leads to clear reflections associated with PdO (34°). Indeed, the average Pd nanoparticle size determined using the Scherrer equation was 17 nm, when a calcination temperature of 800 °C was utilised. This is much lower than that observed when 5 wt. % Pd / TS-1 was calcined at 800 °C (Table 5.2), and may be the reason why the 2.5 wt.

% Au – 2.5% wt. Pd / TS-1 catalyst retains a degree of activity following calcination at 800 °C, as shown in Figure 5.12. The development of XRD reflections associated with PdO with increasing temperature correlates well with analysis by XPS (Appendix 5.3, Table A.2). It is seen that the atomic concentration of Pd decreases with increasing temperature, from 0.4 to 0.13 %, suggesting a decrease in the dispersion of Pd on the support.

Unlike Pd, XRD analysis of bimetallic Au – Pd/ TS-1 shows reflections associated with Au (38°, 44° and 70°) regardless of calcination temperature, suggesting Au is present as larger, poorly dispersed, nanoparticles even when calcined at 400 °C.

Further investigation by XPS shows that the Pd : Au ratio decreases drastically with temperature from a Pd : Au ratio of 40 when calcined at 400 °C to 2.6 at 800 °C, suggesting the migration of Au to the surface of the alloyed metal nanoparticles. It is known that when utilising a variety of oxide supports it is possible for Au-Pd nanoparticles to adopt a Au-core PdO-shell upon calcination and this may explain why Pd : Au ratio is so high when calcined at 400 °C. The decrease in Pd : Au ratio with increasing calcination temperature may be due to the breakdown of this core-shell morphology.

Unlike for the Pd-only supported catalysts it is not possible to investigate AuPd/TS-1 by CO chemisorption due to the need for sub-ambient temperatures when investigating Au, these facilities are not available at Cardiff University. It is suggested that a trend similar to that seen for the Pd-only catalysts would be observed for these AuPd/TS-1; where metal dispersion decreases as calcination temperature increase.

Further investigation of the effect of calcination temperature on 2.5 wt. % Au – 2.5 wt. % Pd / TS-1 was carried out using transmission electron microscopy can be seen in Figure 5.15.

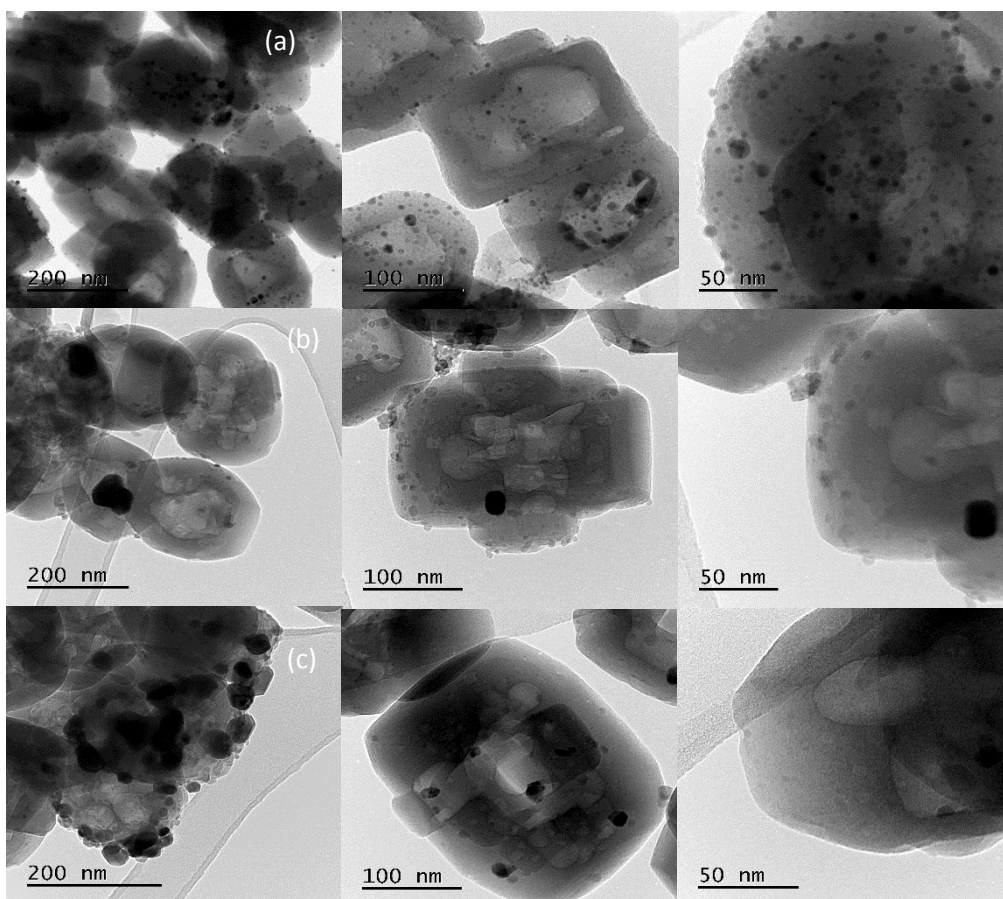


Figure 5.15. Transmission Electron Microscopy of 2.5 wt. % Au – 2.5 wt.% Pd / TS-1 exposed to calcination temperatures of (a) 400 °C, (b) 600 °C, (c) 800 °C (3 h, 20 OC min⁻¹, static air).

As with the 5 wt. % Pd / TS-1 catalyst, shown in Figure 5.4, it is observed that increasing calcination temperature results in larger, less well dispersed metal nanoparticles. However, it is not possible to determine particle size distribution due to the deformation of the metal nanoparticles that is it is not possible to identify individual nanoparticles. Further investigation by STEM-EDX is observed in Figure 5.16.

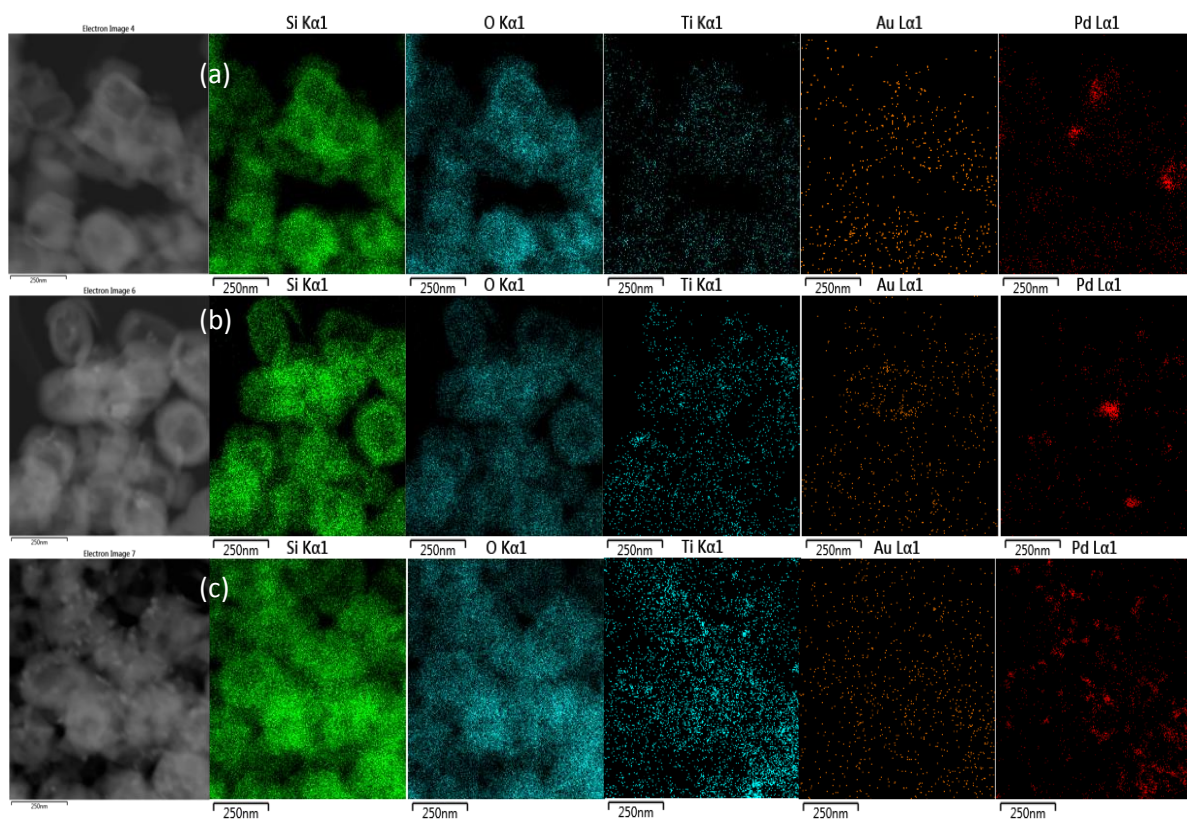


Figure 5.16. STEM-EDX analysis of 2.5 wt. % Au – 2.5 wt. % Pd / TS-1 calcined at (a) 400 °C, (b) 600 °C, (c) 800 °C. Si (Green), O (Blue), Ti (Blue), Au (Orange), Pd (Red).

It is possible that the presence of Au limits the formation of larger Pd nanoparticles at these calcination temperatures. This may either be through alloying of the two metals or due to the presence of additional Cl⁻ anions, found in the Au precursor, HAuCl₄. Indeed, Hutchings and co-workers have previously reported that Cl⁻ increases Pd distribution in a similar manner¹².

Further investigation into the structure of the 2.5 wt. % Au – 2.5 wt. % Pd TS-1 catalysts exposed to increasing calcination temperatures (400 – 800 °C) by FTIR can be seen in Figure 5.17

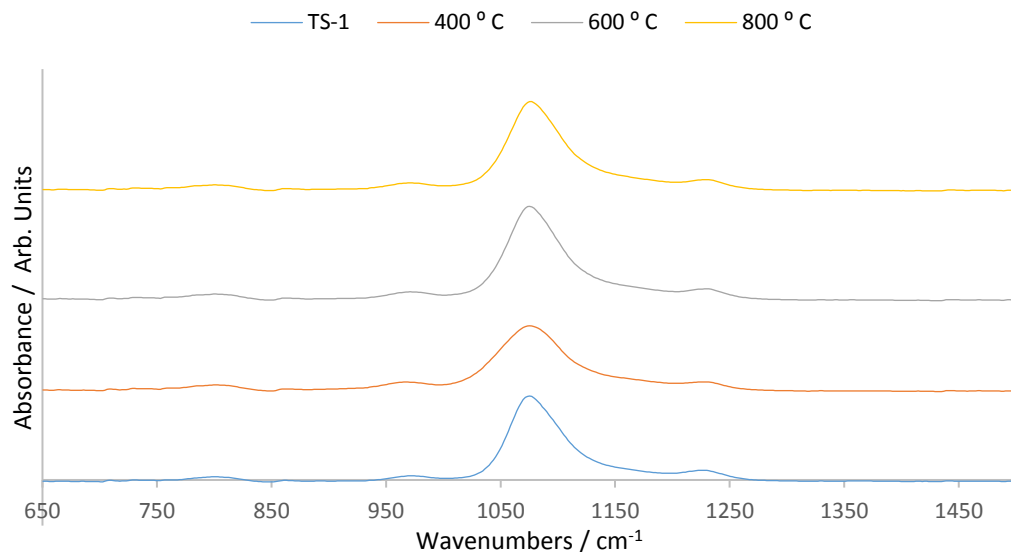


Figure 5.17. FTIR spectra of 2.5 wt. % Au - 2.5 wt. % Pd / TS-1 catalysts calcined at 400 – 800 °C (3 h, static air, 20 °C min⁻¹).

Investigation by FTIR reveals no significant changes in the structure of TS-1, as with the 5 wt. % Pd / TS-1 catalysts shown in Figure 5.6.

5.2.6. Investigation of the effect of total metal loading for Au-Pd catalysts for the ammoxidation of cyclohexanone.

Figure 5.17 shows the effect of changing the total loading of active metal while maintaining the Au : Pd ratio at 1:1 wt/ wt on the ammoxidation of cyclohexanone.

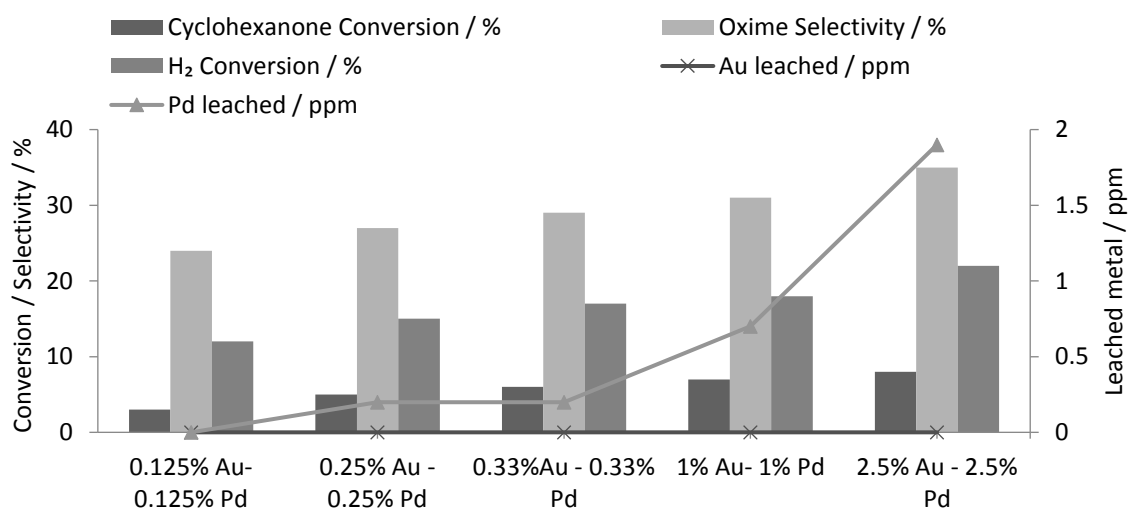


Figure 5.17 The effect of total metal loading on the activity towards ammoxidation of cyclohexanone for Au-Pd/TS-1 catalysts where Au : Pd = 1 : 1 (wt/wt).

Reaction conditions: Catalyst (0.05 g), cyclohexanone (0.13 g, 0.13 mmol), NH₃ (0.08 g, 28 wt. %, 1.3 mmol), total pressure 580 psi, H₂ / O₂ = 0.525, 1200 rpm, 30 min, 5.6 g t-BuOH + 2.69 g H₂O (66 wt. % t-BuOH), 80 °C.

It can be seen that as metal loading increases, oxime selectivity, cyclohexanone conversion and H₂ conversion improve, in a manner similar to that observed for the 5 wt.% Pd / TS-1 catalyst (Figure 5.1). This is attributed to increased rates of catalytic H₂O₂ synthesis. Rates of cyclohexanone conversion are relatively low for all catalysts investigated in Figure 5.17. Interestingly, upon lowering the total metal content by a factor of 20, from 2.5 wt. % Au – 2.5 wt. % Pd / TS-1 to 0.125 wt. % Au – 0.125 wt. % Pd / TS-1, the cyclohexanone conversion rate is only decreased by a factor of 2.6, from 8 to 3 %. Selectivity is observed to decrease across this range, from 36 at 5 wt. % metal loading to 24 % at 0.25 wt. % metal loading. As with the other two metrics used to determine catalyst efficiency (selectivity towards the oxime and cyclohexanone conversion) H₂ conversion also increases with total metal loading, from 12 to 22 % for 0.125 wt. % Au – 0.125 wt.% Pd / TS-1 and 2.5 wt. % Au – 2.5 wt. % Pd / TS-1 respectively. This improvement, as with cyclohexanone conversion and oxime selectivity is ascribed to an increase in the rate of H₂O₂ synthesis. The same catalysts were therefore assessed for H₂O₂ synthesis and degradation with the data shown in Figure 5.18.

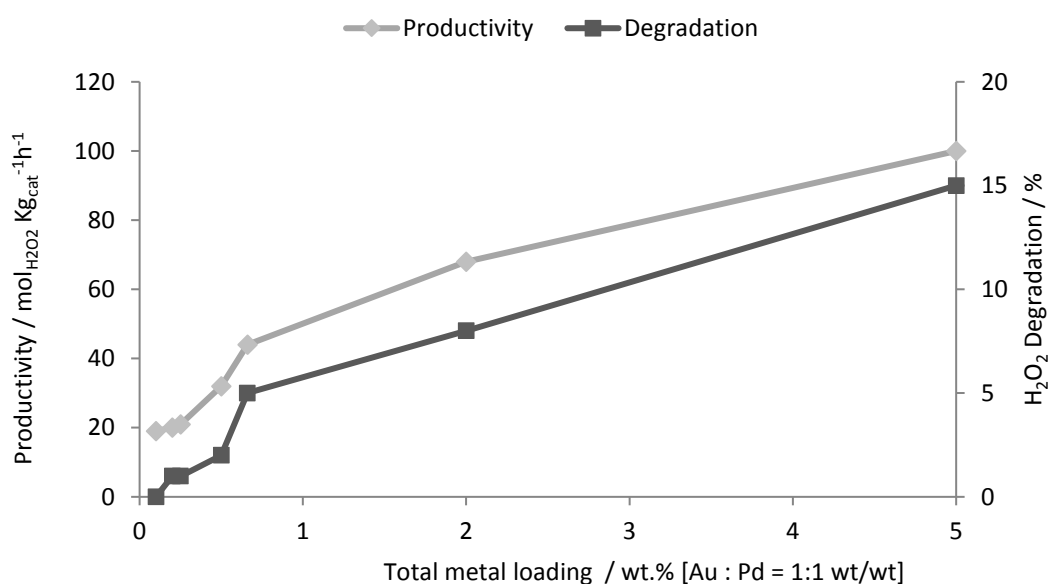


Figure 5.18. The effect of total metal loading on H₂O₂ synthesis and degradation, for Au-Pd/ TS-1 catalysts where Au: Pd = 1: 1 wt/ wt.

Reaction conditions: Catalyst (0.01 g), total pressure 580 psi, H₂/ O₂ = 0.525, 1200 rpm, 30 min, 5.6 g MeOH + 2.9 g H₂O (66 wt. % MeOH), 2 °C.

Catalytic activity towards both H₂O₂ synthesis and degradation is observed to correlate with total metal loading. That is, as the total metal loading decreases so does catalytic activity. This has been observed previously in Section 5.2.1 for Pd loading. It is observed in Figure 5.18 that catalyst activity for the direct synthesis of H₂O₂ increases from 19 to

100 mol_{H₂O₂} Kg_{cat}⁻¹h⁻¹ as the total metal loading increases from 0.1 wt. % to 5 wt. %. A similar trend can be observed for catalytic activity towards H₂O₂ degradation, with the rate of H₂O₂ conversion increasing from 0 to 15 %. It is particularly interesting that the catalyst with the lowest total metal loading (0.05 wt. % Au – 0.05 wt. % Pd / TS-1) shows no activity towards the degradation of H₂O₂, over the timescale investigated (30 min). As such the catalyst is highly selective towards H₂O₂, although when compared to catalysts with higher metal loadings the activity towards H₂O₂ synthesis is relatively low.

5.2.7. Mono – bi – and tri-metallic Pd / Pt / Au / catalysts supported on TS-1 for the ammoximation of cyclohexanone.

Previous studies by Hutchings and co-workers¹³ have reported the activity of Pt - containing Au-Pd catalysts towards the direct synthesis of H₂O₂, while Strukul and co-workers have studied Pd – Pt / ZrO₂ – SO₄ for the direct synthesis of H₂O₂¹⁴.

Preliminary studies are shown in Figure 5.19 comparing the activity of monometallic 5 wt. % Au / Pd / Pt / TS-1 catalysts for the ammoximation of cyclohexanone.

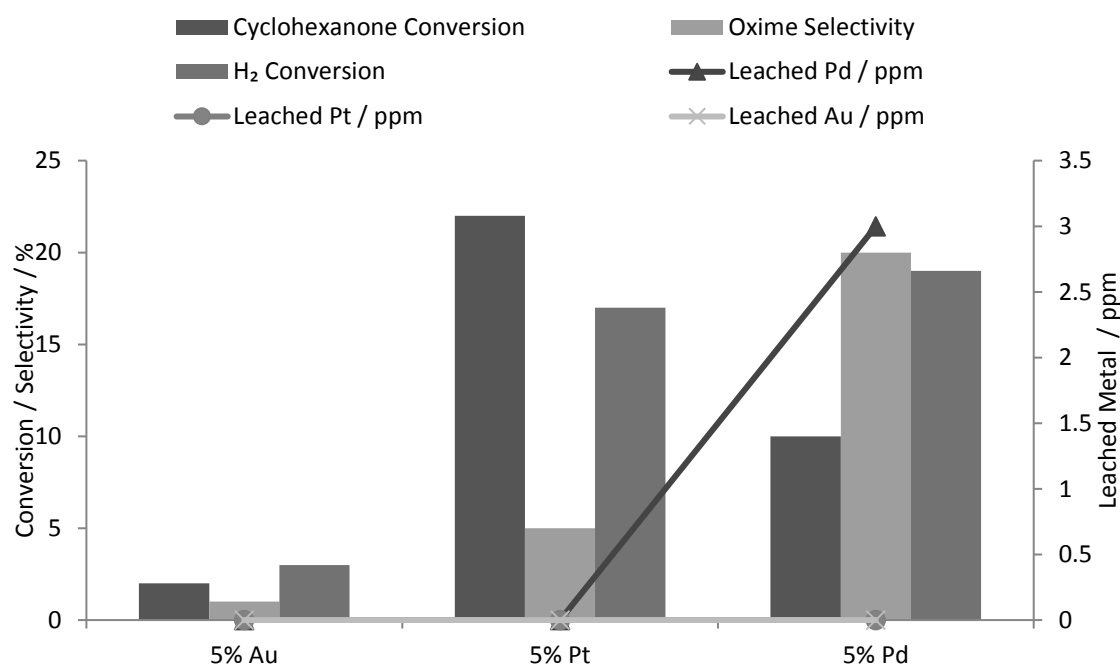


Figure 5.19. Monometallic Au / Pd / Pt catalysts for the ammoximation of cyclohexanone.

Reaction conditions: Catalyst (0.05 g), cyclohexanone (0.13 g, 1.3 mmol), NH₃ (0.08g, 28 wt. %, 1.3 mmol), total pressure 580 psi, H₂ / O₂ = 0.525, 1200 rpm, 30 min, 5.6 g t-BuOH + 2.69 g H₂O (66 wt. % t-BuOH), 80 °C.

It is observed, in Figure 5.19, that cyclohexanone oxime selectivity and H₂ conversion follows the order Pd > Pt > Au. Interestingly, the monometallic Pt catalyst affords higher rates of

conversion than Au or Pd catalysts (22 % compared to 10 and 2 % respectively) though the Pt catalysts shows lower oxime selectivity than the Pd analogue. This is attributed to the greater H₂ affinity displayed by Pt in comparison to Au and Pd. It is suggested that this results in an increase in unwanted hydrogenated by-products such as cyclohexanol.

Bi-metallic catalyst consisting of two component metals (Au, Pd and Pt) were also studied for the ammoximation of cyclohexanone, the results are shown in Figure 5.20.

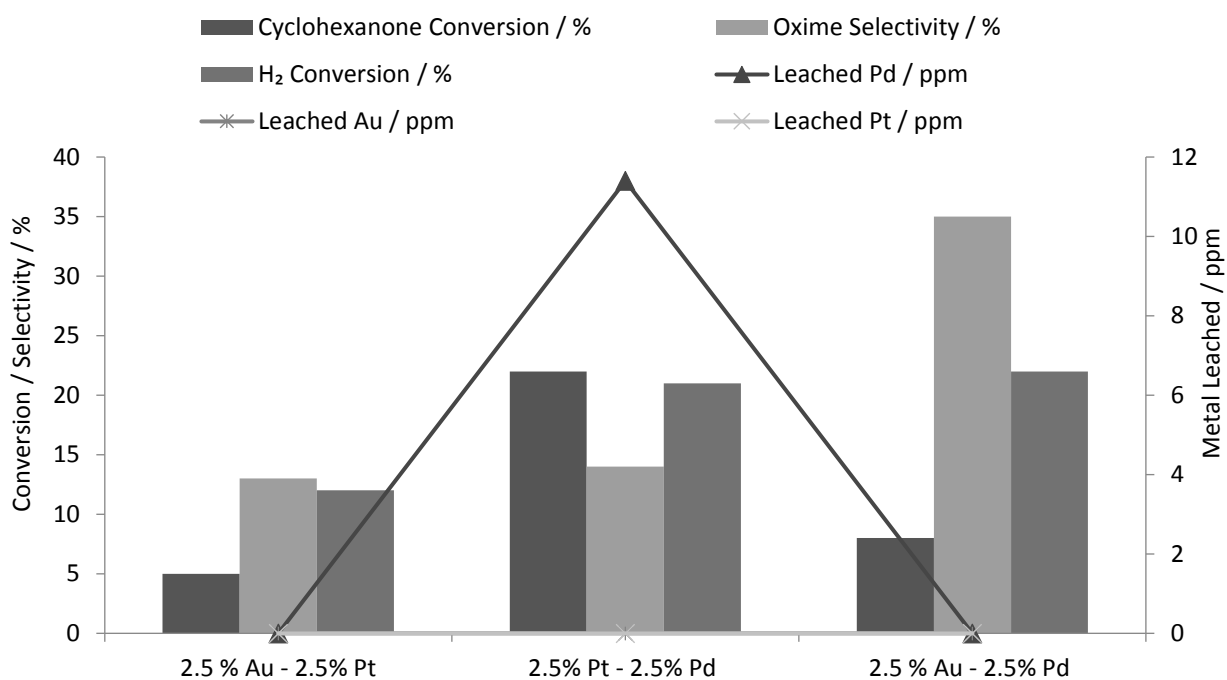


Figure 5.20. Bimetallic catalysts containing Au, Pd or Pt for the ammoximation of cyclohexanone.

Reaction conditions: Catalyst (0.05 g), cyclohexanone (0.13 g, 1.3 mmol), NH₃ (0.08g, 28 wt. %, 1.3 mmol), total pressure 580 psi, H₂ / O₂ = 0.525, 1200 rpm, 30 min, 5.6 g t-BuOH + 2.69 g H₂O (66 wt. % t-BuOH), 80 °C.

Interestingly, even though the monometallic Au/ TS-1 catalyst shows lower rates of conversion and selectivity than the Pt analogue a combination of the two metals results in increased oxime selectivity, from 5 % for 5 wt. % Pt / TS-1 to 13 % for 2.5 wt. % Au – 2.5 wt. % Pt / TS-1.

Comparing the bimetallic catalysts tested, the selectivity afforded by 2.5 wt. % Au – 2.5 wt. % Pd / TS-1 exceeds that observed for 2.5 wt. % Pd- 2.5 wt. %Pt / TS-1 or 2.5 wt. %Au – 2.5 wt. % Pt / TS-1 with oxime selectivities of 35, 14 and 13 % respectively. Interestingly the cyclohexanone conversion observed over 2.5 wt. % Pd- 2.5 wt. % Pt / TS-1 is greater than observed for 2.5 wt. % Au - 2.5 wt. % Pd / TS-1, at 22 and 8 % conversion respectively. This suggests that the hydrogenation ability of the Pd- Pt / TS-1 catalyst is greater than that of the Pd- Au / TS-1 catalyst. It has been reported by Holderich and co-workers¹⁵ that the addition

of Pt to Pd / TS-1 stabilises surface Pd(II)O species, an oxidation state known to favour H₂O₂ formation . This may increase the rate of H₂O₂ synthesis for the 2.5 wt. % Pd – 2.5 wt. % Pt / TS-1 catalyst such that it exceeds the rate of hydroxylamine formation at Ti (IV) sites, which would lead to lower oxime selectivity due to increased H₂O₂ degradation from the reaction conditions. It is suggested that due to the harsh reaction conditions only the Ti (IV) sites in close proximity to the metal nanoparticles responsible for H₂O₂ synthesis are involved in the formation of hydroxylamine and cyclohexanone oxime. Wang *et.al.*¹⁶ have reported that H₂O₂ productivity strongly depends on the Pt : Pd ratio. They report that increasing the Pt to Pd ratio is deleterious to the rate of H₂O₂ synthesis. Further work is required to determine how the Pd : Pt ratio effects catalytic activity for cyclohexanone oxime synthesis and to assess the rates of H₂O₂ synthesis and degradation over the mono- and bi-metallic catalysts in Figures 5.19 and 5.20.

Assessment of the catalytic activity of mono- and bi- metallic catalysts comprising of Au, Pd or Pt in Figures 5.19 and 5.20 provides key information as to potential routes to designing a TS-1 supported catalyst which is not only active for the ammoximation of cyclohexane with *in situ* H₂O₂ generation but also selective towards cyclohexanone oxime as the favoured reaction product. Specifically; high rates of cyclohexanone conversion are favoured over Pt-containing catalysts, due to platinum's high affinity for H₂, however Pt catalysts show low oxime selectivity. Meanwhile Pd- catalysts show appreciable oxime selectivity, at the expense of substrate conversion. Finally addition of Au, which itself shows low rates of substrate conversion, as a second metal with Pt- or Pd increases both oxime selectivity and, in the case of Pd, stabilises the active phase towards chemical leaching. To determine whether the positive effects of Au, Pd and Pt might be combined in a cumulative fashion, trimetallic TS-1 catalysts comprising of Au- Pd (1: 1 wt/wt) and low loadings of Pt were prepared and catalytic data for these is shown in Figure 5.21.

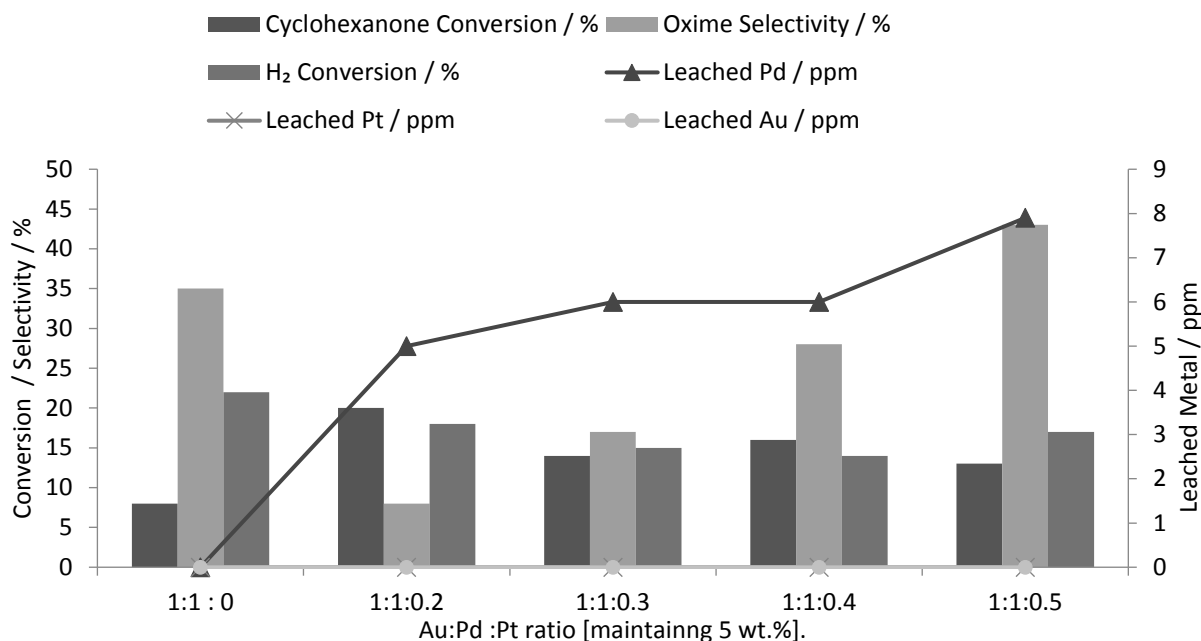


Figure 5.21 Tri-metallic catalysts of varying metal formulations comprising Au, Pd and Pt (total metal loading = 5 wt. %) for the ammoximation of cyclohexanone.

Reaction conditions: Catalyst (0.05 g), cyclohexanone (0.13 g), NH₃ (0.08 g, 28 wt. %), total pressure 580 psi, H₂ / O₂ = 0.525, 1200 rpm, 30 min, 5.6 g t-BuOH + 2.69 g H₂O (66 wt. % t-BuOH), 80 °C.

It is observed that the addition of Pt (≤ 0.45 wt. %) along with Au and Pd (Au : Pd = 1 : 1 wt/wt, total metal loading = 5 wt. %) dramatically decreases oxime selectivity, from 35% for 2.5wt. % Au – 2.5 wt.% Pd / TS-1 to 8% selectivity for 2.4 wt.% Au – 2.4 wt.% Pd – 0.2 wt.% Pt / TS-1 (Au : Pd : Pt wt.% ratio of 1 : 1 : 0.08). This drop in oxime selectivity coincides with a substantial increase in cyclohexanone conversion from 8 % for 2.5 wt. % Au 2.5 wt. % Pd/TS-1 to 20 % for 2.4 wt. % Au 2.5 wt. % Pd 0.2 wt. % Pt/TS-1. Further increasing of the wt. % loading of Pt (at a total metal loading of 5 wt. %) is found to have a beneficial effect upon catalyst performance. As shown in Figure 5.21, the trimetallic catalyst 2 wt. % Au 2 wt. % Pd 1 wt. % Pt/ TS-1 shows optimal catalytic performance, affording 13 % substrate conversion, 43 % oxime selectivity and 17 % H₂ conversion. However, with increasing Pt content/ oxime selectivity, Pd leaching also increases. No apparent leaching of Au or Pt was detected.

The poor selectivity observed in Figure 5.21 at low Pt loadings might be attributed a beneficial effect of Pt upon the catalytic activity towards the direct synthesis of H₂O₂ relative to Au- Pd alone. To further explore this, trimetallic catalysts were assessed for H₂O₂ synthesis and degradation reactions, the results are shown in Figure 5.22.

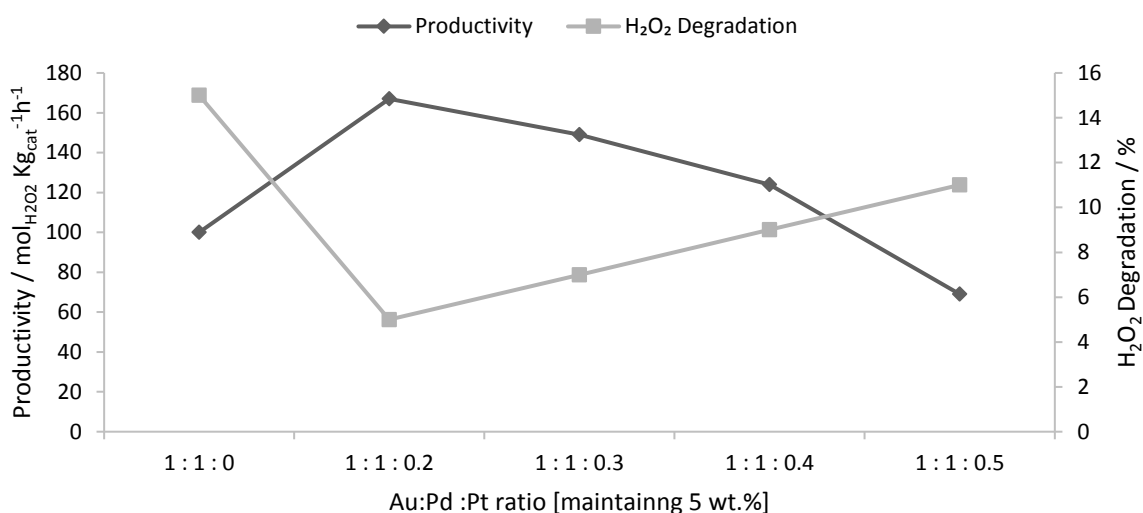


Figure 5.22. Tri-metallic catalysts of varying metal formulations comprising Au, Pd and Pt (total metal loading = 5 wt. %) for the direct synthesis and degradation of H₂O₂.

Reaction conditions: 5 wt. % Pd / TS-1 (0.01 g), total pressure 580 psi, H₂/O₂ = 0.525, 1200 rpm, 30 min, 5.6 g MeOH + 2.69 g H₂O (66 wt. % MeOH), 2°C.

The effect of varying the Pt content in AuPdPt / TS-1 trimetallic catalysts, while maintaining Au : Pd ratio at 1 :1, on the rates of H₂O₂ synthesis and degradation is shown in Figure 5.22. As can be observed, the small addition of Pt reduces the extent of H₂O₂ degradation when compared to the Au-Pd catalyst significantly, from 15 % to for the Au-Pd / TS-1 catalyst to 5% when 0.2 wt. % Pt is included. This corresponds with an increase in the rate of H₂O₂ synthesis, from 100 to 167 mol_{H₂O₂}Kg_{cat}⁻¹h⁻¹. This is in keeping with the findings of Pritchard *et.al.*¹³ who investigated the effect of Pt introduction into Au-Pd supported on CeO₂. Pritchard *et.al.*¹³ reports that the introduction of 0.1 wt. % Pt into a Au Pd/CeO₂ catalyst decreased the rate of H₂O₂ degradation from 145 to 76 mol_{H₂O₂}Kg_{cat}⁻¹h⁻¹, while the rate of H₂O₂ synthesis increased significantly from 68 to 109 mol_{H₂O₂}Kg_{cat}⁻¹h⁻¹. Further investigation by Pritchard *et.al.*¹³ has revealed that the introduction of Pt increased the surface ratio of Pd : Au from a value of 7 for the 2.5 wt. % Au – 2.5 wt. % Pd / CeO₂ catalyst (similar to the value reported herein for the 2.5 wt. % Au – 2.5 wt. % Pd TS-1 catalyst) to 58 for the 2.4 wt. % Au – 2.4 wt. % Pd – 0.2 wt.% Pt / CeO₂ catalyst, with a corresponding increase in catalytic activity towards the direct synthesis of H₂O₂ from 68 mol_{H₂O₂} Kg_{cat}⁻¹h⁻¹ for the 2.5 wt. % Au – 2.5 wt. % Pd / CeO₂ catalyst to 170 mol_{H₂O₂} Kg_{cat}⁻¹h⁻¹ for the 2.4 wt. % Au – 2.4 wt. % Pd – 0.2 wt.% Pt / CeO₂ catalyst. A similar improvement can be seen in Figure 5.22, where catalytic activity towards H₂O₂ formation increases from 100 mol_{H₂O₂} Kg_{cat}⁻¹h⁻¹ for the 2.5 wt. % Au – 2.5 wt. % Pd TS-1 catalyst to 167 mol_{H₂O₂} Kg_{cat}⁻¹h⁻¹ for the 2.4 wt. % Au – 2.4 wt. % Pd – 0.2 wt.% Pt / TS-1

catalyst. Investigation by XPS (Appendix 5.3 Table A.3) indicates that a similar phenomenon is observed as that reported by Pritchard *et.al.*¹³ It is observed that the introduction of a small amount of Pt increases to Pd : Au ratio from 7 for the 2.5 wt. % Au – 2.5 wt. % Pd / TS-1 catalyst to 34 for the catalyst. Further introduction of Pt results in a slight decrease in the Pd : Au ratio and a corresponding decrease in catalytic activity towards H₂O₂ synthesis, as observed in Figure 5.22 Again this is in keeping with the work of Pritchard *et.al.*¹³ who report that ‘the addition of Pt to AuPd nanoparticles significantly affect the surface composition’ and that the presence of Pt results in the improvement off electronic effects through the formation of core-shell structures. It is suggested that a similar effect is observed herein with the addition of Pt to AuPd / TS-1.

Increasing the Pt content affects a decrease in activity for H₂O₂ synthesis of whilst also increasing the rate of H₂O₂ degradation. Catalyst productivity for H₂O₂ synthesis is observed to decrease from 167 to 69 mol_{H₂O₂}Kg_{cat}⁻¹h⁻¹ as the Pt content increases from 0.2 to 1 wt %, while maintaining Au : Pd ratio at 1:1. The rate of H₂O₂ degradation increases across this range, from 5 to 11 %. Interestingly, the incorporation of small amounts of Pt (≤ 0.45 wt %) is observed to increase catalytic activity towards H₂O₂ synthesis beyond that of 2.5% Au – 2.5% Pd / TS-1 while H₂O₂ degradation activity is observed to be lower than the bi-metallic catalyst. These findings correlate well with the work of Wang *et.al.*¹⁶, who reported that an optimal ratio of Pt : Pd is required to improve activity towards H₂O₂ synthesis, and that above this ratio, activity towards the formation of H₂O₂ decreases¹⁶.

It is possible to relate the effect of Pt content on catalytic activity towards H₂O₂ synthesis and activity for cyclohexanone ammoximation. With increasing Pt content, catalytic activity towards H₂O₂ synthesis decreases. This corresponds with decreased cyclohexanone conversion and increased oxime selectivity / an improved mass balance. Increasing selectivity suggests that H₂O₂ plays a role in undesirable further reactions which convert cyclohexanone oxime to nitrocyclohexane which has been reported by Cesana *et.al.*¹⁷

At lower rates of H₂O₂ synthesis the Ti(IV) sites of the support are able to activate a greater proportion of the synthesised H₂O₂, thereby increasing the selectivity with which H₂O₂ is utilised in cyclohexanone oxime formation. Of course not all the H₂O₂ that is synthesised will be utilised in hydroxylamine and in turn cyclohexanone oxime formation due to the harsh reaction conditions utilised and the activity of the catalyst towards H₂O₂ degradation. However by maintaining a H₂O₂ synthesis rate similar to that of hydroxylamine formation it is possible to increase selectivity toward the oxime and utilise H₂ in a more selective manner.

The observed rate of H₂O₂ synthesis over 2.5 wt. % Au -2.5 wt. % Pd/TS-1 and trimetallic catalysts (from Figure 5.22 and corresponding oxime yields / selectivities are shown in Figure 5.23.

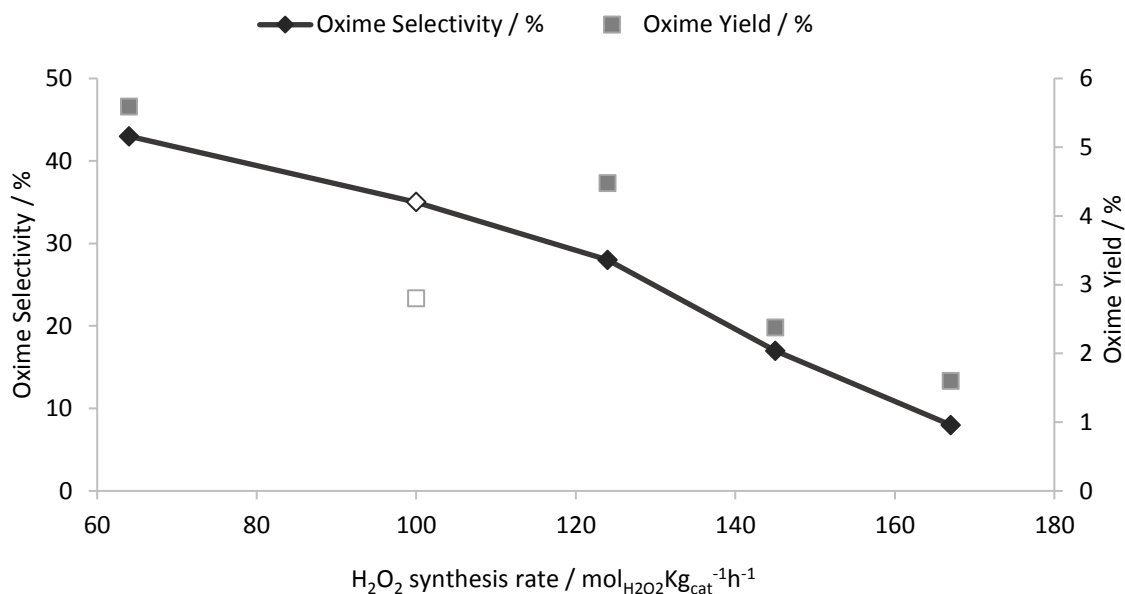


Figure 5.23. A plot of H₂O₂ synthesis rate versus oxime selectivity and yield constructed using data for trimetallic catalysts from Figures 5.21 and 5.22. \diamond and \square represent 2.5 wt. % Au - 2.5 wt. % Pd / TS-1.

Oxime selectivity is shown in Figure 5.23 to decrease linearly with an increase in the observed rate of H₂O₂ synthesis over the same catalysts. This correlates well with decreasing Pt loading (where applicable). At the same time oxime yield decreases and this is due to decreasing cyclohexanone conversion. This is curious, as cyclohexanone conversion would be expected to increase with increasing H₂O₂ concentration, which suggests that mass transfer limitations are suppressing the rate of reaction.

To better understand the structure of Pt containing tri-metallic catalysts, they were analysed by XRD. Diffractograms in Appendix 5.1, Figure A5 do not indicate the presence of either PdO or Pt phases, suggesting that these metals present on the surface as nanoparticles below the XRD detection limit of 5 nm. This suggests that co-impregnation of Pt with Au- Pd does not affect a significant growth in particle size and therefore metal nanoparticle growth cannot be ascribed as the reason why catalyst activity decreases with increasing Pt content.

5.2.8. The effect of calcination temperature on 2 wt. % Au – 2 wt. % Pd – 1 wt. % Pt / TS-1 activity towards the ammoximation of cyclohexanone.

The effect of calcination temperature on catalytic activity towards the ammoximation of cyclohexanone is shown in Figure 5.24.

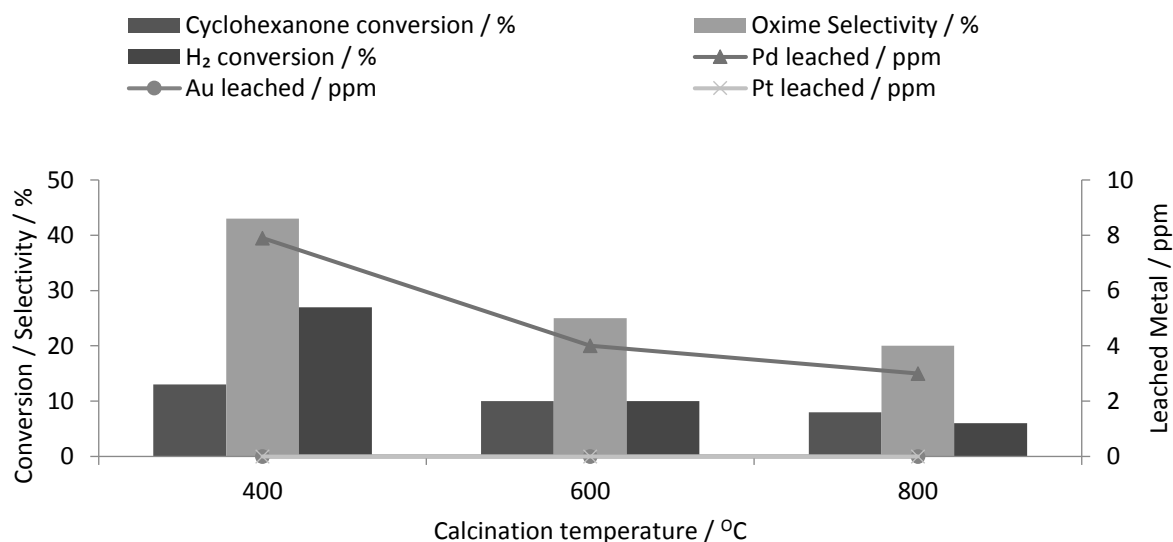


Figure 5.24 Effect of calcination temperature on the catalytic performance of 2 wt. % Au – 2 wt. % Pd – 1 wt. % Pt / TS-1 for the ammoximation of cyclohexanone.

Reaction conditions: Catalyst (0.05 g), cyclohexanone (0.13 g, 1.3 mmol), NH₃ (0.08 g, 28 wt %, 1.3 mmol), total pressure 580 psi, H₂ / O₂ = 0.525, 1200 rpm, 30 min, 5.6 g t-BuOH + 2.69 g H₂O (66 wt % t-BuOH), 80 °C.

As previously shown for 5 wt. % Pd / TS-1 (Figure 5.7) and 2.5 wt. % Au – 2.5 wt. % Pd / TS-1 (Figure 5.13), a decrease in both cyclohexanone conversion and oxime selectivity is observed as the calcination temperature increases from 400 to 800 °C. A significant decrease in oxime selectivity is observed across this range, from 43 to 20 %. When compared with the mono- and bi-metallic catalysts, the decrease in activity is not as pronounced, with cyclohexanone conversions of 13 and 8 % following calcination at 400 and 800 °C respectively.

To rationalise these trends, the same catalysts were assessed for H₂O₂ synthesis and degradation reactions. This data is shown in Figure 5.25.

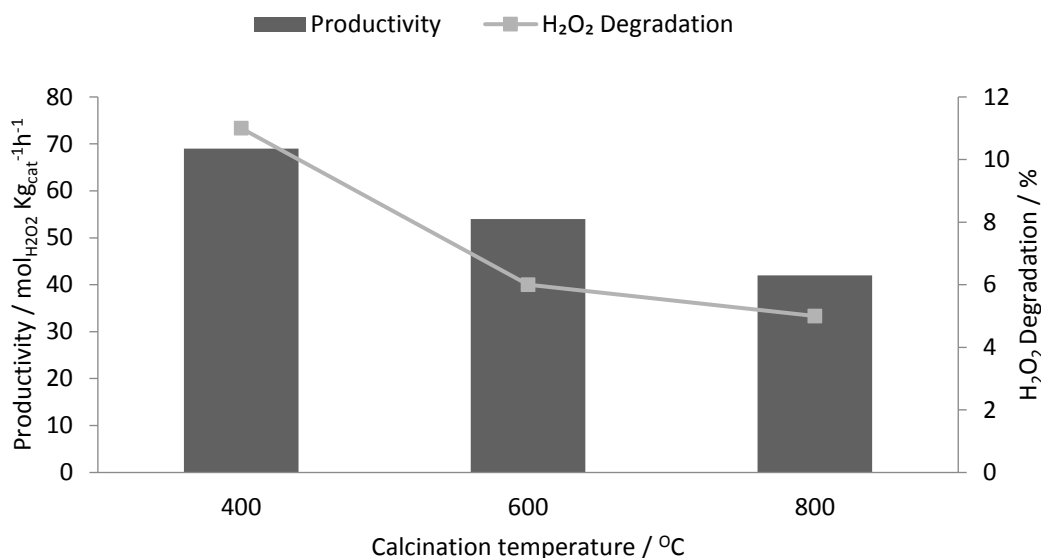


Figure 5.25 The effect of calcination temperature on H₂O₂ synthesis and degradation activity of 2 wt. % Au – 2 wt. % Pd – 1 wt. % Pt / TS-1.

Reaction conditions: Catalyst (0.01 g), total pressure 580 psi, H₂/ O₂ = 0.525, 1200 rpm, 30 min, 5.6 g MeOH + 2.69 g H₂O (66 wt. % MeOH), 2°C.

As previously observed for 5 wt. % Pd/ TS-1 and 2.5 wt. % - 2.5 wt. % Pd / TS-1, increasing the calcination temperature leads to a decrease in catalytic activity for the direct synthesis and degradation of H₂O₂. However in comparison to 5 wt. % Pd / TS-1 and 2.5 wt. % Au – 2.5 wt. % Pd the loss in activity towards H₂O₂ synthesis is less pronounced, with a loss in activity of *ca.* 40 % between upon increasing the calcination temperature from 400 to 800 °C. This is compared with relative decreases in rate of 90 and 70 % for 5 wt. % Pd/ TS-1 and 2.5 wt. % Au – 2.5 wt. % Pd / TS-1 catalyst respectively, across the same temperature range. As with the mono- and bi-metallic catalysts, this loss in catalytic activity is ascribed to an increase in nanoparticle size as eluded to by the development of reflections associated with these metals when studied by XRD (Table 5.2) (diffractograms shown in Appendix 5.3 Figure A3). In particular the increased intensity of the reflection at 40 and 67 ° associated with Pt which is observed at higher calcination temperatures (600 and 800 °C) but not at 400 °C, while the reflection at 38 ° associated with Au is observed regardless of calcination temperature. The development in reflections associated Pt correlates well with analysis by XPS. It is seen in Appendix 5.3 that atomic composition of Pt decreases 0.27 to 0.03 At. % when calcination temperature increases from 400 to 800 °C.

Furthermore as previously determined for 5 wt. % Pd/ TS-1 and 2.5 wt. % Au – 2.5 wt. % Pd / TS-1 there is a significant loss in TS-1 crystallinity upon metal incorporation and calcination, shown in Table 5.2 with the crystallinity of the catalyst calcined at 800 °C seen to be 33.8 % of that of the untreated support. Further investigation in to the TS-1 support by XRD reveals the development of a TiO₂ rutile phase (Appendix 5.2, Table A.1) and this is supported by analysis by XPS (Appendix 5.3, Table A.2)

which indicates a dramatic change in the Si : Ti ratio from 88.2 when the 2 wt.% Au – 2 wt. % Pd -1 wt. % Pt / TS-1 catalyst is calcined at 400 °C to 65.3 when calcined at 800 °C.

Further investigation by TEM and STEM-EDX into the effect of calcination temperature on 2 wt. % Au – 2. Wt % Pd. 1 wt % Pt / TS-1 can be seen in Figures 5.26 and 5.27.

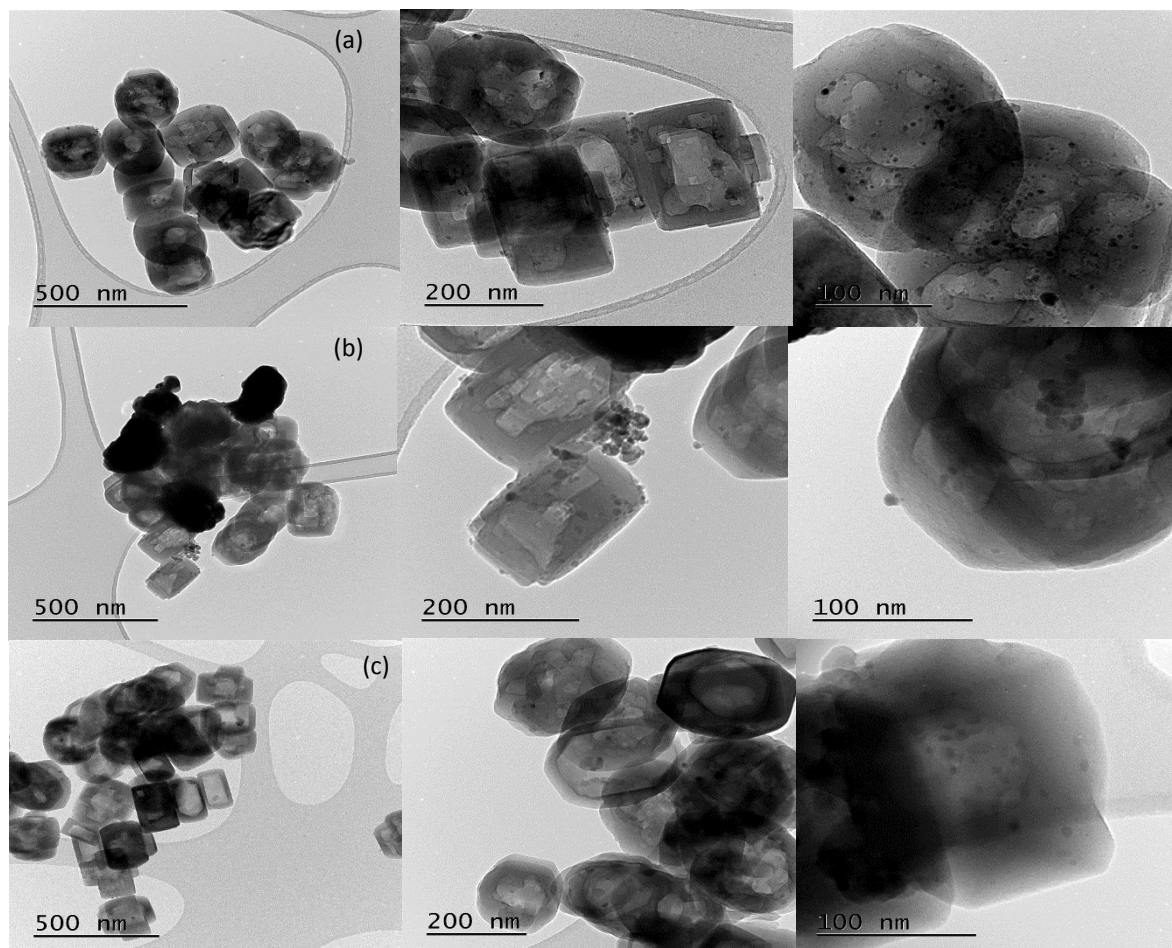


Figure 5.26. Transmission Electron Microscopy of 2 wt. % Au – 2 wt. % Pd – 1 wt. % Pt / TS-1 calcined at (a) 400 °C (b) 600 °C and (c) 800 °C (3 h, 20 °C min⁻¹, static air).

Investigation by TEM indicates the sintering of metal nanoparticles as calcination temperature increases, as with 5 wt. % Pd / TS-1 and 2.5 wt. % Au – 2.5 wt. % Pd / TS-1 it is not possible to determine particle size distribution due to a lack of discernible, individual metal nanoparticles, which is caused by deformation of the metal nanoparticles as calcination temperature increases. As such there are not a statistically relevant number of individual nanoparticles present to determine particle size distribution.

The effect of calcination temperature was also investigated by STEM-EDX, with the results observed in Figure 5.27.

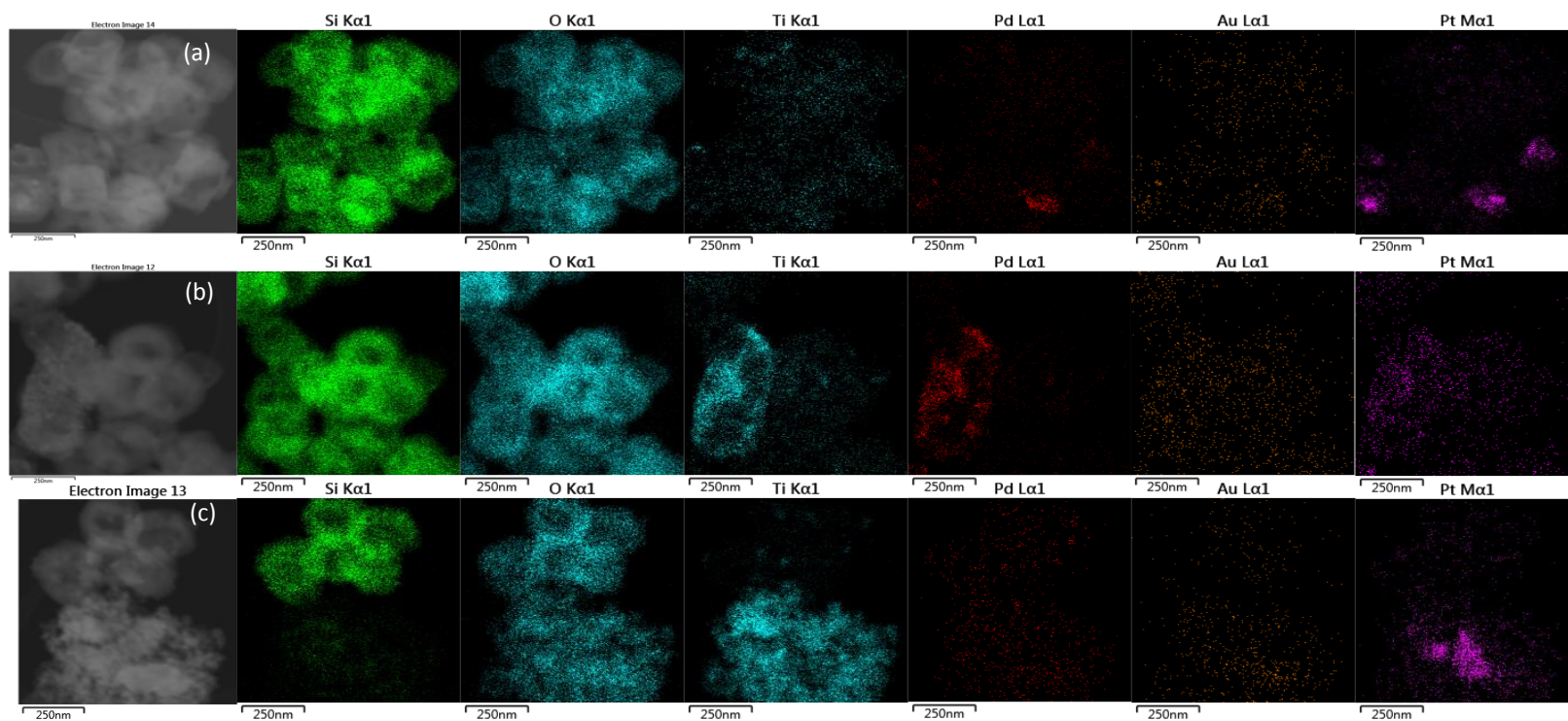


Figure 5.27. STEM-EDX analysis of 2 wt. % Au – 2 wt. % Pd – 1 wt. % Pt / TS-1 calcined at (a) 400 °C, (b) 600 °C, (c) 800 °C. Si (Green), O (Blue), Ti (Blue), Au (Orange), Pd (Red), Pt (Purple).

Investigation by STEM-EDX corroborates analysis by XRD, which indicated a decrease in dispersion of Pd, Au and Pt with increasing calcination temperature, particularly with regards to Pt and Au. As discussed previously investigation of the 2 wt. % Au – 2 wt. % Pd – 1 wt. % Pt / TS-1 catalyst calcined at 800 °C by XRD indicates the development of the TiO₂ rutile phase (6 %), however it should be noted that phase identification is semi-quantitative. This is substantiated via investigated by STEM-EDX, shown in Figure 5.28.

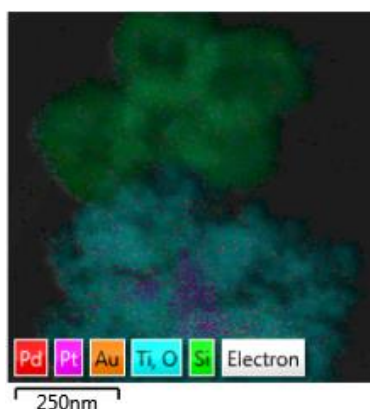


Figure 5.28. STEM-EDX analysis of 2 wt. % Au – 2 wt. % Pd – 1 wt. % Pt / TS-1 catalyst calcined at 800 °C showing development of the TiO₂ rutile phase.

It can be observed that two distinct phases appear upon calcination of the 2 wt. % Au – 2 wt. % Pd – 1 wt. % Pt / TS-1 catalyst at 800 °C; a Ti phase (blue) and a Si phase (green). This supports investigation by XRD which shows both a loss in crystallinity of the support upon increasing calcination temperature (Table 5.2) and development of a TiO₂ phase (Appendix 5.2, Table A.1).

Further investigation by FTIR can be seen in Figure 5.29.

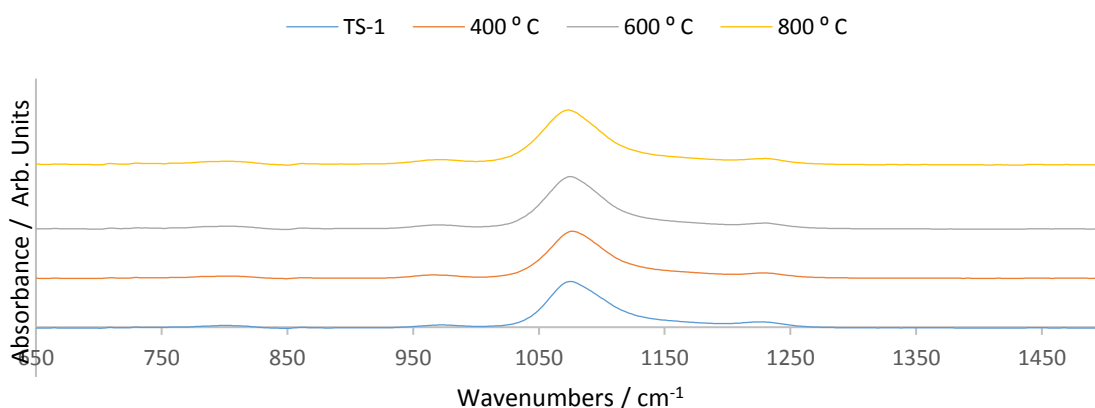


Figure 5.29. FTIR spectra of 2 wt. % Au – 2 wt. % Pd – 1 wt. % Pt / TS-1 catalysts calcined at 400 – 800 °C (3 h, static air, 20 °C min⁻¹).

As with the 5 wt. % Pd / TS-1 and 2.5 wt. % Au – 2.5 wt. % Pd / TS-1 catalysts there is no loss in the structure of TS-1 upon metal incorporation and exposure to calcination temperatures ranging from 400 – 800 °C.

In conclusion the loss in activity for H₂O₂ synthesis and cyclohexanone ammoximation reactions following calcination at 600 and 800 °C, as represented in Figures 5.24 and 5.25, is attributed to the increase in metal nanoparticle size and a decrease in crystallinity of TS-1. It is observed that while PdO is not detected by XRD, suggesting the presence of PdO as nanoparticles smaller than the detection limit of XRD (5 nm), the average particle sizes of Au and Pt by XRD are 50 and 28.7 nm respectively when 2 wt. % Au – 2 wt. % Pd – 1 wt. % Pt / TS-1 is calcined at 800 °C

5.2.9. The effect of calcination temperature of 5 wt. % Au-Pd-Pt / TS-1 catalysts for the ammoximation of cyclohexanone via direct synthesis of H₂O₂.

It is shown above that the incorporation of Pt into a Au-Pd catalyst can improve catalyst selectivity towards cyclohexanone oxime when the loading of Pt is relatively high (1 wt. %). The effect which Pt loading and calcination temperature have on catalytic activity for cyclohexanone ammoximation and the direct synthesis and degradation of H₂O₂ is therefore of great interest.

It has been shown in Figure 5.25 that the decrease in catalytic activity for H₂O₂ synthesis, observed when increasing calcination temperature from 400 to 800 °C, is far greater for 5 wt. % Pd/ TS-1 and 2.5 wt. % Au – 2.5 wt. % Pd / TS-1 than for 2 wt. % Au – 2 wt. % Pd – 1 wt. % Pt / TS-1. To further study the apparent enhanced stability of trimetallic AuPdPt / TS-1 catalysts to high temperature calcination, the effect of Pt content was studied whilst maintaining a Au : Pd ratio of 1:1 wt/wt and a total metal loading at 5 wt. %. The ability of Pt to stabilise catalyst activity with increasing calcination temperature is shown in Table 5.3.

Table 5.3. The observed catalytic performance and metal leaching of trimetallic AuPdPt/ TS-1 catalysts of varying metal formulations and following differing calcination treatments.

wt. % Au	wt. % Pd	wt. % Pt	Calcination Temperature / °C	Cyclohexanone Conversion / %	Oxime Selectivity / %	Oxime Yield/ %	Au leached / ppm	Pd leached / ppm	Pt leached / ppm
2.5	2.5	0	400	8	35	2.8	n.d	3	n.d
			600	4	15	0.6	n.d	0.4	n.d
			800	2	9	0.2	n.d	0.2	n.d
2.4	2.4	0.2	400	20	8	1.6	nd	2	n.d
			600	14	5	0.7	n.d	1	n.d
			800	4	4	0.48	n.d	1	n.d
2.35	2.35	0.3	400	18	12	2.16	n.d	2	n.d
			600	13	9	1.17	n.d	1	n.d
			800	11	7	0.77	n.d	1	n.d
2.28	2.28	0.44	400	16	14	2.24	n.d	3	n.d
			600	11	13	1.43	n.d	3	n.d
			800	10	11	1.1	n.d	1	n.d
2	2	1	400	13	43	5.59	n.d	7.9	n.d
			600	10	25	2.5	n.d	4	n.d
			800	8	20	1.6	n.d	3	n.d

Reaction Conditions: Catalyst (0.05 g), cyclohexanone (0.13 g, 1.3 mmol), NH₃ (0.08 g, 28 wt %, 1.3 mmol), total pressure 580 psi, H₂/ O₂ = 0.525, 1200 rpm, 30 min, 5.6 g t-BuOH + 2.69 g H₂O (66 wt % t-BuOH), 80 °C
n.d signifies not detected.

It was previously shown in Figure 5.21 that, for catalysts calcined at 400 °C, cyclohexanone conversion generally decreases and oxime selectivity increases with increasing Pt content. Data in Table 5.3 shows that this trend holds true when catalysts are calcined at a temperature with the range of 400 – 800 °C, regardless of Pt content. Meanwhile, increasing calcination temperature has previously been shown to result in the formation of larger metal nanoparticles on the surface of the TS-1 support (Sections 5.2.2 and 5.2.5). An increased population of larger metal nanoparticles, which are suggested to be less active towards the direct synthesis and degradation of H₂O₂, is consistent with trends shown in Table 5.3. To determine whether Pt loading and calcination temperature significantly effect H₂O₂ synthesis and degradation rates, catalysts were assessed for these reactions and the data is shown in Table 5.4.

Table 5.4. The performance of trimetallic AuPdPt catalysts for H₂O₂ synthesis and degradation reactions as a function of Pt loading and calcination temperature.

wt. % Au	wt. % Pd	wt. % Pt	Calcination Temperature / °C	H ₂ O ₂ synthesis rate / mol _{H₂O₂} Kg _{cat} ⁻¹ h ⁻¹ (a)	H ₂ O ₂ degradation/ % (b)
2.5	2.5	0	400	100	15
			600	35	9
			800	30	6
2.4	2.4	0.2	400	167	5
			600	96	3
			800	63	3
2.35	2.35	0.3	400	149	7
			600	89	4
			800	59	4
2.28	2.28	0.44	400	124	9
			600	76	5
			800	55	4
2	2	1	400	69	11
			600	54	6
			800	42	5

Reaction Conditions : (a) **H₂O₂ Synthesis Reaction Conditions:** Catalyst (0.01 g), total pressure 580 psi, H₂ / O₂ = 0.525, 1200 rpm, 30 min, 5.6 g MeOH + 2.69 g H₂O (66 wt. % MeOH), 2°C.

(b) **H₂O₂ Degradation Reaction Conditions:** Catalyst (0.01 g), MeOH (5.6 g), H₂O (2.22 g), H₂O₂ (50 wt. % 0.68 g), 5 % H₂/CO₂ (2.9 MPa) 30min, 2 °C, 1200 rpm.

Table 5.4 demonstrates a beneficial effect of Pt content on maintaining catalytic activity towards the direct synthesis and degradation of H₂O₂ with increasing calcination temperature. Increased Pt content reduces the deleterious effect of calcination temperature upon activity, with those catalysts containing more Pt retaining a greater percentage of their activity determined at 400 °C when calcined at higher temperatures. It is observed in Table 5.4 that by increasing the total Pt content it is possible to slow the loss in activity for H₂O₂ synthesis. Indeed, 2.4 wt. % Au – 2.4 wt. % Pd – 0.2 wt. % Pt / TS-1 shows a 62.3 % drop in rate upon increasing the calcination temperature from 400 °C to 800 °C and this is compared with a rate decrease of only 33.1 % observed for 2 wt. % Au – 2 wt. % Pd – 1 wt. % Pt / TS-1 over the same temperature range.

However it should be noted that regardless of calcination temperature, catalytic activity towards the direct synthesis H₂O₂ is related to Pt content, with catalysts of greater Pt content showing lower synthesis rates. As observed in Table 5.4, following calcination at 400 °C a catalyst with 0.2 wt. % Pt loading is more than twice as active for H₂O₂ synthesis when compared to a catalyst containing 1 wt. % Pt, with rates of 167 and 69 mol_{H₂O₂} Kg_{cat}⁻¹h⁻¹ respectively.

With regards to H₂O₂ degradation, those catalysts with higher Pt loadings are observed to be more active than those of lower Pt content. As can be observed in Table 5.4, following calcination at 400 °C

2 wt. % Au – 2 wt. % Pd – 1 wt. % Pt / TS-1 shows almost double the activity towards the degradation of H₂O₂ when compared with 2.4 wt. % Au – 2.4 wt. % Pd – 0.2 wt. % Pt / TS-1 , with values of 11 and 5 % respectively.

5.3. Conclusion.

It has been shown that precious metal catalysts supported on commercial TS-1 are active for the direct synthesis of H₂O₂ from H₂ and O₂ as well as towards the ammoximation of cyclohexanone to cyclohexanone oxime. It is observed that, unlike when oxide supports are utilised no synergistic effect is observed between Au and Pd for the direct synthesis of H₂O₂. Indeed H₂O₂ synthesis rate is observed to correlate with Pd loading, with the greatest activity observed for the 5 wt. % Pd / TS-1 catalysts (116 mol_{H₂O₂}kg_{cat}⁻¹h⁻¹).

Both monometallic Au, Pd and Pt catalysts have been shown to be active towards the ammoximation of cyclohexanone, with 5 wt. % Pd / TS-1 seen to offer the greatest selectivity towards cyclohexanone oxime (20 %). However the overall yield is very low, as with all catalysts investigated within in this work, at 2%. The addition of Au to a Pd only catalyst in a 1:1 ratio produces a catalyst that affords greater selectivity towards cyclohexanone oxime when compared to the mono-metallic Au and Pd catalysts despite the Pd-only catalyst showing greater activity towards the direct synthesis of H₂O₂. The improved conversion allows for a slightly improved yield of cyclohexanone oxime, compared to the 5 wt. Pd / TS-1 catalyst, at 2.8%. Table 5.5 compares catalytic activity towards H₂O₂ synthesis and oxime yield.

Table 5.5. Activity of Au-Pd / TS-1 catalysts towards the direct synthesis of H₂O₂ and the ammoximation of cyclohexanone.

Catalyst	Productivity / mol _{H₂O₂} kg _{cat} ⁻¹ h ⁻¹ ^(a)	Oxime yield / % ^(b)
5 wt. % Au / TS-1		0.1
2.5 wt. % Au – 2.5 wt. % Pd / TS-1	100	2.8
5 wt. % Pd / TS-1	116	2

Reaction Conditions: ^(a)**Direct synthesis of H₂O₂:** Catalyst (0.01 g), total pressure 580 psi, H₂ / O₂ = 0.525, 1200 rpm, 30 min, 5.6 g MeOH + 2.69 g H₂O (66 wt. % MeOH), 2°C.

^(b)**Ammoximation of cyclohexanone:** Catalyst (0.05 g), cyclohexanone (0.13 g, 1.3 mmol), NH₃ (0.08 g, 28 wt %, 1.3 mmol), total pressure 580 psi, H₂ / O₂ = 0.525, 1200 rpm, 30 min, 5.6 g t-BuOH + 2.69 g H₂O (66 wt % t-BuOH), 80 °C.

Further investigation into 5 wt. % Au-Pd-Pt catalysts supported on TS-1 has shown that the addition of small amounts of Pt, while maintaining the Au : Pd ratio at 1 :1 can drastically improve catalyst activity towards the direct synthesis of H₂O₂. The effect of Pt addition on the activity of Au-Pd / TS-1 catalysts towards the direct synthesis of H₂O₂ and the ammoximation of cyclohexanone can be seen in Table 5.6.

Table 5.6. Activity of Au-Pd-Pt / TS-1 catalysts towards the direct synthesis of H₂O₂ and the ammoximation of cyclohexanone.

Catalyst	Productivity / mol _{H₂O₂} kg _{cat} ⁻¹ h ⁻¹ ^(a)	Oxime yield / % ^(b)
2.5 wt. % Au – 2.5 wt. % Pd / TS-1	100	2.
2.4 wt. % Au – 2.4 wt. % Pd / 0.2 wt. % Pt / TS-1	167	1.6
2.35 wt. % Au – 2.35 wt. % Pd / 0.3 wt. % Pt / TS-1	149	2.16
2.4 wt. % Au – 2.4 wt. % Pd / 0.44 wt. % Pt / TS-1	124	2.2
2 wt. % Au – 2 wt. % Pd / 1 wt. % Pt / TS-1	69	5.6

Reaction Conditions : ^(a)**Direct synthesis of H₂O₂:** Catalyst (0.01 g), total pressure 580 psi, H₂ / O₂ = 0.525, 1200 rpm, 30 min, 5.6 g MeOH + 2.69 g H₂O (66 wt. % MeOH), 2 °C.

^(b)**Ammoximation of cyclohexanone:** Catalyst (0.05 g), cyclohexanone (0.13 g, 1.3 mmol), NH₃ (0.08 g, 28 wt %, 1.3 mmol), total pressure 580 psi, H₂ / O₂ = 0.525, 1200 rpm, 30 min, 5.6 g t-BuOH + 2.69 g H₂O (66 wt % t-BuOH), 80 °C.

Catalyst activity is seen to increase from 100 mol_{H₂O₂}kg_{cat}⁻¹h⁻¹ for the 2.5 wt. % Au-2.5 wt. % Pd / TS-1 catalyst to 167 mol_{H₂O₂}kg_{cat}⁻¹h⁻¹ with the incorporation of 0.2 wt.% Pt, while maintaining Au : Pd ratio at 1 : 1. However despite the high activity towards H₂O₂ synthesis this catalyst offers very poor activity towards the ammoximation of cyclohexanone, in comparison to the Au-Pd analogue, with a oxime yield of 1.6 % observed for the 2.4 wt. % Au – 2.4 wt. % Pd – 0.2 wt. % Pt / TS-1 catalyst. By further increasing the Pt content to 1 wt. % it is observed that the rate of H₂O₂ synthesis decreases, while the activity towards cyclohexanone ammoximation increases. Indeed the overall yield of cyclohexanone oxime is seen to be 5.6 % for the 2 wt. % Au – 2.4 wt. % Pd – 0.2 wt. % Pt / TS-1 catalyst, much lower than the other AuPd / TS-1 and AuPdPt/ TS-1 catalysts that have lower rates of H₂O₂ synthesis.

Investigation of catalyst stability shows that under the conditions utilised active metal, in particular Pd, leaching is an issue. It has been shown previously in Chapter 4 Section 4.4 that leached Pd has no activity towards the ammoximation of cyclohexanone however catalyst stability is still considered essential. In an attempt to improve catalytic stability 5 wt. % Pd / TS-1, 2.5 wt. % Au – 2.5 wt. % Pd / TS-1 and 2 wt. % Au – 2 wt. % Pd / 1 wt. % Pt / TS-1 were calcined at elevated temperatures, as high as 800 °C.

It has been shown that loss of metal from the support can be decreased through calcination at higher temperatures, although these catalysts are less active towards H₂O₂ synthesis and the ammoximation of cyclohexanone. Investigation by XPS, XRD, TEM and STEM-EDX indicates the development of larger metal nanoparticles as calcination temperature increases. This is suggested to partly contribute to the decrease in catalyst activity towards the synthesis of H₂O₂ and in turn formation of cyclohexanone oxime.

Interestingly as calcination temperature increases the Au : Pd ratio for both the 2.5 wt. % Au – 2.5 wt. % Pd / TS-1 and 2 wt.% Au – 2 wt. % Pd – 1wt. % Pt / TS-1 catalysts decreases drastically. When analysis by XRD is also taken in to consideration it is possible to suggest that the migration of Au to the surface of the alloyed metal nanoparticles may also contribute to a loss in catalytic activity towards H₂O₂ formation and cyclohexanone ammoximation.

Furthermore, it has been shown that subjecting the TS-1 support to such extreme calcination temperatures can significantly reduce its crystallinity, with the greatest loss observed for the 2 wt. % Au – 2 wt. % Pd – 1 wt. % Pt / TS-1 catalyst, with a decrease in crystallinity of 66% observed when this catalyst is calcined at 800 °C. Further investigation by XRD shows the development of the TiO₂ rutile phase as calcination temperature increases, while XPS investigation of the support shows that the calcination at 800 °C leads to a significant decrease in the Si : Ti ratio, which may explain the loss in crystallinity of the support.

5.4. References.

1. V. R. Choudhary, C. Samanta and A. G. Gaikwad, *Chem. Commun.*, 2004, **10**, 2054-2055.
2. Y.-F. Han and J. H. Lunsford, *J. Catal.*, 2005, **230**, 313-316.
3. J. Lunsford, *J. Catal.*, 2003, **216**, 455-460.
4. J. K. Edwards, A. Thomas, B. E. Solsona, P. Landon, A. F. Carley and G. J. Hutchings, *Catal. Today*, 2007, **122**, 397-402.
5. J. K. Edwards, A. F. Carley, A. A. Herzing, C. J. Kiely and G. J. Hutchings, *Faraday Discuss*, 2008, **138**, 225.
6. J. K. Edwards and G. J. Hutchings, *Angew. Chem. Int. Ed.*, 2008, **47**, 9192-9198.
7. J. Edwards, B. Solsona, P. Landon, A. Carley, A. Herzing, C. Kiely and G. Hutchings, *J. Catal.* 2005, **236**, 69-79.
8. J. K. Edwards, B. Solsona, E. N. N, A. F. Carley, A. A. Herzing, C. J. Kiely and G. J. Hutchings, *Science*, 2009, **323**, 1037-1041.
9. J. K. Edwards, A. Thomas, A. F. Carley, A. A. Herzing, C. J. Kiely and G. J. Hutchings, *Green Chem.*, 2008, **10**, 388.
10. B. E. Solsona, J. K. Edwards, P. Landon, A. F. Carley, A. Herzing, C. J. Kiely and G. J. Hutchings, *Chem. Mater*, 2006, **18**, 2689-2695.
11. J. K. Edwards and G. J. Hutchings, *Angew. Chem. Int. Ed*, 2008, **47**, 9192-9198.
12. M. Sankar, Q. He, M. Morad, J. Pritchard, S. J. Freakley, J. K. Edwards, S. H. Taylor, D. J. Morgan, A. F. Carley, D. W. Knight, C. J. Kiely and G. J. Hutchings, *ACS Nano*, 2012, **6**, 6600-6613.
13. J. K. Edwards, J. Pritchard, P. J. Miedziak, M. Piccinini, A. F. Carley, Q. He, C. J. Kiely and G. J. Hutchings, *Catal. Sci. Technol* 2014, **4**, 3244-3250.
14. G. Bernardotto, F. Menegazzo, F. Pinna, M. Signoretto, G. Cruciani and G. Strukul, *Appl. Catal. A. Gen*, 2009, **358**, 129-135.
15. R. Meiers and W. F. Hölderich, *Catal. Lett*, **59**, 1999, 161-163.
16. X. Wang, Y. Nie, J. L. C. Lee and S. Jaenicke, *Appl. Catal. A Gen*. 2007, **317**, 258-265.
17. A. Cesana, M. A. Mantegazza and M. Pastori, *J. Mol. Catal. A. Chem.*, 1997, **117**, 367-373.

Appendix 5.1

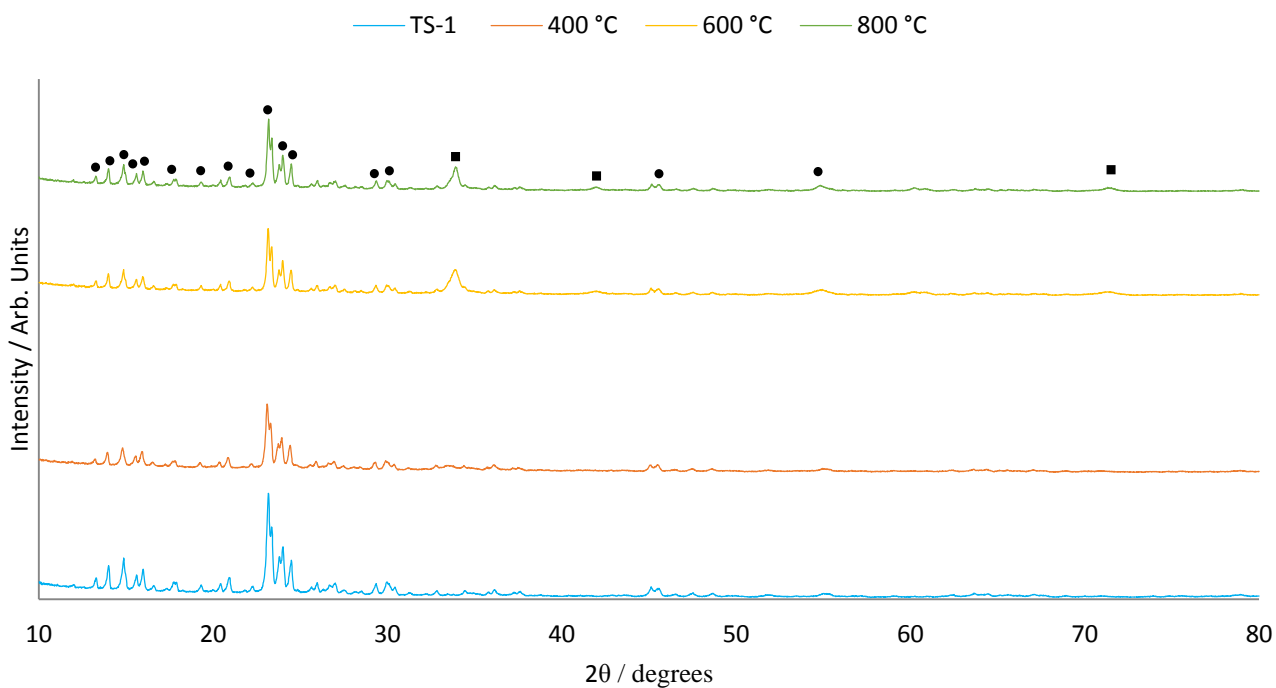


Figure A1. X-ray diffractograms of 5 wt. % Pd / TS-1 prepared by wet impregnation calcined at various temperatures (400 – 800 °C), 3 h, static air, ramp rate = 20 °C min⁻¹. ●: TS-1 ; ■: PdO

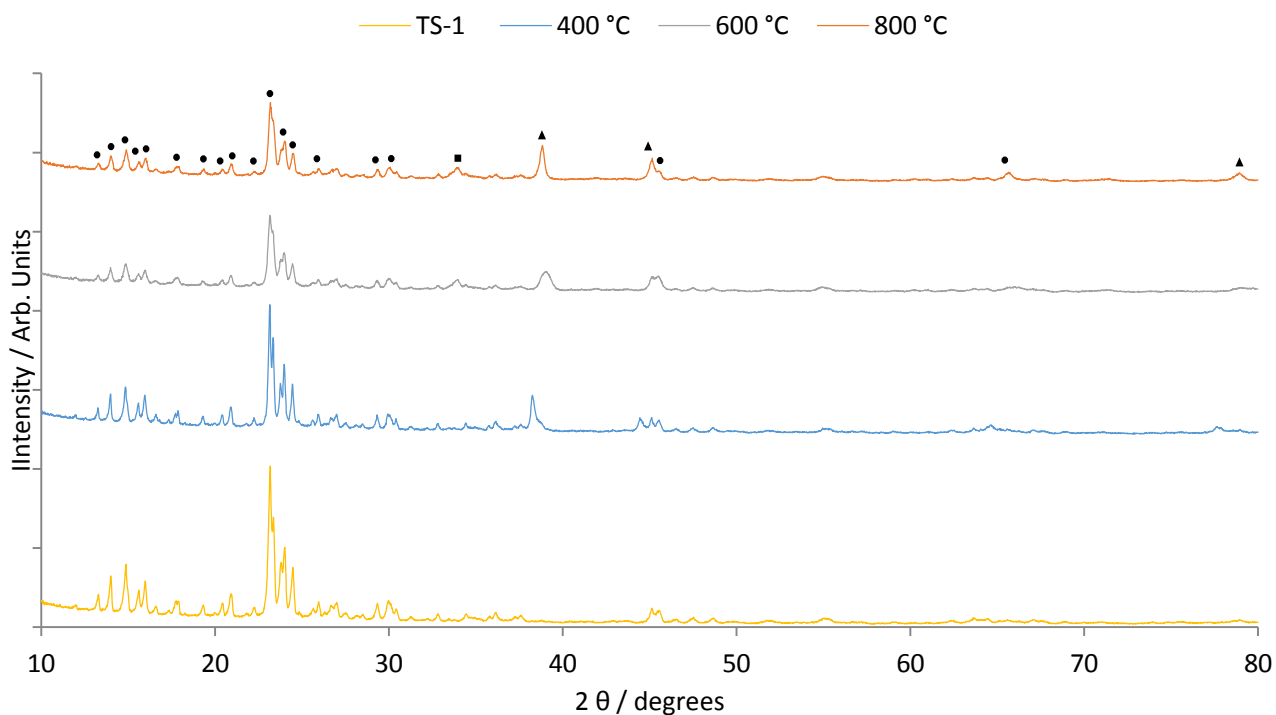


Figure A2. X-ray diffractograms of 2.5 wt. % Au- 2.5 wt. % Pd / TS-1 prepared by wet impregnation, calcined at various temperatures (400 – 800 °C), 3h, static air, ramp rate = 20 °C min⁻¹. ●: TS-1; ▲: Au; ■: PdO

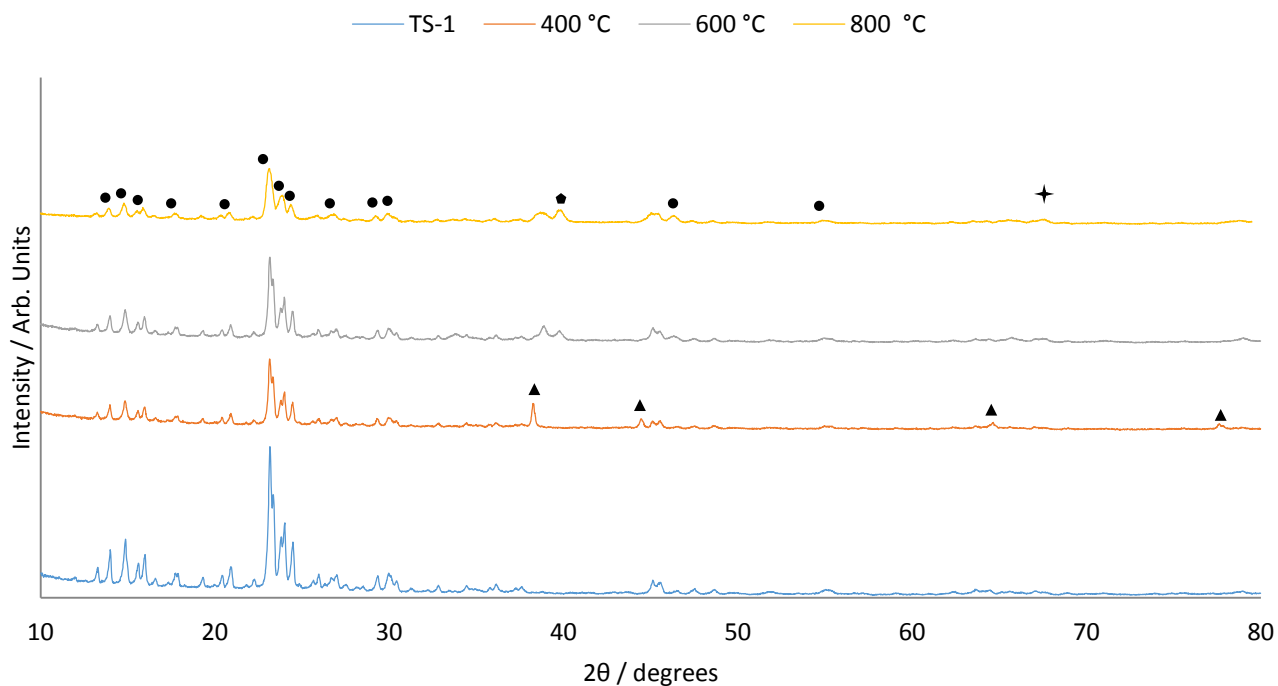


Figure A3. X-ray diffractograms of 2 wt. % Au- 2 wt. % Pd – 1 wt. % Pt / TS-1 prepared by wet impregnation, calcined at various temperatures (400 – 800 °C) 3 h, static air, ramp rate = 20 °C min⁻¹. ●: TS-1; ▲: Au; † Pt

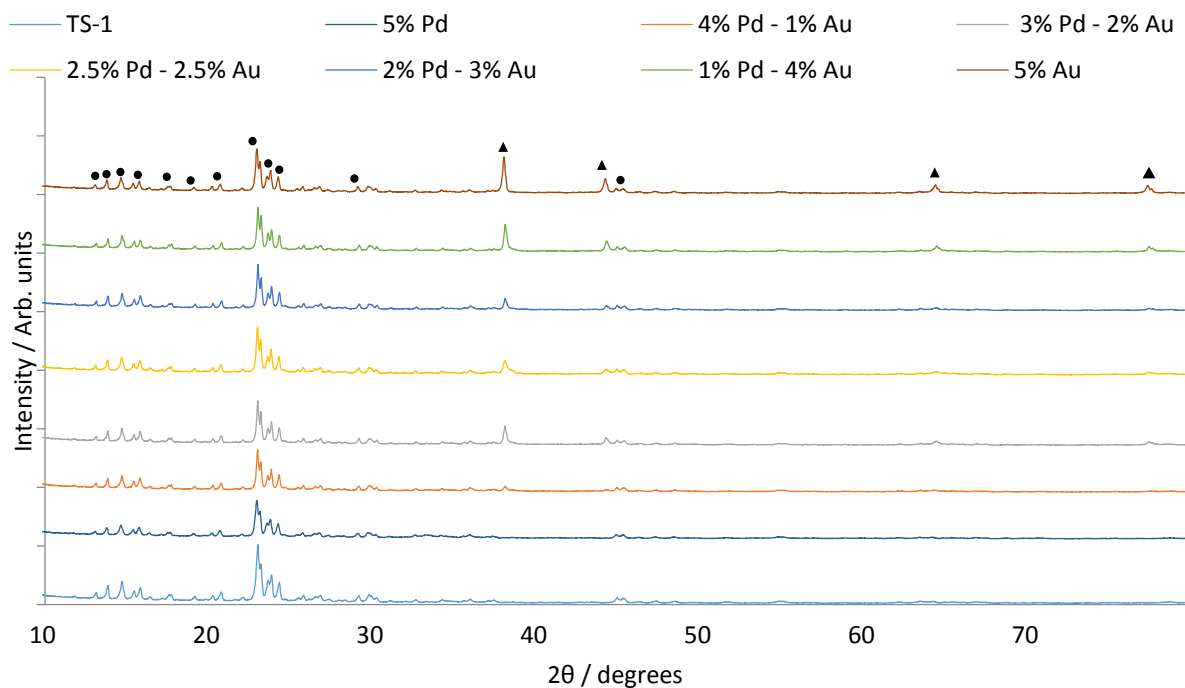


Figure A4. X-ray diffractograms of 2.5 wt. % Au- 2.5 wt. % Pd / TS-1 prepared by wet impregnation calcined at 400 °C, 3 h, static air, ramp rate = 20 °C min⁻¹. ●: TS-1; ▲: Au.

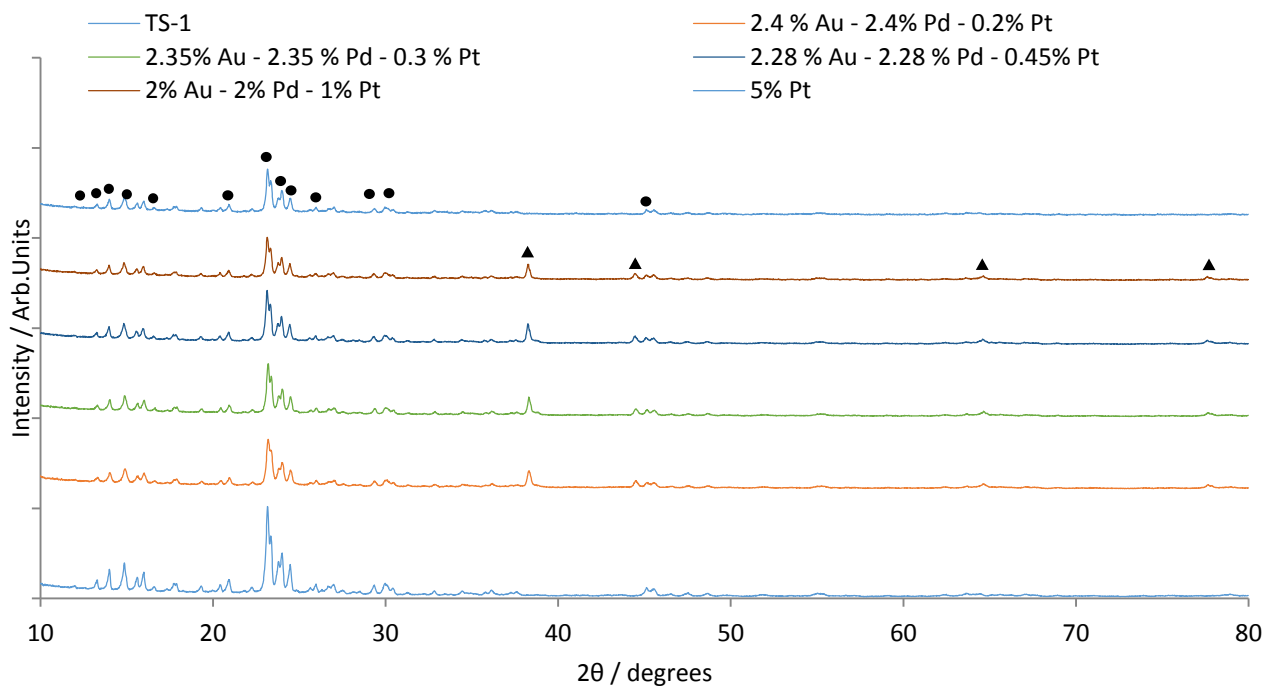


Figure A5. X-ray diffractogram of 5 wt. % Au-Pd-Pt / TS-1 and 5 wt.% Pt / TS-1 prepared by wet impregnation, calcined 400 °C in static air, ramp rate = 20 °C min⁻¹. ●: TS-1; ▲: Au.

Appendix 5.2.

Table A.1. Phase Identification of 5 wt. % Pd, AuPd and AuPdPt / TS-1 calcined at various temperatures (400 – 800 °C).

Catalyst	Calcination temperature / °C	Phase / %				
		TS-1	TiO ₂	PdO	Au	Pt
5 % Pd	400	98	2	-	-	-
	600	96	3	1	-	-
	800	93	5	2	-	-
2.5 % Au – 2.5 % Pd	400	96	3	-	1	-
	600	93	5	1	1	-
	800	91	6	1	2	-
2% Au – 2% Pd – 1% Pt	400	96	3	-	1	-
	600	93	5	-	1	1
	800	90	6	1	2	1

All catalysts calcined X °C, 3 h, 20 °Cmin⁻¹, static air.

Appendix 5.3.

Table A.2. XPS analysis of Pd / TS-1, AuPd / TS-1 and AuPdPt / TS-1 calcined at 400 -800 °C

Catalyst	Calcination Temperature / °C	Composition / At. %								Pd : Au	Pd : Pt	Ti ⁸⁺ : Ti ⁴⁺	Si : Ti
		Pd 3d	Au 4f	Pt 4f	Cl 2p	O 1s	Si 2p	Ti 2p	C 1s				
Pd	400	1.14	-	-	0.75	61.62	34.3	0.33	1.86	-	-	1.49	103.9
	600	1.57	-	-	0.18	61.52	33.36	0.33	3.03	-	-	1.45	101.1
	800	1.01	-	-	-	61.52	34.27	0.43	2.06	-	-	1.95	79.7
AuPd	400	0.4	0.01	-	-	63.2	35.22	0.45	1.54	40	-	2.22	78.3
	600	0.21	0.03	-	-	62.52	35.32	0.54	1.39	7	-	2.25	65.4
	800	0.13	0.05	-	-	62.35	35.4	0.49	1.58	2.6	-	1.95	72.2
AuPdPt	400	0.28	-	0.27	0.57	59.08	103.79	0.37	0	0	1	1.5	88.2
	600	0.19	0.03	0.05	1.37	62.66	103.89	0.41	6.3	6.3	3.8	2.2	86.1
	800	0.12	0.07	0.03	-	62.92	103.65	0.54	1.7	1.7	4	1.2	65.3

All catalysts calcined X °C, 3 h, 20 °Cmin⁻¹, static air.

Table A.3. XPS analysis of AuPdPt / TS-1 catalysts.

Catalyst	Composition / At. %								Pd: Au	Pd : Pt	Ti ⁸ : Ti ⁴	Si : Ti
	Pd 3d	Au 4f	Pt 4f	Cl 2p	O 1s	Si 2p	Ti 2p	C 1s				
2.5 wt.% Au – 2.5 wt. % Pd	0.4	0.01	-	-	63.2	35.22	0.45	1.54	7	-	2.22	78.3
2.4 wt. % Au – 2.4 wt. % -0.2 wt. % Pt	0.34	0.01	0.01	0.34	59.31	36.11	0.45	3.44	34	34	1.33	80.24
2.35 wt. % Au – 2.35 wt. % -0.3 wt. % Pt	0.33	0.01	0.01	0.3	60.13	36.04	0.48	2.79	33	33	1.22	75.08
2.28 wt. % Au – 2.28 wt. % -0.44 wt. % Pt	0.32	0.01	0.01	0.26	59.05	35.34	0.42	4.62	33	32	1.22	84.14
2 wt. % Au – 2 wt. % Pd – 1 wt. % Pt	0.28	-	0.27	0.57	59.08	103.79	0.37	0	0	1	1.5	88.2

All catalysts calcined 400 °C, 3 h, 20 °Cmin⁻¹, static air.

6. Conclusion and Future Work.

6.1 .Conclusion.

As outlined in Chapter 1 the current, industrial, process for H₂O₂ formation via the anthraquinone process offers a number of advantages including H₂ selectivity. However the need to continually replace the organic solvent and the need for this process to be conducted on an industrial scale to be financially viable has led to a great deal of investigation into H₂O₂ synthesis from molecular H₂ and O₂.

The direct synthesis of H₂O₂ represents a possible alternative to the anthraquinone process, however it presents some significant challenges. In particular the subsequent degradation of H₂O₂ to H₂O via decomposition and hydrogenation, a requirement for any industrial application would of course be high selectivity towards H₂O₂, likely in excess of 95 %. The use of acidic reaction conditions^{1,2} and acidified catalysts³⁻⁵ has been shown previously to improve selectivity towards H₂O₂ via reduction or complete inhibition of the subsequent degradation reactions.

Within this work the role of catalyst design has been investigated in improving catalyst activity towards H₂O₂ synthesis (Chapter 3) through the investigation of Cs-exchanged tungstophosphoric acid, with varied Cs content, as an additive for catalysts already established for the direct synthesis of H₂O₂, in particular 2.5 wt. % Au – 2.5 wt. % Pd / TiO₂. The results presented within this chapter show some promise, with great improvement in catalytic activity towards H₂O₂ observed. It has been demonstrated that the incorporation of Cs into the Keggin unit decreases the solubility of the heteropolyacid, with the concentration of W within the reaction solution decreasing from 1834 ppm when H₃PW₁₂O₄₀ is utilised as an additive to 240 ppm when Cs₃PW₁₂O₄₀ is used. However, as W is detected regardless of Cs incorporation it is possible to conclude that it is not possible to produce a totally insoluble material through the incorporation of Cs into the Keggin unit of H₃PW₁₂O₄₀.

As with W, Cs is detected regardless of the extent of its incorporation. A general trend can be observed where Cs concentration within the reaction solution increases as to a maximum of 183 ppm for the Cs₂HPW₁₂O₄₀, further addition of Cs decreases the concentration of Cs

detected within the reaction solution, to a minimum of 95 ppm when $\text{Cs}_3\text{HPW}_{12}\text{O}_{40}$ is used in addition to 2.5 wt. % Au – 2.5 wt. % Pd / TiO_2 .

Furthermore it has been demonstrated that the use of $\text{Cs}_x\text{H}_{3-x}\text{PW}_{12}\text{O}_{40}$ as an additive for 2.5 wt. % Au – 2.5 wt. % Pd / TiO_2 results in significant leaching of Pd from the support, with leaching of up to 30 % of the total Pd loading when $\text{H}_3\text{PW}_{12}\text{O}_{40}$ is used in addition to the catalyst. This coincides with the greatest catalytic activity towards H_2O_2 synthesis with catalytic activity of $301 \text{ mol}_{\text{H}_2\text{O}_2}\text{Kg}_{\text{cat}}^{-1}\text{h}^{-1}$.

It is possible to conclude that both the 2.5 wt. % Au – 2.5 wt. % Pd / TiO_2 catalyst and $\text{Cs}_x\text{H}_{3-x}\text{PW}_{12}\text{O}_{40}$ are unstable under the reaction conditions investigated and that in particular the presence of $\text{Cs}_x\text{H}_{3-x}\text{PW}_{12}\text{O}_{40}$ promotes the leaching of Pd from the catalyst support, while no Au is detected in the reaction solution, suggesting that this metal is more stable than Pd.

Furthermore it is demonstrated that although the $\text{Cs}_x\text{H}_{3-x}\text{PW}_{12}\text{O}_{40}$ salts have no activity towards the direct synthesis of H_2O_2 they are active towards the degradation of H_2O_2 , with the activity of the $\text{Cs}_x\text{H}_{3-x}\text{PW}_{12}\text{O}_{40}$ salt towards H_2O_2 degradation correlating with Cs content. It is observed that the activity of the $\text{H}_3\text{PW}_{12}\text{O}_{40}$ parent material is $35 \text{ mol}_{\text{H}_2\text{O}_2}\text{Kg}_{\text{cat}}^{-1}\text{h}^{-1}$ while that of $\text{Cs}_3\text{HPW}_{12}\text{O}_{40}$ is $213 \text{ mol}_{\text{H}_2\text{O}_2}\text{Kg}_{\text{cat}}^{-1}\text{h}^{-1}$ and this increase can be related, in part, to the amount of Cs leached from the $\text{Cs}_x\text{H}_{3-x}\text{PW}_{12}\text{O}_{40}$ salt.

From investigation of the reusability of a physical mixture of 2.5 wt. % Au – 2.5 wt. % Pd / TiO_2 and $\text{Cs}_x\text{H}_{3-x}\text{PW}_{12}\text{O}_{40}$ it is possible to conclude that only when the value of x in $\text{Cs}_x\text{H}_{3-x}\text{PW}_{12}\text{O}_{40}$ is equal to 2.5 is the catalyst reusable. With a catalyst activity of $188 \text{ mol}_{\text{H}_2\text{O}_2}\text{Kg}_{\text{cat}}^{-1}\text{h}^{-1}$ retained over two uses. However it has also been shown that Pd, Cs and W are all detected in the reaction solution post reaction and as such catalyst stability is a concern.

Finally comparison between catalytic activity towards H_2O_2 synthesis when either HNO_3 , H_2WO_3 or $\text{Cs}_x\text{H}_{3-x}\text{PW}_{12}\text{O}_{40}$ salts are used in addition to 2.5 wt. % Au – 2.5 wt. % Pd / TiO_2 suggests that the decrease in the reaction solution pH is not the only reason for improved H_2O_2 synthesis activity. It is suggested that the presence of phosphate ions within the reaction solution improves H_2O_2 stability and is responsible for the observed increase in catalytic activity towards H_2O_2 . It is observed that as Cs incorporation decreases so does the stability of the $\text{Cs}_x\text{H}_{3-x}\text{PW}_{12}\text{O}_{40}$ salt and it is proposed that this results in an increase in the availability of PO_4^{3-} ions and improved H_2O_2 stability.

It has been shown previously that the utilisation of exchanged tungstophosphoric acid as a support for metals active towards the synthesis of H₂O₂ produces highly active catalysts^{6,7}. In particular activity is considered to be relatively high when using conditions considered to be detrimental to H₂O₂ synthesis, *i.e.* elevated temperatures and H₂O only solvents^{8,9}. However both of these conditions are likely to be favoured by any industrial application due to the reduction in costs associated with ambient temperatures and a H₂O only solvent. The future investigation of supported Au-Pd catalysts in addition to Cs-exchanged heteropolyacids under these harsh conditions may make the direct synthesis of H₂O₂ considerably more attractive. Although it is suggested that the low stability of Cs_xH_{3-x}PW₁₂O₄₀ salts limit its application in any future use in the direct synthesis process in the liquid phase.

Chapters 4 and 5 investigate the ammoximation of cyclohexanone to cyclohexanone oxime via the in-situ synthesis of H₂O₂. As discussed previously the economic requirement of large scale H₂O₂ synthesis ensures that costs for the ammoximation and other subsequent reactions that utilise H₂O₂ as an oxidant can be particularly high and variable, both of these factors are clearly unattractive to industrial use. An attractive alternative to the current process, where preformed H₂O₂ is added to the reaction mixture would be the *in-situ* synthesis of H₂O₂ and ammoximation of cyclohexanone in a one-pot synthesis process.

Chapter 4 investigates the ability of monometallic Au, Pd and bimetallic Au-Pd catalysts supported on TS-1 to catalyse the formation of H₂O₂ from H₂ and O₂. The results are summarised in Table 6.1.

Table 6.1. The activity of TS-1 supported Au-, Pd- and Au-Pd catalysts towards the direct synthesis of H₂O₂.

Catalyst	Temperature / °C	Solvent	Productivity / mol _{H₂O₂} kg _{cat} ⁻¹ h ⁻¹
5 wt. % Au /TS-1 ^(a)	2	H ₂ O / MeOH	2
2.5 wt. % Au – 2.5 wt. % Pd /TS-1 ^(a)	2	H ₂ O / MeOH	100
5 wt. % Pd/TS-1 ^(a)	2	H ₂ O / MeOH	116
5 wt. % Pd/ TS-1 ^(a)	30	H ₂ O / MeOH	26
5 wt. % Pd /TS-1 ^(b)	30	H ₂ O / t-BuOH	60
5 wt. % Pd /TS-1 ^(b)	50	H ₂ O / t-BuOH	12
5 wt. % Pd / TS-1 ^(b)	80	H ₂ O / t-BuOH	7

Reaction conditions: ^(a) Catalyst (0.01 g), 580 psi, H₂ / O₂ = 0.525, 1200 rpm, 30 min, 5.6 g MeOH + 2.9 g H₂O (66 wt. % CH₃OH), X °C. ^(b) Catalyst (0.01 g), 580 psi, H₂ / O₂ = 0.525, 1200 rpm, 30 min, 5.6 g t-BuOH + 2.9 g H₂O (66 wt. % CH₃OH), X °C.

Firstly it is observed that no synergistic effect is observed between Au and Pd when using TS-1 as a support in a manner that has been reported by Hutchings and co-workers when using a variety of oxide supports including; TiO_2 ¹⁰ and SiO_2 ¹¹. Indeed the productivity of the 5 wt. % Pd / TS-1 catalyst is seen to be $116 \text{ mol}_{\text{H}_2\text{O}_2} \text{ kg}_{\text{cat}}^{-1} \text{ h}^{-1}$, while the productivity of the 2.5 wt. % Au – 2.5 wt. % Pd / TS-1 catalyst is $100 \text{ mol}_{\text{H}_2\text{O}_2} \text{ kg}_{\text{cat}}^{-1} \text{ h}^{-1}$, when using a water/MeOH solvent at 2 °C. The activity of both the Pd / TS-1 and Au-Pd / TS-1 catalysts are comparable to that reported by Hutchings and co-workers for the 2.5 wt. % Au – 2.5 wt. % Pd / carbon catalyst ($110 \text{ mol}_{\text{H}_2\text{O}_2} \text{ kg}_{\text{cat}}^{-1} \text{ h}^{-1}$), under comparable reduction conditions. It is possible to conclude that using TS-1 as a support for Au and Pd results in catalysts that have significant activity towards the direct synthesis of H_2O_2 , under conditions optimised for this process.

It is further demonstrated that the use of a t-BuOH – water solvent offers greater rates of H_2O_2 synthesis than MeOH – water at elevated reaction temperatures, with the activity of the 5 wt. % Pd / TS-1 catalyst observed to be 26 and 60 $\text{mol}_{\text{H}_2\text{O}_2} \text{ kg}_{\text{cat}}^{-1} \text{ h}^{-1}$ when MeOH – water and t-BuOH – water is used as the solvent at 30 °C. This is ascribed to increased H_2 solubility in t-BuOH in comparison to MeOH. The application of a t-BuOH-water solvent system may warrant further investigation for its use in the direct synthesis of H_2O_2 from H_2 and O_2 .

Chapter 4 further outlines the feasibility of the ammoximation of cyclohexanone via *in-situ* generation of H_2O_2 using 5 wt. % Pd / TS-1 and investigates the role that the reaction conditions can play in improving both oxime yield and catalyst stability. It is demonstrated that there is some activity towards the ammoximation of cyclohexanone via *in-situ* H_2O_2 synthesis is observed when utilising a 5 wt. % Pd / TS-1 catalyst. Table 6.2 summarises how the optimisation of reaction conditions can improve cyclohexanone oxime yield when utilising 5 wt. % Pd / TS-1, with the optimal reaction conditions highlighted in bold. Although optimal conditions have been established the effect of their combination on catalyst selectivity and cyclohexanone conversion have not been established. It is suggested that future work investigate the combination of the optimal reaction conditions in an attempt to improve the yield of cyclohexanone oxime.

Table 6.2. The effect of optimal reaction conditions on cyclohexanone oxime yield.

Temperature / °C	H ₂ :O ₂	Catalyst Mass / g	H ₂ O : t- BuOH	[Cyclohexanone] / mmol	[NH ₃] / mmol	Time / min	Stirring Speed / rpm	Total Pressure / psi	Oxime Yield / %
120	0.525	0.05	0.5	1.3	1.3	90	1200	580	10
80	1	0.05	0.5	1.3	1.3	90	1200	580	7
80	0.525	0.2	0.5	1.3	1.3	90	1200	580	17
80	0.525	0.05	0.5	1.3	1.3	90	1200	580	4
80	0.525	0.05	0.5	0.65	1.3	90	1200	580	8
80	0.525	0.05	0.5	1.3	1.3	90	800	580	5

It has been shown that catalyst stability is an issue, in particular the presence of cyclohexanone, NH₃ and a water containing solvent has been shown to result in the leaching of Pd from the support. Investigation into the activity of leached Pd towards the ammoximation of cyclohexanone in the presence of TS-1 is observed to result in no additional formation of cyclohexanone oxime. It is suggested that the elevated temperatures and presence of basic reaction conditions, that is the presence of NH₃, ensures that any H₂O₂ synthesised is unable to diffuse to the Ti(IV) sites present on the TS-1 support to be involved in the formation of hydroxylamine. However catalyst stability is of great concern and it is suggested that future work investigate methods of stabilising TS-1 supported catalysts.

Chapter 5 investigates catalyst design for the generation of H₂O₂ *in-situ* and the subsequent ammoximation process. It is observed that the addition of Au to a Pd only catalyst in a 1 : 1 ratio does not result in an improvement in catalytic activity towards H₂O₂ synthesis, that is no synergistic effect is observed between the two metals, as reported when utilising a number of other common supports¹¹. Table 6.3 compares the catalytic activity of Au-Pd catalysts supported on TS-1 towards the direct synthesis of H₂O₂ and the ammoximation of cyclohexanone.

Table 6.3. Activity of Au-Pd / TS-1 catalysts towards the direct synthesis of H₂O₂ and the ammoximation of cyclohexanone.

Catalyst	Productivity / mol _{H₂O₂} kg _{cat} ⁻¹ h ⁻¹ (<i>a</i>)	Oxime yield / % (<i>b</i>)
5 wt. % Au / TS-1	2	0.1
2.5 wt. % Au – 2.5 wt. % Pd / TS-1	100	2.8
5 wt. % Pd / TS-1	116	2

Reaction Conditions: (*a*) **Direct synthesis of H₂O₂**: Catalyst (0.01 g), total pressure 580 psi, H₂ / O₂ = 0.525, 1200 rpm, 30 min, 5.6 g MeOH + 2.69 g H₂O (66 wt. % MeOH), 2°C.

(*b*) **Ammoximation of cyclohexanone**: Catalyst (0.05 g), cyclohexanone (0.13 g, 1.3 mmol), NH₃ (0.08 g, 28 wt %, 1.3 mmol), total pressure 580 psi, H₂ / O₂ = 0.525, 1200 rpm, 30 min, 5.6 g t-BuOH + 2.69 g H₂O (66 wt % t-BuOH), 80 °C.

It is observed that the greatest yield of cyclohexanone oxime is achieved utilising a 2.5 wt. % Au – 2.5 wt. % Pd / TS-1 catalyst, despite the greater activity of the 5 wt. % Pd / TS-1 catalyst towards the direct synthesis of H₂O₂. It is suggested that by lowering the rate of H₂O₂ synthesis it becomes similar to the rate of hydroxylamine formation and as such H₂O₂ is utilised more selectively, in the formation of cyclohexanone oxime, rather than in the formation of H₂O.

Further investigation into TS-1 Au-Pd-Pt supported catalysts has shown that it is possible to improve the rate of H₂O₂ synthesis through the introduction of small amount of Pt, while maintaining the Au : Pd ratio at 1 : 1. The results of Pt incorporation into a Au-Pd / TS-1

catalyst on catalytic activity towards the direct synthesis of H₂O₂ and the ammoximation of cyclohexanone is summarised in Table 6.4.

Table 6.4. Activity of Au-Pd-Pt / TS-1 catalysts towards the direct synthesis of H₂O₂ and the ammoximation of cyclohexanone.

Catalyst	Productivity / mol _{H₂O₂} kg _{cat} ⁻¹ h ⁻¹ (<i>a</i>)	Oxime yield / % (<i>b</i>)
2.5 wt. % Au – 2.5 wt. % Pd / TS-1	100	2.8
2.4 wt. % Au – 2.4 wt. % Pd / 0.2 wt. % Pt / TS-1	167	1.6
2.35 wt. % Au – 2.35 wt. % Pd / 0.3 wt. % Pt / TS-1	149	2.16
2.4 wt. % Au – 2.4 wt. % Pd / 0.44 wt. % Pt / TS-1	124	2.2
2 wt. % Au – 2 wt. % Pd / 1 wt. % Pt / TS-1	69	5.6

Reaction Conditions: (*a*) **Direct synthesis of H₂O₂**: Catalyst (0.01 g), total pressure 580 psi, H₂ / O₂ = 0.525, 1200 rpm, 30 min, 5.6 g MeOH + 2.69 g H₂O (66 wt. % MeOH), 2°C.

(*b*) **Ammoximation of cyclohexanone**: Catalyst (0.05 g), cyclohexanone (0.13 g, 1.3 mmol), NH₃ (0.08 g, 28 wt %, 1.3 mmol), total pressure 580 psi, H₂ / O₂ = 0.525, 1200 rpm, 30 min, 5.6 g t-BuOH + 2.69 g H₂O (66 wt % t-BuOH), 80 °C.

It can be seen that the incorporation of 0.2 wt% Pt can dramatically improve catalytic activity towards H₂O₂ synthesis, from 100 mol_{H₂O₂}kg_{cat}⁻¹h⁻¹ for the 2.5 wt. % Au – 2.5 wt. % Pd / TS-1 catalyst to 167 mol_{H₂O₂}kg_{cat}⁻¹h⁻¹ for the 2.4 wt. % Au – 2.4 wt. % Pd / 0.2 wt. % Pt / TS-1 catalyst. However the oxime yield decreases from 2.8 % to 1.6 % upon the incorporation of 0.2 wt. % Pt. Further incorporation of Pt decreases the catalytic activity towards H₂O₂ synthesis, while cyclohexanone oxime yield increases, to a maximum of 5.6 % for the 2 wt. % Au – 2 wt. % Pd / 1 wt. % Pt / TS-1 catalyst. It is suggested that, as shown previously with the 2.5 wt. % Au – 2.5 wt. % Pd / TS-1 catalyst, by lowering the rate of H₂O₂ synthesis it is possible to ensure that H₂O₂ is utilised more selectively and not degraded, either catalytically or by the reaction conditions to H₂O and as such oxime yield is improved.

Investigation into the use of elevated calcination temperatures to improve catalyst stability has shown that it is possible to reduce the leaching of metals, in particular Pd, from the TS-1 support. However exposure to such elevated temperatures leads to the sintering of the metal nanoparticles and a resultant decrease in catalytic activity towards H₂O₂ synthesis and cyclohexanone ammoximation. Table 6.5 shows the effect of calcination temperature on catalytic activity towards H₂O₂ synthesis and cyclohexanone ammoximation.

Table 6.5. The effect of calcination temperature on catalytic activity towards the direct synthesis of H₂O₂ and the ammoximation of cyclohexanone.

Catalyst	Calcination temperature / °C	Productivity / mol _{H₂O₂} kg _{cat} ⁻¹ h ⁻¹ ^(a)	Oxime yield / % ^(b)
5 wt. % Pd / TS-1	400	116	2.8
	600	25	0.72
	800	10	0
2.5 wt. % Au – 2.5 wt. % Pd / TS-1	400	100	2.8
	600	35	0.6
	800	30	0.2
2 wt. % Au – 2 wt. % Pd / 1 wt. % Pt / TS-1	400	69	5.59
	600	54	2.5
	800	42	1.6

Reaction Conditions: ^(a)**Direct synthesis of H₂O₂:** Catalyst (0.01 g), total pressure 580 psi, H₂ / O₂ = 0.525, 1200 rpm, 30 min, 5.6 g MeOH + 2.69 g H₂O (66 wt. % MeOH), 2°C.

^(b)**Ammoximation of cyclohexanone:** Catalyst (0.05 g), cyclohexanone (0.13 g, 1.3 mmol), NH₃ (0.08 g, 28 wt %, 1.3 mmol), total pressure 580 psi, H₂ / O₂ = 0.525, 1200 rpm, 30 min, 5.6 g t-BuOH + 2.69 g H₂O (66 wt % t-BuOH), 80 °C.

It is observed that increasing calcination temperature results in a decrease in activity towards both H₂O₂ synthesis and cyclohexanone ammoximation, regardless of catalyst composition. However it is also observed that the incorporation of Au into a Pd-only catalyst and Pt into a Au-Pd catalyst is able to offset the deleterious effect of calcination temperature on catalyst activity. Investigation by XRD shows that the incorporation of Au into a mono-metallic Pd catalyst, so that the ratio of Au : Pd is 1 : 1, is able to decrease the development of large Pd nanoparticles and a more pronounced effect is observed when Pt is introduced into a Au-Pd / TS-1 catalyst in Au : Pd : Pt ratio of 1 : 1 : 0.5. It is suggested that small Pd nanoparticles provide greater activity towards H₂O₂ synthesis and as such by limiting the agglomeration of Pd it is possible to ensure some catalytic activity is retained.

In conclusion the utilisation of many metals active for the direct synthesis of H₂O₂ supported on a commercial TS-1 support has led to improvement to the ammoximation reaction and it is suggested that through further catalyst design and process optimisation it may be possible for the ammoximation of cyclohexanone to cyclohexanone oxime via *in-situ* H₂O₂ generation to present an alternative to the current industrial process.

6.2. Future Work.

A great deal of work published in the literature prior to and during this thesis has concerned improving catalytic selectivity towards H_2O_2 , through the partial or complete inhibition of H_2O_2 degradation pathways^{3 12} (hydrogenation and decomposition). In all three chapters reported within this thesis it is recommended that further work concentrates on improving catalyst selectivity, particularly through catalyst design.

6.2.1 Improved use of metal.

By increasing the dispersion of metals active for the direct synthesis of H_2O_2 it may be possible to produce a cheaper catalyst, with lower total metal loading. It has previously been shown that metal dispersion can be improved by the use of HCl during catalyst preparation¹³. Sankar *et.al.* have reported that the particle size distribution (PSD) for a Au-Pd / TiO_2 catalyst prepared by conventional impregnation, the method used for catalyst preparation throughout this thesis, ranges from 10 nm to sub 1 nm with the mean particle size reported as 4.7 nm¹³. Despite this work focusing on the use of TiO_2 as a support it is reasonable to assume that the PSD for the catalysts utilising a TS-1 support, such as those investigated in Chapters 4 and 5 would be similar.

Investigation of other catalyst preparation techniques that allow for better control over particle size such as; modified impregnation, sol-immobilisation and deposition precipitation may show some promise in improving catalytic activity towards H_2O_2 synthesis as well as the ammoximation of cyclohexanone. By improving the dispersion of metals active for the direct synthesis of H_2O_2 it may be possible to ensure that a greater proportion of the Ti (IV) sites present in the TS-1 support are available to produce hydroxylamine. It is suggested that by increasing dispersion of metals the diffusion path of H_2O_2 from the metal nanoparticles to Ti (IV) sites is reduced.

It would also be of interest to determine how H_2O_2 degradation, as well as H_2O_2 synthesis, is altered by lowering the total metal loading of the catalysts studied within Chapter 3, in particular the 5 % Au- Pd / TiO_2 catalyst.

6.2.2. Catalyst Stability.

The stability of catalysts for the ammoximation of cyclohexanone has been observed to be an issue, with leaching of Pd in particular observed to be of greatest concern. Further

investigation into methods to produce a stable catalyst is of the utmost concern although this issue may need a combination of catalyst and process design to overcome. It is suggested that by utilising a catalyst preparation technique that leads to a smaller mean particle size, such as modified impregnation and then exposing these catalyst to greater calcination temperatures it may be possible to retain a greater catalyst activity towards both the direct synthesis of H₂O₂ and the ammoximation of cyclohexanone, in comparison to catalysts prepared by conventional impregnation, as well as improving catalyst stability.

The stability of the TS-1 support must also be determined as both the support and metals supported on it are key for the overall process and a greater understanding of both of these phases will be important for future development.

In comparison the activity to H₂O₂ synthesis of Au-Pd catalysts prepared on TiO₂ have been observed to be stable over two uses when Cs_{2.5}H_{0.5}PW₁₂O₄₀ is utilised as an additive, despite the loss of Pd from the support. However, for any large scale use catalyst stability must be investigated over an extended reaction time and utilising a system more akin to that which will be used upon scale up of the process, be that a flow or slurry type reactor for example. Possibly a flow style reactor will allow for greater control of the reaction conditions, in particular flow rates of solvent over the catalyst and allow for on stream analysis of catalyst stability through the continual sampling of reaction solution and analysis of leached metal content. However, it is suggested that catalytic activity be monitored over multiple uses in a batch reactor to provide information on catalyst stability.

6.2.3. Catalyst synthesis technique.

The catalysts studied within this thesis are synthesised using a standard wet impregnation technique, as outlined in Chapter 2. However a variety of catalyst preparation techniques have been reported to produce catalysts active for the direct synthesis of H₂O₂, including modified impregnation¹³, sol-immobilisation¹⁴ and physical grinding¹⁵. Although investigation of catalyst preparation should not be limited to these techniques it is recommended that they represent a good place to begin initial research. Principally into producing catalysts for the ammoximation of cyclohexanone via *in-situ* H₂O₂ formation. It is suggested that the use of the modified impregnation technique to produce catalysts for the ammoximation of cyclohexanone may show some promise. Particularly if exposure to increased calcination temperatures is required to improve catalyst stability, as with the catalysts investigated within Chapter 5. Modified impregnation is known to produce a

catalysts with a narrow particle size distribution and a smaller mean particle size than conventional wet impregnation. By producing a greater population of smaller metal nanoparticles it is possible that a greater metal dispersion may be retained as catalysts are exposed to increased calcination temperatures and as such greater catalyst activity is preserved.

6.2.4. The use of cheaper metals.

The replacement of Au with Sn has been studied by Hutchings and co-workers¹² for the direct synthesis of H₂O₂ and is briefly touched upon within this thesis. In particular the ability of Cs-exchanged tungstophosphoric acid to promote a Pd-Sn / TiO₂ catalyst for H₂O₂ synthesis. Further investigation of these systems utilising exchanged heteropolyacids and non-precious metal containing catalysts would be of great interest. It is known that the by optimising both the Pd : Sn ratio and heat treatment cycle applied it is possible to produce a catalyst which is totally selective towards H₂O₂, that is there is no activity towards the degradation of H₂O₂. In this way it is possible to limit the degradation of H₂O₂ to that observed for the heteropolyacid only. It is suggested that future work investigate the activity of a catalyst that is totally selective towards H₂O₂ when used in utilisation with H₃PW₁₂O₄₀ and its Cs-exchanged salts.

While for the '*in-situ*' ammoximation reaction only precious metals (Au, Pd and Pt) were studied. However the use of cheaper base metals as replacements for one or more of the precious metals may be of great interest to any industrial application particularly if catalyst activity can be retained.

6.2.5. Particle composition.

It is known that when Au-Pd catalysts are prepared by impregnation, on a range of oxide supports it is possible to form Au-Pd alloyed nanoparticles with a bimodal distribution of particle size. The morphology of these Au-Pd particles have been observed to often exhibit a core-shell structure, with a Pd-rich shell and Au-rich core.¹⁶⁻¹⁸ Often the smaller particles are found to be Pd rich and the larger ones Au rich. It has been shown that when supported on TiO₂ the addition of Pt to Au-Pd results in a significant narrowing of the particle size distribution¹⁹. It would be of great interest to determine if this effect is also observed when catalysts are prepared on TS-1. In addition to this it would be of interest to truly determine whether or not alloying between Au and Pd is observed in these bi-metallic catalysts is

responsible for the improvement in catalytic activity towards cyclohexanone oxime formation, or if there is another means by which improvement occurs. Furthermore it has been suggested that the role of Pt is to enhance the surface Pd : Au ratio when utilising CeO₂ as a support for these Au-Pd-Pt catalysts²⁰. A similar improvement is observed for the AuPdPt / TS-1 catalysts however it is unclear if the increase in Pd : Au surface ratio is due to an enhancement of Au-core Pd-shell morphology or simply due to improved dispersion of the metal. It is suggested further work be conducted to determine the role Pt plays in promoting catalytic activity when using TS-1 as a support.

6.2.6. Determine the activity of TS-1 supported catalysts towards the ammoximation of other substrates.

It is known that the combination of H₂O₂ and TS-1 is able to catalyse a number of oxidation reactions, including alkanes, alkenes, alcohols and aromatics under mild conditions. These reactions often require the continuous addition of H₂O₂ and a significant proportion of the process costs are associated with the transportation and storage of preformed H₂O₂. Application of in-situ H₂O₂ synthesis for the various oxidation processes provides a more environmentally friendly, cheaper and safer alternative to the use of pre-formed H₂O₂. Particularly if H₂ generation can be achieved via electrolytic splitting of water. It is suggested that the approach utilised within Chapters 4 and 5 for the ammoximation of cyclohexanone should first be investigated for other ketone substrates, such as 2-butanone, to determine the efficiency of the one-pot approach and then expanded to alcohols and other substrates if possible.

6.2.7. Determine the role of phosphate present in Cs_xH_{3-x}PW₁₂O₄₀ salts in improving the stability H₂O₂.

It was postulated in Chapter 3 that the improvement in H₂O₂ activity observed when Cs_xH_{3-x}PW₁₂O₄₀ salts are used in conjunction with 2.5 wt. % Au – 2.5 wt. % Pd / TiO₂ is not solely due to the decrease in reaction solution pH but also due to improved stability of H₂O₂ through the presence of PO₄³⁻, a known H₂O₂ stabilising agent²¹. It is suggested that further work be carried out to investigate the availability of PO₄³⁻ when utilising Cs_xH_{3-x}PW₁₂O₄₀ salts in a polar medium and how the incorporation of Cs into the Keggin cage structure of H₃PW₁₂O₄₀ can limit the availability of PO₄³⁻.

6.3. References.

1. V. V. Krishnan, A. G. Dokoutchaev and M. E. Thompson, *J.Catal.*, 2000, **196**, 366-374.
2. Y.-F. Han and J. H. Lunsford, *J.Catal*, 2005, **230**, 313-316.
3. J. K. Edwards, B. Solsona, E. N. N, A. F. Carley, A. A. Herzing, C. J. Kiely and G. J. Hutchings, *Science*, 2009, **323**, 1037-1041.
4. J. K. Edwards, S. F. Parker, J. Pritchard, M. Piccinini, S. J. Freakley, Q. He, A. F. Carley, C. J. Kiely and G. J. Hutchings, *Catal. Sci. Technol.*, 2013, **3**, 812.
5. J. K. Edwards, E. Ntainjua N, A. F. Carley, A. A. Herzing, C. J. Kiely and G. J. Hutchings, *Angew.Chem. Int.Ed.*, 2009, **48**, 8512-8515.
6. S. Park, T. J. Kim, Y.-M. Chung, S.-H. Oh and I. K. Song, *Res.Chem. Intermed.*, 2010, **36**, 639-646.
7. S. Park, S. Lee, S. Song, D. Park, S. Baeck, T. Kim, Y. Chung, S. Oh and I. Song, *Catal. Commun.* 2009, **10**, 391-394.
8. E. N. Ntainjua, M. Piccinini, S. J. Freakley, J. C. Pritchard, J. K. Edwards, A. F. Carley and G. J. Hutchings, *Green Chem.*, 2012, **14**, 170.
9. S. J. Freakley, R. J. Lewis, D. J. Morgan, J. K. Edwards and G. J. Hutchings, *Catal. Today*, 2015, **248**, 10-17.
10. J. Edwards, B. Solsona, P. Landon, A. Carley, A. Herzing, C. Kiely and G. Hutchings, *J. Catal.*, 2005, **236**, 69-79.
11. J. K. Edwards, A. Thomas, A. F. Carley, A. A. Herzing, C. J. Kiely and G. J. Hutchings, *Green Chem.* 2008, **10**, 388.
12. S. J. Freakley, Q. He, J. H. Harry, L. Lu, D. A. Crole, D. J. Morgan, E. N. Ntainjua, J. K. Edwards, A. F. Carley, A. Y. Borisevich, C. J. Kiely and G. J. Hutchings, *Science*, 2016, **351**, 965-968.
13. M. Sankar, Q. He, M. Morad, J. Pritchard, S. J. Freakley, J. K. Edwards, S. H. Taylor, D. J. Morgan, A. F. Carley, D. W. Knight, C. J. Kiely and G. J. Hutchings, *ACS Nano*, 2012, **6**, 6600-6613.
14. J. A. Lopez-Sanchez, N. Dimitratos, P. Miedziak, E. N. Ntainjua, J. K. Edwards, D. Morgan, A. F. Carley, R. Tiruvalam, C. J. Kiely and G. J. Hutchings, *Phys. Chem. Chem. Phys.*, 2008, **10**, 1921-1930.
15. P. J. Miedziak, S. A. Kondrat, N. Sajjad, G. M. King, M. Douthwaite, G. Shaw, G. L. Brett, J. K. Edwards, D. J. Morgan, G. Hussain and G. J. Hutchings, *Catal. Sci. Technol.*, 2013, **3**, 2910-2917.
16. J. K. Edwards, B. E. Solsona, P. Landon, A. F. Carley, A. Herzing, C. J. Kiely and G. J. Hutchings, *J. Catal.*, 2005, **236**, 69-79.
17. J. K. Edwards, B. Solsona, P. Landon, A. F. Carley, A. Herzing, M. Watanabe, C. J. Kiely and G. J. Hutchings, *J. Mater. Chem.*, 2005, **15**, 4595-4600.
18. B. E. Solsona, J. K. Edwards, P. Landon, A. F. Carley, A. Herzing, C. J. Kiely and G. J. Hutchings, *Chem. Mater.*, 2006, **18**, 2689-2695.
19. J. K. Edwards, J. Pritchard, P. J. Miedziak, M. Piccinini, A. F. Carley, Q. He, C. J. Kiely and G. J. Hutchings, *Catal. Sci. Technol.*, 2014, **4**, 3244-3250.
20. J. K. Edwards, Pritchard, J., Lu, L., Piccinini, M., Shaw, G., Carley, A. F., Morgan, D. J., Kiely, C. J. and Hutchings, G. J. , *Angew. Chem. Int. Ed*, 2014, **53**, 2381-2384.
21. P. Wegner, *US patent number US20030151024 A1*, 2003, Hydrogen peroxide stabilizer and resulting product and applications